Journal of FMBA of Russia

ISSN Print 2713-2757
ISSN Online 2713-2765

EXTREME MEDICINE

Vol. 26 No. 3 / 2024
EXTREMEMEDICINE.RU

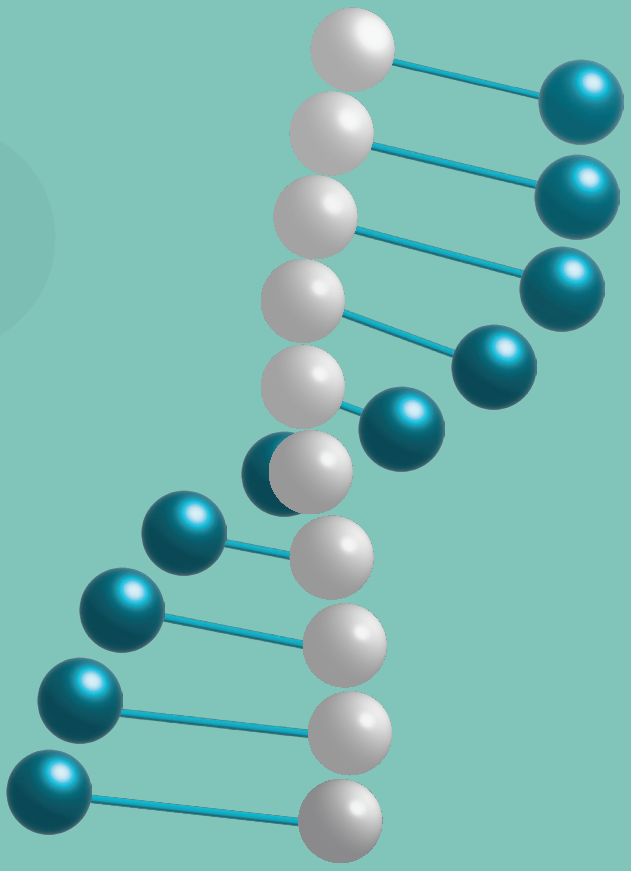

RETROSPECTIVE BIODOSIMETRY. CONVERSION OF THE CHROMOSOMAL TRANSLOCATIONS RATE INTO THE ORGANS DOSE

Molecular genetic characteristics and phylogenetic analysis of Russian and foreign measles virus variants

Assessment of the cardiobiomarkers level in end-to-end space flight simulation

EXTREME MEDICINE

SCIENTIFIC AND PRACTICAL JOURNAL OF FMBA OF RUSSIA
Frequency of 4 issues per year. Founded in 1999

Founder: FMBA OF RUSSIA, Volokolamskoe shosse, 30, str. 1, Moscow, 123182, Russia

Publisher: Centre for Strategic Planning, of the Federal medical and biological agency, 10 bld. 1 Pogodinskaya Str., Moscow, 119121, Russia

Postal address of the editorial office: Pogodinskaya ul., d. 10, str. 1, Moskva 119121, extrememedicine@cspfmba.ru; www.extrememedicine.ru

Contract publisher: NEICON ISP LLC: 4/5 Letnikovskaya St., Moscow 115114

Printing office: Triada Publishing House LLC: 9 Tchaikovsky Ave, office 514, Tver 170034

Print run: 100 copies. Free price

Passed for printing: 5 Dec. 2024

Date of publication: 9 Dec. 2024

The journal is registered as a mass medium by the Federal Service for Supervision of Communications, Information Technologies and Mass Communications. Certificate PI No. FS 77-25124 dated 27 July 2006

Indexed in Scopus in 2022

Indexed in RSCI. IF 2021: 0,450

Listed in HAC 08.10.2024 (№ 1668)

Open access to archive

МЕДИЦИНА ЭКСТРЕМАЛЬНЫХ СИТУАЦИЙ

НАУЧНО-ПРАКТИЧЕСКИЙ ЖУРНАЛ ФМБА РОССИИ
Периодичность 4 номера в год. Основан в 1999 году

Учредитель: ФМБА России, 123182, Москва, Волоколамское шоссе, д. 30, стр. 1

Издатель: ФГБУ «ЦСП» ФМБА России, 119121, Москва, Погодинская ул., д. 10, стр. 1

Адрес редакции: 119121, Москва, Погодинская ул., д. 10, стр. 1
extrememedicine@cspfmba.ru; www.extrememedicine.ru

Исполнитель: ООО «НЭИКОН ИСП»: 115114, Москва, ул. Летниковская, д. 4, стр. 5

Типография: ООО «Издательство «Триада»: 170034, Тверь, Чайковского пр., д. 9, оф. 514

Тираж: 100 экз. Цена свободная

Подписано в печать: 05.12.2024.

Дата выхода в свет: 09.12.2024

Журнал зарегистрирован в Федеральной службе по надзору в сфере связи, информационных технологий и массовых коммуникаций. Свидетельство ПИ № ФС77-25124 от 27 июля 2006 г.

Журнал включен в Scopus в 2022 г.

Журнал включен в РИНЦ. IF 2021: 0,450

Журнал включен в Перечень 08.10.2024 (№ 1668)

Здесь находится открытый архив журнала

CONTENTS

VOL. 26, NO. 3, 2024

СОДЕРЖАНИЕ

ТОМ 26, № 3, 2024

CONTENTS

VOL. 26, NO. 3, 2024

СОДЕРЖАНИЕ

ТОМ 26, № 3, 2024

https://doi.org/10.47183/mes.2024-26-3-5-14

RETROSPECTIVE BIODOSIMETRY: CONVERSION OF FREQUENCY OF CHROMOSOMAL TRANSLOCATIONS INTO ORGAN DOSES

Evgenia I. Tolstykh[1]✉, Yulia R. Akhmadullina[1,2], Pavel A. Sharagin[1], Elena A. Shishkina[1,2], Aleksander V. Akleyev[1,2]

[1] Urals Research Center for Radiation Medicine, Chelyabinsk, Russia

[2] Chelyabinsk State University, Chelyabinsk, Russia

Introduction. One of the techniques used in retrospective biodosimetry according to the fluorescence in situ hybridization (FISH) method involves the estimation of stable chromosome aberrations (translocations) in human peripheral blood T-lymphocytes. In the case of uniform external and internal exposure, the interpretation of FISH data does not pose any problem, since the dose to T-lymphocytes that effects the translocation frequency can be simply interpreted as the dose to other organs and tissues. However, when the internal exposure is non-uniform and the doses to the organs differ by an order of magnitude, conversion from frequency of translocation to dose estimates becomes a complicated task.

Objective. To review the main parameters necessary for the retrospective assessment of doses using the FISH method in the case of internal uneven and prolonged β-irradiation.

Findings. The present analytical review considers problems associated with determining the following parameters: (1) Frequency of radiation-induced and background translocations; (2) Conversion factors from the frequency of radiation-induced translocations to the dose to T-lymphocytes (α); (3) Conversion factors from the dose to T-lymphocytes (cytogenetic dose) to the dose to critical organs and tissues (B_{org}), which depend on age at the time of exposure. General approaches and estimates of (α) based on the construction of *in vivo* and *in vitro* calibration curves for external and internal exposure were analyzed. The dose-accumulation features in different T-cell populations from prolonged internal non-uniform exposure (using ^{90}Sr as an example) were considered in terms of the applicability of the model approach to assessing accumulated doses. Uncertainties of dose estimates in retrospective biodosimetry are discussed and further research directions proposed.

Conclusions. In the case of non-uniform internal exposure with a low dose rate, converting translocation frequency to dose estimates becomes a complex task. The α and B_{org} conversion coefficients, which are derived from independent data sets, can be based on various approaches, including modelling. Currently, approaches to assessing their uncertainties, as well as the uncertainties of the dose obtained using the FISH method, remain undeveloped. Therefore, these coefficients require further studies.

Keywords: chromosomal aberrations; translocations; circulating T-lymphocytes; biodosimetry; internal non-uniform internal exposure

For citation: Tolstykh E.I., Akhmadullina Y.R., Sharagin P.A., Shishkina E.A., Akleev A.V. Retrospective biodosimetry: Conversion of frequency of chromosomal translocations into organ doses. *Extreme Medicine*. 2024;26(3):5–14. https://doi.org/10.47183/mes.2024-26-3-5-14

Funding: the work was carried out with the financial support of the Federal Medical and Biological Agency of Russia, state registration number of research work in EGISU 122040400135-0.

Acknowledgments: the authors express their gratitude to Viktor A. Krivoshchapov and Svetlana B. Epifanova, specialists of the Urals Research Center for Radiation Medicine, for technical assistance.

Compliance with ethical principles: all ethical standards were observed when working with information sources.

Potential conflict of interest: Aleksander V. Akleyev has been a member Advisory Board of the journal “Extreme Medicine” since 2020. The other authors declare no conflict of interest.

✉ Evgenia I. Tolstykh evgenia.tolstykh@yandex.ru

Received: 1 July 2024 **Revised:** 28 Sep. 2024 **Accepted:** 14 Oct. 2024

РЕТРОСПЕКТИВНАЯ БИОДОЗИМЕТРИЯ. ПРОБЛЕМА КОНВЕРТАЦИИ ЧАСТОТЫ ХРОМОСОМНЫХ ТРАНСЛОКАЦИЙ В ДОЗУ НА ОРГАНЫ

Е.И. Толстых[1]✉, Ю.Р. Ахмадуллина[1,2], П.А. Шарагин[1], Е.А. Шишкина[1,2], А.В. Аклеев[1,2]

[1] Уральский научно-практический центр радиационной медицины Федерального медико-биологического агентства, Челябинск, Россия

[2] Челябинский государственный университет, Челябинск, Россия

Введение. Одним из методов ретроспективной биодозиметрии является учет стабильных хромосомных аберраций (транслокаций) в Т-лимфоцитах периферической крови человека с использованием метода FISH (fluorescence in situ hybridization). В случае равномерно внешнего или внутреннего облучения интерпретация данных FISH не вызывает проблем: доза на Т-лимфоциты, определяющая частоту транслокаций, трактуется как доза на другие органы и ткани. В случае неравномерного внутреннего облучения, когда дозы облучения органов различаются на порядок величины, переход от частоты транслокаций к оценкам дозы требует особых подходов.

Цель. Рассмотреть основные параметры, которые необходимы для ретроспективной оценки доз с использованием метода FISH в случае внутреннего неравномерного и пролонгированного β-облучения.

Обсуждение. В аналитическом обзоре были проанализированы проблемы, связанные с определением следующих параметров.

(1) Частота радиационно-индуцированных и фоновых транслокаций.

(2) Коэффициенты перехода от частоты радиационно-индуцированных транслокаций к дозе на Т-лимфоциты (α). Были рассмотрены общие подходы и оценки переходных коэффициентов на основе построения калибровочных кривых *in vivo* и *in vitro* при внешнем и внутреннем облучении.

(3) Коэффициенты перехода от дозы на Т-лимфоциты (цитогенетической дозы) к дозе на критические органы и ткани (B_{org}), которые существенно зависят от возраста.

Были проанализированы особенности накопления дозы в различных популяциях Т-клеток при длительном внутреннем неравномерном облучении (на примере ^{90}Sr), а также применимость модельного подхода к оценке накопленных доз. В работе обсуждаются неопределенности дозовых оценок и дальнейшие направления исследований в рамках ретроспективной биодозиметрии.

Заключение. В случае неравномерного внутреннего облучения с низкой мощностью дозы конвертация частоты хромосомных транслокаций в значения доз является сложной задачей. Коэффициенты конвертации α и B_{org} определяются по независимым наборам данных и опираются на разные, в том числе модельные подходы. Эти коэффициенты требуют дальнейшего уточнения. В настоящее время подходы к оценке их неопределенностей, а также неопределенностей дозы, получаемой с помощью метода FISH, остаются неразработанными.

Ключевые слова: хромосомные аберрации; транслокации; циркулирующие Т-лимфоциты; биодозиметрия; внутреннее неравномерное облучение

Для цитирования: Толстых Е.И., Ахмадуллина Ю.Р., Шарагин П.А., Шишкина Е.А., Аклеев А.В. Ретроспективная биодозиметрия. Проблема конвертации частоты хромосомных транслокаций в дозу на органы. *Медицина экстремальных ситуаций.* 2024;26(3):5–14. https://doi.org/10.47183/mes.2024-26-3-5-14

Финансирование: работа выполнена при финансовой поддержке ФМБА России, номер государственного учета НИР 22040400135-0.

Благодарности: авторы выражают благодарность специалистам Уральского НП Центра радиационной медицины В.А. Кривощапову и С.Б. Епифановой за техническую помощь в работе.

Потенциальный конфликт интересов: А.В. Аклеев — член редакционного совета журнала «Медицина экстремальных ситуаций». Остальные авторы заявляют об отсутствии конфликта интересов.

✉ Толстых Евгения Игоревна evgenia.tolstykh@yandex.ru

Статья поступила: 01.07.2024 **После доработки:** 28.09.2024 **Принята к публикации:** 14.10.2024

INTRODUCTION

In cases of radiation exposure when a dosimeter was not available at the time of radiation exposure, retrospective biodosimetry can be used to reconstruct the radiation dose. One of the available biodosimetry approaches is based on the accounting of stable chromosomal aberrations (translocations) in human peripheral blood T-lymphocytes [1–3]. The application of this method is based on the following assumptions: the frequency of chromosomal translocations in T-lymphocytes is proportional to the exposure dose; the frequency remains constant for a long time (does not decrease with time); the radiation dose received by T-lymphocytes resulting in the formation of translocations corresponds to the dose of exposure to other organs and tissues, in particular to red bone marrow (RBM). The latter postulate is true in the case of uniform external or internal exposure. However, in case of non-uniform internal irradiation, for example, due to ^{89,90}Sr, when doses to the RBM and other organs may differ by an order of magnitude, difficulties arise when interpreting the results of cytogenetic methods. This problem has been discussed in detail in a number of reviews [1–2]. For the purposes of biodosimetry, a model of T-lymphocyte exposure was developed in the case of ^{89,90}Sr accumulation in mineralized tissues of the human body [4–6].

The fluorescence in situ hybridization (FISH) method is used to estimate the frequency of translocations in the cell. The main parameters required for retrospective dose estimation using FISH in case of internal non-uniform and prolonged β-irradiation are as follows.

(1) The number of y_i translocations in $n_{cell,}$ counted in T-lymphocytes of a subject or a group of subjects is estimated using the FISH method. The characteristics of application and requirements for unification of the method are described in a number of regulatory documents [1, 7]. To estimate the dose level, the translocation frequency (μ_i) is used; this should be presented per one genomic equivalent (Genomic Equivalent GE) — or, according to an alternative terminology, per one cell equivalent (Cell Equivalent CE). The conversion factor (G_j) from the number of counted cells (metaphases) n_{cell} to the number of genomic equivalents n_{ge} depends on the set of stained chromosomes and the type of staining (single-color or multicolor). If 24-color staining is used, no conversion to GE is required.

(2) Background (non-radiation) translocation frequency $\mu_0(\tau)$ depending on age. Here, since translocations may occur under the influence of other (non-radiation) unfavorable endogenous and exogenous factors, correction for background values (subtraction of background values) is necessary. The number of translocations in T-lymphocytes accumulates with age over an individual's lifetime. According to the scientific literature, sex does not have a significant effect on the formation of translocations; the influence of smoking and alcohol is also insignificant. The dependence of translocation frequency obtained in a joint international study of unexposed donors in terms of the number of translocations per GE is used as already known background values [8].

(3) Coefficients of the dose-effect relationship (C — free term, α — linear coefficient, β — quadratic coefficient), whose combination permits age-adjusted translocation frequency μ_{i_age} to be transposed onto the dose absorbed in T-lymphocytes (D_L). The coefficients are determined on the basis of the calibration curve (linear-quadratic or linear). For the construction of the calibration curve, the reliability of radiation dose estimation and uniformity of translocation counting criteria are of fundamental importance. The shape and parameters of the calibration curve depend on the type of radiation (linear energy transfer LET); sparsely ionizing gamma and beta radiation are dependent on the dose rate. Calibration curves are discussed in detail in the literature [1, 7, 9].

(4) Conversion factor (B_{rbm}) from lymphocyte dose (D_L) to red bone marrow dose (D_{rbm}). For osteotropic ^{89,90}Sr, this coefficient depends on age at the time of irradiation onset (τ_1) and time following irradiation onset ($\tau_s - \tau_1$), where τ_s is the age of the donor at the time of blood collection. In addition, the coefficient depends on sex due to variable strontium metabolism and its accumulation in bone tissue [10].

The purpose of this analytical review is to consider the main parameters[1] that are necessary for retrospective dose estimation using the FISH method in the case of internal nonuniform and prolonged β-irradiation.

FINDINGS

Chromosome translocations taken into consideration under retrospective biodosimetry

For good reproducibility of the biodosimetry method, it is important to unambiguously define the types of chromosomal translocations that are considered. Radiation cytogenetics uses different nomenclature approaches, typically PAINT (Protocol for Aberration Identification Nomenclature Terminology) [11], S&S (Savage and Simpson) [12]), and a combined approach using International System for Human Cytogenomic Nomenclature (ISCN) medical genetics terminology [13]. In the Russian-language literature, this leads to a large number of synonyms for translocations.

Under the action of sparsely ionizing β-radiation characteristic of ^{89,90}Sr, most of the registered translocations are reciprocal (synonyms: complete, bilateral, two-way). In this case, there is a mutual exchange of end sites between two non-homologous chromosomes without loss of genetic material. Despite the involvement of fact that two chromosomes, reciprocal translocation is considered as a single event, i.e., one translocation. A small proportion are nonreciprocal (incomplete, unilateral, one-way) translocations, when the transfer of material occurs only from one nonhomologous chromosome to another — i.e., unidirectionally — and is counted as a single event. It has been suggested [1, 14, 15] that an incomplete translocation may actually be complete, but that the second chromosome segment involved in the exchange is too small to visualize. Reciprocal and nonreciprocal (complete and incomplete) translocations are also referred to as simple translocations. Here, the main indicator on the basis of which the radiation dose is calculated when using the FISH method is their frequency.

Complex translocations, when three or more chromosomes are involved in the exchange, make up a small fraction of the total number of translocations under prolonged sparsely ionizing radiation [16, 14]. Difficulties can arise due to counting complex translocations as the sum of simple translocations, whose number is determined by the number of color transitions [17]. Under conditions of densely ionizing radiation, the proportion of complex translocations increases significantly [18, 19].

In the publication of the International Atomic Energy Agency, 2011 [1], chromosomal translocations also include insertions in cases when a visible insertion of a region of one chromosome into the arm of a nonhomologous chromosome is observed. The authors note that the frequency of insertions may or may not be taken into account when estimating the radiation dose.

Cytogenetic analysis may also take into account inversions representing intrachromosomal aberrations in which there is a 180° reversal of a chromosome segment. Indication of inversions requires more complex staining — for example, by Multicolor Banding Probes (mBAND) or by combining whole chromosome probes together with telomeric probes. The frequency of inversions is significantly increased by exposure to densely ionizing radiation [18, 19].

If several lymphocytes contain identical translocations (the numbers of chromosomes involved in the exchange and the length of the translocated sites are the same), such cells are considered to be clones [1]. In this case, it is assumed that a single translocation occurred in one cell regardless of the number of cells with identical translocations.

Estimation of the frequency of chromosomal translocations for the purposes of retrospective biodosimetry is usually performed in so-called stable cells, i.e., cells that do not contain unstable chromosomal aberrations such as rings and dicentrics that prevent normal cell cycle progression. Unstable cells contain the aberrations mentioned above.

CONVERSION FACTORS FROM THE FREQUENCY OF RADIATION-INDUCED TRANSLOCATIONS TO THE DOSE TO T-LYMPHOCYTES

General approaches

The description of dose-effect relationships for translocation frequency are described in detail in the literature along with approaches to parameter determination [1, 7, 9, 13, 20]. In our case, the dependences for sparsely ionizing radiation are of interest.

Numerous experiments have demonstrated a linear-quadratic dependence of the frequency of radiation-induced translocations (μ_i) of lymphocyte radiation dose D_L at high dose rates (irradiation time less than 2 hours):

$$\mu_i = C + \alpha \cdot D_L + \beta \cdot D_L^2, \quad (1)$$

where:
C — absolute term of the dose-effect relationship;
α — linear dose-effect coefficient;
β — quadratic coefficient of the dose-effect relationship.

Such a dependence can be explained as follows. It is assumed that the quadratic term β takes into account DNA damage (the source of translocation formation *Tr*) arising from repeated hits of ionizing particles into the cell nucleus with a short time interval (<2 h). In other words, the coefficient β takes into account aberrations that can be altered by repair mechanisms if they manage to "work" during prolonged exposure or in periods between intermittent (fractionated) acute exposures. Most lesions resulting in chromosomal aberrations are either repaired or become unavailable for repair within about five to six hours after exposure. Therefore, an additional coefficient is proposed for the quadratic term in the form of a G-function [1, 21, 22], which takes into account the time required for damage repair, i.e., the dose rate:

$$\mu_i = C + \alpha \cdot D_L + \beta \cdot G(x) \cdot D_L^2, \quad (2)$$

$$G(x) = 2/x^2 \cdot [x - 1 + e^{-x}], \quad (3)$$

[1] 1. Frequency of radiation-induced and background translocations and requirements for their estimation.
2. Transition coefficients from the frequency of radiation-induced translocations to the dose to T lymphocytes (α). General approaches and estimates of transition coefficients based on the construction of *in vivo* and *in vitro* calibration curves under external and internal irradiation were reviewed.
3. Transition factors from T-lymphocyte irradiation dose (cytogenetic dose) to the dose to critical organs and tissues (B_{org})

in this case, $x = t / t_0$, (4)

where:

t — time (duration) of irradiation,

t_0 — average rupture lifetime, which has been shown to be about 2 hours.

When a dose accumulates over a long period of time, $G(x)$ decreases about to zero. Consequently, even if prolonged irradiation occurs with a high dose (>1.0 Gy), the dose dependence of the translocation frequency becomes linear:

$$\mu_i = C + \alpha \cdot D_L. \quad (5)$$

It is also evident that most aberrations due to the action of sparsely ionizing radiation at low doses (<0.3 Gy) but with high power occur during the passage of single ionizing tracks, resulting in a dependence close to linear.

Thus, a dependence close to linear is observed when there is has been prolonged irradiation (duration of irradiation was days, months, years), including with high accumulated doses (up to 2–3 Gy), or in the case of acute irradiation with low doses when no acute radiation syndrome was detected. Therefore, for retrospective assessment of doses in cases of internal exposure to ^{89,90}Sr, the estimation of the linear coefficient α is of fundamental importance.

As the analysis of experimental data [1] shows, the linear coefficient in formula 5 will be the same both when studying the dose dependence of the translocation frequency and when analyzing the dose dependence of the yield of unstable aberrations (dicentrics, rings). As noted in [23, 24], the ratio of dicentrics to radiation-induced translocations is approximately 1:1; as a result, similar ratios in the dose-effect relationship can be expected. According to the dicentrics data, the linear coefficient for translocations for high-energy gamma rays in the case of uniform prolonged irradiation is 0.015–0.020 Tr/GE per Gy [25], which can be used to convert from translocation frequency to dose to lymphocytes. In [26], the recommended value is ~0.015.

Thus, based on (5) and taking into account the background values for the corresponding age ($\mu_0(\tau_s)$), the dose to T-lymphocytes is obtained using the formula:

$$D_L = \frac{[\mu_i - \mu_0(\tau_s)] - [C - \mu_0(\tau_s)]}{\alpha}. \quad (6)$$

Since the absolute term C is mainly due to the background translocation frequency, the expression $[C - \mu_0(\tau_s)]$ is assumed to be close to zero, so:

$$D_L = \frac{\mu_{i\_age}}{\alpha}. \quad (7)$$

Approaches to estimating the coefficients of α are discussed below.

Estimates of the parameter α obtained by acute external gamma irradiation of donor lymphocytes *in vitro*

Recently, a number of studies have appeared aimed at obtaining calibration curves for translocations estimated by the FISH method under the condition of standardization [1, 9, 20], which assumes acute irradiation, application of a linear-quadratic model, standard statistical approaches, etc. In order to use the parameters of these dependencies for retrospective dosimetry, translocations must be calculated in stable cells where there are no unstable aberrations interfering with the cell cycle. Since at prolonged irradiation the dose dependence of translocation yield is close to linear, the linear coefficient α should be considered from the obtained parameters of the linear-quadratic dependence for the transition from the translocation frequency to the dose to lymphocytes.

The article [9] gives an overview of the parameters of calibration curves for translocations (determination of coefficients α and β of the linear-quadratic dependence) obtained by FISH following subtraction of background values. As well as being sporadic, such works also differ in their approaches to accounting for translocations (Tr). Table 1 summarizes the results of the most appropriate cytogenetic studies where the α coefficient was statistically significantly determined by in vitro lymphocyte irradiation. In all cases, the authors irradiated donor blood from a ^{60}Co source with a high dose rate; the irradiation time was measured in minutes and the dose-effect was described by a linear-quadratic relationship (formula 1). Table 1 shows that the variation of α values is significant (from 0.012 to 0.0447); the median value is equal to 0.0178 (95% 0.012-0.044) Tr/GE per Gy.

Evaluation of α parameter used in irradiation process *in vivo*

For in vivo irradiation, the dose to T-lymphocytes and other organs is calculated on the basis of dosimetric measurements. In this case, dose measurements are not made directly in the target cells or tissues, but either by means of a dosimeter located close to the body (in professionals) or by measuring the radionuclide content in the body in the population (measurement of ^{90}Sr content in the bodies of residents of coastal villages of the Techa River), or by reconstructing gamma fields and radiation spectra as in the case of the nuclear bombings of Hiroshima and Nagasaki.

Acute external irradiation of complex spectrum with high power (Hiroshima and Nagasaki populations)

In the cases of atomic bombing, there was an acute single exposure of the population with high dose rate and different LET. Therefore, in order to analyze the dose dependence it is necessary to introduce coefficients that take into account the relative biological effectiveness (RBE) of radiation, which introduces additional uncertainty in dose estimates. In addition, it is known that densely ionizing radiation leads to a large number of complex (compound) damages of DNA and chromosomes [18, 19]. This makes it difficult to directly use these data for cases of sparsely ionizing radiation. On the other hand, the cohort of those exposed due to atomic bombardments is the most studied, so the results of cytogenetic studies deserve attention. Dose-dependent analysis of the frequency of stable chromosomal aberrations for the residents of Hiroshima and Nagasaki has been

Table 1. Values of the linear coefficient α (Tr/GE per Gy) of the linear-quadratic dependence of the translocation frequency (with correction of background values) on the lymphocyte dose

Coefficient α±SE	Number of observations, *n*	Values, comments	Source
0.0119±0.0083 CV= 70%	2	Only reciprocal translocations in all cells (stable and unstable) were considered. $\mu_i = (0.0014 \pm 0.0005) + (0.0119 \pm 0.0083)D_L + (0.0357 \pm 0.0135) D_L^2$	[27]
0.0178±0.0037 CV=21%	5	All simple translocations were counted and attributed to all cells (stable and unstable). Complex translocations were converted to an equivalent number of simple translocations. $\mu_i = (0.0005 \pm 0.0001) + (0.0178 \pm 0.0037) D_L + (0.0901 \pm 0.0054) D_L^2$	[9]
0.0152±0.0108 CV=71%	11	All simple translocations in stable cells only were considered. $\mu_i = (0.0001 \pm 0.0021) + (0.0152 \pm 0.0108) D_L + (0.0809 \pm 0.0061) D_L^2$	[28]
0.0447±0.0144 CV=30%	1	All simple translocations were considered and attributed to stable cells only. $\mu_i = (0.001 \pm 0.0008) + (0.0447 \pm 0.0144) D_L + (0.0142 \pm 0.0195)D_L^2$	[29]
0.0343±0.0107 CV=31%	5	All simple translocations were counted and attributed to all cells (stable and unstable). Complex translocations were converted to an equivalent number of simple translocations. No correction was made for background translocations. $\mu_i = (0.0040 \pm 0.0017) + (0.0343 \pm 0.0107) D_L + (0.0779 \pm 0.0052) D_L^2$	[30]

Table prepared by the authors using data from references [9, 27–30]

Note: *n* is the number of blood donors, adults aged 25 to 45 years.

conducted since the 1960s. The results were published as cytogenetic data accumulated and/or as the system for calculating individual doses improved [31–34]. The analysis of cytogenetic data of key interest to us (but using routine Gimza staining of chromosomes) was performed in [34], where reciprocal translocations, pericentric inversions, or small deletions (or their combinations) were considered as stable. Translocations in stable cells — i.e., cells without dicentrics and rings — were counted. The dose-effect relationship was described by a linear-quadratic function (Formula 1). A total of 1703 individuals were included in the study. Individual equivalent doses were calculated with correction for the RBE of neutrons and γ-radiation. The maximum individual doses were 1.5 Sv. The following values of the linear coefficient were obtained:

For Hiroshima inhabitants α = 0.03915 ± 0.00315 Tr to the cell per Zv

$\mu_i = (0.01274 \pm 0.01399) + (0.03915 \pm 0.00315) D_L + (0.00970 \pm 0.00155) D_L^2$.

For Nagasaki inhabitants α = 0.02350 ± 0.00246 Tr to the cell on Zv

$\mu_i = (0.01274 \pm 0.11399) + (0.02350 \pm 0.00246) D_L + (0.01870 \pm 0.00099) D_L^2$.

In general, these values are higher than those obtained for the calibration curves (Table 1), but fall within the range of scatter of their values.

The last analysis of the data obtained using FISH and the updated version of the dosimetry system was performed in [35]. Reciprocal and nonreciprocal translocations, insertions (insertions), and complex exchanges were taken into account. The excess relative rate (ERR) of translocation frequency was calculated with correction for background. Although dose-effect parameters for ERR cannot be directly used for quantitative comparison with literature data, the authors noted interesting patterns. Linear-quadratic dependence of translocation frequency (in terms of ERR) on dose was observed up to 1.25 Gy. Thus, the dependence had a more complex character. It was shown that age at the time of irradiation is a significant factor affecting the dose-effect parameters. The lowest values of translocation frequency per 1 Gy were observed in the group of children aged 0–5 years, then the frequency increased to decrease again after 25 years of age.

Prolonged external γ-irradiation with low dose rate (professionals)

The analysis was performed as described in [36]; male workers (*n* = 459) were included in the study; the dose was up to 1.6 Gy (the accumulated dose was determined on the basis of individual dosimeter data as the dose per RBM). Using the FISH method, simple Tr translocations in stable cells per GE were counted. Data were described by linear regression (Poisson distribution of translocation frequency was tested for each dose group). The AMFIT module of the EPICUR program was used for calculations: α = 0.01174 ± 0.00164.

These values fall within the lower limit of the interval of estimates of the α coefficient from the in vitro calibration curves.

Prolonged external and internal exposure of residents of riverside villages of the Techa River (Southern Urals) with decreasing dose rate

The inhabitants of the riverside villages of the Techa river suffered from radiation expose (mixed γ-, β-irradiation with low dose rates, both external and internal) following discharges of radioactive waste from the Mayak Production Association into the Techa River during the 1950s. External exposure was more pronounced in the upper reaches of the Techa River near to site of radioactive waste discharges. However, throughout the river, the main contribution to the internal dose to the RBM was made by ^{89,90}Sr. Dose-response analysis was performed in 2023 and described in detail [37]. We used pooled data for a long period of studies from 1994 to 2021 (197 donors, 212 blood samples). For each donor, the dose to T-lymphocytes was calculated taking into account age-related dynamics and kinetics of

T-cell populations. Simple translocations and complex exchanges in stable cells were taken into account. As in the above-mentioned study [33], the dose dependence of translocation frequency was described by linear regression (Poisson distribution of translocation frequency was checked for each dose group); the AMFIT module of the EPICUR program was used for calculations.

Table 2 shows the values of linear coefficients of α-dose-effect dependence for donors of different ages at the time of the beginning of irradiation in 1950.

The lowest values of translocation frequency per 1 Gy dose to T-lymphocytes were obtained for children of the first years of life (Table 2). The maximum values were observed in the group from 5 to 18 years of age. The data of Table 2 do not contradict the results obtained in vitro (Table 1) and in vivo for professionals [36]. It should be noted that these data are consistent with the results on the evaluation of the effect of age at the time of irradiation on the translocation rate in the Japanese cohort [35], where relatively low values of ERR per 1 Gy were observed in children of the first years of life, followed by an increase in the translocation rate and subsequent decrease in adults after 25 years of age.

To summarize, the in vitro calibration curves described in the literature were obtained by irradiating blood samples with high dose rates (irradiation lasting minutes). Adults aged 25 to 45 years were taken as donors.

The number of donors for the construction of one calibration curve is small (a maximum of 11 people [7], of which sharply falling out values were obtained for two donors, who differed from the rest of the group by almost 10 times. The International Organization for Standardization (ISO) [7] recommends that biodosimetry laboratories develop their own calibration curves to take into account the staining and translocation counting methods adopted by the laboratory and the age range of the subjects. Examples of such work include [20, 30].

Although estimates obtained in vivo are based on the study of a large number of donors, the accuracy of dose estimates is much lower. In these studies, parameter values may change with improvements in dosimetric approaches, as is done in the Japanese cohort studies and the Techa River studies.

CONVERSION FACTORS FROM THE DOSE TO T-LYMPHOCYTES (CYTOGENETIC DOSE) TO THE DOSE TO CRITICAL ORGANS AND TISSUES

In the case of uneven internal irradiation, the dose to T lymphocytes is not the same as the dose to other organs and tissues, of which the dose to RBM is of most interest. Coefficient (B_{org}) can be used to relate the dose to lymphocytes (D_L) to the dose on the body (D_{org}). Thus, taking into account formula (7), the dose to a particular organ based on cytogenetic data will be calculated according to the formula:

$$D_{org} = D_L \cdot B_{org}(sex, \tau_1, \tau_s) = \frac{\mu_{i\_age}}{\alpha} B_{org}(sex, \tau_1, \tau_s). \quad (8)$$

Table 2. Values of the coefficient α in the linear dependence of the translocation frequency on T-lymphocyte doses, according to Techa River data

Age at the beginning of exposure, years	Number of probes	Number of translocations on GE per 1 Gy α±SE (95% CI)
0–5	58	0.0093±0.013 (0.0067–0.0119)
5–18	108	0.0153±0.0015* (0.0124–0.0183)
18–38	46	0.0119±0.0029 (0.0063–0.0178)

Table prepared by the authors using their own data [37]

Note: * — statistically significant differences relative to the 0–5 year's group.

Dose shaping to different T-cell populations during prolonged internal non-uniform irradiation (on the example of ^{90}Sr)

If the irradiation occurred decades ago, the donor's blood contains a mixture of T-lymphocytes, which are descendants of T-cells irradiated at different doses. Two groups of T-lymphocytes can be distinguished, the dose to which differs most significantly in the case of local irradiation of RBM ^{90}Sr.

(1) T-lymphocytes are the descendants of lymphocytes formed (emerged from the thymus) before exposure. Their proportion can be quite significant if the exposure occurred during adolescence and adulthood. Despite the fact that the lifespan of individual lymphocytes is several years (varies in different subpopulations) [38-40], T-lymphocytes are able to proliferate in peripheral lymphoid organs, maintaining quantitative constancy of the peripheral pool of T-cells [41–42] against the background of a sharp age-related decrease in thymus production [39, 40, 43]. These T-lymphocytes are irradiated only when circulating in the body, spending a certain time, including the bone marrow.

(2) T-lymphocytes, progenitors of progenitors (stem cells) irradiated in the RBM after ^{90}Sr enters the body. The dose load on these cells is much higher than on T-lymphocytes from the first group due to the accumulation of ^{90}Sr in bone tissue to locally irradiate RBM, including T-progenitors. After passing through the stages of differentiation and proliferation in the RBM and in the thymus, the formed T-lymphocytes continue to circulate and in some cases proliferate in the body; their descendants may appear in the donor's blood sample decades after the beginning of irradiation.

The works [4, 6, 37, 44] describe in detail approaches to modeling the dynamics and biokinetics of T cells based on the concept of T-cell lineage, when the modeling unit is the progenitor and all its progeny (potential carriers of stable aberration). Modeling approaches can be used to determine weighting coefficients for these two groups of T-lymphocytes and estimate the weighted average dose per T-lymphocyte. The evaluations rely on dose calculations to the RBM and other organs and tissues based on dosimetric and biokinetic models for ^{90}Sr [45–46].

Evaluation of transition factors from dose to T-lymphocytes (D_L) to dose to critical organs using ^{90}Sr as an example

The estimation of the conversion factors from dose to T lymphocytes to dose to critical organs (B_{org}) using ^{90}Sr as an example was described earlier [10]. This factor is the

ratio of the corresponding dose coefficients — i.e., the values of the accumulated dose in the case of a single intake of the radionuclide. For a single intake, the following formula is used:

$$B_{org}(sex, \tau_1, \tau_s) = \frac{Dc_{org}(sex, \tau_1, \tau_s)}{Dc_L(sex, \tau_1, \tau_s)}, \quad (9)$$

where:

τ_1 — the age of the donor at the moment of ^{90}Sr intake (years)

τ_s — the age of the donor at the time of blood collection for FISH cytogenetic study

$Dc_{org}(sex, \tau_1, \tau_s)$ — the dose accumulated in the organ *org* during the period of time $(\tau_s - \tau_1)$ after a single intake with food 1 Bq ^{90}Sr; is calculated using dosimetric [45] and biokinetic models [46] that take into account the sex and age of the individual;

$Dc_L(sex, \tau_1, \tau_s)$ — weighted average dose accumulated over a period of time $(\tau_s - \tau_1)$ in a series of T-cell generations after a single food intake of 1Bq ^{90}Sr; calculated using the model of age dynamics and T-cell kinetics, as well as known values of D_{org} doses for organs and tissues in which T-cells spend some time [47]; Gy/Bq. The computer program "Lymphocytes" was used for calculations. Numerical values $Dc_{org}(sex, \tau_1, \tau_s)$ for ^{90}Sr are shown in the study [47]. In the case of chronic ingestion, the sum of the dose values from activity ingestion was calculated $A_i(t)$ in every marked period of time. Therefore, for B_{org} we consider the following:

$$B_{org}(\tau_1, \tau_s) = \frac{\Sigma_{t1}^{ts}[Dc_{org}(sex, \tau_1, \tau_s) \cdot A_i(t)]}{\Sigma_{t1}^{ts}[Dc_L(sex, \tau_1, \tau_s) \cdot A_i(t)]}. \quad (10)$$

Since the values of $A_i(t)$ in the numerator and denominator of formula (10) are reduced in the case of uniform arrival:

$$B_{org}(\tau_1, \tau_s) = \frac{\Sigma_{t1}^{ts}[Dc_{org}(sex, \tau_1, \tau_s)]}{\Sigma_{t1}^{ts}[Dc_L(sex, \tau_1, \tau_s)]}. \quad (11)$$

However, if the chronic intake was uneven (function $A_i(t)$ is not constant), coefficient B_{org} must be calculated considering this function.

Numerical values of coefficients B_{org}, which connect the dose on T-lymphocytes and dose to RBM, were counted and analyzed for ^{89,90}Sr (B_{rbm}^{Sr}), [10]. Coefficients B_{rbm}^{Sr} turned out to significantly depend on the age at the beginning of ^{89,90}Sr intake. The older a person is at the beginning of exposure, the more the cytogenetic dose differs from the dose to the RBM because the coefficient B_{rbm}^{Sr} is growing with age and can and may exceed the value of 5.

This is due to the age-related dynamics of T-cell populations: it is only legitimate to assume that the cytogenetic dose corresponds to the dose to RBM for newborns and children in the first years of life for whom the values of B_{rbm}^{Sr} are close to one.

Sex does not have a significant impact on B_{rbm}^{Sr}. If homogeneous enrollment was stretched in time by six months, it did not significantly affect the value of the B_{rbm}^{Sr}. The study of the effect of the longer intake of ^{90}Sr to B_{rbm}^{Sr} (up to 5 years) showed that the most sensitive group is adolescents of 15 years old. For this cohort, the differences of B_{rbm}^{Sr} in the case of a single and 5-year even ^{90}Sr intake are about 13%.

UNCERTAINTY OF DOSE ESTIMATES IN RETROSPECTIVE BIODOSIMETRY, RESEARCH DIRECTIONS

In the case of acute whole-body gamma irradiation, the approaches to dose estimation uncertainty are described in detail in [7]. The uncertainties of all input parameters are taken into account: the uncertainty of the translocation frequency estimate, the uncertainty of the calibration curve, and the uncertainty of the age-specific background translocation frequency estimate. These approaches allow estimating the limits of the 95% confidence interval (CI) of the radiation dose to T-lymphocytes, which differs little from the dose to RBM and other organs and tissues. The simplest method [48] is based on estimating the lower and upper limits of CI for the frequency of chromosomal aberrations (in the Poisson distribution approximation) and comparing them with the CI of the calibration curve. In this case, the CI width for the frequency of chromosomal aberrations is chosen to be 83%, which gives 95% CI for the transition to dose uncertainty estimation [49].

More complicated is the method of uncertainty propagation or delta method [1, 7], which is based on estimates of the variation (and covariance) of the calibration curve parameters and aberration frequency variance in terms of standard deviation. In this case, the 95% CI of the dose estimate is calculated in the approximation of a normal distribution. This is a conservative method used, for example, for "alien" calibration curves. The need to switch from dose to T-lymphocytes to dose to other organs and tissues is relevant for non-uniform external and internal irradiation.

For the case of non-uniform (partial) *external irradiation*, scenarios of local irradiation of different segments of the human body containing RBM (e.g., sternum, pelvis, head, etc.) are considered. However, all the proposed statistical methods for estimating the dose accumulated by tissues in the irradiated area (with an estimate of their uncertainty) are based on dicentrics analysis, i.e., they should be applied in a short period of time after exposure [1, 50]. The methods are based on the use of the "contaminated" Poisson method, which allows dose estimation to take into account the distribution of dicentrics among all affected cells, as well as providing additional information about the irradiated body volume and RBM. The above methods — in particular, using the Bayesian approach [51] — are implemented in the BiodoseTool, DoseEstimate, and CABAS [50–53] computer programs. However, the applicability of these statistical methods for retrospective dosimetry of internal exposure (using the translocation frequency) is highly questionable, since, as noted above, by the time of blood sampling, different subpopulations of lymphocytes have accumulated different doses depending on the age of the donor at the time of 90Sr intake making it impossible to divide the Poisson distribution into two components.

Under uneven *inner irradiation* as in the case with ^{90}Sr, the total uncertainty should include — but not be limited to — the uncertainty of factor estimates B_{org} (Formula 11). Approaches to its assessment currently being developed represent one of the most important directions of our work. It should be noted that individual donor differences in the ability to repair DNA damage (individual differences in the

efficiency of repair enzymes) — as well as donor lifestyle, which determines the occurrence of other endogenous and exogenous factors that influence the background frequency of translocations — contribute to the uncertainty of dose estimates.

The total uncertainty determines the threshold of individual doses that can be detected using the FISH method (minimum detectable value). A review by Edwards et al. [26] indicates that supra-phononuclear individual doses of the order of 0.5 Gy can be measured using FISH. In general, reviews on the application of retrospective dosimetry methods note a detectable individual dose value of 0.25–0.3 Gy [54-57] or 0.25–0.4 Gy [3]. In the case of internal ^{90}Sr exposure, this value can be expected to be higher.

For the purposes of retrospective dosimetry, not only individual but also mean group dose estimates using the FISH method are in demand. Such assessments are used in the case of radiation accidents in which large populations are affected or where there is a need to estimate average doses in a locality with a conditionally uniform level of contamination/exposure. In this mean group approach, the total number of translocations detected in all donors in the group is summarized along with the number of background translocations according to the age of each donor in the group. The difference between these numbers considered as radiation-induced translocations refers to the total number of genome-equivalents calculated in the group. Such an approach avoids the null and negative values that often occur when background is subtracted at the individual level at low radiation doses, thus significantly lowering the threshold for detecting dose exceeding the background values. However, the mean group approach requires careful formation of groups with maximally similar exposure conditions. Mean group estimates can also be used to validate individualized dose estimates derived from models and/or other retrospective dosimetry techniques, which include:

- reconstructing external dose to human organs and tissues from soil contamination levels (includes calculations using human body phantoms);
- reconstructing internal doses from dietary contamination (includes the use of dosimetric and biokinetic models);
- using other biodosimetry techniques such as electron paramagnetic resonance (EPR) method for tooth enamel;
- dosimetry using materials sensitive to ionizing radiation (e.g., thermoluminescent dosimetry using ceramic samples).

The use of cytogenetic data for the purposes of validation of external doses is exemplified in the studies on the Techa River [58, 59], where good convergence of the results of estimation of doses to members of epidemiological cohorts estimated on the basis of direct measurements of gamma fields, human body exposure models, data from cytogenetic FISH studies, studies of tooth enamel by the EPR method, etc., was shown.

CONCLUSION

The used of translocation frequency to provide dose estimates is challenging especially in cases of non-uniform internal irradiation with low dose rates. The conversion factors from chromosomal translocation frequency to T-lymphocyte dose (α) and further from T-lymphocyte dose to organ and tissue dose B_{org}, which are determined from independent data sets, rely on different approaches.

The α coefficient requires experimental characterization of the calibration curves, since its estimates vary widely, often differing by a factor of two; in addition, values depend on the specific FISH technique used. Calibration curves obtained in vitro for children and adolescents at the time of exposure, whose parameters may differ from those for adults, are not described. No *in vitro* calibration curves are available for prolonged irradiation at low dose rates. Due to the small number of donors, the curves may involve systematic bias in the dose-effect parameters.

The estimation of the B_{org} coefficient relies on a set of models, which, in turn, are based on a large amount of experimental data on human physiology, mineral metabolism, anatomical structure of organs, etc. The coefficients depend significantly on age at the time of exposure. Unfortunately, approaches to estimating their uncertainties remain undeveloped to date.

References

1. IAEA, International Atomic Energy Agency. Cytogenetic dosimetry: applications in preparedness for and response to radiation emergencies. EPR-Biodosimetry. IAEA, Vienna, Austria. 2011.
2. Giussani A, Lopez MA, Romm H, Testa A, Ainsbury EA, Degteva M, et al. Eurados review of retrospective dosimetry techniques for internal exposures to ionising radiation and their applications. *Radiat Environ Biophys.* 2020;59(3):57–387. https://doi.org/10.1007/s00411-020-00845-y
3. Nakayama R, Abe Y, Goh Swee Ting V, Nakayama R, Takebayashi N, Nakata A, A Riyoshi K et al. Cytogenetic Biodosimetry in Radiation Emergency Medicine: 4. Overview of Cytogenetic Biodosimetry. *Radiation Environment and Medicine.* 2022;11(2):91–103. https://doi.org/10.51083/radiatenvironmed.11.2_91
4. Tolstykh EI, Degteva MO, Vozilova AV, Anspaugh LR. Local bone-marrow exposure: how to interpret the data on stable chromosome aberrations in circulating lymphocytes? (some comments on the use of FISH method for dose reconstruction for Techa riverside Residents). *Radiat Environ Biophys*. 2017;56(4):389–403. https://doi.org/10.1007/s00411-017-0712-7
5. Tolstykh EI, Degteva MO, Vozilova AV, Akleyev AV. Interpretation of FISH Results in the Case of Nonuniform Internal Radiation Exposure of Human Body with the Use of Model Approach. *Russian Journal of Genetics*. 2019;55(10):1227–33. https://doi.org/10.1134/S1022795419100132
6. Tolstykh EI, Vozilova AV, Akleyev AV, Zalyapin VI. Model of age-dependent dynamics and biokinetics of T-cells as natural biodosimeters. *Radiat Environ Biophys*. 2024 Aug;63(3):405–21. https://doi.org/10.1007/s00411-024-01072-5
7. Radiological protection — Performance criteria for laboratories using Fluorescence In Situ Hybridization (FISH) translocation assay for assessment of exposure to ionizing radiation. ISO 20046. 2019.
8. Sigurdson AJ, Ha M, Hauptmann M, Bhatti P, Sram RJ, Beskid O, et al. International study of factors affecting human chromosome translocations. *Mutat Res*. 2008;652(2):112–21. https://doi.org/10.1016/j.mrgentox.2008.01.005
9. Goh VST, Fujishima Y, Abe Y, Sakai A, Yoshida MA, Ariyoshi K et al. Construction of fluorescence in situ hybridization (FISH) translocation dose-response calibration curve with multiple do-

nor data sets using R, based on ISO 20046:2019 recommendations. *Int J Radiat Biol*. 2019;95(12):1668–84. https://doi.org/10.1080/09553002.2019.1664788
10. Tolstykh E. I. Conversion from the frequency of chromosome translocations in T-lymphocytes to the bone marrow dose in the long-term period after internal ^{89,90}Sr exposure. *Radiation Hygiene*. 2024;17(2):53–63. (In Russ). https://doi.org/10.21514/1998-426X-2024-17-2-53-63
11. Tucker JD, Morgan WF, Awa AA, Bauchinger M, Blakey D, Cornforth MN, et al. PAINT: a proposed nomenclature for structural aberrations detected by whole chromosome painting. *Mutat Res*. 1995 Jun;347(1):21–4. https://doi.org/10.1016/0165-7992(95)90028-4
12. Savage JR, Tucker JD. Nomenclature systems for FISH-painted chromosome aberrations. *Mutat Res*. 1996 Nov;366(2):153–61. https://doi.org/10.1016/s0165-1110(96)90036-6
13. Stevens-Kroef M, Simons A, Rack K, Hastings RJ. Cytogenetic Nomenclature and Reporting. *Methods Mol Biol*. 2017;1541:303–9. https://doi.org/10.1007/978-1-4939-6703-2_24
14. Nugis VYu. FISH-method: technique of cytogenetic retrospective dose evaluation (review). *Saratov Journal of Medical Scientific Research*.2016;12(4):671–8 (In Russ). EDN: YPYFKV
15. Fomina J, Darroudi F, Natarajan AT. Accurate detection of true incomplete exchanges in human lymphocytes exposed to neutron radiation using chromosome painting in combination with a telomeric PNA probe. *Int J Radiat Biol*. 2001;77(12):1175–83. https://doi.org/10.1080/09553000110083951
16. Vozilova AV, Krivoshchapova YV. Investigation of the Frequency of Inversions and Complex Translocations in T-Lymphocytes in Exposed Residents of the Southern Urals. *Biology Bulletin*. 2023;(50):2979–85. https://doi.org/10.1134/s1062359023110237
17. Pouzoulet F, Roch-Lefèvre S, Giraudet AL, Vaurijoux A, Voisin P, Buard V et al. Monitoring translocations by M-FISH and three-color FISH painting techniques: a study of two radiotherapy patients. *J Radiat Res*. 2007;48(5):425–34. https://doi.org/10.1269/jrr.07013
18. Sotnik NV, Azizova TV, Zhuntova GV. Bioindication of internal radiation exposure following accidental radionuclide intake. Extreme Medicine. 2019;21(4):540–7 (In Russ.). EDN: YZWAFI
19. Hada M, Wu H, Cucinotta FA. mBAND analysis for high- and low-LET radiation-induced chromosome aberrations: a review. *Mutat Res*. 2011;711(1–2):187–92. https://doi.org/10.1016/j.mrfmmm.2010.12.018
20. Nugis VY, Snigiryova GP, Lomonosova EE, Kozlova MG, Nikitina VA. Three-Color FISH Method: Dose-Effect Curves for Translocations in Peripheral Blood Lymphocyte Cultures after Gamma-Irradiation In Vitro. *Medical Radiology and radiation safety*. 2021; 5: 12–20. https://doi.org/10.12737/1024-6177-2020-65-5-12-20
21. Lea DE, Catcheside DG. The mechanism of the induction by radiation of chromosome aberrations in Tradescantia. *Journal of Genetics*. 1942; 44(2):216–45. https://doi.org/10.1007/BF02982830
22. Bauchinger M, Schmid E, Dresp J. Calculation of the dose-rate dependence of the decentric yield after Co gamma-irradiation of human lymphocytes. *Int J Radiat Biol Relat Stud Phys Chem Med*. 1979;35(3):229–33. https://doi.org/10.1080/09553007914550261
23. Bauchinger M, Schmid E, Zitzelsberger H, Braselmann H, Nahrstedt U. Radiation-induced chromosome aberrations analysed by two-colour fluorescence in situ hybridization with composite whole chromosome-specific DNA probes and a pancentromeric DNA probe. *Int J Radiat Biol*. 1993;64(2):179–84. https://doi.org/10.1080/09553009314551271
24. Fernández JL, Campos A, Goyanes V, Losada C, Veiras C, Edwards AA. X-ray biological dosimetry performed by selective painting of human chromosomes 1 and 2. *Int J Radiat Biol*. 1995;67(3):295–302. https://doi.org/10.1080/09553009514550351
25. Sasaki MS. Advances in the biophysical and molecular bases of radiation cytogenetics. *Int J Radiat Biol*. 2009;85(1):26–47. https://doi.org/10.1080/09553000802641185
26. Edwards AA, Lindholm C, Darroudi F, Stephan G, Romm H, Barquinero J, et al. Review of translocations detected by FISH for retrospective biological dosimetry applications. *Radiat Prot Dosimetry*. 2005;113(4):396–402. https://doi.org/10.1093/rpd/nch452
27. Lindholm C, Luomahaara S, Koivistoinen A, Ilus T, Edwards AA, Salomaa S. Comparison of dose-response curves for chromosomal aberrations established by chromosome painting and conventional analysis. *Int J Radiat Biol*. 1998;74(1):27–34. https://doi.org/10.1080/095530098141690
28. Barquinero JF, Beinke C, Borràs M, Buraczewska I, Darroudi F, Gregoire E, et al. RENEB biodosimetry intercomparison analyzing translocations by FISH. *Int J Radiat Biol*. 2017;93(1):30–5. https://doi.org/10.1080/09553002.2016.1222092
29. Rodríguez P, Montoro A, Barquinero JF, Caballín MR, Villaescusa I, Barrios L. Analysis of translocations in stable cells and their implications in retrospective biological dosimetry. *Radiat Res*. 2004;162(1):31–8. https://doi.org/10.1667/rr3198
30. Jeong SK, Oh SJ, Kang YR, Kim H, Kye YU, Lee SH, et al. Biological dosimetry dose-response curves for residents living near nuclear power plants in South Korea. *Sci Prog*. 2023;106(3):368504231198935. https://doi.org/10.1177/00368504231198935
31. Sposto R, Stram DO, Awa AA. An estimate of the magnitude of random errors in the DS86 dosimetry from data on chromosome aberrations and severe epilation. *Radiat Res*. 1991;128(2): 157–69. PMID: 1947012
32. Stram DO, Sposto R, Preston D, Abrahamson S, Honda T, Awa AA. Stable chromosome aberrations among A-bomb survivors: an update. *Radiat Res*. 1993;136(1):29–36. PMID: 8210335
33. Awa A. Analysis of chromosome aberrations in atomic bomb survivors for dose assessment: studies at the Radiation Effects Research Foundation from 1968 to 1993. *Stem Cells*. 1997;15 Suppl 2:163–73. https://doi.org/10.1002/stem.5530150724
34. Sasaki MS, Endo S, Ejima Y, et al. Effective dose of A-bomb radiation in Hiroshima and Nagasaki as assessed by chromosomal effectiveness of spectrum energy photons and neutrons. *Radiat Environ Biophys*. 2006;45(2):79–91. https://doi.org/10.1007/s00411-006-0051-6
35. Sasaki MS, Endo S, Ejima Y, Saito I, Okamura K, Oka Y, et al. The Association of Radiation Exposure with Stable Chromosome Aberrations in Atomic Bomb Survivors Based on DS02R1 Dosimetry and FISH Methods. *Radiat Res*. 2023;199(2):170–81. https://doi.org/10.1667/RADE-22-00154.1
36. Tawn EJ, Curwen GB, Jonas P, Gillies M, Hodgson L, Cadwell KK. Chromosome Aberrations Determined by FISH in Radiation Workers from the Sellafield Nuclear Facility. *Radiat Res*. 2015;184(3):296–303. https://doi.org/10.1667/RR14125.1
37. Tolstykh EI, Vozilova AV, Degteva MO, et al. Dependence of the Translocation Frequency in Blood Lymphocytes on the Dose and Age at the Onset of Exposure in Residents of the Techa Riverside Settlements. *Radiacionnaya biologiya. Radioekologiya*. 2023;63(2):3184–95. https://doi.org/10.31857/S086980312302011X
38. Vrisekoop N, den Braber I, de Boer AB, Ruiter AF, Ackermans MT, van der Crabben SN, et al. Sparse production but preferential incorporation of recently produced naive T cells in the human peripheral pool. *Proc Natl Acad Sci USA*. 2008;105(16):6115–20. https://doi.org/10.1073/pnas.0709713105
39. De Boer RJ, Perelson AS. Quantifcation T lymphocyte turnover. *J Theor Biol*. 2013;(327):45–87. https://doi.org/10.1016/j.jtbi.2012.12.025
40. De Boer RJ, Tesselaar K, Borghans JAM. Better safe than sorry: Naive T-cell dynamics in healthy ageing. *Semin Immunol*. 2023;(70):101839. https://doi.org/10.1016/j.smim.2023.101839

41. Yan J, Greer JM, Hull R, O'Sullivan JD, Henderson RD, Read SJ, et al. The effect of ageing on human lymphocyte subsets: comparison of males and females. *Immun Ageing*. 2010;(7):4. https://doi.org/10.1186/1742-4933-7-4
42. Den Braber I, Mugwagwa T, Vrisekoop N, Westera L, Mögling R, de Boer AB, et al. Maintenance of peripheral naive T cells is sustained by thymus output in mice but not humans. *Immunity*. 2012;36(2):288–97. https://doi.org/10.1016/j.immuni.2012.02.006
43. Steinmann GG, Klaus B, Muller-Hermelink HK. The involution of the ageing human thymic epithelium is independent of puberty. A morphometric study. *Scand J Immunol*. 1985;(22):563–75. https://doi.org/10.1111/j.1365–3083.1985.tb01916.x
44. Tolstykh EI, Vozilova AV, Degteva MO, et al. Concept of T-cell genus as the basis for the analysis of FISH results after local bone marrow exposure. *Biology Bulletin*. 2020;47(11):1495–506. https://doi.org/10.1134/S1062359020110151
45. Degteva MO, Tolstykh EI, Shishkina EA, Sharagin PA, Zalyapin VI, Volchkova AY, et al. Stochastic parametric skeletal dosimetry model for humans: General approach and application to active marrow exposure from bone-seeking beta-particle emitters. *PLoS One*. 2021;16(10):e0257605. https://doi.org/10.1371/journal.pone.0257605
46. Shagina NB, Tolstykh EI, Degteva MO, Anspaugh LR, Napier BA. Age and sex specific biokinetic model for strontium in humans. *J Radiol Prot*. 2015;35(1):87–127. https://doi.org/10.1088/0952-4746/35/1/87
47. Tolstykh EI, Degteva MO. Estimation of radiation doses on lymphocytes and their progenitors after ingestion of strontium-89,90. Radiatsionnaya Gygiena = Radiation Hygiene. 2022;15(3):82–91 (In Russ.). https://doi.org/10.21514/1998-426X-2022-15-3-82-91
48. Merkle W. Statistical methods in regression and calibration analysis of chromosome aberration data. *Radiat Environ Biophys*. 1983;21(3):217–33.
49. Austin PC, Hux JE. A brief note on overlapping confidence intervals. *J Vasc Surg*. 2002;36(1):194–5. https://doi.org/10.1067/mva.2002.125015
50. Hernández A, Endesfelder D, Einbeck J, Puig P, Benadjaoud MA, Higueras M, et al. Biodose Tools: An R Shiny Application for Biological Dosimetry. 2023;99(9):1378–90. https://doi.org/10.1080/09553002.2023.2176564
51. Higueras M, Puig P, Ainsbury EA, Vinnikov VA, Rothkamm K. A new Bayesian model applied to cytogenetic partial body irradiation estimation. *Radiat Prot Dosimetry*. 2016;168(3):330–6. https://doi.org/10.1093/rpd/ncv356
52. Ainsbury EA, Lloyd DC: Dose estimation software for radiation biodosimetry. *Health Phys*. 2010;98(2):290–5. https://doi.org/10.1097/01.HP.0000346305.84577.b4
53. Deperas J, Szluinska M, Deperas-Kaminska M, Edwards A, Lloyd D, Lindholm C, et al. CABAS: a freely available PC program for fitting calibration curves in chromosome aberration dosimetry. *Radiat Prot Dosimetry*. 2007;124(2):115–23. https://doi.org/10.1093/rpd/ncm137
54. Gnanasekaran TS. Cytogenetic biological dosimetry assays: recent developments and updates. *Radiat Oncol J*. 2021;39(3):159–66. https://doi.org/10.3857/roj.2021.00339
55. Beinke C, Siebenwirth C, Abend M, Port M. Contribution of Biological and EPR Dosimetry to the Medical Management Support of Acute Radiation Health Effects. *Appl Magn Reson*. 2022;(53):265–87. https://doi.org/10.1007/s00723-021-01457-5
56. M'Kacher R, Colicchio B, Junker S, El Maalouf E, Heidingsfelder L, Plesch A, et al. High Resolution and Automatable Cytogenetic Biodosimetry Using In Situ Telomere and Centromere Hybridization for the Accurate Detection of DNA Damage: An Overview. *Int J Mol Sci*. 2023;24(6):5699. https://doi.org/10.3390/ijms24065699
57. Herate C, Sabatier L. Retrospective biodosimetry techniques: Focus on cytogenetics assays for individuals exposed to ionizing radiation. *Mutat Res Rev Mutat Res*. 2020;(783):108287. https://doi.org/10.1016/j.mrrev.2019.108287
58. Degteva MO, Shagina NB, Shishkina EA, Vozilova AV, Volchkova AY, Vorobiova MI, et al. Analysis of EPR and FISH studies of radiation doses in persons who lived in the upper reaches of the Techa River. *Radiat Environ Biophys*. 2015;54(4):433–44. https://doi.org/10.1007/s00411-015-0611-8
59. Degteva MO, Shishkina EA, Tolstykh EI, et al. Application of the EPR and FISH Methods to Dose Reconstruction for People Exposed in the Techa River Area. *Radiats Biol Radioecol*. 2017;57(1):30–41. English, Russian. https://doi.org/10.7868/S0869803117010052

Authors' contributions. All the authors confirm that they meet the ICMJE criteria for authorship. The most significant contributions were as follows. E.I. Tolstykh — the main idea of the article, writing the text, table preparation; Yu.R. Akhmadullina — literature analysis, section on the analysis of chromosomal translocations, text editing; P.A. Sharagin — literature analysis, section on uncertainties of dose estimates; E.A. Shishkina — section on uncertainties of dose estimates; A.V. Akleev — discussion of results, editing of the text.

AUTHORS

Evgenia I. Tolstykh, Dr. Sci. (Biol.),
https://orcid.org/0000-0002-4958-3214
evgenia.tolstykh@yandex.ru

Yulia. R. Akhmadullina, Cand. Sci. (Biol.)
https://orcid.org/0000-0003-4394-2228
akhmadullina@urcrm.ru

Pavel A. Sharagin
https://orcid.org/0000-0002-1457-4916
sharagin@urcrm.ru

Elena A. Shishkina, Dr. Sci. (Biol.)
https://orcid.org/0000-0003-4464-0889
lena@urcrm.ru

Aleksander V. Akleyev, Dr. Sci. (Med.), prof.
https://orcid.org/0000-0003-2583-5808
akleyev@urcrm.ru

https://doi.org/10.47183/mes.2024-26-3-15-21

SPI1 AND *GATA3* GENE EXPRESSION AND COMPOSITION OF T-HELPER CELL SUBPOPULATIONS IN CHRONICALLY EXPOSED PEOPLE

Vladislav S. Nikiforov[1,2]✉, Alisa I. Kotikova[1,2], Alexander V. Akleyev[1,2]

[1] Ural Scientific and Practical Center for Radiation Medicine of the Federal Medical and Biological Agency of Russia, Chelyabinsk, Russia

[2] Chelyabinsk State University, Chelyabinsk, Russia

Introduction. The influence of adverse factors including ionizing radiation leads to a violation of key transcription factors expression and the ratio of the main types of T-helper cells, which in turn initiates a wide range of immunopathological disorders.

Objective. The objective of this research was to study the mRNA expression of the *SPI1* and *GATA3* genes, as well as the composition of T-helper type 1 and 2 subpopulations, in chronically exposed people during the period of radiation exposure late effects development.

Materials and methods. The study was carried out on peripheral blood mononuclear cells obtained from 98 residents of the Techa riverside settlements. Two study groups were formed: the group of exposed individuals (average accumulated dose for the red bone marrow radiation was 706.8 ± 62.7 mGy) and the comparison group (radiation dose did not exceed 70 mGy). The median age of the studied individuals at examination was 71.1 ± 0.9 years (58–87 years). The relative mRNA content of the studied genes was assessed using real-time PCR. The number of T-helpers of types 1 and 2 in the populations of T-helpers of central and effector memory was calculated using the flow cytometry method.

Results. There was a decrease in the absolute and relative number of type 2 T-helpers included in the T-helpers of central memory in chronically exposed individuals. In people with accumulated doses ≥1000 mGy, an increase in the Th1/Th2 ratio of T-helpers of the central memory (p = 0.01), as well as the positive correlation relationship between the relative content of type 2 T-helpers of the effector memory and the expression of the *GATA3* gene were registered relative to unexposed individuals.

Conclusions. The obtained results indicate that changes in the composition of T-helper cell subpopulations in chronically exposed individuals are not pronounced in the long-term period. However, these changes may directly depend on the total absorbed dose, which in turn determines the prospects for further analysis of the health status of people exposed to chronic high-dose radiation.

Keywords: gene expression; chronic radiation exposure; T-helpers 1 type; T-helpers 2 type; Techa River; low doses

For citation: Nikiforov V.S., Kotikova A.I., Akleyev A.V. Expression of genes *SPI1* and *GATA3* and T-helpers subpopulation combination in chronically exposed people. *Extreme Medicine.* 2024;26(3):15–21. https://doi.org/10.47183/mes.2024-26-3-15-21

Funding: the study was carried out within the framework of the state assignment of the Federal Medical and Biological Agency of Russia "Investigation of the influence of chronic radiation exposure on the state of the T-cell link of the human immune system" No. 388-03-2023-112 from 01/19/2023.

Compliance with ethics principles: the study was approved by ethics committee of Ural Scientific and Practical Center for Radiation Medicine of FMBA of Russia (protocol No. 8 from 12/19/2022). All patients enrolled in the study had previously signed voluntary informed consent as a part of the 2013 Declaration of Helsinki.

Potential conflict of interest: Alexander V. Akleyev has been a member of the Advisory Board of "Extreme Medicine" since 1999. The other authors declare no conflict of interest.

✉ Vladislav S. Nikiforov nikiforovx@mail.ru

Received: 2 Aug. 2024 **Revised:** 27 Sep. 2024 **Accepted:** 4 Oct. 2024

ЭКСПРЕССИЯ ГЕНОВ *SPI1* И *GATA3* И СУБПОПУЛЯЦИОННЫЙ СОСТАВ Т-ХЕЛПЕРОВ У ХРОНИЧЕСКИ ОБЛУЧЕННЫХ ЛЮДЕЙ

В.С. Никифоров[1,2]✉, А.И. Котикова[1,2], А.В. Аклеев[1,2]

[1] Уральский научно-практический центр радиационной медицины Федерального медико-биологического агентства, Челябинск, Россия

[2] Челябинский государственный университет, Челябинск, Россия

Введение. Влияние неблагоприятных факторов, в том числе ионизирующего излучения, приводит к нарушению экспрессии ключевых транскрипционных факторов и соотношения основных типов Т-хелперных клеток, что, в свою очередь, инициирует широкий спектр иммунопатологических расстройств.

Цель. Изучение экспрессии мРНК генов *SPI1* и *GATA3*, а также субпопуляционного состава Т-хелперов 1-го и 2-го типов у хронически облученных людей в период реализации отдаленных последствий радиационного воздействия.

Материалы и методы. Объектом изучения служили мононуклеарные клетки периферической крови, полученные от 98 жителей прибрежных сел реки Течи, среди которых были выделены группа облученных лиц (средняя накопленная доза облучения красного костного мозга составила 706,8 ± 62,7 мГр) и группа сравнения (доза облучения не превышала 70 мГр). Средний возраст людей на время проведения обследования составлял 71,1 ± 0,9 года (58–87 лет). Оценка относительного содержания мРНК исследуемых генов осуществлялась с использованием метода ПЦР-РВ. Исследование количества Т-хелперов 1-го и 2-го типов проводилось методом проточной цитометрии в составе популяций Т-хелперов центральной и эффекторной памяти.

Результаты. Отмечено снижение абсолютного и относительного количества Т-хелперов 2-го типа, входящих в состав Т-хелперов центральной памяти у хронически облученных лиц. У людей с накопленными дозами более 1000 мГр зафиксированы увеличение соотношения Th1/Th2 в популяции Т-хелперов центральной памяти по отношению к необлученным лицам (p = 0,01), а также положительная корреляционная связь между относительным содержанием Т-хелперов 2-го типа эффекторной памяти и экспрессией гена *GATA3*.

Выводы. Результаты исследования показывают, что изменения в субпопуляционном составе Т-хелперных клеток в отдаленные сроки у хронически облученных людей носят невыраженный характер. Однако эти изменения могут напрямую зависеть от суммарной поглощенной дозы облучения, что определяет перспективы для дальнейшего анализа состояния здоровья людей, подвергшихся хроническому облучению в высоких дозах.

Ключевые слова: экспрессия генов; хроническое облучение; Т-хелперы 1-го типа; Т-хелперы 2-го типа; река Теча; малые дозы

Для цитирования: Никифоров В.С., Котикова А.И., Аклеев А. А. Экспрессия генов *SPI1* и *GATA3* и субпопуляционный состав Т-хелперов у хронически облученных людей. *Медицина экстремальных ситуаций.* 2024;26(3):15–21. https://doi.org/10.47183/mes.2024-26-3-15-21

Финансирование: работа выполнена в рамках государственного задания ФМБА России по теме «Исследование влияния хронического радиационного воздействия на состояние Т-клеточного звена иммунной системы человека» № 388-03-2023-112 от 19.01.2023 г.

Соответствие принципам этики: исследование одобрено этическим комитетом ФГБУН УНПЦ РМ ФМБА России (протокол № 8 от 19.12.2022). Все пациенты, участвовавшие в исследовании, подписали добровольное информированное согласие на исследование в рамках Хельсинкской декларации 2013 г.

Потенциальный конфликт интересов: Аклеев А.В. — член редакционного совета журнала «Медицина экстремальных ситуаций». Остальные авторы заявляют об отсутствии конфликта интересов.

✉ Никифоров Владислав Сергеевич nikiforovx@mail.ru

Статья поступила: 02.08.2024 **После доработки:** 27.09.2024 **Принята к публикации:** 04.10.2024

INTRODUCTION

The human immune system is marked by extremely high radiosensitivity and post-radiation changes in the immune system of exposed individuals can remain for a long time [1, 2]. This is most remarkably manifested in persons who have been internally irradiated as a result of deposition of osteotropic radionuclides, in particular Strontium-90 (^{90}Sr), in the body. By accumulating in bone tissue, ^{90}Sr has a prolonged irradiation effect on the red bone marrow (RBM), which is responsible for the formation and development of blood cells, including immunocompetent cells.

Long-term changes in the immune systems of chronically exposed residents of the villages along the banks of the Techa River included a decrease in the expression of differentiation antigens of T-lymphocytes, suppression of T-cells functional activity, a decrease in serum IL-4 level, and an increase in TNFα (tumor necrosis factor-alpha) and IFNɣ (interferon-ɣ). Together, these changes characterize the immune response associated with marked inflammatory reactions [3].

One of the mechanisms involved in the process of immunosuppression found in irradiated individuals is a shift in the balance between cell-mediated immunity (Th1-response) and humoral immunity (Th2-response) [4]. Type 1 (Th1) T-helper cells are responsible for eliminating intracellular pathogens and are associated with organ-specific autoimmune diseases, while type 2 (Th2) T-helper cells initiate immune response to extracellular parasites such as helminths, as well as playing a key role in the development of asthma and other allergic diseases [5]. The balance between T-helper 1 and T-helper 2 plays a key role in the immune response. Normally, cytokines produced by Th2 cells suppress the production of Th1 cytokines and the activity of natural killer cells. In turn, Th1 cells can inhibit the differentiation and proliferation of basophils and eosinophils, whose functions are regulated by Th2 cytokines [6]. However, exposure to high doses of ionizing radiation triggers more pronounced immunosuppressive reactions from the production of Th2-mediated cytokines, while the effect of low doses of radiation on the balance of T-helper cells remains controversial [7, 8].

The mechanisms controlling a wide range of T-helper phenotypes, especially under the influence of unfavorable factors, remain poorly understood. Nevertheless, several key genes that play an important role in the regulation of Th1 and Th2 differentiation are currently known [9].

The transcription factor PU.1, encoded by the proto-oncogene SPI1, and the GATA-3 protein, which is encoded by the GATA-3 gene of the same name, are involved in a variety of processes of hematopoiesis and immune system functioning. In immunocompetent cells of the system, these factors are able to trigger the activation of a number of factors such as chemokines, cytokines and cytokine receptors that regulate the processes of differentiation and functioning of T-helper cells. The interaction between PU.1 and GATA-3 controls immune development and homeostasis by regulating the expression of genes specific for Th1 and Th2 subpopulations [10].

Taking into account the above mentioned, the aim of the present work was to study mRNA expression of SPI1 and GATA3 genes, as well as subpopulation composition of T-helpers of types 1 and 2 in chronically irradiated people during the realization of remote consequences of radiation exposure.

MATERIALS AND METHODS

The study was conducted more than 65 years after the beginning of chronic exposure. The object of the study was peripheral blood mononuclear cells obtained from 98 human residents of the villages along the banks of the Techa River. The irradiation of these people was characterized by its low intensity, the value of absorbed doses mainly falling in the range of small- and medium, low intensity and long-term irradiation of red bone marrow (RBM) with pronounced compensatory mechanisms in the hematopoiesis system. Internal irradiation was due to accumulation of radionuclides in the body through consumption of river water and local products. External gamma radiation was caused by contamination of bottom sediments and floodplain soils with radionuclides [11].

The study participants underwent medical examination in the clinical department of Ural Scientific and Practical Center for Radiation Medicine of the Federal Medical and Biological Agency of Russia. Biological material was obtained with the patients' consent (basis — voluntary informed consent in accordance with the Declaration of Helsinki).

Patients who were in a period of acute or exacerbation of chronic inflammatory diseases, who had oncological

and autoimmune diseases, who were taking antibiotics, hormonal and cytostatic drugs during the examination, or who had contact with genotoxic agents in the course of their professional activity, were excluded from the study.

The main dosimetric values determining the measures of ionizing radiation (IR) impact on the organism of the examined persons were personalized radiation doses to the RBM, thymus and peripheral lymphoid organs, as calculated by the specialists of the biophysical laboratory of the Federal state budgetary institute of Ural Scientific and Practical Center for Radiation Medicine of FMBA of Russia using the TRDS-2016 dosimetric system [12].

According to the value of the accumulated radiation dose to the RBM, the patients were divided conditionally into two groups: the comparison group of 45 people, whose dose accumulation occurred during life mainly due to natural radioactive background and medical diagnostic procedures (accumulated doses did not exceed 55 mGy), and the group of 53 chronically irradiated persons, whose average dose to the red bone marrow amounted to 782.0 ± 82.3 mGy.

Patients chronically irradiated were divided into three subgroups depending on the magnitude of the accumulated radiation dose to the RBM.

- Subgroup 1. Irradiated individuals with accumulated doses to the RBM not exceeding 500 mGy (n = 20);
- Subgroup 2. Irradiated persons with accumulated doses to RBM from 500 to 1000 mGy (n = 20);
- Subgroup 3. Irradiated persons with accumulated doses at the RBM of more than 1000 mGy (n = 13).

The ages of the people from all subgroups did not differ statistically significantly. Table 1 presents the characteristics of the studied groups, including the average age of the subjects and the average radiation doses calculated on the RBM, thymus, and peripheral lymphoid organs. The subjects were of Slavic and Turkic origin (Tatars and the Bashkirs).

Blood was collected from the cubital vein in a volume of 3 mL into sterile vacuum tubes Tempus Blood RNA Collection Tubes (Thermo Scientific™, USA) to assess the relative mRNA content of methyltransferases. RNA was isolated by column method using a commercial GeneJET Stabilized and Fresh Whole Blood RNA Kit (Thermo Scientific™, USA). Quantitative and qualitative characteristics of isolated total RNA samples were evaluated using a NanoDrop 2000C spectrophotometer (Thermo Scientific™, USA). The purity of the preparation was assessed by absorbance values at 260 nm and 280 nm wavelengths (A260/280). Reverse transcription reactions were performed as a separate step using a commercial reagent kit MMLV RT kit (Eurogen, Russia). The relative quantitative content of mRNA was determined by real-time PCR using CFX96 Touch amplifier (Bio-Rad Laboratories, USA). Oligonucleotide sequences of primers and probes were developed by the commercial company "DNK-SYNTEZ" LLC. Relative gene production was calculated using the $2^{-\Delta\Delta Ct}$ method, which is based on the calculation of quantitative assessment of expression of genes of interest relative to the "housekeeping gene" based on real-time PCR- analysis [13]. The "housekeeping gene" ACTB (Actin Beta) was used as an endogenous control and data normalization. Calculation was performed using the software of the Real-Time CFX96 Touch instrument ("BioRad", USA).

A detailed description of the methodology for the study of peripheral blood T-helper subpopulations by flow cytofluorimetry described by Kotikova AI. et al. [14]. The following cell populations were selected for this study: Type 1 T-helpers in the central memory T-helper population (CD3+CD4+CD45RA-CD62L+CXCR5-CXCR3+CCR6-CCR4- phenotype), Type 1 T-helpers in the effector memory T-helper population (CD3+CD4+CD45RA-CD62L-CXCR5-CXCR3+CCR6-CCR4- phenotype), Type 2 T-helpers in the central memory T-helper population (CD3+CD4+CD45RA-CD62L+CXCR5-CXCR3-CCR6-CCR4+ phenotype) and type 2 T-helpers in the effector memory T-helper population (CD3+CD4+CD45RA-CD62L-CXCR5-CXCR3-CCR6-CCR4+ phenotype).

Statistical processing of the results was carried out using SPSS Statistics 17.0 and Graph Pad Prism 8.4.3. The normality of the distribution of quantitative indicators was checked using the Kolmogorov-Smirnov test of agreement. The median (Me) and 25–75th percentiles (Q1–Q3) were used to describe the obtained indicators whose distribution differed from normal. Comparison of data samples was performed using the Mann-Whitney U-criterion due to the distribution of most values not following the law of normal distribution. The Kraskell-Wallis test was used for multivariate comparison. For all criteria and tests, differences were considered statistically significant at $p<0.05$.

STUDY RESULTS

In the course of the study, statistically significant differences were obtained in the content of type 2 T-helper cells,

Table 1. Characteristics of the examined persons

Parameter	Comparison Group	Dose subgroups of exposed persons, RBM dose, mGy			All exposed persons
		Subgroup 1	Subgroup 2	Subgroup 3	
Number of patients, n	45	20	20	13	53
Age of patients, years,	68.2 ± 1.0	70.5 ± 1.1	72.5 ± 0.8	72.5 ± 0.6	71.7 ± 1.0
Absorbed dose to RBM, mGy	17.3 ± 2.3 (0–55.0)	286.5 ± 27.8 (73.4–485.1)	695.1 ± 34.8 (509.6–968.6)	1371.5 ± 71.8 (1032.0–1867.6)	706.8 ± 62.7 (73.4–1867.6)
Absorbed dose to thymus and peripheral lymphoid organs, mGy	7.17 ± 1.30 (0–39.52)	46.4 ± 7.4 (4.6–160.9)	86.2 ± 16.4 (25.5–354.6)	165.5 ± 17.7 (103.6–357.9)	90.6 ± 10.2 (4.6–357.9)

Table prepared by the authors using their own data

Note: RBM — red bone marrow, N — number of subjects studied; the data are presented as an average value and the standard error of the average (M ± SE) (max-min).

which are part of central memory T-helper cells in the peripheral blood of exposed subjects and subjects from the comparison group. The corresponding data are presented in Figures 1A and 1B.

Thus, a statistically significant decrease in the absolute number of type 2 T-helper cells was observed in subjects from subgroups with different dose of RBM irradiation compared to the results of subjects from the comparison group, namely: 6.00×10^9/L (p=0.03) in the total group of exposed subjects, 3.63×10^9/L (p=0.03) in subjects from the first subgroup, and 5.88×10^9/L (p=0.02) in subjects from the second subgroup versus 13.14×10^9/L in subjects from the comparison group. A statistically significant decrease in the relative number of type 2 T-helper cells was also found in the exposed subjects from the subgroups with different dose of BCC irradiation compared to the same index in the subjects from the comparison group (Fig. 1B).

At the same time, a statistically significant increase in the Th1/Th2 ratio in the population of central memory T-helper cells was found in the third subgroup — 14.26%, in irradiated subjects from the general group — 12.54% relative to the index in subjects from the comparison group — 7.25% (Fig. 2). At the same time, in the first and second subgroups of the exposed persons, this index was increased relative to the subjects from the comparison group only at the trend level (p=0.06 and p=0.07, respectively). No statistically significant intergroup differences were found for other studied indicators of the T-helper cells.

Correlation analysis was performed to assess the degree of association between the concentration of T-helper cells, exposure to radiation factors (accumulated radiation doses to RBM, thymus and peripheral lymphoid organs), and the age of patients at the time of examination.

The analysis revealed no statistically significant correlation between the absolute and relative number of type 2 T-helpers in the population of central memory T-helpers and the Th1/Th2 ratio in the population of central memory T-helpers with the RBM cumulative exposure, thymus and peripheral lymphoid organs in the combined study group. There were also no statistically significant correlations between the selected indices of T-helper cells and the ages of the studied individuals whether in the comparison group or in the group of irradiated individuals.

The results of the study of relative expression of SPI1 and GATA-3 genes in the examined patients are presented in Table 2. The data presented in Table 2 indicate that there were no statistically significant differences in the relative mRNA content of SPI1 and GATA3 genes in the individuals from the main group and the comparison group even as

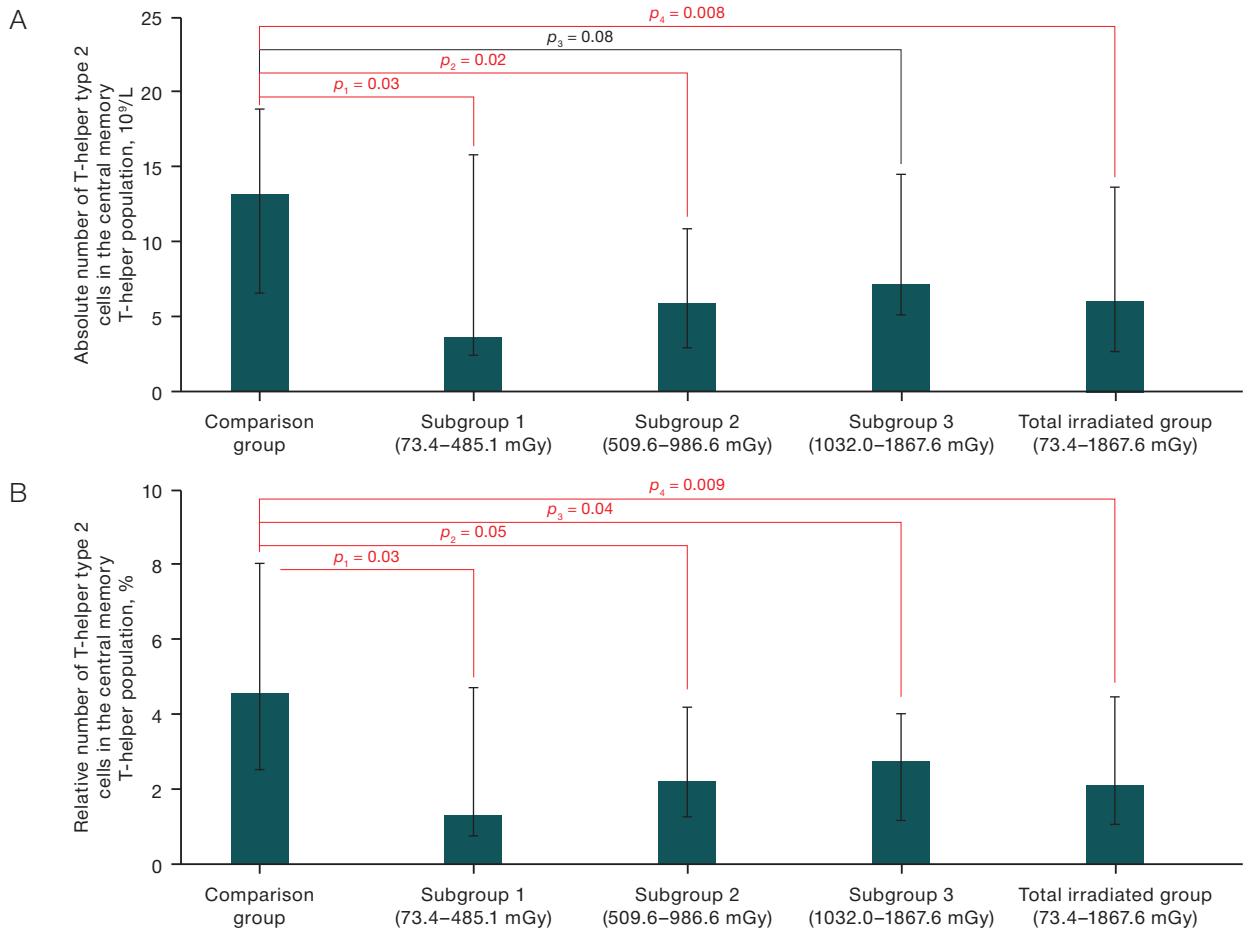

Figures prepared by the author using his own data

Fig. 1. Absolute (A) and relative (B) content of T-helper type 2 cells in the central memory T-helper population in peripheral blood, Me (Q1–Q3)
Note: *p* — indicates the confidence level of differences relative to the comparison group (Mann-Whitney *U* test).

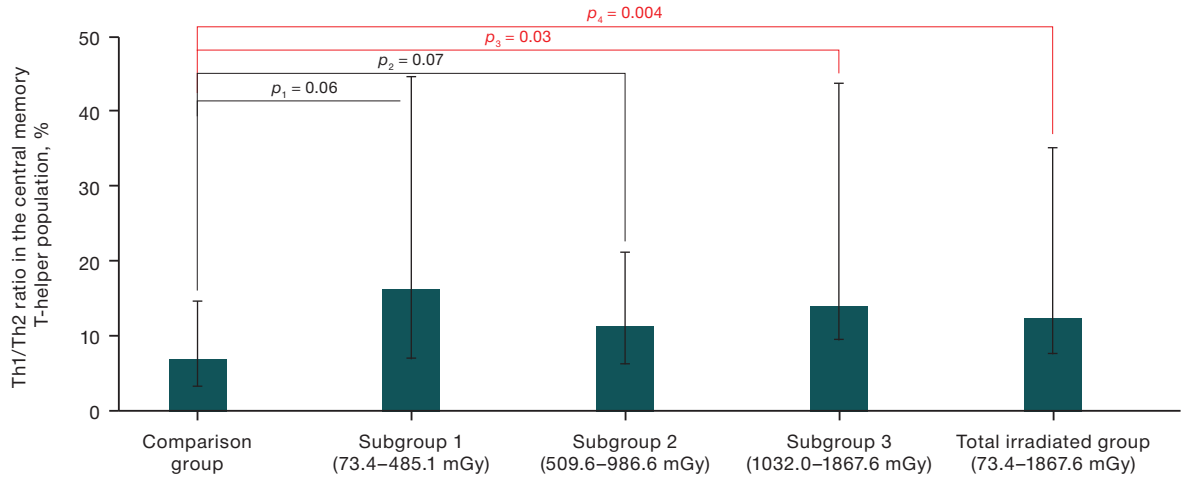

Figure prepared by the author using his own data

Fig. 2. Difference in the Th1/Th2 ratio in the central memory T-helper population between the comparison group and individuals exposed at a wide dose range, Me (Q1–Q3)
Note: *p* — indicates the confidence level of differences relative to the comparison group (Mann-Whitney *U* test)

the values of the accumulated dose of irradiation of RBM increased.

No statistically significant correlations were found between the relative mRNA content of SPI and GATA3 genes and the RBM radiation absorbed doses, thymus and peripheral lymphoid organs and factors of non-radiation nature (achieved age, sex and ethnicity).

In all chronically irradiated persons, no statistically significant correlations were found between the relative content of SPI1 gene mRNA and the absolute number and frequency of T-helper cells of type 1 and type 2 in the distant terms after the beginning of radiation exposure. At the same time, in the group of irradiated people whose accumulated radiation doses to RBM were in the range of high values (exceeding 1000 mGy), a positive correlation between GATA3 gene expression and the relative content of type 2 effector memory T-helper cells was found (Rs=0.70; p=0.02).

RESULTS AND DISCUSSION

According to earlier data, prolonged exposure to ionizing radiation, even in the range of low doses, can cause a decrease in cellular immunity against the background of changes in the composition of circulating cells of the immune system [15].

T-helper cells representing T-lymphocyte subpopulations play an important role in the regulation of immunity. By mediating the interaction between immunocompetent cells, they determine the type of immune response (cellular or humoral) [16]. In modern literature, there is increasing evidence in favor of radiation-induced changes in the composition and function of T-cell subpopulations, which determines the formation of a specific inflammatory profile of the immune system, disturbance of the balance between Th1 and Th2 subpopulations, and changes in the expression level of transcription factors [17].

The study revealed a statistically significant decrease in the number of type 2 T-helpers in the population of central memory T-helpers in irradiated people. The lowest cellularity indices were observed among individuals whose absorbed doses ranged from 73.4 to 485.1 mGy. In this regard, irradiated individuals showed an increase in the Th1/Th2 ratio in the central memory T-helper population relative to individuals in the comparison group. However, these changes were not related to age or RBM irradiation dose in the thymus and peripheral lymphoid organs. A similar suppression of the Th2 response in mice was demonstrated in an experiment under low-dose radiation exposure conditions [18]. Karimi G. et al., who monitored radiologists with radiation exposure levels of less than 50 mGy, additionally noted a shift in their immune response towards the production of type 1 T-helper cells [19]. Previously, we also described a decrease in the number of type 2 T-helper cells, which are part of central memory T-helper cells, in individuals exposed to chronic low-intensity radiation [20].

Within the framework of the present work, we found no changes in the mRNA expression of the genes of

Table 2. Relative mRNA content of the SPI1 and GATA 3 genes in the studied groups

Relative mRNA level of the gene	Comparison group *n* = 45)	Dose subgroups of exposed persons, RBM dose, mGy			
		Subgroup 1 *n* = 20	Subgroup 2 *n* = 20	Subgroup 3 *n* = 13	All exposed persons (*n* = 53)
SPI1, rel. un.	1.09 (0.30–2.69)	1.09 (0.33–3.11)	1.00 (0.24–2.71)	0.96 (0.28–2.66)	1.03 (0.29–2.71)
GATA3, rel. un.	1.10 (0.05–5.62)	0.84 (0.01–7.37)	1.10 (0.19–3.16)	0.83 (0.02–4.06)	0.85 (0.02–4.06)

Table prepared by the author using his own data

Note: The data are presented in Me (Q1–Q3) format

transcription factors SPI and GATA3 in the remote terms after exposure to IR in the residents of the villages along the banks of the Techa River exposed to chronic training. However, it is noteworthy that a statistically significant positive correlation between the relative mRNA content of the GATA3 gene and type 2 effector memory T-helper cells was characteristic of individuals whose absorbed doses of RBM exposure were in the range of high values (more than 1000 mGy). Indeed, GATA3 protein plays an important role in the development of the Th2 phenotype by activating the secretion of cytokines IL-4, IL-5 and IL-13 in Th2 cells, as well as inhibiting specific Th1 transcription factors such as T-bet, NF-AT1, FOXP3 and others [21].

The results obtained in the course of the study, which are consistent with modern scientific data, show that the changes in the immune system in people exposed to chronic low-intensity radiation exposure are not pronounced in the long term. However, further work is required to study the study of key transcription factors involved in the differentiation of immunocompetent cells and their continued functioning in people exposed to high doses.

CONCLUSION

The results of the study recorded a decrease in the absolute number of type 2 T-helper cells, which are part of the central memory T-helper cells, in remote periods of time in individuals exposed to chronic radiation exposure. In individuals with accumulated doses of more than 1000 mGy, an increase in the ratio of Th1/Th2 in the population of central memory T-helpers in relation to unirradiated individuals and a positive correlation between GATA3 gene expression and the relative number of type 2 effector memory T-helpers were observed.

The results obtained confirm the fact that radiation-induced immune changes may directly depend on the total absorbed radiation dose, which determines the prospects for further analysis of the health status of people exposed to chronic high-dose irradiation.

References

1. UNSCEAR Biological mechanisms relevant for the inference of cancer risks from low-dose and low-dose-rate radiation. United Nations Scientific Committee on the Effects of Atomic Radiation. United Nations. New York. 2021.
2. Stewart FA, Akleyev AV, Hauer-Jensen M. Proceedings of the ICRP. Publication 118. ICRP report on tissue reactions, early and late effects in normal tissues and organs — threshold doses for *tissue reactions in the context of radiation protection*. Chelyabinsk: Kniga;2012 (In Russ.).
3. Akleyev AA. Immune Status of a Man Long after Chronic Radiation Exposure. *Medical Radiology and Radiation Safety*. 2020;65(4):29–35 (In Russ.). https://doi.org/10.12737/1024-6177-2020-65-4-29-35
4. Chalmin F, Humblin E, Ghiringhelli F, Vegran F. Transcriptional programs underlying Cd4 T cell differentiation and functions. *International Review of Cell and Molecular Biology*. 2018;(341):1–61. https://doi.org/10.1016/bs.ircmb.2018.07.002
5. Luckheeram RV, Zhou R, Verma AD, Xia B. CD4+ T cells: differentiation and functions. *Clin Dev Immunol*. 2012;(2012):925135. https://doi.org/10.1155/2012/925135
6. Mazzarella G, Bianco A, Catena E, De Palma R, Abbate GF. Th1/Th2 lymphocyte polarization in asthma. *Allergy*. 2000;55(61):6–9. https://doi.org/10.1034/j.13989995.2000.00511.x
7. Han SK, Song JY, Yun YS and Yi SY. Effect of gamma radiation on cytokine expression and cytokine-receptor mediated STAT activation. *International Journal of Radiation Biology*. 2006;(82):686–97. https://doi.org/10.1080/09553000600930699
8. Gao H, Dong Z, Gong X, Dong J, Zhang Y, Wei W. et al. Effects of various radiation doses on induced T-helper cell differentiation and related cytokine secretion. *Journal of Radiation Research*. 2018;(59):395–403. https://doi.org/10.1093/jrr/rry011
9. Nikiforov VS., Akleyev AV. mRNA Expression of GATA3, FOXP3, TBX21, STAT3, NFKB1, and MAPK8 Transcription Factors in Humans and Their Cooperative Interactions Long-Term after Exposure to Chronic Radiation. *Biology Bulletin*. 2022;49(6):588–95. https://doi.org/10.1134/S1062359022060103
10. Rothenberg EV, Hosokawa H, Ungerback J. Mechanisms of action of hematopoietic transcription factor PU.1 in initiation of T-cell development. *Frontiers in Immunology*. 2019;(10):228. https://doi.org/10.3389/fimmu.2019.00228
11. Akleev AV, ed. *Consequences of radioactive contamination of the Techa river*. Chelyabinsk: Kniga; 2016. EDN: VYWFDT
12. Degteva MO, Napier BA, Tolstykh EI, Shishkina EA, Bougrov NG, Krestinina LYu et al. Individual dose distribution in cohort of people exposed as a result of radioactive contamination of the Techa river. *Medical Radiology and Radiation Safety*. 2019;64(3):46–53 (In Russ.). https://doi.org/10.12737/article_5cf2364cb49523.98590475
13. Livak KJ, Schmittgen TD. Analysis of relative gene expression data using real-time quantitative PCR and the 2(-Delta Delta C(T)). *Methods*. 2001;25(4):402–8. https://doi.org/10.1006/meth.2001.1262
14. Kotikova AI., Blinova EA., Akleyev AV. Subpopulation Composition of T-Helpers in the Peripheral Blood of Persons Chronically Exposed to Radiation in the Long Term. *Extreme Medicine*. 2022; 24(2): 65–73 (In Russ.). https://doi.org/10.47183/mes.2022.018
15. Kodintseva EA, Akleyev AA. Delayed correlated parameters of adaptive and innate immunity in chronically irradiated subjects. *Russian journal of immunology*. 2020;23(2):225–30 (In Russ.). https://doi.org/10.46235/1028-7221-399-DCP
16. Alberts B, Johnson A, Lewis J et al. Molecular Biology of the Cell. 4th edition. New York: Garland Science; 2002. Helper T Cells and Lymphocyte Activation. Available from: https://www.ncbi.nlm.nih.gov/books/NBK26827.
17. McKelvey KJ, Hudson AL, Back M, Eade T, Diakos CI. Radiation, inflammation and the immune response in cancer. *Mammalian Genome*. 2018;29(11):843–65. https://doi.org/10.1007/s00335-018-9777-0
18. Gao H, Dong Z, Gong X, Dong J, Zhang Y, Wei W,et al. Effects of various radiation doses on induced T-helper cell differentiation and related cytokine secretion. *Journal of radiation research*. 2018;59(4):395–403. https://doi.org/10.1093/jrr/rry011
19. Karimi G, Balali-Mood M, Alamdaran SA, Badie-Bostan H, Mohammadi E, Ghorani-Azam A, Sadeghi M, & Riahi-Zanjani B. Increase in the Th1-Cell-Based Immune Response in Healthy Workers Exposed to Low-Dose Radiation — Immune System Status of Radiology Staff. *Journal of pharmacopuncture*. 2017;20(2):107–11. https://doi.org/10.3831/KPI.2017.20.014
20. Nikiforov VS, Kotikova AI, Blinova EA, Akleyev AV. Transcriptional Activity of Genes Regulating T-Helper Differentiation in the

Accidentally Exposed Population of the Southern Urals. *Dokl Biochem Biophys.* 2024.
https://doi.org/10.1134/S1607672924701114
21. Shih H-Y, Sciumè G, Poholek AC, Vahedi G, Hirahara K, Villarino AV et al. Transcriptional and epigenetic networks that drive helper T cell identities. *Immunological Reviews*. 2014;261(1):23–49.
https://doi.org/10.1111/imr.12208

Authors' contributions. All the authors confirm that they meet the ICMJE criteria for authorship. The most significant contributions were as follows. Vladislav S. Nikiforov — design, information collection, data processing, text writing; Alisa I. Kotikova — design, information collection, data processing, text writing; Alexander V. Akleyev — the concept and design of the study, general guidance, editing.

AUTHORS

Vladislav S. Nikiforov, Cand. Sci. (Biol.), Associate Professor
https://orcid.org/0000-0002-6685-1823
nikiforovx@mail.ru

Alisa I. Kotikova, Junior Researcher, Graduate Student
https://orcid.org/0000-0002-1695-1340
kotikova@urcrm.ru

Alexander V. Akleyev, Doc. Sci. (Med.), Professor
https://orcid.org/0000-0003-2583-5808
akleyev@urcrm.ru

https://doi.org/10.47183/mes.2024-26-3-22-29

SUBPOPULATIONS OF HUMAN PERIPHERAL BLOOD MONOCYTES AND NATURAL KILLER CELLS IN THE LONG-TERM PERIOD OF CHRONIC EXPOSURE

Polina O. Khomenko[1]✉, Ekaterina A. Kodintseva[1], Andrey A. Akleyev[2]

[1] Urals Research Center for Radiation Medicine of the Federal Medical and Biological Agency, Chelyabinsk, Russian Federation

[2] South Ural State Medical University, Chelyabinsk, Russian Federation

Introduction. An increased risk of malignancy and cardiovascular diseases is revealed in exposed individuals from different cohorts. Monocyte and natural killer (NK) cells modulate inflammation and carcinogenesis.

Objective. To evaluate absolute and relative cell counts in monocyte and natural killer cell subpopulations in the peripheral blood of individuals exposed to chronic irradiation.

Materials and methods. Thirty-five persons from the Techa River cohort were examined, divided into three subgroups depending on the radiation absorbed dose calculated to the red bone marrow (RBM) (70–249 mGy; 250–699 mGy; 700–1429 mGy, respectively). The mean age of patients was 74.9 years; the mean value of the radiation absorbed dose to RBM was 542.0±65.3 mGy, while that of the radiation absorbed dose to thymus and peripheral lymphoid organs was 99.7±14.4 mGy. The comparison group consisted of 10 persons without a history of anthropogenic irradiation of similar gender and ethnicity, mean age — 71.8 years.

Results. In the second dose subgroup, the proportion of $CD14^-CD16^+$ monocytes was statistically significantly higher (8.47%) than in the comparison group (5.52%, p=0.014), and the absolute $CD14^-CD16^+$ monocytes count (0.040×10^9/l) was also higher than in the third subgroup (0.018×10^9/l, p=0.044) without correlations with radiation and non-radiation factors. No statistically significant differences of other studied parameters between the groups were revealed.

Conclusion. In persons from the second subgroup the relative number of $CD14^-CD16^+$ monocytes was statistically significantly higher than in the comparison group; the absolute $CD14^-CD16^+$ monocytes count was also higher than in the third subgroup without correlations with factors of a radiation and non-radiation nature. The findings are preliminary.

Keywords: chronic radiation exposure; Techa River; subpopulations; peripheral blood monocytes; natural killer cells; long-term period; molecular markers

For citation: Khomenko P.O., Kodintseva E.A., Akleyev A.A. Subpopulations of monocytes and natural killer cells of human peripheral blood in the long-term period of chronic irradiation. *Extreme Medicine*. 2024;26(3):22–29. https://doi.org/10.47183/mes.2024-26-3-22-29

Finding: the research work was performed within the framework of the state assignment of the Federal Medical and Biological Agency of Russia on the topic "Study of the functional state of effector cells of human antitumor immunity during the realization of carcinogenic effects of chronic radiation exposure" (Agreement on granting a subsidy from the federal budget for financial provision of the state assignment for public services (works) No. 388-03-2024-155 dated January 24, 2024).

Acknowledgements: the authors thank N.V. Startsev, Head of the Human Database Department (FGBUN UNPC RM FMBA of Russia) for assistance in the formation of the study groups.

Compliance with ethical principles: the study was approved by the Ethical Committee of FGBUN FGUBUN UNPC RM FMBA of Russia (protocol No. 8 of 19.12.2022). All patients participating in the study had previously signed voluntary informed consent within the framework of the Helsinki Declaration of 2013.

Potential conflict of interest: the authors declare that there is no conflict of interest.

✉ Polina O. Khomenko polinahomenko@mail.ru

Received: 31 July 2024 **Revised:** 26 Sep. 2024 **Accepted:** 03 Oct. 2024

СУБПОПУЛЯЦИИ МОНОЦИТОВ И НАТУРАЛЬНЫХ КИЛЛЕРОВ ПЕРИФЕРИЧЕСКОЙ КРОВИ ЧЕЛОВЕКА В ОТДАЛЕННОМ ПЕРИОДЕ ХРОНИЧЕСКОГО ОБЛУЧЕНИЯ

П.О. Хоменко[1]✉, Е.А. Кодинцева[1], А.А. Аклеев[2]

[1] Уральский научно-практический центр радиационной медицины Федерального медико-биологического агентства, Челябинск, Россия

[2] Южно-Уральский государственный медицинский университет, Челябинск, Россия

Введение. Повышенный риск развития злокачественных новообразований и заболеваний сердечно-сосудистой системы установлен для разных когорт облученных людей. При этом известна важная роль моноцитов и натуральных киллеров в модуляции воспаления и канцерогенеза.

Цель. Оценка абсолютного и относительного количества клеток в субпопуляциях моноцитов и натуральных киллеров в периферической крови у лиц, подвергшихся хроническому радиационному воздействию.

Материалы и методы. Обследованы 33 человека из когорты реки Течи, средний возраст пациентов — 74,9 года. Пациенты были разделены на три подгруппы в зависимости от величины поглощенной дозы облучения в красном костном мозге (70–249 мГр, 250–699 МГр, 700–1429 мГр соответственно), средняя поглощенная доза облучения красного костного мозга — 542,1 ± 65,3 мГр, средняя поглощенная доза облучения тимуса и периферических лимфоидных органов — 99,7 ± 14,4 мГр. Группу сравнения составили 10 человек, средний возраст — 71,8 года, без техногенного облучения в анамнезе, сопоставимых по полу и этнической принадлежности.

Результаты. Во второй дозовой подгруппе доля $CD14^-CD16^+$ моноцитов была статистически значимо выше (8,47%), чем в группе сравнения (5,52%, p = 0,014), а абсолютное количество $CD14^-CD16^+$ моноцитов ($0,040\times10^9$/л) — больше, чем в третьей подгруппе ($0,018\times10^9$/л, p = 0,044). Не обнаружено статистически значимых корреляций указанных показателей с факторами радиационной и нерадиационной природы.

Выводы. У людей из второй подгруппы относительное количество $CD14^-CD16^+$ моноцитов было статистически значимо выше, чем в группе сравнения, в то время как абсолютное число $CD14^-CD16^+$ моноцитов — больше, чем в третьей подгруппе, без статистически значимой взаимосвязи с факторами радиационной и нерадиационной природы.

Ключевые слова: хроническое радиационное воздействие; река Теча; субпопуляции; моноциты периферической крови; натуральные киллеры; отдаленные сроки; молекулярные маркеры

Для цитирования: Хоменко П.О., Кодинцева Е.А., Аклеев А.А. Субпопуляции моноцитов и натуральных киллеров периферической крови человека в отдаленном периоде хронического облучения. *Медицина экстремальных ситуаций*. 2024;26(3):22–29. https://doi.org/10.47183/mes.2024-26-3-22-29

Финансирование: научно-исследовательская работа выполнена в рамках государственного задания ФМБА России по теме «Исследование функционального состояния клеток-эффекторов противоопухолевого иммунитета человека в период реализации канцерогенных эффектов хронического радиационного воздействия» (Соглашение о предоставлении субсидии из федерального бюджета на финансовое обеспечение выполнения государственного задания на оказание государственных услуг (выполнение работ) № 388-03-2024-155 от 24 января 2024 года).

Благодарности: Н.В. Старцеву, заведующему отделом базы данных «Человек» (ФГБУН «Уральский научно-практический центр радиационной медицины» Федерального медико-биологического агентства) за помощь в формировании исследуемых групп.

Соответствие принципам этики: исследование одобрено этическим комитетом ФГБУН «Уральский научно-практический центр радиационной медицины» Федерального медико-биологического агентства (протокол № 8 от 19.12.2022). Все пациенты, участвовавшие в исследовании, предварительно подписывали добровольное информированное согласие в рамках Хельсинкской декларации 2013 г.

Потенциальный конфликт интересов: авторы заявляют об отсутствии конфликта интересов.

✉ Хоменко Полина Олеговна polinahomenko@mail.ru

Статья поступила: 31.07.2024 **После доработки:** 26.09.2024 **Принята к публикации:** 03.10.2024

INTRODUCTION

The increased risk of malignant neoplasms (MN) among inhabitants of settlements located along the Techa River affected by ionizing radiation (IR) is a scientifically identified fact confirmed by epidemiological studies [1, 2]. The works of many authors have revealed a correlation between IR dose and risk of hypertension, ischemic heart disease, and cerebrovascular diseases in exposed people in long-term periods following exposure [3]. However, the mechanism of the influence of radiation exposure on the key immune reactions mediating neoplastic processes and/or the development of cardiovascular pathology in irradiated people in long-term periods of exposure to radiation [4] is still insufficiently studied.

A number of authors emphasize that people exposed to technogenic radioactive contamination affecting the Techa River had lower intracellular oxygen-dependent metabolism of monocytes, lower levels of interleukin-4 (IL-4), higher levels of tumor necrosis factor alpha (TNF-α) and interferon gamma (IFN-γ) in serum [5] as compared to unexposed persons. At the same time, TNF-α is weakly correlated with the absorbed dose of red bone marrow irradiation (RBM) [6].

Monocyte–macrophages are of special interest in studying the pathogenesis of the long-term effects of chronic irradiation. The poorly understood role of these cells in the regulation of hematopoiesis and regeneration of RBM represents a promising area of research [7] both under physiological conditions and when RBM are affected by osteotropic radionuclides. Monocyte–macrophages make a significant contribution to the development of both innate and adaptive immune response reactions. As well as participating in the formation of immunological memory, they recognize a wide range of antigenic substances, participate in antigen presentation to T-lymphocytes and regulation of immune responses depending on the type of reaction, its intensity and duration [8].

For many types of oncopathology, the development of inflammatory process caused by active monocytes/macrophages is understood to potentiate the transformation of premalignant tissue into fully malignant tissue. It has been noted earlier that immune cells play a dual role in the pathogenesis of MN. On the one hand, they are able to efficiently and rapidly recognize damaged, transformed and tumor cells in order to neutralize and eliminate them from the body. On the other hand, immunocytes, which typically provide inflammation and removal of genetically foreign agents from the body, contribute to the formation of a pro-tumor microenvironment by producing cytokines and growth factors that stimulate tumor development. In particular, the macrophage migration inhibitory factor (MIF) produced by macrophages suppresses the expression of the *P53* gene, one of the key regulators of cell cycle and apoptosis, which leads to an insufficiently effective response to DNA damage, increased cell life spans, and consequent accumulation of mutations.

Monocyte–macrophages produce a spectrum of growth factors — in particular, vascular endothelial growth factor (VEGF) — which promotes tumor vascularization and metastasis. In turn, tumor signaling molecules provide chemotaxis of monocytes from peripheral blood to the focus of malignant growth and their differentiation into macrophages. The combination of hypoxia and mediators released by tumor cells initiates reprogramming of *de novo* recruited macrophages of the microenvironment into tumor growth promoters — “tumor-associated macrophages” [9]. The presence of macrophages, mast cells, and neutrophils in the tumor microenvironment is usually associated with increased angiogenesis and poor prognosis. However, some clusters of macrophages in the tumor microenvironment may be associated with tumor regression [10].

The cytolytic activity of natural killer (NK) cells is determined by the balance between activating and inhibitory signals and is realized by perforation of the target cell membrane. NK cells can express CD8 α-chain on the membrane but at a lower density than cytotoxic T-cells. Human NK subpopulations expressing αα-homodimer CD8 have greater cytotoxicity than NK cells without a CD8 molecule on the membrane. $CD38^{+}CD8^{+}$ NK-cells have been reported to have high cytolytic activity [11].

Full activation of immunocytes in response to tumor antigens can lead to tumor cell elimination, whereas ineffective immune responses against the background of chronic age-associated inflammation [12] can lead to tumor progression. Chronically activated cells of innate immunity (monocytes/macrophages, natural killer cells, neutrophils

and others) may contribute to the development of MN by suppressing immune reactions, hyperproduction of reactive oxygen species damaging biological membranes and cell DNA, secretion of growth factors and in other ways. Based on the abovementioned, the study of the peculiarities of the quantitative composition of monocyte subpopulations in irradiated people residing along the Techa River, who have now reached the age of realization of oncogenic effects associated with the impact of IR, is a priority direction of research.

In this work, we aim to evaluate absolute and relative cell counts in the subpopulations of monocyte and NK cells in the peripheral blood of persons affected by chronic radiation exposure in the long-term.

MATERIALS AND METHODS

The study was carried out on the basis of the Ural Scientific and Practical Center of Radiation Medicine of FMBA of Russia. Forty-five chronically exposed rural residents permanently residing in areas along the Techa River, which was subject to technogenic contamination during the 1950s due to the activities of the Mayak Production Association, were examined. For each patient, the individualized doses were preliminarily calculated using the Techa River Dosimetry System-2016 (TRDS-2016) [13].

The main group included 33 people, whose absorbed dose calculated on the RBM at the time of examination was 70 mGy or more. The minimum radiation dose calculated on RBM in people from this group was 88.5 mGy, while the maximum dose was 1429 mGy, and the range of doses calculated on thymus and peripheral/secondary lymphoid organs (TSLO) was from 12 to 460 mGy. To permit a detailed study of the dose-effect relationship, the main group was divided into three subgroups depending on the value of the cumulative radiation dose calculated on the RBM: 1st subgroup — 11 people with doses from 70 to 249 mGy; 2nd subgroup — 10 people with doses from 250 to 699 mGy; 3rd subgroup — 12 people with doses from 700 to 1429 mGy.

The comparison group consisted of 10 people with no history of anthropogenic IR exposure, whose absorbed radiation dose was calculated at an RBM less than 70 mGy. The radiation dose calculated on the RBM in the persons included in the comparison group was in the range from 4 to 55 mGy, while the dose on TSLO was from 1 to 20 mGy.

Table 1. Characteristics of the study groups

Parameter, unit of measurement		Comparison group *n* = 10	Main group *n* = 33
RBM dose, mGy		22.5±5.9	542.1±65.3
Dose for TSLO, mGy		8.7±2.4	99.7±14.4
Gender composition, %	male	20.0	27.3
	female	80.0	72.7
Ethnic composition, %	Slavic	50.0	21.2
	Turkic	50.0	78.8

Table prepared by the authors using their own data

Note: The data are presented as average value (*M* ± *SE*)

The mean age of the examined persons in the comparison group was equal to 71.8 ± 1.2 years; in the main group — 74.9 ± 0.6 years. The studied groups of people did not differ statistically significantly in ethnic and gender composition but differed in age ($p = 0.026$). The data on the value of the average radiation dose at RBM, TSLO, gender and ethnic composition in the studied groups of people are presented in Table 1.

Criteria for exclusion of subjects from the study were: signs of acute inflammatory diseases; chronic diseases in exacerbation; renal or hepatic insufficiency; symptoms of acute cerebral circulatory failure or craniocerebral trauma within three months before the study; confirmed oncological and autoimmune diseases; courses of hormone, antibiotic, chemotherapy and (or) radiotherapy; medical procedures involving the use of ionizing radiation within six months before the study.

Human peripheral blood served as a material for immunologic study. Peripheral blood samples (3 mL) were obtained from the ulnar vein in the morning on an empty stomach into a vacuum tube filled with K3-EDTA (tripotassium ethylenediaminetetraacetic acid). The subpopulation composition of monocytes and natural killer cells in peripheral blood was assessed on a LongCyte C3111 flow cytometer (Chenglang Biotechnology, PR China) after preliminary staining with monoclonal antibodies labeled with fluorochromes: CD14-PE, CD16-PerCP, CD45-APC (Elabscience, PRC) — panel for the analysis of monocytes, CD3-FITC, CD56-PE, CD16-PerCP, CD8-PC7, CD45-APC (Elabscience, PRC), CD38-PO (Exbio, Czech Republic), a panel for NK analysis, followed by lysis of erythrocytes with VersaLyse solution (Beckman Coulter Inc., USA) according to the reagent manufacturers' instructions using standardized methods [14]. On the day of blood collection for the study of immunologic parameters in the clinical diagnostic laboratory of Ural Scientific and Practical Center for Radiation Medicine of FMBA of Russia, patients underwent a general blood count with leukoform counting in accordance with the established procedure [15].

Statistical processing of the data was performed in the Statistica 12 software package (demo version). The data were checked for normal distribution using the Kolmogorov–Smirnov test of agreement. The arithmetic mean (M), minimum and maximum values were used to describe normally distributed data. For data that were statistically significantly different from the normal distribution, median, 25th and 75th percentile values were given.

Student's T-test was used to compare parametric data sets; the Mann-Whitney *U*-test was used for nonparametric data. Qualitative data were compared using the χ^2 criterion. Differences were considered statistically significant when the confidence level (p) was less than 0.05. For correlation analysis of abnormally distributed data, the Spearman rank correlation coefficient was calculated with a confidence level of 5%.

RESULTS

When comparing the values of the studied parameters in chronically irradiated people with different dose loads, a statistically significant increase in the absolute monocyte $CD14^{-}CD16^{+}$ count was found in the peripheral blood of

patients from the second subgroup in comparison with those from the third subgroup (p^* = 0.044), and non-exposed patients (p = 0.014) (Table 2).

However, in the process of analyzing the results of quantitative assessment of monocyte subpopulations in the examined persons with different dose loads, no statistically significant differences were found between the median values of the studied parameters in the main group and the comparison group.

The results of quantitative analysis of subpopulations of natural killer cells expressing CD8 and CD38 activation molecules on cell membranes in the examined persons with different absorbed dose of irradiation are presented in Table 3.

Table 2. Results of quantitative analysis of monocyte subpopulations in the examined persons

Indicator, unit of measure	Comparison group *n* = 10	Main group, *n* = 33			
		Subgroups, radiation doses			Median values within the group
		70–249 mGy, *n* = 11	250–699 mGy, *n* = 10	700–1429 mGy, *n* = 12	
Leukocytes, ×10⁹/L	6.14 (5.25–6.60)	5.96 (5.30–6.51)	5.74 (4.70–6.41)	6.23 (5.45–7.05)	5.96 (5.30–6.51)
Monocytes, %	8.2 (7.00–9.90)	8.20 (6.40–11.00)	7.95 (5.00–8.10)	6.00 (3.50–9.15)	8.00 (5.00–9.00)
Monocytes, ×10⁹/L	0.452 (0.364–0.630)	0.467 (0.376–0.679)	0.417 (0.350–0.464)	0.381 (0.185–0.588)	0.420 (0.330–0.567)
$CD14^+CD16^-$ monocytes, %	67.86 (62.45–74.00)	65.58 (54.96–75.66)	69.48 (62.73–73.63)	66.96 (57.50–75.57)	67.68 (58.36–74.80)
$CD14^+CD16^-$ monocytes, ×10⁹/L	0.336 (0.263–0.376)	0.281 (0.218–0.415)	0.305 (0.187–0.314)	0.267 (0.128–0.328)	0.287 (0.187–0.341)
$CD14^+CD16^+$ monocytes, %	4.77 (2.92–6.13)	4.04 (2.85–8.66)	4.25 (2.26–7.30)	3.92 (2.57–5.81)	4.04 (2.48–7.05)
$CD14^+CD16^+$ monocytes, ×10⁹/L	0.024 (0.007–0.031)	0.032 (0.006–0.034)	0.015 (0.004–0.030)	0.095 (0.007–0.019)	0.014 (0.006–0.023)
$CD14^-CD16^+$ monocytes, %	5.52 (3.30–7.50)	6.56 (3.64–8.93)	8.47 (7.98–11.27) p=0.014	6.25 (2.76–9.01)	7.94 (4.67–9.47)
$CD14^-CD16^+$ monocytes, ×10⁹/L	0.018 (0.012–0.034)	0.036 (0.023–0.042)	0.040 (0.033–0.051) p^*=0.044	0.011 (0.007–0.029)	0.033 (0.009–0.042)

Table prepared by the authors using their own data

Notes:
1 — The data are presented as median (25th–75th percentiles).
2 — p — confidence probability of differences relative to the comparison group (Mann–Whitney U test).
3 — p^* p^*=0.044 — confidence probability of differences with respect to the subgroup of people with the highest doses (Mann–Whitney U test).

Table 3. Results of quantitative analysis of NK subpopulations in the examined persons

Parameter, unit of measure	Comparison group, *n* = 10	Main group, *n* = 33			
		Subgroups, radiation doses			Median values in the group
		70–249 mGy, *n* = 11	250–699 mGy, *n* = 10	700–1429 mGy, *n* = 12	
Lymphocytes, %	37.00 (32.40–45.00)	35.00 (30.00–40.90)	39.15 (29.60–46.00)	36.35 (33.55–38.50)	35.70 (30.20–41.00)
Lymphocyte, ×10⁹/L	2.211 (1.701–2.619)	1.979 (1.700–2.600)	1.903 (1.680–2.381)	2.145 (1.863–2.946)	1.979 (1.739–2.600)
NK ($CD3^-CD16^+CD56^+$), %	11.75 (9.00–15.63)	10.87 (6.65–13.93)	10.70 (9.56–14.72)	13.80 (12.00–16.37)	12.00 (7.49–15.63)
NK ($CD3^-CD16^+CD56^+$), ×10⁹/L	0.266 (0.163–0.350)	0.237 (0.117–0.353)	0.195 (0.161–0.349)	0.302 (0.223–0.417)	0.269 (0.160–0.353)
$CD3^-CD16^+CD56^+CD8^-CD38^-$, % of NK	52.39 (17.65–65.45)	42.95 (14.98–66.46)	12.36 (7.83–64.86)	22.11 (4.94–53.73)	26.44 (10.13–64.94)
$CD3^-CD16^+CD56^+CD8^-CD38^-$, ×10⁹/L	0.111 (0.040–0.224)	0.045 (0.031–0.102)	0.020 (0.014–0.046)	0.061 (0.015–0.166)	0.043 (0.015–0.114)
$CD3^-CD16^+CD56^+CD8^+CD38^+$, % of NK	7.13 (2.75–20.00)	2.99 (0–18.92)	10.84 (2.60–30.50)	12.15 (2.03–32.86)	7.10 (1.16–21.90)
$CD3^-CD16^+CD56^+CD8^+CD38^+$, ×10⁹/L	0.011 (0.005–0.036)	0.006 (0–0.045)	0.021 (0.001–0.049)	0.036 (0.009–0.049)	0.021 (0.001–0.049)
$CD3^-CD16^+CD56^+CD8^-CD38^+$, % of NK	22.00 (9.27–44.51)	18.07 (4.83–50.64)	8.44 (0.78–29.03)	21.28 (2.85–47.14)	18.82 (4.83–47.14)
$CD3^-CD16^+CD56^+CD8^-CD38^+$, ×10⁹/L	0.077 (0.015–0.085)	0.046 (0.014–0.154)	0.010 (0.002–0.085)	0.066 (0.011–0.099)	0.063 (0.008–0.101)
$CD3^-CD16^+CD56^+CD8^+CD38^-$, % of NK	9.14 (4.58–18.15)	4.19 (2.48–34.05)	18.94 (2.41–38.74)	5.21 (1.23–22.67)	5.44 (2.41–34.05)
$CD3^-CD16^+CD56^+CD8^+CD38^-$, ×10⁹/L	0.015 (0.008–0.042)	0.010 (0.006–0.024)	0.010 (0.005–0.056)	0.012 (0.003–0.070)	0.010 (0.005–0.056)

Table prepared by the authors using their own data

Notes:
1 — The data are presented as median (25th–75th percentiles).
2 — p — confidence probability of differences relative to the comparison group (Mann–Whitney U test).
3 — p^* — confidence probability of differences with respect to the subgroup of people with the highest doses (Mann–Whitney U test).

Despite a decrease in the median number of natural killer cells not expressing CD38 and CD8 molecules and in the absolute $CD38^+$ NK count in chronically exposed people from the main group relative to the comparison group, no statistical significance of differences was established due to the significant scatter of individual values in people from the main group with relatively small sample sizes, confidence intervals of median values overlap.

At the same time, no statistically significant differences were found between the relative and absolute natural killer cells count expressing in various combinations of CD8 and CD38 molecules on the cell membrane in chronically irradiated people from different dose subgroups and in persons from the comparison group.

When examining the dose-effect relationship, weak inverse correlations were found between the dose calculated on RBM and the relative, absolute monocyte count, absolute $CD14^+CD16^-$ and $CD14^+CD16^+$ monocyte count, and relative $CD3^-CD16^+CD56^+CD8^-CD38^-$ cell count. A direct weak correlation was found between the relative NKs and the dose calculated per RBM. The correlations between the studied indices of innate immunity and doses of RBM and TSLO irradiation were not statistically significant. In order to clarify the results of the analysis of the dependence of the studied indicators of innate immunity on radiation doses, the sample of the examined persons will be expanded in future research. In chronically exposed people in the long-term period following the beginning of radiation exposure, no statistically significant correlations were established by the Spearman criterion between the quantitative characteristics of leukocytes, lymphocytes or monocytes, as well as the analyzed subpopulations of monocytes and natural killer cells and such factors of non-radiation nature as age, sex and ethnos, or between the studied indicators of innate immunity and the doses of radiation exposure.

The data presented in Table 4 show a statistically significant positive correlation between age at the time of examination and the proportion of inactivated NKs, as well as a negative correlation between the ethnicity of the subjects and the proportion of $CD14^-CD16^+$ monocyte in the peripheral blood. At the same time, a reliable correlation was established between the gender of the subjects and the relative or absolute cell count in the subpopulation of inactivated NKs and the proportion of NKs simultaneously expressing CD8 and CD38 molecules on the cell membrane. No such correlations were found in people from the comparison group.

The results are preliminary. In future research, the study groups will be enlarged.

DISCUSSION

The results of the study agree with and complement previously obtained results of immunological examinations of chronically exposed people from the Techa River cohort. The main dose-forming radionuclide was osteotropic strontium-90 (^{90}Sr), whose characteristic feature is a long half-life (about 30 years), accumulation in bone tissue, and prolonged impact of IR on the central organ of the immune system and hematopoiesis (RBM). The unique nature of radiation exposure — in particular, the combination of external and internal γ-radiation, mainly β-radiation due to ^{90}Sr — apparently underlies the long-term changes in the immune system in the residents of the Techa River cohort. No changes in the absolute leukocyte count or relative and absolute monocyte content in blood were detected between exposed and unexposed study participants.

The subpopulation composition of monocytes and expression of activation molecules on NK cells in the peripheral blood of people from the Techa River cohort in long-term periods following chronic radiation exposure was investigated for the first time.

Monocyte–macrophages represent a heterogeneous cluster of cells having great plasticity and multiple functions determined by the type of activating signal. They are radioresistant cells whose functions can be modulated by exposure (AI); depending on the radiation dose and fractionation, such cells exert both pro- or anti-inflammatory, as well as pro- or antitumor activity. At present, it is not possible to systematize information on specific radiation-induced modulations of monocyte–macrophages [16].

CD14 molecule, a type of Toll-like receptor (TLR), appears at the early stages of monocyte maturation and is its specific marker [16]. Differentiation of classical $CD14^{++}CD16^-$ monocytes occurs from a medullary myeloid precursor. Outside the BCC they mature into intermediate $CD14^{++}CD16^+$ monocytes, differentiate into non-classical $CD14^+CD16^{++}$ monocytes and further as tissue

Table 4. The results of the correlation analysis between some non-radiation factors and the studied indicators of immunity

Pairs of parameters, units	Comparison group, *n* = 10		Main group, *n* = 33	
	SR	*p*	*SR*	*p*
$CD14^-CD16^+$ monocytes, $\times10^9$/L & Ethnicity	–0.59	0.072	–0.41	0.019
$CD3^-CD16^+CD56^+CD8^-CD38^-$, % of NK & Age at the time of examination	0.42	0.228	0.39	0.036
$CD3^-CD16^+CD56^+CD8^-CD38^-$, % of NK & Gender	0.09	0.811	0.50	0.005
$CD3^-CD16^+CD56^+CD8^-CD38^-$, $\times10^9$/L & Gender	–0.17	0.631	0.46	0.010
$CD3^-CD16^+CD56^+CD8^+CD38^+$, % of NK & Gender	0.17	0.631	0.36	0.050

Table prepared by the authors using their own data

Notes: *SR* — Spearman correlation coefficient, *p* — Confidence probability

macrophages and dendrocytes perform remodeling and repair of damaged tissues [17, 18]. Late maturation of peripheral monocytes is accompanied by the expression of FcγRIII (CD16) on the cell membrane with a simultaneous decrease in the number of CD14 molecules. At the same time, CD16 expression is associated with an increased ability of monocytes to present antigen, which increases with the loss of CD14 expression on the cell membrane [7]. The relatively low phagocytic activity and enhanced ability to produce cytokines and antigen presentation in such cells is due to higher expression of major histocompatibility complex class II (MHC II) molecules [19].

Monocyte subpopulations perform different functions, which are determined either by the state of their microenvironment representing a complex cytokine-cell system, or by their linear differentiation [18]. Functionally, all monocytes/macrophages are conventionally classified into two types: proinflammatory (M1), which mainly produce IL-18, IL-12, IL-26 and thus stimulate Th1 and Th17 responses, and anti-inflammatory (M2), which mainly produce IL-10 and transforming growth factor beta (TGF-β) and participate in immunoregulation and tissue repair. There are many intermediate and transitional forms between these two clusters of cells, and a dynamic balance of cytokines is maintained depending on the current needs of the macroorganism [7].

The ability of macrophages to respond to various endogenous and exogenous pro- and anti-inflammatory stimuli ensures a high heterogeneity of their phenotype. IFN-γ activates pro-inflammatory macrophages (M1), which participate in the Th1-dependent immune response to oncotransformed target cells. Anti-inflammatory macrophages (M2) are involved in Th2-dependent immune responses, repair processes, and the pathogenesis of some tumors. The spectrum of cytokines produced by M2 cells includes IL-1, IL-6, IL-10, vascular endothelial growth factor (VEGF), and TGF-β, which under certain conditions provide proliferation and metastasis of tumor cells. The subpopulation of monocytes with the $CD14^{low}CD16^{bright}$ phenotype "non-classical monocytes" corresponds to anti-inflammatory cells [7].

Normal monocytes/macrophages play an important role in antitumor immune surveillance by antigen-mediated activation of T-cytotoxic cells or direct lysis of tumor cells in the activated state. Activated macrophages exhibit antitumor activity due to lysing enzymes, TNF-α synthesis and free radical production. Intermediate monocytes in comparison with monocytes of other subpopulations are the main producers of IL-1β, IL-6 and TNF-α, have the greatest ability to perform transendothelial migration and formation of reactive oxygen species [20, 21].

Oncotransformed cells are characterized by reduced expression of major histocompatibility complex class I molecules, which modifies inhibitory signals from other NK receptors. Activating NK receptors interact with stress-inducible proteins that are expressed by tumor cells. The secretory process is triggered in NK cells representing cytoplasmic vesicles containing serine esterases (granzymes A and B) are released by local exocytosis into the space between the effector cell and the target. In NK, a specialized mechanism of transformed cell killing is associated with perforin contained within the granules, which has lytic activity against target cells. Immediately after lymphocyte binding to the target cell, pores are formed in its membrane, NK granules are exocytosed and their contents — granzymes and perforin — are released. Further, a cascade of lytic processes is triggered in the target cell, which leads to deoxyribonucleic acid (DNA) degradation and subsequent cell death. The ability of NK to synthesize cytokines — primarily IFN-γ — determines their participation in the regulation of other parts of antitumor immunity [11].

The scientific literature discusses the hypothesis that in the long-term period following exposure of the organism to IR, senescent cells (primarily leukocytes and macrophages, as well as fibroblasts and others) are one of the main and constant sources of reactive oxygen species and reactive nitrogen species in tissues. These contribute to the maintenance of a high level of free radicals therein and can lead to damage of cells and subcellular structures up to fibrosis and neoplastic transformation [22, 23].

It should be emphasized that the revealed features of immune status, which are more pronounced in chronically exposed people with maximum absorbed doses calculated per RBM, were registered during the period of realization of carcinogenic effects of irradiation and may play a certain role in their development. The results of correlation analysis of the influence of factors of non-radiation nature in people from the studied groups require considerable caution in interpretation due to the relatively small sample size, a factor that introduces significant uncertainty in the assessment of pairwise correlations.

CONCLUSION

The study revealed statistically significant changes in monocyte subpopulations in people exposed to chronic radiation. In particular, in persons irradiated in the dose range of 250 and up to 699 mGy, the relative $CD14^-CD16^+$ monocyte count was significantly higher than in the comparison group; their absolute count exceeded the similar index in persons from the third subgroup with a maximal radiation burden. The preliminary results obtained in practically healthy exposed people from the Techa River cohort may indicate some latent tension of regulatory mechanisms in the immune system — in particular, the monocyte–macrophage systems and NK, which act according to the feedback principle and are aimed at compensating proinflammatory immune shifts [23] — that are to a lesser extent expressed in non-exposed people.

In all examined people from the main group and the comparison group, the absolute leukocyte count, relative and absolute monocyte count, as well as the relative and absolute monocyte with phenotypes $CD14^+CD16^-$, $CD14^+CD16^+$, $CD14^-CD16^+$ count, did not differ statistically significantly. Relative and absolute amounts of NK cells expressing in various combinations of CD8 and CD38 molecules on the cell membrane did not differ statistically significantly between chronically exposed people and those from the comparison group.

No statistically significant Spearman correlations were found between the studied indices of innate immunity and factors of radiation nature in chronically irradiated people.

The study of subpopulations of monocytes and natural killer cells in peripheral blood in chronically exposed population of the Techa River embankment zone will be continued.

References

1. Krestinina LY, Silkin SS, Degteva MO, Akleyev AV. Risk of death from circulatory system diseases in the Urals cohort of emergency-exposed population from 1950 to 2015. *Radiatsionnaya Gigiena.* 2019;12(1):52–61 (In Russ.). https://doi.org/10.21514/1998-426X-2019-12-1-52-61
2. Krestinina LY, Silkin SS, Mikryukova LD, Epifanova SB, Akleyev AV. Risk of solid malignant neoplasms incidence in the Urals cohort of emergency-exposed population: 1956–2017. *Radiatsionnaya Gigiena.* 2020;13(3):6–17 (In Russ.). https://doi.org/10.21514/1998-426X-2020-13-3-6-17
3. Azizova TV, Haylock RGE, Moseeva MB, Bannikova MV, Grigoryeva ES. Cerebrovascular diseases incidence and mortality in an extended Mayak worker cohort 1948-1982. *Radiat Research.* 2014;182(5):529–44. https://doi.org/10.1667/RR13680.1
4. Sources, effects and risks of ionizing radiation. United Nations Scientific Committee on the Effects of Atomic Radiation UNSCEAR 2020/2021. Report to the General Assembly, with Scientific Annexes. New York: United Nations; 2021. https://doi.org/10.18356/9789210010030
5. Akleyev AA. Human immune status in the late period of chronic radiation exposure. *Meditsinskaya radiologiya i radiatsionnaya bezopasnost'.* 2020;65(4):29–35 (In Russ.). https://doi.org/10.12737/1024-6177-2020-65-4-29-35
6. Kodintseva EA, Akleyev AA, Blinova EA. Cytokine profile of people exposed to chronic radiation exposure in the long-term post-exposure period. *Radiatsionnaya biologiya. Radioekologiya.* 2021;61(5):506–14 (In Russ.). https://doi.org/:10.31857/S0869803121050076
7. Lambert C, Sack U. monocyte–macrophages in flow: an ESCCA initiative on advanced analyses of monocyte lineage using flow cytometry. *Cytometry Part B.* 2017;92(3):180-8. https://doi.org/10.1002/cyto.b.21530
8. Gratchev AN, Samoilova DV, Rashidova MA, Petrenko AA, Kovaleva OV. Tumor-associated macrophages: current research status and prospects for clinical use. *Uspekhi Molekulyarnoy Onkologii.* 2018;5(4):20–8 (In Russ.). https://doi.org/10.17650/2313-805X-2018-5-4-20-28
9. Balpanova GT, Bizhigitova BB. Chronic inflammation and cancer. *Vestnik KazNMU.* 2017;(4):424–6 (In Russ.). EDN: YOSNUQ
10. Conniot J., Silva JM, Fernandes JG. Cancer immunotherapy: nanodelivery approaches for immune cell targeting and tracking. *Frontiers in Chemistry.* 2014;(2):1–27. https://doi.org/10.3389/fchem.2014.00105
11. Abakushina EV. Flow cytometry method for evaluating NK cells and their activity. *Klinicheskaya Laboratornaya Diagnostika*. 2015;60(11):37–44 (In Russ.). EDN: VEARRP
12. Khatami M. Chronic inflammation: synergistic interactions of recruiting macrophages (TAMs) and eosinophils (Eos) with host mast cells (MCs) and tumorigenesis in CALTs. M-CSF, suitable biomarker for cancer diagnosis. *Cancers*. 2014;6(1):297–322. https://doi.org/2072-6694/6/1/297
13. Degteva MO, Napier BA, Tolstykh EI, Shishkina EA, Bugrov NG, Krestinina LY, et all. Distribution of individual doses in the cohort of people exposed due to radioactive contamination of the Techa River. *Meditsinskaya radiologiya i radiatsionnaya bezopasnost'*. 2019;64 (3):46–53 (In Russ.). https://doi.org/10.12737/article_5cf2364cb49523.98590475
14. Khaydakov SV, Baydun LV, Zurochka AV, Totolyan AA. Standardized technology research of subpopulational structure of lymphocytes in peripheral blood with flowing cytofluorimeters — analyzers. *Ross Immunol Zh*. 2014;8(17):974–992 (In Russ.). EDN: PFIUVZ
15. Kishkun AA, Beganskaya LA. *Clinical laboratory diagnostics*: textbook: in 2 vol. 2nd ed., revised and supplemented. *Moscow:* GEOTAR-Media; 2021 (In Russ.). https://doi.org/10.33029/9704-6084-9-CLD1-2021-1-784
16. Deloch L, Rückert M, Weissmann T, Lettmaier S, Titova E, Wolff T et all. The various functions and phenotypes of macrophages are also reflected in their responses to irradiation: A current overview. *International review of cell and molecular biology.* 2023;(376):99–120. https://doi.org/10.1016/bs.ircmb.2023.01.002
17. Poveshchenko AF, Shkurat GA, Kolesnikov AP, Konenkov VI. Functional and phenotypic characteristics of macrophages in acute and chronic inflammation. Sentinels of lymph nodes. *Uspekhi Fiziologicheskikh Nauk.* 2015;46(1):105–12 (In Russ.). EDN: PQOEMX
18. Zemskov VM, Revishvili AS, Kozlova MN, Shishkina NS, Kulikova AN, Balbutsky AV et all. Analysis of monocyte subpopulations with cardiovascular, burn and other pathologies (2010 classification). *Meditsinsky Sovet*. 2023;17(4):154–63 (In Russ.). https://doi.org/10.21518/ms2023-002
19. Gu BJ, Sun C, Fuller S, Skarratt KK, Petrou S, Wiley JS. A quantitative method for measuring innate phagocytosis by human monocytes using real-time flow cytometry. *Cytometry*. Part A. 2014;85(4):313–21. https://doi.org/10.1002/cyto.a.22400
20. Aw NH, Canetti E, Suzuki K, Goh J. Monocyte subsets in atherosclerosis and modification with exercise in humans. *Antioxidants*. 2018;7(12):1–12. https://doi.org/2076-3921/7/12/196
21. Williams H, Mack CD, Li SCH, Fletcher JP, Medbury HJ. Nature versus number: monocytes in cardiovascular disease. *International Journal of Molecular Sciences.* 2021;22(17):1–21. https://doi.org1422-0067/22/17/9119
22. Citrin DE, Mitchell JB. Mechanisms of normal tissue injury from irradiation. Seminars in radiation oncology. *Seminars in Radiation Oncology*. 2017;27(4):316–24. https://doi.org/10.1016/j.semradonc.2017.04.001
23. Kim JH, Brown SL, Gordon MN. Radiation-induced senescence: therapeutic opportunities. *Radiation Oncology*. 2023;1(1):1–11. https://doi.org/10.1186/s13014-022-02184-2

Authors' contributions. All the authors confirm that they meet the ICMJE criteria for authorship. The most significant contributions were as follows. Polina O. Khomenko — information collection, data processing, text writing; Ekaterina A. Kodintseva — research concept and design, information collection, data processing, text writing; Andrey A. Akleyev — the concept and design of the study, general guidance, editing.

AUTHORS

Polina O. Khomenko
https://orcid.org/0009-0009-1984-715X
polinahomenko@mail.ru

Ekaterina. A. Kodintseva, Cand. Sci. (Biol.)
https://orcid.org/0000-0003-1156-1922
ovcharova.cat@mail.ru

Andrey A. Akleyev, Dr. Sci. (Med.),
https://orcid.org/0000-0001-9781-071X
andrey.akleev@yandex.ru

https://doi.org/10.47183/mes.2024-26-3-30-39

ASSESSMENT OF DEPRESSIVE-LIKE BEHAVIOR IN MICE AFTER FRACTIONAL GAMMA IRRADIATION

Nadezhda A. Obvintseva✉, Natalia I. Atamanyuk, Irina A. Shaposhnikova, Andrej A. Peretykin, Evgeny A. Pryakhin

Urals Research Center for Radiation Medicine, Chelyabinsk, Russia

Introduction. Exposure of the brain to high doses of ionizing radiation is an established risk factor for the development of neoplasms and associated cognitive disorders. However, the impact of long-term low-dose irradiation on the brain and higher nervous system, including the development of anxiety-depressive disorders, remains an unsolved problem.

Objective. To study the effect of fractionated gamma-irradiation in doses of 0.1 Gy, 1 Gy and 5 Gy in the early postnatal period on indices of depression-like states in C57Bl/6 mice at the age of 1 and 6 months.

Materials and methods. The animals were irradiated during the first month of life. Cumulative doses (0.1 Gy, 1 Gy and 5 Gy) were obtained in the mode of fractionated irradiation (20 fractions). 2 control groups were formed comprising intact animals and falsely irradiated animals. The presence of a depression-like state was evaluated in the "tail holding" test at the age of 1 month and 6 months.

Results. Age-related changes were manifested by a decrease in depression-like behavior in 6-month-old mice compared with 1-month-old mice. Stress induced by performing radiation-related manipulations, which had no significant effect on 1-month-old mice, led to the development of marked depression-like states in the same animals at 6 months of age. Radiation exposure led to the development of a dose-dependent antidepressant-like effect, which was more pronounced in animals at the age of 6 months after fractionated irradiation at doses of 0.1 Gy and higher.

Conclusions. Fractionated gamma-irradiation does not lead to the development of depression-like symptomatology in mice in the early postnatal period, but, on the contrary, is characterized by antidepressant action.

Keywords: ionizing radiation; low doses; fractional irradiation; mice; depressive-like state; tail suspension test

For citation: Obvintseva N.A., Atamanyuk N.I., Shaposhnikova I.A., Peretykin A.A., Pryakhin E.A. Assessment of depression-like behavior in mice after fractional gamma irradiation. *Extreme Medicine*. 2024;26(3):30–39. https://doi.org/10.47183/mes.2024-26-3-30-39

Funding: the work was performed within the framework of the state assignment of FMBA of Russia No. 388-03-2024-155.

Compliance with ethical principles: the study was approved by the Ethical Committee of the Ural Scientific and Practical Center for Radiation Medicine (Protocol No. 1 dated April 03, 2023). The work with animals was performed in accordance with the provisions of the European Convention for the Protection of Vertebrate Animals Used for Experimental and Other Scientific Purposes (1986, Strasbourg), Directive 2010/63/EU of the European Parliament and the Council of the European Union of 09/22/2010 on the protection of animals used for scientific purposes.

Disclosure: the authors declare that there is no conflict of interest.

✉ Nadezhda A. Obvintseva n_obvintseva@mail.ru

Recived: 2 Aug. 2024 **Revised:** 30 Aug. 2024 **Accepted:** 1 Sep. 2024

ОЦЕНКА ДЕПРЕССИВНОПОДОБНОГО ПОВЕДЕНИЯ У МЫШЕЙ ПОСЛЕ ФРАКЦИОНИРОВАННОГО ГАММА-ОБЛУЧЕНИЯ

Н.А. Обвинцева✉, Н.И. Атаманюк, И.А. Шапошникова, А.А. Перетыкин, Е.А. Пряхин

Уральский научно-практический центр радиационной медицины Федерального медико-биологического агентства, Челябинск, Россия

Введение. Облучение мозга в больших дозах ионизирующего излучения является установленным фактором риска развития новообразований и когнитивных нарушений. Однако нерешенной проблемой остается влияние длительного облучения в малых дозах на головной мозг и высшую нервную деятельность, в том числе на развитие тревожно-депрессивных расстройств.

Цель. Изучить влияние фракционированного гамма-облучения в дозах 0,1 Гр, 1 Гр и 5 Гр в ранний постнатальный период на показатели депрессивноподобного состояния у мышей линии C57Bl/6 в возрасте 1 и 6 мес.

Материалы и методы. Животных облучали в течение первого месяца жизни. Необходимые кумулятивные дозы (0,1 Гр, 1 Гр и 5 Гр) были получены в режиме фракционированного облучения (20 фракций). Были сформированы 2 контрольные группы: интактные животные и ложно облученные животные. Депрессивноподобное состояние оценивали в тесте «удержания хвоста» в возрасте 1 и 6 мес.

Результаты. Возрастные изменения проявлялись в снижении депрессивноподобного поведения у мышей в возрасте 6 мес. по сравнению с мышами в возрасте 1 мес. Стресс, вызванный выполнением манипуляций, связанных с облучением, не оказывал существенного влияния на мышей в возрасте 1 мес., но вызывал развитие выраженного депрессивноподобного состояния у этих же животных в возрасте 6 мес. Радиационное воздействие привело к развитию зависимого от дозы антидепрессивноподобного эффекта, который был более выражен у животных в возрасте 6 мес. после фракционированного облучения в дозах 0,1 Гр и выше.

Выводы. Фракционированное гамма-облучение в ранний постнатальный период не приводит к развитию депрессивноподобной симптоматики у мышей, а, напротив, характеризуется антидепрессивным действием.

Ключевые слова: ионизирующее излучение; малые дозы; фракционированное облучение; мыши; депрессивноподобное состояние; тест «удержание хвоста»

Для цитирования: Обвинцева Н.А., Атаманюк Н.И., Шапошникова И.А., Перетыкин А.А., Пряхин Е.А. Оценка депрессивноподобного поведения у мышей после фракционированного гамма-облучения. *Медицина экстремальных ситуаций*. 2024;26(3):30–39. https://doi.org/10.47183/mes.2024-26-3-30-39

Финансирование: работа выполнена в рамках государственного задания Федерального медико-биологического агентства № 388-03-2024-155.

Соответствие принципам этики: исследование одобрено этическим комитетом ФГБУН «Уральский научно-практический центр радиационной медицины» (протокол № 1 от 3 апреля 2023 г.). Работа с животными выполнена в соответствии с положениями Европейской конвенции по защите позвоночных животных, используемых в экспериментальных и других научных целях (1986 г., Страсбург), Директивы 2010/63/EU Европейского парламента и Совета Европейского союза от 22.09.2010 по охране животных, используемых в научных целях.

Потенциальный конфликт интересов: авторы заявляют об отсутствии конфликта интересов.

✉ Обвинцева Надежда Александровна n_obvintseva@mail.ru

Статья поступила: 02.08.2024 **После доработки:** 30.08.2024 **Принята к публикации:** 01.09.2024

INTRODUCTION

It is known that acute irradiation of the brain in high doses leads to cognitive dysfunction, which is generally manifested as a deficit of hippocampus-dependent functions of learning and memory, and that these effects are correlated with the irradiation dose [1–3]. However, despite the considerable body of information on the influence of ionizing radiation on the human body, the formation of mental disorders and the nature of mental disorders in humans depending on the irradiation dose remains under-researched.

In addition to changes in cognitive function, a number of studies have also noted changes in emotional behavior — in particular, the development of signs of anxiety and depression. Thus, a high prevalence of cerebrovascular diseases, organic psychiatric and depressive disorders, cognitive impairment and dementia were noted among the Chernobyl accident liquidators, which cases grew with increasing radiation dose, some effects being registered at doses from 50 mSv [4, 5]. An increased incidence of depression and suicidal ideation has been reported among adolescents exposed at an early age to radioactive fallout from the Chernobyl accident [6]. A wide range of depressive pathologies against a background of organic disorders was revealed in persons irradiated in the radiation accidents zone of the Southern Urals [7].

However, when analyzing data on radiation effects in populations irradiated as a result of radiation incidents, it should be considered whether the stress associated with receiving information about possible radiation exposure regardless of whether the background doses were actually exceeded may be responsible for the increased incidence of psychiatric disorders [8].

In order to exclude the effect of factors other than radiation exposure, it is of interest to study the peculiarities of radiation exposure on mental states in experimental animals. Behavioral changes characterized by increased anxiety have been detected in rodents under irradiation at doses in the range of 0.25–1 Gy [9–11]. Dos Santos M et al. registered depressive-like symptoms in animals, which were manifested in the increase of immobility time in the forced swimming (Porsolt) test at brain irradiation in the dentate gyrus region at doses from 0.25 Gy [10]. At the same time, a group of authors Wang H, Ma Z, Shen H, et al. noted depressive-like behavior in rats irradiated at the level of 5 Gy at an early age as manifested in the forced swimming test and tail holding test, which remained the same within 4 months after irradiation [12].

Brain exposure to high doses of ionizing radiation is an established risk factor for the development of neoplasms and cognitive disorders [1]. However, the effect of long-term low-dose irradiation on the central nervous system (CNS) and higher nervous activity remains poorly understood. Long-term exposure due to radiation incidents is characteristic both of emergency professionals and the general population living in the proximate zones. This type of radiation exposure will be additionally characteristic for astronauts during long space flights outside the Earth's magnetic field (flights to the Moon, Mars, etc.).

It should be noted that the available data on the effects of chronic or fractionated radiation and their impact on the higher nervous activity of experimental animals, especially in the aspect of long-term irradiation at low doses, are contradictory [1, 3]. Most studies of the effects of ionizing radiation on mental functions were conducted using a single acute exposure, while clinically and environmentally significant effects on humans occur predominantly in the mode of chronic or fractionated irradiation. Due to the fact that sex differences in depression-related behavior can be registered in humans and mice [13], studies to assess the effect of fractionated irradiation on depression-like behavior in mice should take gender specifics in the implementation of radiation-induced behavioral changes into account.

The present work set out to evaluate the effect of early fractionated irradiation at cumulative doses of 0.1 Gy, 1 Gy and 5 Gy on depression-like behavior in mice of different sexes both immediately after irradiation and over longer periods of time.

MATERIALS AND METHODS

Male and female mice of the C57BL/6 line (SPF-vivarium nursery of Institute of Cytology and Genetics SB RAS, Novosibirsk) were used in this work. The animals were kept under standard vivarium conditions on a standard diet under natural light.

The effect of prolonged radiation exposure in the early postnatal period, which is characterized by the greatest sensitivity of the brain to the action of ionizing radiation, was evaluated at low (0.1 Gy), medium (1 Gy) and high (5 Gy) doses. Starting from 0–3 days after birth and continuing for the first month of life, the animals were subjected to fractionated total external gamma-irradiation 5 days a week for 4 weeks (20 fractions in total).

All experimental animals were divided into groups according to sex and the level of external gamma irradiation:

1. 5 Gy group — mice (40 males and 40 females) irradiated at a cumulative dose of 5 Gy (20 fractions of 0.25 Gy each);
2. 1 Gy group — mice (40 males and 40 females) irradiated at a cumulative dose of 1 Gy (20 fractions of 0.05 Gy);
3. 0.1 Gy group — mice (40 males and 40 females) irradiated at a cumulative dose of 0.1 Gy (20 fractions of 0.005 Gy);
4. 0 Gy group — false irradiation (0 Gy) (40 males and 40 females). Animals in this group were treated with similar manipulations and in the same amount as in the "irradiation" groups, but without exposure to ionizing radiation. Stress associated with manipulations included: early postnatal stress in the form of short-term (3–5 min) deprivation from the mother; stress associated with cell transfer, sound, light simulation of irradiation at the IGUR-1M facility;
5. Biological control group (BC) — intact animals (40 males and 40 females).

Irradiation was carried out at the IGUR-1M experimental radiobiological unit with 137Cs-sources (CJSC "Kvant", Russia). The irradiation dose rate at single doses of 0.25 Gy and 0.05 Gy was 0.72 Gy/min; to obtain a single

dose of 0.005 Gy, lead collimators were used to reduce the dose rate to 0.015 Gy/min. Gamma field irregularity in the working space was not more than 10%. For irradiation, mice were placed inside the facility in home cages, removing from them lactating females for the duration of irradiation.

On the IGUR-1M unit, five cages with simultaneously irradiated animals were vertically arranged on top of each other. Each day, the position of cells in the row of five was changed. The absorbed dose in each irradiation cycle was monitored using a DKS5350/1 clinical dosimeter (UE "Atomteh", Republic of Belarus) fitted with a TM31010 cylindrical ionization chamber (PTW-Freiburg, Germany having a volume of 0.125 cm^3 in the mode of K(a) kerma measurement in the air of X-ray and gamma radiation. For each cage containing animals, the actual absorbed dose for 20 fractions of irradiation was individually calculated taking into account the dosimeter readings and the calculated value of dose uncertainty.

When calculating the actually received cumulative absorbed dose for animals of each experimental group as based on the DKS5350/1 dosimeter readings in each irradiation cycle and calculated values of standard uncertainties of irradiation doses on the IGUR-1M unit, the following values were obtained for mice: for the 0.1 Gy group — (0.11 ± 0.01) Gy; for the 1 Gy group — (1.00 ± 0.08) Gy; for the 5 Gy group — (5.2 ± 0.4) Gy [14].

At the age of 1 month, 10 individually labelled mice of the same sex were placed in separate cages. Testing was performed at the age of 35–37 days (one week after completion of irradiation and weaning) and again at the age of 6 months (5 months after completion of irradiation). In each experimental group, 80 animals (40 males and 40 females) were tested.

The depression-like state in mice was assessed via the tail-holding test (analog of the Porsolt forced swimming test), which represents the animal's reaction to a short-term unavoidable stress in the form of immobile suspension (immobility). The test assessed the time, during which the animal switches from active attempts to free itself from an unpleasant position (suspension by the tail) to immobility, which is interpreted as a manifestation of despair behavior and reflects a depression-like state of rodents [15].

To perform the test, mice were suspended by their tails with 15 cm long pieces of painter's tape from a bar located on two racks. Four animals were tested at a time, separating them from each other with cardboard partitions. Plastic tubes 2/3 the length of the tail attached to the tail to prevent the mouse from being able to climb up it. At least 30 cm was left between the nose of the mouse and the table surface. After suspension, the behavior of the mice was recorded by video (Sony α37 camera) for 6 min, after which the animals were released [15]. The total time during which the mice hung motionless without making active attempts to free themselves (total immobility time); the number of such immobile suspensions; the time until the first immobile suspension; and the average time of one immobile suspension were recorded. The indicators were recorded using the RealTimer program ("Open science" research and production company LLC, Russia).

Data were analyzed in Microsoft Excel and using the R programming language [16]; the results were expressed as mean values and standard errors ($M \pm SE$). We evaluated the conformity of the measured parameters in each group to the normal distribution using the Kolmogorov-Smirnov test of agreement with a statistical significance level of 0.05. Since all analyzed indicators corresponded to normal distribution, the experimental groups were compared using Student's t-criterion. A significance level of 0.05 was considered reliable. Multivariate variance analysis was performed using a generalized linear model to assess the linear dependence of the studied parameters on the radiation dose, sex, and stress factor associated with manipulations during irradiation of animals (animals from the biological control group were assumed not to experience stress, while animals from the other groups, including the 0 Gy group, were exposed to stress).

RESULTS

In the BC group of mice at 1 month and 6 months of age, all analyzed parameters in mice at 6 months of age had no statistically significant differences between males with the exception of mean time to one immobile suspension ($t = 2.33$, $p = 0.02$): time to first immobile suspension at 1 month of age — $t = 1.03$, $p = 0.31$; at age 6 months — $t = 0.74$, $p = 0.46$); total immobile time at age 1 month — $t = 0.20$; $p = 0.84$; at age 6 months — $t = 1.41$, $p = 0.16$; number of immobile suspensions in mice at age 1 month — $t = 0.17$, $p = 0.86$; at 6 months of age — $t = 1.25$, $p = 0.22$; mean time per immobile suspension in mice at 1 month of age — $t = 0.86$, $p = 0.39$. In the experimental groups, there were generally no differences between males and females. However, sex differences were observed in animals in the false irradiation group (0 Gy) at 1 month of age: males had shorter time to first immobile suspension ($t = 2.13$, $p = 0.04$), as well as a longer total immobile time ($t = 2.5$, $p = 0.01$) and mean time to one immobile suspension ($t = 2.3$, $p = 0.02$) compared to females. Among the exposed animals, only one group (1 month, 1 Gy) showed differences between females and males in terms of time to first immobile suspension ($t = 2.6$, $p = 0.01$), which was shorter in males. Further, the test results in each experimental group were analyzed without sex separation (Table 1).

Significant behavioral differences in mice aged 1 and 6 months in the BC group were observed. Thus, the time to the first immobile suspension in mice aged 1 month was 39 ± 3 s, while in the same mice at attainment of the age of 6 months, the value of this index was 2.7 times greater ($t = 11.3$, $p < 0.001$). Total immobility time decreased 2-fold with age ($t = 15.7$, $p < 0.001$); the number of immobile suspensions decreased from 10.8 ± 0.3 times to 7.5 ± 0.3 times ($t = 7.8$, $p < 0.001$). The mean time per immobile suspension also decreased from 23.0 ± 1.2 seconds to 15 ± 1.1 seconds ($t = 4.9$, $p < 0.001$).

In the false irradiation group (0 Gy), stress caused by manipulations related to irradiation (cell transfer, removal of infant mice from their mothers for up to 5 min, simulation of irradiation at the IGUR-1M facility) in mice at

the age of 1 month led to a change in only one indicator — a decrease in the total immobility time by 8% (t = 2.2; p = 0.03) (Table 1). However, such stress led to pronounced changes in 3 out of 4 analyzed parameters (time to the first immobile suspension, total immobility time, number of immobile suspension) when these mice reached the age of 6 months. Thus, in the 0 Gy group mice as compared to the BC group, the time to first static suspension decreased by 16% (t = 2.2, p = 0.03), total immobility time increased by 75% (t = 6.4, p < 0.001), and the number of static suspensions increased by 71% (t = 6.2, p < 0.001). These behavioral changes in mice in the 0 Gy group can be interpreted as a manifestation of a depression-like state. Due to the revealed differences in the BC and 0 Gy groups, the analyzed parameters of the irradiated mice were compared with those of the 0 Gy group of the corresponding age.

In mice at the age of 1 month, no statistically significant differences were found between the 0.1 Gy and 1 Gy groups, or with the 0 Gy group, for all the parameters studied (time to the first immobile suspension, total immobility time, number of immobile suspensions, average time of one immobile suspension). In animals irradiated at a dose of 5 Gy, a lengthening of the time to the first immobile suspension (t = 2.6, p = 0.01), as well as a reduction in total immobility time (t = 4.1, p < 0.001) and mean time per immobile suspension (t = 4.0, p < 0.001) were observed. Such changes can be interpreted as a manifestation of antidepressant-like effect of fractionated irradiation at a total dose of 5.2 Gy.

In mice at the age of 6 months, a statistically significant decrease in the total time of static suspension and the number of static suspensions was detected in all dose groups (Table 2). There was also a statistically significant increase in the time to the first immobile suspension in the 5 Gy group (t = 2.6, p = 0.01) and a decrease in the mean time of one immobile suspension in the 1 Gy group (t = 2.9, p = 0.005). Such changes can be interpreted as manifesting an antidepressant-like effect 5 months after exposure to irradiation at doses of 0.1 Gy and higher.

An important stage in researching the causal relationships between the analyzed factor and its effects is the assessment of dose-effect relationship. The revealed changes depended on the level of radiation exposure. Regression analysis showed that the dose of radiation exposure has a statistically significant effect on the time to the first immobile suspension at the age of 1 month (R^2 = 0.03; F = 12.5; p < 0.001) and at the age of 6 months (R^2 = 0.02; F = 8.3; p = 0.004) (Fig. 1).

At the same time, the slope coefficients in the equations of dependence of time to the first immobile suspension in mice of different ages did not differ (t = 0.2, p = 0.8), indicating that the effect of fractionated irradiation on the indicator of time to the first immobile suspension did not differ in the same animals at the age of 1 and 6 months. Nevertheless, pronounced age changes are registered in the form of increased time to the first immobile suspension in mice at the age of 6 months compared to one-month-old animals.

Table 1. Tail suspension test results in 1 month old mice in different experimental groups

Group	Gender	Time to the first immobile suspension, sec	Total immobility time, sec	Number of immobile suspensions (*M±SE*)	Average time of one immobile suspension (*M±SE*), sec
BC	♂	42 ± 5	230 ± 7	10.9 ± 0.5	24 ± 2.1
	♀	36 ± 3	228 ± 7	10.8 ± 0.3	22 ± 1.0
	♂+♀	39 ± 3	229 ± 5	10.8 ± 0.3	23.0 ± 1.2
0 Gy	♂	*28 ± 4	226 ± 8	11 ± 0.5	23.2 ± 1.8
	♀	51 ± 10	*194 ± 10	10.6 ± 0.4	*18.3 ± 1.1
	+♀	39 ± 5	*211 ± 7	10.8 ± 0.3	20.9 ± 1.1
0.1 Gy	♂	†44 ± 3	222 ± 7	10.9 ± 0.5	21.7 ± 1.3
	♀	*50 ± 4	†222 ± 5	10.9 ± 0.4	†22.3 ± 1.0
	♂+♀	47 ± 3	226 ± 5	10.9 ± 0.3	22 ± 0.8
1 Gy	♂	†41 ± 4	212 ± 8	11.1 ± 0.4	20.6 ± 1.2
	♀	*54 ± 3	†230 ± 6	11.4 ± 0.4	20.7 ± 1.0
	♂+♀	*47 ± 2.5	217 ± 5	11.2 ± 0.3	20.6 ± 0.8
5 Gy	♂	†49 ± 4	*†181 ± 9	11.4 ± 0.5	*†16.8 ± 1.1
	♀	*64 ± 8	*†163 ± 9	11.4 ± 0.6	*†14.7 ± 1.0
	♂+♀	*†56 ± 5	*†172 ± 7	11.4 ± 0.4	*†15.7 ± 0.8

Table prepared by the authors using their own data

Note: ♂ — males; ♀ — females; * — statistically significant differences from the index in the biological control group, p<0.05; † — statistically significant differences from the index in the 0 Gy group, p<0.05.

Table 2. Tail suspension test results of 6-month-old mice in different experimental groups

Groups	Gender	Time to the first immobile suspension, sec	Total immobility time, sec	Number of immobile suspensions	Average time of one immobile suspension, sec
BC	♂	‡101 ± 9	‡97 ± 8	‡7.9 ± 0.5	‡12.5 ± 1.0
	♀	‡109 ± 6	‡114 ± 9	‡7.1 ± 0.4	‡17.5 ± 1.9
	♂+♀	‡105 ± 5	‡106 ± 6	‡7.5 ± 0.3	‡15.0 ± 1.1
0 Gy	♂	88 ± 8	*168 ± 17	*11.7 ± 1.0	14.5 ± 1.0
	♀	*87 ± 8	*204 ± 13	*13.9 ± 1.1	16.7 ± 1.2
	♂+♀	*88 ± 6	*186 ± 11	*12.8 ± 0.8	15.6 ± 0.8
0.1 Gy	♂	82 ± 8	*133 ± 9	*9.7 ± 0.5	13.4 ± 0.9
	♀	95 ± 5	†135 ± 8	*†8.7 ± 0.4	16.2 ± 1.2
	♂+♀	*88 ± 5	*†134 ± 6	*†9.2 ± 0.3	14.8 ± 0.8
1 Gy	♂	96 ± 9	†106 ± 8	†8.9 ± 0.5	12.1 ± 0.9
	♀	99 ± 8	†95 ± 9	†7.7 ± 0.4	*†12.5 ± 1.3
	♂+♀	98 ± 6	†101 ± 6	†8.3 ± 0.3	*†12.3 ± 0.8
5 Gy	♂	113 ± 10	†104 ± 10	†7.2 ± 0.6	14.9 ± 1.6
	♀	†111 ± 9	†103 ± 9	†7.9 ± 0.5	*†12.9 ± 1.1
	♂+♀	†112 ± 7	†104 ± 7	†7.6 ± 0.4	13.9 ± 1.0

Table prepared by the authors using their own data

Note: ♂ — males; ♀ — females; * — statistically significant differences from the index in the biological control group, $p<0.05$; † — statistically significant differences from the index in the 0 Gy group, $p < 0.05$; ‡ — statistically significant differences in the BC groups in mice aged 1 and 6 months, $p < 0.05$.

Total immobility time was dose-dependent at both 1 month of age ($R^2 = 0.14$; $F = 66.6$; $p << 0.001$) and 6 months of age ($R^2 = 0.13$; $F = 49.8$; $p < 0.001$) (Figure 2).

Despite the dependence of this index on radiation dose being satisfactorily described by linear functions with close slope angles, this dependence for mice at the age of 6 months (Fig. 2) has a nonlinear character and is better described by a logarithmic function ($R^2 = 0.19$; F = 75.6; $p < 0.001$), suggesting an age-related change in the reaction of animals to radiation exposure: in mice at the age of 6 months, a decrease in the severity of depressive-like behavior is registered starting from the radiation exposure level of 0.1 Gy, whereas in mice aged 1 month, a statistically significant radiation-induced decrease in depressive-like state is observed only at an irradiation dose of 5 Gy.

The number of immobile suspensions in animals at 1 month of age did not statistically significantly change with increasing radiation dose, whereas in the same mice at 6 months of age, a highly reliable dependence on the level of radiation exposure was observed, which was also best

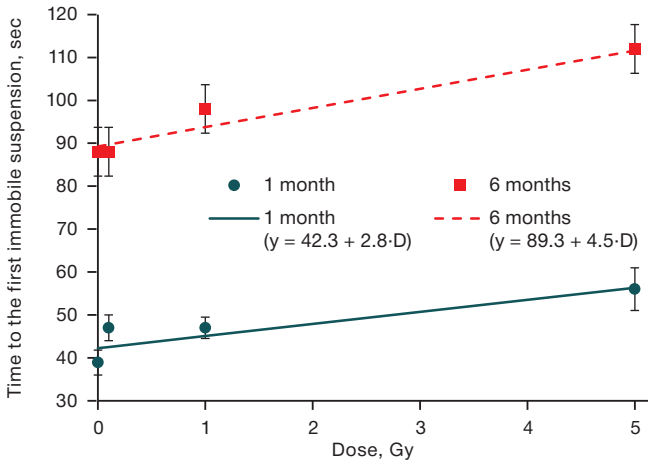

Figure prepared by the authors using their own data

Fig. 1. Dependence of the time to the first immobile suspension on the dose of gamma irradiation in mice aged 1 and 6 months

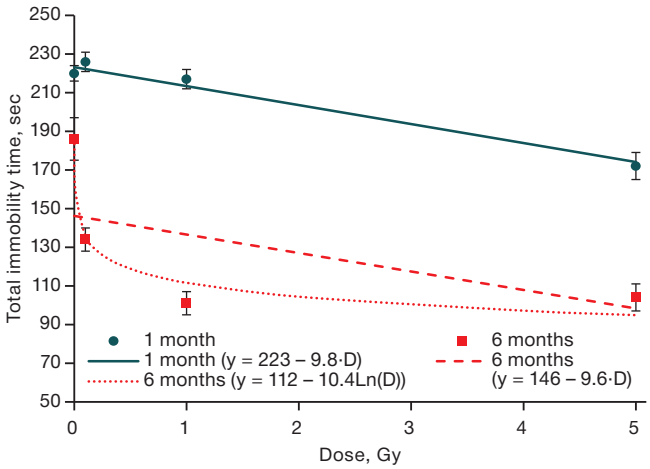

Figure prepared by the authors using their own data

Fig. 2. Dependence of total immobility time on the dose of gamma irradiation in mice aged 1 and 6 months

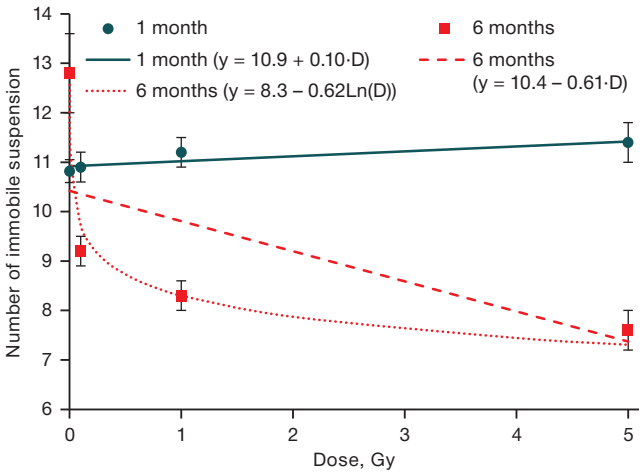

Figure prepared by the authors using their own data

Fig. 3. Dependence of the number of immobile suspensions on the dose of gamma irradiation in mice aged 1 and 6 months

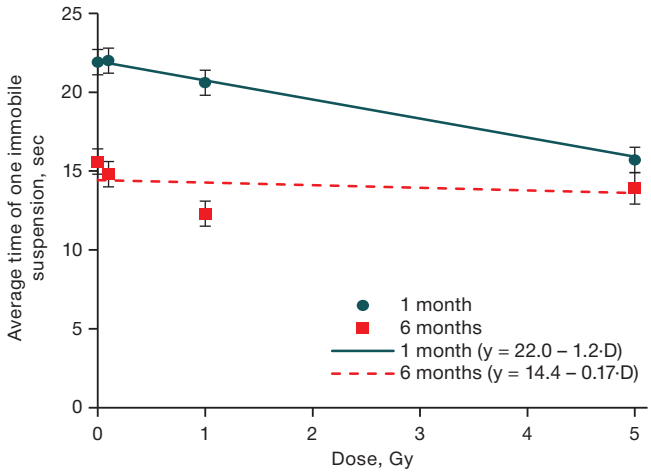

Figure prepared by the authors using their own data

Fig. 4. Dependence of the average time of one immobile suspension on the gamma irradiation dose in mice aged 1 and 6 months

described by a logarithmic function (R^2 = 0.18; F = 67.1; p < 0.001) (Fig. 3).

The indicator "number of immobile suspensions clearly shows that irradiated animals react differently to short-term unavoidable stress (suspension by the tail) five months after fractionated irradiation in comparison with the non-irradiated control group: in irradiated one-month-old animals, there were no differences from mice from the false irradiation group, while, in the same mice at the age of 6 months, there was registered a dose-dependent decrease of this indicator starting from the level of 0.1 Gy.

Analysis of the average duration of one immobile suspension also revealed age-related changes in the response to short-term unavoidable stress in mice aged 1 and 6 months: in one-month-old animals, a linear dependence of this index on the radiation dose was revealed (R^2 = 0.09; F = 40.5; p < 0.001), while in mice aged 6 months, the average duration of one immobile suspension did not depend on the level of radiation exposure (Fig. 4).

The peculiarities of the long-term experiment to assess the effect of fractionated gamma irradiation on physiological processes associated with the development of a depression-like state are the inevitable influence of such factors as age, sex, stress associated with manipulations during irradiation of animals. While the separate effects of these factors are as given above, in order to obtain a holistic picture of the relationship between these factors, it is necessary to conduct a multivariate analysis. The multivariate variance analysis using the generalized linear model showed that the time to the first immobile suspension was statistically significantly influenced by such factors as sex, age, irradiation dose, while the stress factor had a statistically significant effect only on mice aged 6 months. It was found that the "time to the first immobile suspension" in females was 8 ± 3 s longer than in males (Table 3).

While stress had no statistically significant effect on the time to the first immobile suspension in mice at the age of 1 month, the value of this index significantly decreased in the same animals at 6 months. Radiation exposure had a statistically significant effect on the time to the first static suspension; the value of this index increased by 3 ± 0.8 s with increasing dose by 1 Gy.

According to multivariate variance analysis, the total immobility time depended on age, stress, and radiation dose and was independent of the sex of the mice. The stress factor calculated for animals from the 0 Gy, 0.1 Gy, 1 Gy, and 5 Gy groups caused an average increase of 40 ± 8 s, with the value of this parameter being lower by an average of 49 ± 11 s in mice aged 1 month. Radiation exposure had a statistically significant effect on total immobility time, which decreased by 9.4 ± 1.1 s with increasing dose of 1 Gy (Table 3).

The number of immobile suspensions statistically significantly depended on age, stress, irradiation dose, but did not depend on the sex of animals. Mice aged 6 months showed a decrease in the number of immobile suspensions compared to one-month-old mice. Stress, on average, resulted in an increase in the number of immobile suspensions by 2.9 ± 0.5 in groups exposed to procedures involving irradiated mice. Moreover, stress had an effect on animals at 6 months of age and no effect at 1 month of age. In multivariate variance analysis, such age differences in stress response were expressed as an increase in the coefficient for the stress factor and an equal magnitude decrease in the coefficient for the stress*age factor for mice at 1 month of age, where the stress factor had no effect on the number of immobile suspensions. As the dose increased by 1 Gy, the number of immobile suspensions decreased on average by 0.6 ± 0.1. Such changes were determined mainly by the responses of mice aged 6 months, in which the regression analysis revealed a highly significant dependence of the analyzed index on the irradiation dose (Fig. 3). In mice at the age of 1 month, the number of fixed suspensions according to the regression analysis did not depend on the dose. Such age-related peculiarities are expressed in the decrease of the coefficient for the factor "Irradiation dose" by 0.6 ± 0.1 and compensatory increase of the coefficient for the factor "Age*dose" in mice aged 1 month (Table 2).

The mean time of one static suspension, which statistically significantly depended on age and exposure

Table 3. Results of assessing the influence of various factors on the indices in the tail-suspension test using multivariate variance analysis in a general linear model

Factors	*F*	*F*	Coefficients	
Time to first suspension, sec (R^2 = 0.28)				
Gender of animals	6.44	0.011	male: 8 ± 3	female: 0
Age of animals	222.23	< 0.001	1 month: 0	6 months: 49 ± 3
Stress	1.96	0.16	stress–: 0	stress+: 0
Radiation dose	19.85	< 0.001	D · (3 ± 0.8)	
Stress*Age	4.59	0.032	stress–, 1 month: 0 stress+, 1 month: 0	stress–, 6 months: 0 stress+, 6 months: -16 ± 8
Total suspension time, sec (R^2 = 0.356)				
Gender of animals	0.027	0.87	male: 0	female: 0
Age of animals	320.9	< 0.001	1 month: 0	6 months: -75 ± 5
Stress	7.57	0.006	stress–: 0	stress+: 40 ± 8
Radiation dose	73.42	< 0.001	D · (-9.4 ± 1.1)	
Stress*age	19.17	< 0.001	stress–, 1 month: 0 stress+, 1 month: -49 ± 11	stress–, 6 months: 0 stress+, 6 months: 0
Number of suspensions (R^2 = 0.126)				
Gender of animals	0.004	0.95	male: 0	female: 0
Age of animals	30.04	< 0.001	1 month: 0	6 months: -0.5 ± 0.04
Stress	18.78	< 0.001	stress–: 0	stress+: 2.9 ± 0.5
Radiation dose	15.2	< 0.001	D · (-0.6 ± 0.1)	
Stress*age	15.79	< 0.001	stress–, 1 month: 0 stress+, 1 month: 0	stress–, 6 months: 0 stress+, 6 months: -2.8 ± 0.7
Age*dose	28.17	< 0.001	1 months: D · (-0.5 ± 0.04)	6 months: D 0
Average time of one suspension, sec (R^2 = 0.126)				
Gender of animals	0.002	0.97	male: 0	female: 0
Age of animals	114.97	< 0.001	1 month: 0	6 months: -5.7 ± 0.9
Stress	1.67	0.2	stress–: 0	stress+: 0
Radiation dose	19.42	< 0.001	D · (-0.14 ± 0.021)	
Gender*age	8.57	0.004	male, 1 month: 3.3 ± 1.1 male, 6 months: 0	female, 1 month: 0 female, 6 months: 0
Age*dose	13.33	< 0.001	1 month: D (-1.0 ± 0.27)	6 months: D · 0

Table prepared by the authors using their own data

Note: "stress–" — absence of a stress factor associated with animal irradiation (group BK); "stress+" — presence of a stress factor associated with animal irradiation (groups 0 Gy, 0.1 Gy, 1 Gy, 5 Gy)

dose, was independent of sex and stress. In animals aged 6 months, the mean time of one static suspension was 5.7 ± 0.9 s shorter than in animals aged 1 month. Upon irradiation, this index decreased with increasing dose of 1 Gy by an average of 0.14 ± 0.021 s. It should also be noted that a combination of the factors "Sex*age" and "Age*dose" had a statistically significant effect on the value of the average time of one static suspension. In males at the age of 1 month, the time of one static suspension was 3.3 ± 1.1 seconds longer than in the same males at the age of 6 months and females at the age of 1 and 6 months. The influence of modifying effect of age was manifested in the absence of statistically significant dependence of this index on the irradiation dose at the age of 6 months, although at the age of 1 month the mean time of one static suspension decreased with dose by 1.0 ± 0.27 s with increasing dose by 1 Gy (Table 3).

DISCUSSION

The study revealed that fractionated irradiation at an early age led to a dose-dependent reduction of depression-like behavior in mice in the tail retention test, maximally expressed at a total dose of 5.2 Gy. This is indicated by changes in all the parameters recorded in this test: the total time of immobility, interpreted as despair behavior, is reduced; animals make longer attempts to free themselves from an unpleasant position before suspension motionless for the first time; the number of such acts of immobile suspension and the average duration of one immobile suspension are reduced.

In animals at the age of 6 months, less pronounced signs of depression-like behavior were observed than at the earlier age: thus, in the biological control group, the total immobility time decreased more than 2-fold with age, while 2.5-fold longer mice tried to actively free themselves

before motionless suspension for the first time. At the same time, the previously revealed effects of irradiation were fully preserved: the signs of depression-like behavior of irradiated animals decreased with increasing dose of irradiation.

This effect of irradiation was rather unexpected: the development of depression-like behavior in rodents has been described in the literature at acute irradiation at comparable doses. Thus, when rats at the age of 3 days were irradiated at a dose of 5 Gy, an increase in immobility time in the tail retention test and the Porsolt forced swimming test was observed after 120 days without any change in their general motor activity [12]. In this study, the authors also revealed hypoplasia of the granular layer of the dentate gyrus of the hippocampus, impaired division of neuronal stem cells, and changes in the process of their migration and maturation, which may represent the physiological basis of the behavioral changes [12].

An important role of neurogenetic changes in the dentate gyrus of the hippocampus in the development of post-tradiation depression was also revealed when studying the effects of targeted irradiation of the dentate gyrus compared to total brain irradiation in mice at the age of 10 days [10]. Here, 3 months after irradiation, an increase in anxiety was detected in the elevated cruciform maze at acute irradiation at doses of 0.25 Gy, along with an increase in anxiety detected in the test of glass bead burying at acute irradiation at doses of 0.5 Gy and an increase in manifestations of depressive behavior in the forced swimming test at acute irradiation at doses of 0.25 Gy. All effects were more pronounced at targeted irradiation of the ventral part of the dentate gyrus.

At fractionated X-ray irradiation in cumulative doses of 0.4 and 0.5 Gy (single dose of 0.1 Gy), more anxious behavior in the open-field test was observed in mice [17]. In long-term modeling of chronic neutron-photon irradiation, an increase in anxiety in the open-field test was revealed in mice at a cumulative dose of 0.4 Gy over 600 days of irradiation [18]. However, a decrease in the severity of the effects with dose fractionation was also shown compared to acute irradiation: while acute irradiation at a dose of 5 Gy resulted in inhibition of neurogenesis in the dentate gyrus, as well as learning and memory deficits in the test for contextual fear conditioning and memory deficits in the test for recognition of new objects, when this dose was divided into 10 daily fractions, no such behavioral changes were observed, and the inhibition of neurogenesis was insignificant [19].

In our studies, fractionated gamma-irradiation during the first month of life at a cumulative dose of 5.2 Gy led not only to a decrease in depression-like behavior, but also, as previously reported, to the formation of the least anxious phenotype: anxiety indices in the elevated cross-shaped maze and the glass bead burial test decreased in animals irradiated at this dose [20]. An increase in anxiety and neophobic behavior was observed at a cumulative dose of 0.1 Gy [20], which, however, was not accompanied by an increase in the manifestations of depression.

It is important to note the revealed influence of early-life stress on the development of signs of depression over long periods following the end of stress exposure. The stress factor in this study is manipulation in the process of irradiation or its imitation over the course of the first month of the animals' life. Thus, while at the age of 1 month the indices of depression-like behavior of mice in the 0 Gy false irradiation group were close to those of intact animals of the biological control group, at the age of 6 months significant differences were observed indicating the development of depression-like behavior in mice of the false irradiation group. These results are quite consistent with both the results of modeling stress at an early age in mice [21] and clinical data on the increased risk of developing anxiety and depressive psychopathologies in people who have suffered mental traumas in childhood [22, 23].

However, according to the obtained data, the indices of depression-like behavior in animals exposed to both stress factor and fractionated irradiation decreased in a dose-dependent manner up to the biological control values at an irradiation dose of 5.2 Gy. Similar results were obtained in a study of diazepam-induced depression in rats, where X-ray irradiation at a dose of 3 Gy divided into 6 fractions led to a decrease in depressive symptomatology and normalization of neurotransmitter levels [24].

A number of studies have also revealed weak neuroprotective effects of a single irradiation at doses up to 0.1 Gy, such as a decrease in signs of proinflammatory activation of microglia, an increase in the density of neurons in the dentate gyrus of the hippocampus, and an increase in the functional activity of mitochondria [1, 25, 26]. Such changes in the hippocampal dentate gyrus may underlie the described antidepressant symptomatology of irradiated animals.

CONCLUSIONS

1. A dose-dependent change in depressive-like behavior in mice under fractionated irradiation in the first month of life (the period of active brain maturation) was revealed; with increasing total dose from 0.1 Gy to 5 Gy, indices of depressive behavior decreased. This pattern is shown both in the early period immediately following the completion of irradiation (at the age of 1 month) and over longer periods of time (at the age of 6 months).

2. Stress suffered in early age led to the development of depression-like behavior in adult unexposed mice; however, under simultaneous exposure to stress and fractionated irradiation in doses of 1–5 Gy, the indices of depression-like behavior of mice at the age of 6 months did not differ from intact animals.

References

1. Atamanyuk NI. The effect of moderate and low doses of ionizing radiation of higher nervous activity of human and animals. *Extreme medicine.* 2023;25(3):5–13 (In Russ.). https://doi.org/10.47183/mes.2023.029
2. Tanguturi SK, Alexander BM. Neurologic complications of radiation therapy. *Neurol Clin*. 2018;36(3):599–625. https://doi.org/10.1016/s0733-8619(02)00031-2
3. Pasqual E, Boussin F, Bazyka D, Nordenskjold A, Yamada M, Ozasa K et al. Cognitive effects of low dose of ionizing radiation — Lessons learned and research gaps from epidemiological and biological studies. *Environ Int*. 2021;147:106295. https://doi.org/10.1016/j.envint.2020.106295
4. Loganovsky K, Marazziti D. Mental health and neuropsychiatric aftermath 35 years after the chernobyl catastrophe: current state and future perspectives. *Clin Neuropsychiatry*. 2021;18(2):101–6. https://doi.org/10.36131/cnfioritieditore20210204
5. Loganovsky KN, Masiuk SV, Buzunov VA, Marazziti D, Voychulene YS. Radiation risk analysis of neuropsychiatric disorders in ukrainian chornobyl catastrophe liquidators. *Front Psychiatry*. 2020;(11):553420. https://doi.org/10.3389/fpsyt.2020.553420
6. Contis G, Foley TP, Jr. Depression, suicide ideation, and thyroid tumors among ukrainian adolescents exposed as children to chernobyl radiation. *J. Clin. Med. Res*. 2015;(7):332–8. https://doi.org/ 10.14740/jocmr2018w
7. Balashov PP, Bujkov VA, Kolmogorova VV, Burtovaja EJ. Clinic variants of organic disorders with depressive manifestation in exposed to radiation population in the area of radioactive accidents in the South Urals. *Siberian herald of psychiatry and addiction psychiatry.* 2009;(3):92–5 (In Russ.). EDN: KTYYGB
8. Collett G, Craenen K, Young W, Gilhooly M, Anderson RM. The psychological consequences of (perceived) ionizing radiation exposure: a review on its role in radiation-induced cognitive dysfunction. *Int J Radiat Biol*. 2020; 96 (9): 1104–1118. https://doi.org/10.1080/09553002.2020.1793017
9. Njamnshi AK, Ahidjo N, Ngarka L, Nfor LN, Mengnjo MK, Njamnshi WY et al. Characterization of the Cognitive and motor changes revealed by the elevated plus maze in an experimental rat model of radiation-induced brain injury. *Adv Biomed Res*. 2020;9:72. https://doi.org/10.4103/abr.abr_62_20
10. Dos Santos M, Kereselidze D, Gloaguen C, Benadjaoud MA, Tack K, Lestaevel P, Durand C. Development of whole brain versus targeted dentate gyrus irradiation model to explain low to moderate doses of exposure effects in mice. *Sci Rep*. 2018;8(1):17262. https://doi.org/10.1038/s41598-018-35579-x
11. Whoolery CW, Walker AK, Richardson DR, Lucero MJ, Reynolds RP, Beddow DH et al. Whole-Body exposure to 28Si-radiation dose-dependently disrupts dentate gyrus neurogenesis and proliferation in the short term and new neuron survival and contextual fear conditioning in the long term. *Radiat Res*. 2017;188(5):532–51. https://doi.org/10.1667/RR14797.1
12. Wang H, Ma Z, Shen H, Wu Z, Liu L, Ren B et al. Early life irradiation-induced hypoplasia and impairment of neurogenesis in the dentate gyrus and adult depression are mediated by MicroRNA- 34a-5p/T-Cell intracytoplasmic antigen-1 pathway. *Cells*. 2021;10(9):2476. https://doi.org/10.3390/cells10092476
13. Pitzer C, Kurpiers B, Eltokhi A. Sex differences in depression-like behaviors in adult mice depend on endophenotype and strain. *Front Behav Neurosci*. 2022; 16: 838122. https://doi.org/10.3389/fnbeh.2022.838122
14. Shishkina EA, Atamanyuk NI, Peretykin AA, Pryakhin EA. Whole organism doses and their uncertainties during mice exposure at the gamma radiobiological installation IGUR-1M. *ANRI.* 2024; 117(2): 63–75 (In Russ.). https://doi.org/0.37414/2075-1338-2024-117-2-63-75
15. Can A, Dao DT, Terrillion CE, Piantadosi SC, Bhat S, Gould TD. The tail suspension test. *J Vis Exp*. 2012;59:e3769. https://doi.org/10.3791/3769
16. R Core Team. R: A language and environment for statistical computing. R Foundation for Statistical Computing, Vienna, Austria; 2022. Available at: https://www.R-project.org.
17. Koturbash I, Jadavji NM, Kutanzi K, Rodriguez-Juarez R, Kogosov D, Metz GAS et al. Fractionated low-dose exposure to ionizing radiation leads to DNA damage, epigenetic dysregulation, and behavioral impairment. *Environ Epigenet*. 2017;2(4):dvw025. https://doi.org/10.1093/eep/dvw025
18. Perez RE, Younger S, Bertheau E, Fallgren CM, Weil MM, Raber J. Effects of chronic exposure to a mixed field of neutrons and photons on behavioral and cognitive performance in mice. *Behav Brain Res*. 2020;379:112377. https://doi.org/10.1016/j.bbr.2019.112377
19. Tang FR, Loke WK, Wong P, Khoo BC. Radioprotective effect of ursolic acid in radiation-induced impairment of neurogenesis, learning and memory in adolescent BALB/c mouse. *Physiol Behav*. 2017;175:37–46. https://doi.org/10.1016/j.physbeh.2017.03.027
20. Atamanyuk NI, Obvintseva NA, Peretykin AA, Pryakhin EA. The dose-dependent effect of fractionated γ-radiation on anxiety-like behavior in neonatal mice. *Bull Exp Biol Med*. 2024;176(6):727–30. https://doi.org/10.1007/s10517-024-06097-w
21. He T, Guo C, Wang C, Hu C, Chen H. Effect of early life stress on anxiety and depressive behaviors in adolescent mice. *Brain Behav*. 2020;10(3):e01526. https://doi.org/10.1002/brb3.1526
22. Ochi S, Dwivedi Y. Dissecting early life stress-induced adolescent depression through epigenomic approach. *Mol Psychiatry*. 2023;28(1):141–53. https://doi.org/10.1038/s41380-022-01907-x
23. Juruena MF. Early life stress, depression and epigenetics. *Vitam Horm*. 2023;(122):307–37. https://doi.org/10.1016/bs.vh.2023.01.004
24. Kaur A, Singla N, Dhawan DK. Low dose X-irradiation mitigates diazepam induced depression in rat brain. *Regul Toxicol Pharmacol*. 2016;(80):82–90. https://doi.org/10.1016/j.yrtph.2016.06.004
25. Casciati A, Dobos K, Antonelli F, Benedek A, Kempf SJ, Bellés M et al. Age-related effects of X-ray irradiation on mouse hippocampus. *Oncotarget*. 2016;7(19):28040–58. https://doi.org/10.18632/oncotarget.8575
26. Ung MC, Garrett L, Dalke C, Leitner V, Dragosa D, Hladik D et al. Dose-dependent long-term effects of a single radiation event on behaviour and glial cells. *Int J Radiat Biol*. 2021;97(2):156–69. https://doi.org/10.1080/09553002.2021.1857455

Authors' contributions. All the authors confirm that they meet the ICMJE criteria for authorship. The most significant contributions were as follows: Nadezhda A. Obvintseva — writing the manuscript, conducting experiments, analyzing data; Natal'ya I. Atamanyuk — planning and conducting experiments, article design; Irina A. Shaposhnikova — test analysis; Andrej A. Peretykin — animal irradiation, statistical data analysis; Evgeny A. Pryakhin — development of research design, approval of the final version of the manuscript for publication.

AUTHORS

Nadezhda A. Obvintseva
https://orcid.org/0000-0001-5914-8913
n_obvintseva@mail.ru

Natal'ya I. Atamanyuk, Cand. Sci. (Biol.)
https://orcid.org/0000-0001-8293-2730
vita_pulhra@mail.ru

Irina A. Shaposhnikova, Cand. Sci. (Biol.)
https://orcid.org/0000-0002-0769-8267
shaposhnikova@lenta.ru

Andrej A. Peretykin
https://orcid.org/0000-0003-0929-9531
peretykin@urcrm.ru

Evgeny A. Pryakhin, Dr. Sci. (Biol.), Professor
https://orcid.org/0000-0002-5990-9118
pryakhin@urcrm.ru

https://doi.org/10.47183/mes.2024-26-3-40-50

MOLECULAR AND GENETIC CHARACTERISTICS FROM PHYLOGENETIC ANALYSIS OF RUSSIAN AND FOREIGN VARIANTS OF MEASLES VIRUS 2020–2024

Ekaterina N. Chernyaeva[1], Kirill V. Morozov[1]✉, Alina D. Matsvay[1], Maria S. Guskova[1], Andrey Y. Nekrasov[1], Ivan F. Stetsenko[1], Anastasiya O. Nosova[1], Olga G. Kurskaya[2], Alexander M. Shestopalov[2], German A. Shipulin[1]

[1] Centre for Strategic Planning and Management of Biomedical Health Risks of the Federal Medical Biological Agency, Moscow, Russia

[2] Federal Research Center for Fundamental and Translational Medicine, Novosibirsk, Russia

Introduction. Over the past two years, there has been an increase in measles morbidity in Russia and other countries. In order to assess the heterogeneity of clinically significant strains of *Measles morbillivirus* to reveal the sources of infection and transmission routes strains, a molecular genetic study thus becomes an urgent task. In this paper, a genetic identification of clinical strains of measles virus detected in 2023–2024 is compared with global variants as well as Russian strains detected in previous years.

Materials and methods. Forty measles virus genome sequences isolated from nasopharyngeal swab samples obtained in Moscow and Novosibirsk in 2023–2024 were included in the study. The data were then compared with strains collected in Russia in May 2023 and deposited at the Central Research Institute of Epidemiology, as well as strains collected in 2020 and 2021 in Moscow.

Results. The nucleotide sequences of studied *Measles morbillivirus* strains were categorized into different phylogenetic groups within genotype D8. For samples of genotype B3 collected in 2020 and 2023, a comparative analysis was performed to identify the region of origin. Phylogenetic analysis of Russian and foreign variants of measles virus suggests that strains currently circulating in Russia may be a variety of strains that had previously circulated in other countries and independently spread to Russia in 2023. After analyzing the most frequent nucleotide substitutions in various measles virus genes, the most variable genes were identified to provide a basis for the extension of phylogenetic analysis.

Conclusions. The proposed approach to molecular genetic testing of complete and partial genome sequences of clinical isolate of measles virus detected in 2023–2024 in Moscow and Novosibirsk made it possible to identify strain subgroups that differ in origin. The comparison of the *Measles morbillivirus* strains sequenced in the present research with global sequences allowed us to detect similar sequences identified both in 2023 and in previous years in various countries of the world. The analysis of epidemiologically significant strains of *Measles morbillivirus* shows that N gene can be used to reliably determine the main genotype; however, this approach is not sufficient for studying the transmission pathways of the virus.

Keywords: measles; measles virus; molecular genetic testing; phylogenetic testing; full genome sequencing

For citation: Chernyaeva EN, Morozov KV, Matsvay AD, Guskova MS, Nekrasov AY, Stetsenko IF, Nosova AO, Kurskaya OG, Shestopalov AM, Shipulin GA. Molecular and genetic characteristics from phylogenetic analysis of Russian and foreign variants of measles virus 2020–2024. *Extreme Medicine*. 2024;26(3):40–50. https://doi.org/10.47183/mes.2024-26-3-40-50

Funding: the study was performed within the framework of the state assignment of FMBA of Russia No. 388-03-2024-155.

Compliance with ethical principles: the study was approved by the local ethical committee of the Federal Research Center for Fundamental and Translational Medicine (protocol #7/1 of March 16, 2023). All patients signed voluntary informed consent for the study.

Potential conflict of interest: German A. Shipulin is a member of the Editorial Council of the Journal “Extreme Medicine”. The other authors declare no conflict of interest.

✉ Kirill V. Morozov kmorozov@cspfmba.ru

Received: 20 Aug. 2024 **Revised:** 11 Oct. 2024 **Accepted:** 14 Oct. 2024

МОЛЕКУЛЯРНО-ГЕНЕТИЧЕСКАЯ ХАРАКТЕРИСТИКА И ФИЛОГЕНЕТИЧЕСКИЙ АНАЛИЗ РОССИЙСКИХ И ЗАРУБЕЖНЫХ ВАРИАНТОВ ВИРУСА КОРИ 2020–2024 гг.

Е.Н. Черняева[1], К.В. Морозов[1]✉, А.Д. Мацвай[1], М.С. Гуськова[1], А.Ю. Некрасов[1], И.Ф. Стеценко[1], А.О. Носова[1], О.Г. Курская[2], А.М. Шестопалов[2], Г.А. Шипулин[1]

[1] Центр стратегического планирования и управления медико-биологическими рисками здоровью Федерального медико-биологического агентства, Москва, Россия

[2] Федеральный исследовательский центр фундаментальной и трансляционной медицины, Новосибирск, Россия

Введение. Молекулярно-генетическое исследование штаммов *Measles morbillivirus*, позволяющее оценивать гетерогенность клинически значимых штаммов, определять источники заражения и пути передачи инфекции, в настоящее время является актуальной задачей. В последние два года наблюдается рост заболеваемости корью в России и других странах. В данной работе мы даем генетическую характеристику клинических штаммов вируса кори, выявленных в 2023–2024 гг., и сравниваем их с глобальными вариантами, а также с российскими штаммами, выявленными в предыдущие годы.

Цель. Молекулярно-генетическая характеристика штаммов вируса кори, выявленных в России в период повышенной заболеваемости в 2023–2024 гг. в двух крупных городах — Москве и Новосибирске, и их дальнейший филогенетический анализ.

Материалы и методы. В исследование включены 40 полученных в Москве и Новосибирске в 2023–2024 гг. последовательностей генома вируса кори, выделенного из образцов назофарингеального мазка. Данные сравнивали со штаммами, собранными в России в мае 2023 г., депонированными ЦНИИ эпидемиологии Роспотребнадзора, и штаммами, собранными в 2020 и 2021 гг. в Москве.

Результаты. Изученные нуклеотидные последовательности *Measles morbillivirus* разделены на разные филогенетические группы в пределах генотипа D8. Для образцов генотипа B3, собранных в 2020 и 2023 гг., проведен сравнительный анализ с целью определения региона происхождения. Филогенетический анализ российских и зарубежных вариантов вируса кори позволяет предположить, что штаммы, циркулирующие в настоящее время в России, могут быть разновидностью штаммов, ранее циркулировавших в других странах и независимо распространившихся в России в 2023 г. Проведен анализ наиболее частых нуклеотидных замен в различных генах вируса кори. Определены наиболее вариабельные гены, на основе которых можно расширить филогенетический анализ.

Выводы. Предложенный подход к молекулярно-генетическому исследованию полных и частичных последовательностей геномов клинических штаммов вируса кори, обнаруженных в 2023–2024 гг. в Москве и Новосибирске, дал возможность выделить подгруппы, отличающиеся по происхождению. Сравнение секвенированных нами штаммов *Measles morbillivirus* с глобальными последовательностями позволило обнаружить близкие последовательности, выявленные как в 2023 г., так и в предыдущие годы на территории различных стран мира. Из анализа эпидемически значимых штаммов *Measles morbillivirus* следует, что использование гена N позволяет с высокой достоверностью определять основной генотип, однако не является достаточным для изучения путей передачи вируса.

Ключевые слова: корь; вирус кори; молекулярно-генетический анализ; филогенетический анализ; полногеномное секвенирование

Для цитирования: Черняева Е.Н., Морозов К.В., Мацвай А.Д., Гуськова М.С., Некрасов А.Ю., Стеценко И.Ф., Носова А.О., Курская О.Г., Шестопалов А.М., Шипулин Г.А. Молекулярно-генетическая характеристика и филогенетический анализ российских и зарубежных вариантов вируса кори 2020–2024 гг. *Медицина экстремальных ситуаций*. 2024;26(3):40–50. https://doi.org/10.47183/mes.2024-26-3-40-50

Финансирование: Работа выполнена в рамках государственного задания ФМБА России № 388-03-2024-155.

Соответствие принципам этики: исследование одобрено локальным этическим комитетом Федерального государственного бюджетного научного учреждения «Федеральный исследовательский центр фундаментальной и трансляционной медицины» (протокол № 7/1 от 16 марта 2023 г.). Все пациенты подписали добровольное информированное согласие на исследование.

Потенциальный конфликт интересов: Г.А. Шипулин — член редакционного совета журнала «Медицина экстремальных ситуаций». Остальные авторы заявляют об отсутствии конфликта интересов.

✉ Морозов Кирилл Владимирович kmorozov@cspfmba.ru

Статья поступила: 20.08.2024 **После доработки:** 11.10.2024 **Принята к публикации:** 14.10.2024

INTRODUCTION

Measles is a highly infectious acute disease caused by an RNA virus belonging to the genus *Morbillivirus* in the family *Paramyxoviridae*. Despite the existence of a safe and effective vaccine, measles remains one of the leading causes of child mortality worldwide.

According to WHO, in 2022, after years of declining measles vaccination coverage, the number of measles cases increased by 18%, while the number of deaths due to measles infection increased by 43% (compared to data for 2021, when the number of deaths was 128,000) [1]. The incidence of measles in Russia in previous years ranged from 100 cases in 2010 to 4,500 cases in 2019, which were distributed in more than 60 regions of the country. Only one case was registered in 2021 and 100 cases in 2022 [2]. During the SARS-CoV-2 pandemic, more than 61 million doses of measles vaccine were delayed or missed in a number of countries around the world, including as part of routine childhood vaccination. For this reason, an increase in the vulnerable proportion of the population, and consequently the risk of localized measles outbreaks was only to be expected [3, 4].

In early 2023, measles outbreaks were detected in almost all regions of the world. By the end of November 2023, more than 42,200 cases of measles virus infection had been reported in the European Union, five of which were fatal [5, 6]. According to Russian Federal Service for Surveillance on Consumer Rights Protection and Human Wellbeing (Rospotrebnadzor), more than 13,000 people (8.9 per 100,000 population) contracted measles in 44 regions of Russia in 2023. Most cases (67.9%) of the total number of registered cases were detected in children aged 0 to 17 years inclusive, two of which were fatal. In 2023, 2,244 cases of measles (17.18 per 100,000 population) were registered in Moscow; in the same year, 266 cases of measles (9.5 per 100,000 population) were registered in Novosibirsk [7]. The head of the Russian Federal Service for Surveillance on Consumer Rights Protection and Human Wellbeing (Rospotrebnadzor) noted that, since all outbreaks were local and quickly controlled, no global restrictive measures were required. [8].

In addition to local outbreaks, migrant and refugee flows can pose a great threat to Russia. According to the UN, as of July 2022, about 1.8 million Ukrainian refugees had arrived in Russia [9]. According to WHO, in the European region Ukraine had the worst situation in terms of detected measles cases in recent years (more than 57,000 cases were reported in 2019) [10]. In 2023, large measles outbreaks also occurred in Russia's neighboring countries with which there is reduced migration control, such as Azerbaijan, Kazakhstan, Uzbekistan, Tajikistan and Armenia. Some of these countries had also experienced measles outbreaks in previous years, such as Uzbekistan in 2019 [11]. Since this situation may lead to a significantly increased incidence of measles in Russia in the near future, is crucial to monitor the spread of different strains of measles virus and conduct timely phylogenetic analysis to determine the origin of each specific strain.

In order to trace and determine the origin of a measles virus strain, genotyping by sequencing is most commonly carried out on the nucleoprotein gene, which is considered to be the most variable. The sequencing of 450 nucleotides encoding 150 amino acids of the C-terminal domain of the nucleoprotein (N450) is the most common approach for genotyping measles virus strains. Over 11,000 nucleotide sequence records for this domain have been uploaded to the MeaNS2 database from 2019–2022 alone [12]. However, the N450 sequence is often insufficient to separate endemic strain lineages circulating in neighboring regions of the country. The resolution of measles molecular epidemiologic analysis can be improved by using a larger measles virus genome fragment for nucleotide sequence analysis. Although full-genome sequencing may be most effective in this case, this method has the significant disadvantage of high cost. The feasibility of extended genome

fragment sequencing should be evaluated in comparison with full-genome sequencing data.

In this work, we aim to carry out a molecular genetic testing of measles virus strains detected in Russia during the period of increased morbidity in 2023–2024 in the major cities of Moscow and Novosibirsk and conduct their further phylogenetic analysis.

MATERIALS AND METHODS

40 clinical specimens were collected from Novosibirsk and Moscow patients diagnosed with measles during outbreaks that occurred in 2023–2024. They were collected at the Federal Research Center for Basic and Translational Medicine (Novosibirsk) and the Center for Strategic Planning and Management of Biomedical Health Risks of the Federal Medical and Biomedical Agency (FMBA). Archival samples identified in Moscow in 2020 were also investigated. Genotyping was performed to identify the strain of measles virus for all samples included in the study. For genetic typing of measles virus, the data of comparative analysis of nucleotide sequences of the C-terminal domain of the nucleoprotein N gene (450 nt (nucleotides), 1,126–1,575 nt) are used; in order to achieve a more detailed characterization, fragments (850 nt) of the hemagglutinin H gene were additionally analyzed in some samples (n = 15). Since these genes are the most variable structural genes of the virus, they are best suited for determining the origin and pathways of individual measles virus strains. In addition, full genome sequencing was performed for three measles virus samples. The data obtained were compared with strains collected in Russia in May 2023 and deposited in the Central Research Institute of Epidemiology (see Table 1 for a complete list of measles virus samples from Russia used in this work).

For the comparative phylogenetic analysis of measles virus, both N and H gene fragments and full-genome sequencing data strains prevalent in Russia in 2020–2024, as well as global genetic variants, were used. Measles virus samples obtained from 40 patients from Moscow (n = 11) and Novosibirsk (n = 29) in 2023–2024, as well as two samples from Moscow detected in 2020 and 2021, were included in the analysis. All samples were obtained with full informed consent of the donors and in compliance with all necessary ethical standards.

Viral RNA isolated from clinical nasopharyngeal swab samples using the previously developed Ribo-prep purification kit was subjected to reverse transcription using AmpliTest Revert (AmpliTest, Russia) [13]. Fragments of the C-terminal domain of the N-gene as well as a fragment of the H-gene were amplified using LongAmp® Taq DNA polymerase (New England Biolabs, USA) and primers described in Table 2. Sanger sequencing was performed using BigDye™ Terminator v3.1 cyclic sequencing kit (Thermo Fisher Scientific, USA) and Applied Biosystems 3500 genetic analyzer (Thermo Fisher Scientific, USA). Three samples were sequenced by full-genome sequencing: total RNA was used for library preparation using NEBNext® Ultra™ II RNA Library Prep kit (NEB, USA); sequencing was performed using MiSeq platform and MiSeq Reagent Kit v2 (500 cycles) (Illumina, USA). The primers were taken from Schulz et al. and further optimized for our task [14].

As well as the full-genome sequences of six Russian measles virus samples isolated in 2023 and studied at the Central Research Institute of Epidemiology obtained from the NCBI GeneBank database [15], the gene sequences of N and H strains detected in 2019–2024 in different countries were additionally selected, along with the full-genome sequences for the same period from the open GenBank database. To permit a deeper comparison, the genome sequences of vaccine strains available in the GenBank database [15] were added to the study.

Metagenomic assembly of complete measles virus genome sequences was performed using Trimmomatic v0.39 software to remove adapter sequences and SPAdes Genome Assembler v3.15.5 to assemble the viral genome [16]. The sequences of N and H gene fragments obtained by Sanger sequencing were combined into one for further alignment and analysis.

Multiple alignment was performed using the MAFFT v7.505 package [17]. Phylogenetic analysis was performed using the FastTree program version 2.1.11 SSE3 [18] using the GTR+CAT model (a general time reversible model with a fixed rate for each site (an approximation of the CAT model)) and 100 bootstrap replications. The dolphin measles virus genome sequence (AJ608288) was used as an outgroup for cladogram generation.

Phylogenetic trees were analyzed using the FigTree v.1.4.4 program. The results of comparative analysis were visualized using the Matplotlib 3.6.2 and Seaborn 0.13.2 packages for the Python programming language.

RESULTS

According to the results of genotypic analysis, most of the samples (n = 44) collected in 2023–2024 turned out to belong to genotype D8 and only one to genetic variant B3 (Table 1). Phylogenetic analysis of partial sequencing of the N gene (Fig.1) showed that most of the samples from Russia formed a cluster within the D8 genotype, which also included some strains found abroad:

- PP056610 (2023) from China, which has the highest similarity to Mea12 from Moscow;
- OR733283 (2021) from Tajikistan, PP319645 (2023) from the USA and PP229487 (2023) from Switzerland, which are located phylogenetically closer on the tree to the Mea6 specimen from Novosibirsk;
- PP319658 (2023) from USA and PP274936 (2024) from Bosnia and Herzegovina are closest to Mea49 from Novosibirsk and a group of specimens from Moscow including Mea43 and Mea2.

This phylogenetic cluster includes two subclusters, one of which was formed by samples from Novosibirsk (A), while the second cluster includes three samples from Moscow and two from Novosibirsk (B). The strains sequenced formed a phylogenetic group with samples Mea2 and Mea43 from Moscow.

Only two sequences of the N gene of measles virus samples detected in 2023 in Russia could be classified as representatives of phylogenetic group B3 — Mea48 registered in Novosibirsk and OR290098 sequenced by the Central Research Institute of Epidemiology with an unknown region

Table 1. List of samples collected in different Russian cities

No.	Internal sample identifier	Year of sample taken	City of detection	Sequenced section of the genome	Genotype of measles virus strain	Data source
1	Mea01	2023	Moscow	WGS	D8	Centre for Strategic Planning of FMBA of Russia
2	Mea02	2023	Novosibirsk	WGS	D8	Centre for Strategic Planning of FMBA of Russia
3	Mea04	2020	Moscow	WGS	B3	Centre for Strategic Planning of FMBA of Russia
4	Mea05	2023	Moscow	N	D8	Centre for Strategic Planning of FMBA of Russia
5	Mea06	2023	Novosibirsk	N,H	D8	Centre for Strategic Planning of FMBA of Russia
6	Mea07	2023	Novosibirsk	N,H	D8	Centre for Strategic Planning of FMBA of Russia
7	Mea08	2023	Novosibirsk	N,H	D8	Centre for Strategic Planning of FMBA of Russia
8	Mea10	2021	Moscow	N	B3	Centre for Strategic Planning of FMBA of Russia
9	Mea11	2023	Moscow region	N,H	D8	Centre for Strategic Planning of FMBA of Russia
10	Mea12	2023	Moscow	N,H	D8	Centre for Strategic Planning of FMBA of Russia
11	Mea13	2023	Moscow	N,H	D8	Centre for Strategic Planning of FMBA of Russia
12	Mea14	2023	Moscow	N,H	D8	Centre for Strategic Planning of FMBA of Russia
13	Mea15	2023	Novosibirsk	N	D8	Centre for Strategic Planning of FMBA of Russia
14	Mea16	2023	Novosibirsk	N	D8	Centre for Strategic Planning of FMBA of Russia
15	Mea17	2023	Novosibirsk	N	D8	Centre for Strategic Planning of FMBA of Russia
16	Mea18	2023	Novosibirsk	N	D8	Centre for Strategic Planning of FMBA of Russia
17	Mea20	2023	Novosibirsk	N	D8	Centre for Strategic Planning of FMBA of Russia
18	Mea21	2023	Novosibirsk	N	D8	Centre for Strategic Planning of FMBA of Russia
19	Mea22	2023	Novosibirsk	N	D8	Centre for Strategic Planning of FMBA of Russia
20	Mea23	2023	Novosibirsk	N	D8	Centre for Strategic Planning of FMBA of Russia
21	Mea24	2023	Novosibirsk	N	D8	Centre for Strategic Planning of FMBA of Russia
22	Mea25	2023	Novosibirsk	N	D8	Centre for Strategic Planning of FMBA of Russia
23	Mea26	2023	Novosibirsk	N	D8	Centre for Strategic Planning of FMBA of Russia
24	Mea27	2023	Novosibirsk	N	D8	Centre for Strategic Planning of FMBA of Russia
25	Mea28	2023	Novosibirsk	N	D8	Centre for Strategic Planning of FMBA of Russia
26	Mea29	2023	Novosibirsk	N	D8	Centre for Strategic Planning of FMBA of Russia
27	Mea30	2023	Novosibirsk	N	D8	Centre for Strategic Planning of FMBA of Russia
28	Mea31	2023	Novosibirsk	N	D8	Centre for Strategic Planning of FMBA of Russia
29	Mea32	2023	Novosibirsk	N	D8	Centre for Strategic Planning of FMBA of Russia
30	Mea33	2023	Novosibirsk	N	D8	Centre for Strategic Planning of FMBA of Russia
31	Mea34	2023	Novosibirsk	N	D8	Centre for Strategic Planning of FMBA of Russia
32	Mea35	2023	Novosibirsk	N	D8	Centre for Strategic Planning of FMBA of Russia
33	Mea36	2023	Novosibirsk	N	D8	Centre for Strategic Planning of FMBA of Russia
34	Mea37	2023	Novosibirsk	N	D8	Centre for Strategic Planning of FMBA of Russia
35	Mea39	2023	Moscow	N, H	D8	Centre for Strategic Planning of FMBA of Russia
36	Mea43	2023	Moscow	N, H	D8	Centre for Strategic Planning of FMBA of Russia
37	Mea44	2023	Moscow	N, H	D8	Centre for Strategic Planning of FMBA of Russia
38	Mea45	2023	Moscow	N, H	D8	Centre for Strategic Planning of FMBA of Russia
39	Mea46	2023	Moscow	N, H	D8	Centre for Strategic Planning of FMBA of Russia
40	Mea47	2024	Novosibirsk	N, H	D8	Centre for Strategic Planning of FMBA of Russia
41	Mea48	2024	Novosibirsk	N, H	B3	Centre for Strategic Planning of FMBA of Russia
42	Mea49	2024	Novosibirsk	N, H	D8	Centre for Strategic Planning of FMBA of Russia
43	OR290097	2023	No data	Full genome	D8	Central Research Institute of Epidemiology
44	OR290098	2023	No data	Full genome	B3	Central Research Institute of Epidemiology
45	OR290099	2023	No data	Full genome	D8	Central Research Institute of Epidemiology
46	OR290100	2023	No data	Full genome	D8	Central Research Institute of Epidemiology
47	OR290101	2023	No data	Full genome	D8	Central Research Institute of Epidemiology
48	OR290102	2023	No data	Full genome	D8	Central Research Institute of Epidemiology

Table prepared by the authors using their own data

Table 2. List of primer sequences for the sequencing of the N and H genes

Sequenced gene	Direct primer nucleotide sequence	Nucleotide sequence of reverse primer
gene N	TGGAGCTATGCCATGGGAGT	TAACAATGATGGAGGGTAGG
gene H (region 1)	CTGAAATTGTCTCYGGCTTC	GACCCAGGATTGCATGTC
gene H (region 2)	GATTTCAGCAACTGYATGGT	CTGATGTCTGRGTGACATCATG

Table prepared by the authors using their own data

of collection (Fig. 1, cluster B). These samples did not form a cluster with the gene sequences of viral strains detected in Russia in 2020 and 2021. In addition to the Russian samples, three more strains from Brazil, USA and Iran detected in 2023, as well as two strains from China and Switzerland detected in 2024, fell into phylogenetic cluster B3. Most *Measles morbillivirus* strains assigned to genotype B3 were detected before 2023.

According to phylogenetic analysis of N and H gene fragments, the Russian samples formed a subcluster within the D8 genotype. The results were used to clarify the phylogenetic structure of the population of the studied Russian strains. In particular, subcluster B within the D8 genetic group formed by samples Mea7, Mea8, Mea13, Mea44, and Mea45 was not confirmed (Figs. 2, 3) based on the analysis of the N gene alone.

The comparison of the results of phylogenetic analysis using only the N fragment and the sequence obtained by combining the sequences of the N and H gene fragments supports the conclusion that sequencing of the N gene is

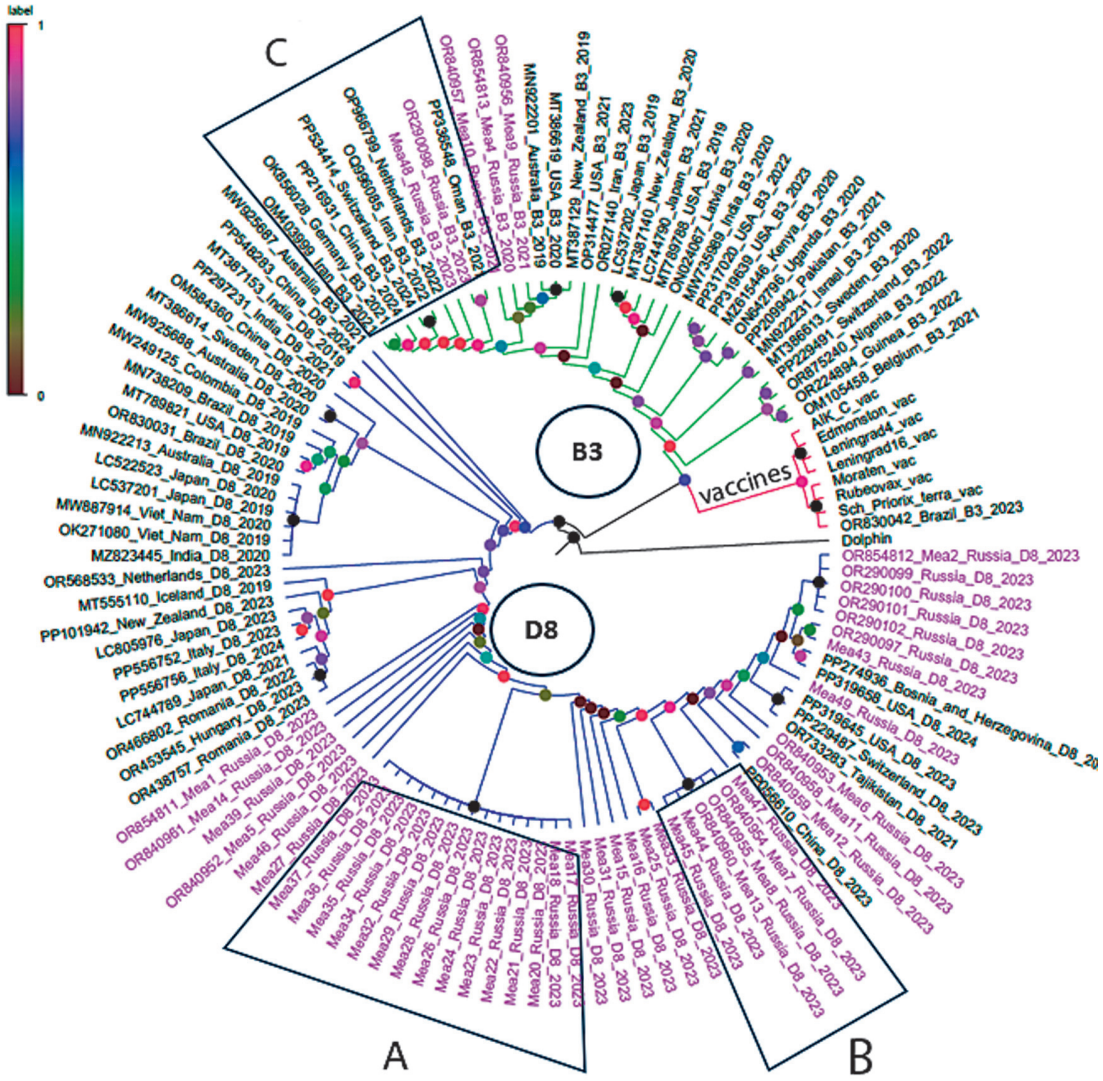

Figure prepared by the authors using their own data

Fig. 1. Phylogenetic relationships of *Measles morbillivirus* strains based on N-gene fragment sequencing data.
Phylogenetic group D8 is shown in blue, phylogenetic group B3 in green, and the group of vaccine strains in red. Genomes from Russia included in the analysis and sequenced in 2020, 2021 and 2023–2024 are highlighted in pink. Subcluster A consists of samples from Novosibirsk; subcluster B consists of samples from Moscow and Novosibirsk, which belong to the D8 genotype. Subcluster C of phylogenetic group B3 includes two samples — Mea48, discovered in Novosibirsk in 2023, and OR290098, sequenced by the Central Research Institute of Epidemiology with an unknown collection region.

sufficient to determine the genetic group of measles virus strains; however, in order to study the virus transmission routes, an extended analysis involving additional genome regions is necessary. An additional study of the H gene allows a more precise determination of genetic similarity between measles virus samples.

Complete genome sequencing was performed for two samples of genotype D8, which belong to two phylogenetically distant and identified in different cities strains: Mea1 (Moscow, 2023) and Mea2 (Novosibirsk, 2023). Full-genome sequencing was also performed for the Mea4 sample obtained in 2020 and belonging to genotype B3.

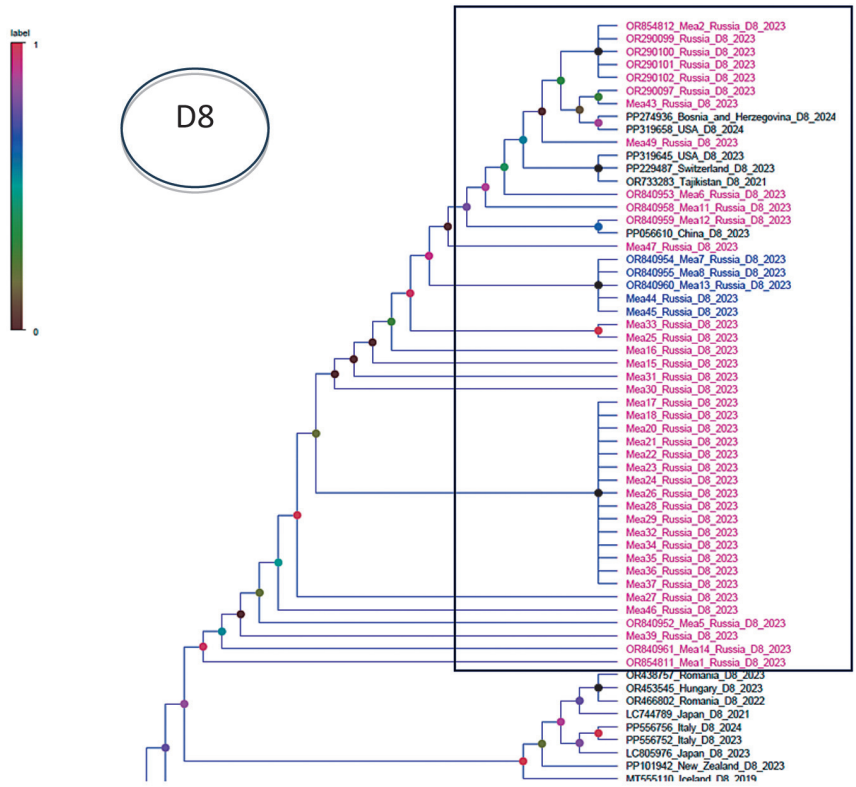

Figure prepared by the authors using their own data

Fig. 2. Position of the investigated Russian samples in cluster D8 obtained as a result of the phylogenetic analysis carried out using a fragment of the N gene sequence. The cluster formed by the studied Russian samples is highlighted with a rectangular frame; the samples are colored in blue and purple test colors. Samples Mea7, Mea8, Mea13, Mea44 and Mea45, which form subcluster B, are highlighted in blue.

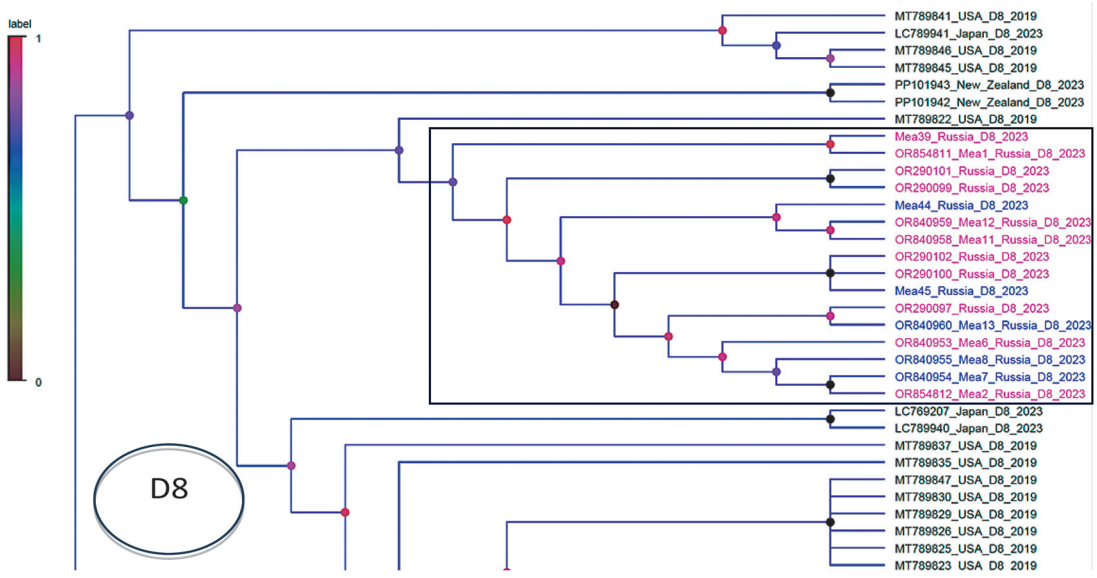

Figure prepared by the authors using their own data

Fig. 3. Position of the investigated Russian samples in cluster D8 obtained as a result of the phylogenetic analysis carried out using the combined sequence of the N and H genes. The cluster formed by the studied Russian samples is highlighted with a rectangular frame; the samples are colored in blue and purple test colors. Samples Mea7, Mea8, Mea13, Mea44 and Mea45, which form subcluster B, are highlighted in blue

Comparative analysis of the genomes revealed 145 nucleotide differences between Mea1 and Mea2, of which 39 fall in the intergenic space and 106 substitutions in various protein-coding fragments of the genes. The highest number of these are in the L (52 substitutions), N (17 substitutions), and H (15 substitutions) genes. This result suggests that these measles virus strains may have different origins.

For phylogenetic analysis of full-genome sequences, all available genomes from the GenBank database identified in the last 5 years and belonging to groups B3, D8, as well as sequences of vaccine strains, were included in the study. Phylogenetic analysis of full genome sequences of Russian strains with sequences found in other regions of the world showed that Russian strains are closest to the samples isolated in the USA and India in 2019, as well as to those collected in Japan and New Zealand in 2023; the corresponding data are presented in Figure 4.

The differences in the formed subgroups within measles virus genotypes obtained from phylogenetic analysis of virus strains raise the question of the efficiency of analysis based on the N gene alone. To further investigate this issue, a comparative analysis of phylogenetic trees generated based on the N gene, N and H genes, along with full-genome sequences, was performed by estimating the Hamming distance between pairs of strains within and between the B3 and D8 genotypes. The results of the analysis (Fig. 5) reflect the discriminatory power of phylogenetic analysis based on different numbers of genes.

The results of the analysis clearly demonstrate the sufficient discriminatory power of the N gene fragment analysis in determining D8 and B3 genotypes, but insufficient efficiency in separating phylogenetic groups within genotypes. The simultaneous analysis of N and H genes allows strains to be separated both within and between phylogenetic groups with higher accuracy, thus increasing the statistical significance and reliability of the study. Analysis of all protein-coding fragments and full-genome sequences significantly increases the accuracy of the study of virus transmission pathways within the same phylogenetic group (Fig. 5).

To assess the variability of *Measles morbillivirus* genes, we performed a comparative analysis of gene sequences in the study sample consisting of full-length genomes of measles virus strains from different countries belonging to the D8 and B3 genetic groups. The results of the comparative analysis were used to determine the total number of single-nucleotide variants in the genes of proteins N, L, M, F, PVC and H. The number and proportion of synonymous and nonsynonymous nucleotide variants were estimated (Fig. 6). The highest number of nucleotide substitutions was found in the L gene, which is the largest and encodes a viral RNA polymerase protein of 2183 amino acids. The distribution profile of mutations in the M gene encoding the virus matrix protein of 335 amino acids differed most markedly from the other genes. In particular, this gene had more nonsynonymous substitutions (n = 114) than synonymous substitutions (n = 71). The PVC gene, which encodes several

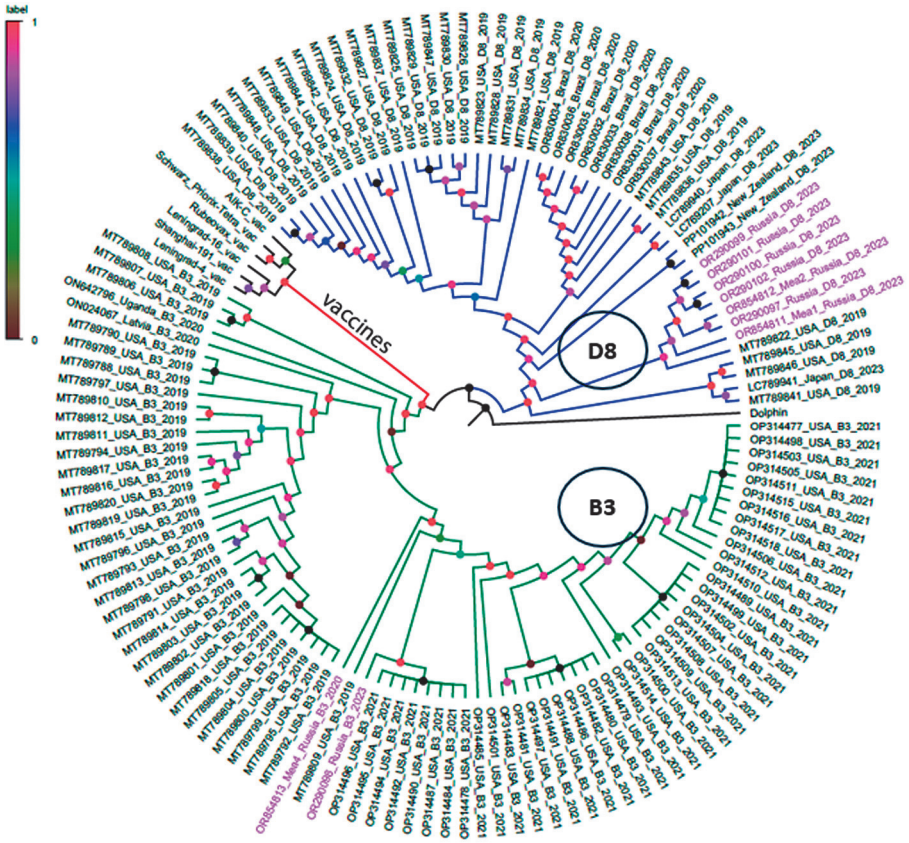

Figure prepared by the authors using their own data

Fig. 4. Phylogenetic relationships of full-genome sequences of 1 virus strains detected in Russia and other countries. The D8 genotype phylogenetic group is shown in blue, the B3 genotype group in green, and the vaccine strain group in red. Genomes from Russia included in the analysis, which were sequenced in 2020 and 2023, are highlighted in pink text

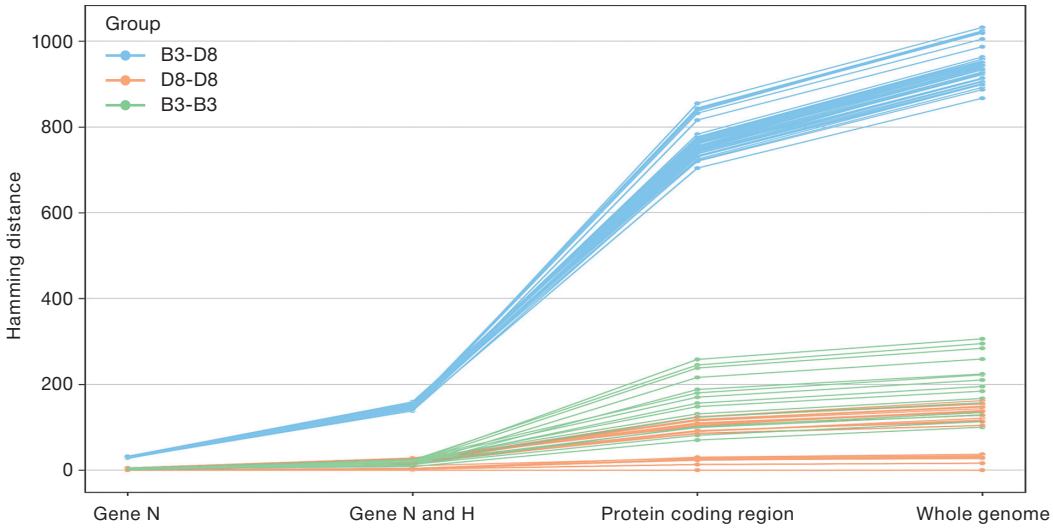

Figure prepared by the authors using their own data

Fig. 5. Pairwise Hamming distance between sequences of 1 virus strains belonging to genetic groups D8 and B3. The vertical axis shows the Hamming distance values for pairwise comparison of sequences, while the horizontal axis shows the fragments of the 1 virus genome analyzed — the N gene fragment, the union of the N and H gene fragments, and the union of all protein-coding sequences and the complete genome. The color indicates the values for the pairwise comparison of sequences within the B3 and D8 groups and between the strain groups: blue — B3-D8, green — D8-D8, orange — B3-B3

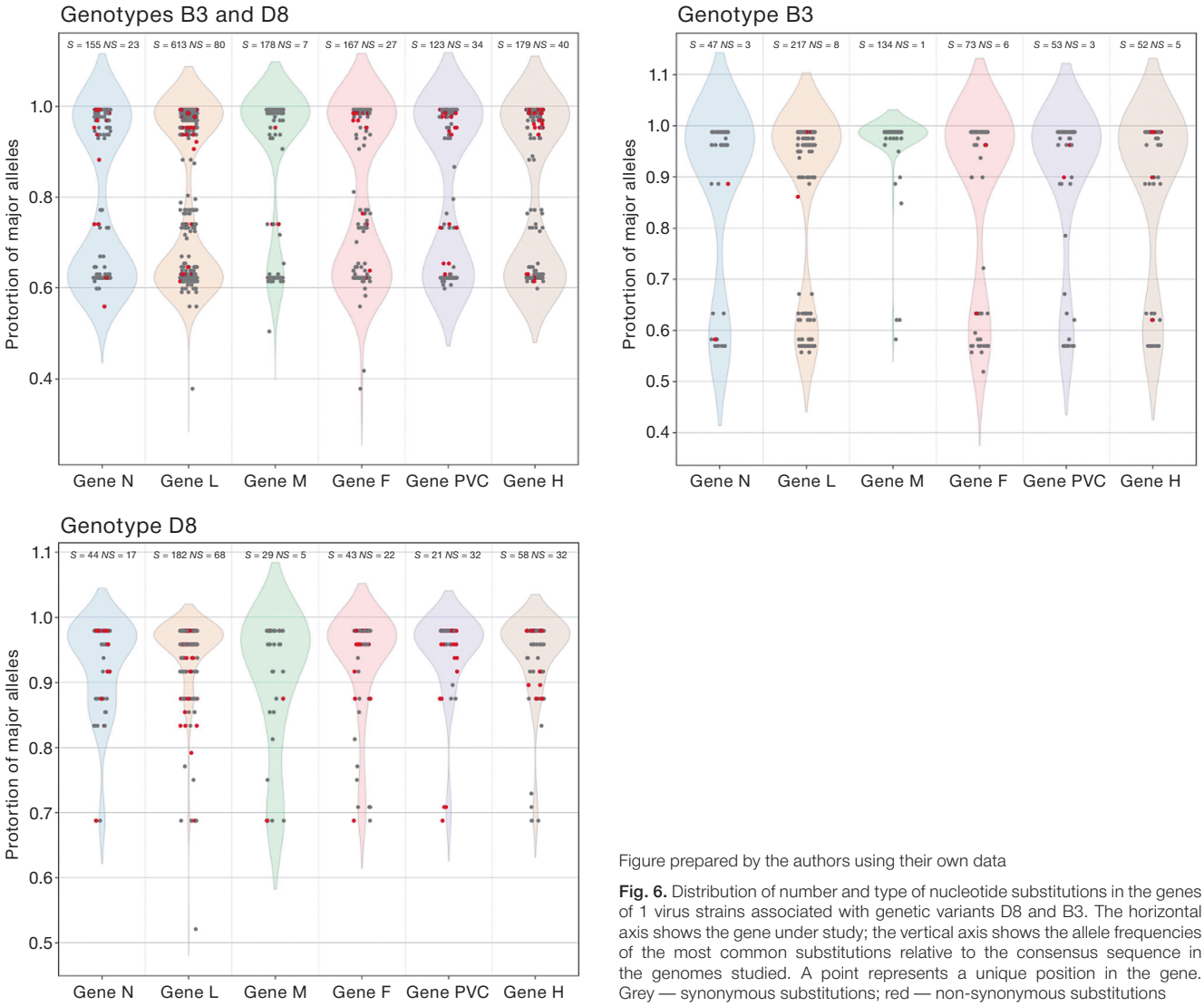

Figure prepared by the authors using their own data

Fig. 6. Distribution of number and type of nucleotide substitutions in the genes of 1 virus strains associated with genetic variants D8 and B3. The horizontal axis shows the gene under study; the vertical axis shows the allele frequencies of the most common substitutions relative to the consensus sequence in the genomes studied. A point represents a unique position in the gene. Grey — synonymous substitutions; red — non-synonymous substitutions

viral proteins (phosphoprotein (P), nonstructural protein V, and protein C), was also found to contain more nonsynonymous substitutions (n = 88) than synonymous substitutions (n = 69).

As well as demonstrating that the N gene is not the most variable, the analysis of nucleotide substitution frequencies in *Measles morbillivirus* genes (Fig. 6) shows that the M and H genes are also important targets for clarifying phylogenetic relationships between pathogen strains.

DISCUSSION

The results of comparative analysis of the examined measles virus samples suggest genetic similarity between Russian circulating variants and strains that have been found in other regions of the world, such as Central Europe or Asia. The published data for 2019–2022 are consistent with our results. Thus, the D8 and B3 genotypes are dominant in the global pattern of measles virus genetic diversity. However, their ratio is shown to vary in different regions of the world. In particular, the B3 genotype was dominant in the African, American, and Eastern Mediterranean regions, while the D8 genotype was dominant in the European, Northeast Asian, and Western Pacific regions [19]. The information presented on the website of the Nextstrain database [20] also indicates the dominant distribution of B3 and D8 genotypes in different regions of the world from 2020 (Fig. 7).

Most of the studied variants identified by us in 2023–2024 belong to the D8 genotype, which includes a widespread group of strains [12, 19]. In total, the open GenBank database contains more than 6 thousand gene sequences or genomes of strains belonging to this group.

Among Russian strains, in addition to the D8 genotype, strains belonging to the B3 genotype were also detected. Although the B3 genotype variant was detected in only two Russian samples in 2023, both samples obtained in Moscow in 2020 and 2021 belong to this group, which is currently prevalent in Africa, Europe and North America. Among the *Measles morbillivirus* genomes or genome

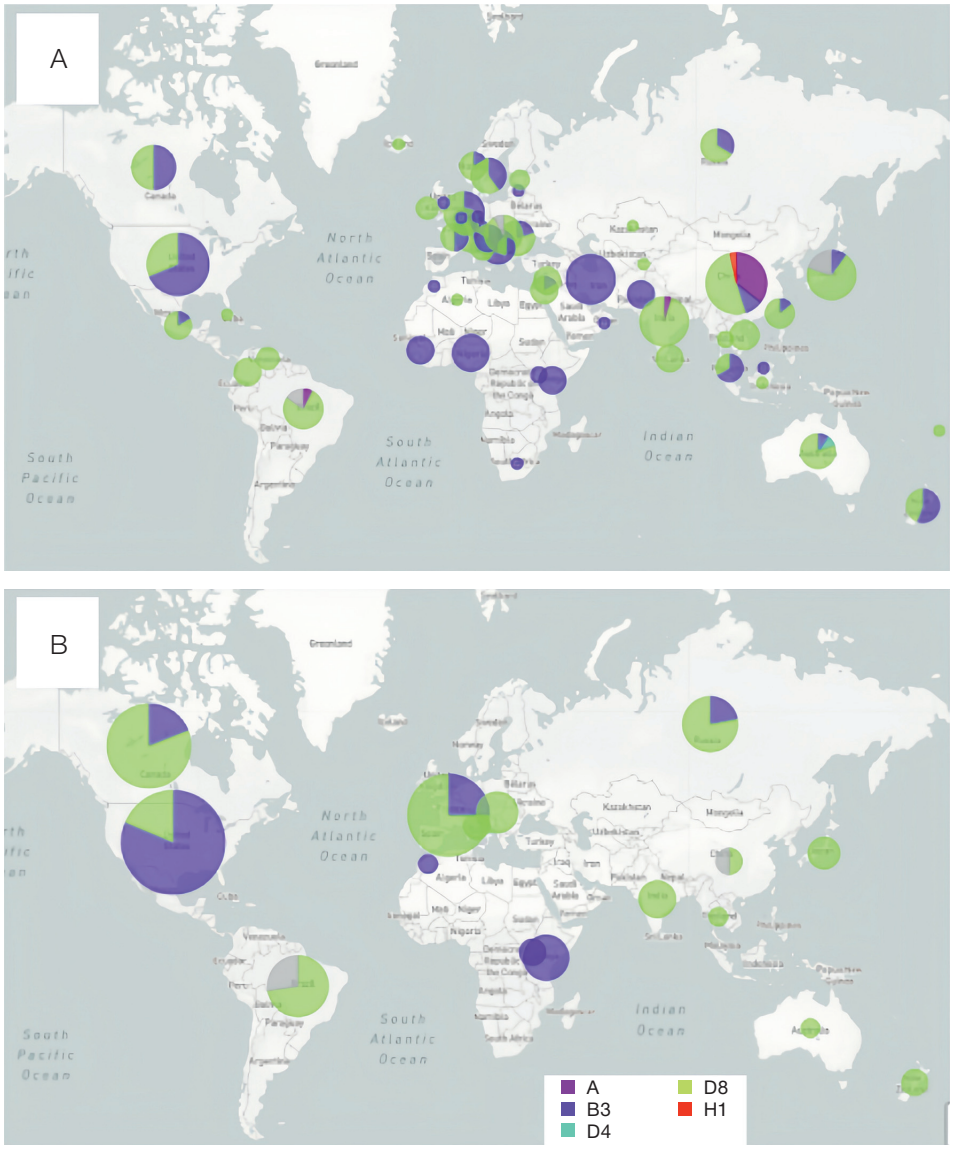

Figure prepared by the authors

Fig. 7. Global distribution of known 1 virus genotypes. Graphs based on A–N gene fragment sequencing data, B — whole genome sequencing data from January 2020 to September 2024. The figure was generated using the internet resource https://nextstrain.org/1/

fragments obtained from patient samples in 2023 and available in public databases such as the National Center for Biotechnology Information (NCBI) database, only 60 belonged to this group; these were found predominantly in the United States and Iran. The phylogenetic analysis of this group of strains shows that the variants detected in Russia in 2020 and 2023 do not form a common cluster, which suggests a different origin. The work by Erokhov et al. [12] demonstrated in the outbreaks of 2018–2020 the presence of genetic lines and variants of measles virus that probably did not circulate in Russia, but were imported from neighboring countries. A similar conclusion was reached in the retrospective analysis of measles outbreaks in the Astrakhan Oblast carried out by Kuzmenkov et al. [21], who identified the process of migration of virus variants from neighboring countries as a key factor in the formation of new outbreaks.

Based on the above, we can assume that the majority of measles outbreaks in Russia in 2023–2024 are caused by D8 variants, which were also identified in various regions of the world during this period. This is supported by statistical data on the distribution of genotypes among measles cases for the period from 2020 to 2024 in the European region [6].

Most of the studied *Measles morbillivirus* nucleotide sequences associated with recent measles outbreaks in Russia can be divided into phylogenetic subgroups according to the place of origin or pathway of spread within the D8 genotype. The distance dependence between subgroups (Fig. 5) confirms that the resolution of phylogenetic analysis depends on the size of the fragment of the nucleotide sequence of the virus genome used in the analysis. The comparative analysis of phylogenetic tree structures obtained by analyzing the sequence of the N gene, along with the combination of the N and H genes, showed that the use of the N gene alone is sufficient to determine the main genotype with high reliability, but does not allow for the study of virus transmission routes. The comparison of *Measles morbillivirus* gene variability also showed that the N gene is not the most variable gene; thus, additional genes, such as M and H, are required to investigate transmission pathways. To achieve an optimal ratio of labor and resolution in the future, at least the three most variable genes for a selected genotype, such as N, H, and M, should be used to analyze measles virus transmission pathways.

CONCLUSIONS

The described approach to the molecular genetic study of complete and partial genome sequences of clinical measles virus strains detected in 2023–2024 in Moscow and Novosibirsk was used to identify subgroups differing in terms of their origin. Among the sequencing data of strains detected in 2023, we also identified two samples belonging to genotype B3, which do not form a common origin group with sequences of the same genotype detected in Moscow in 2020–2021.

The comparison of *Measles morbillivirus* strains sequenced by us with global sequences provides a basis for detecting both those close sequences detected both in 2023 and those identified in previous years in different countries of the world.

The study of the N gene in the analysis of epidemically significant strains of *Measles morbillivirus* is sufficient for determining the main genotype with high reliability, but not to study the pathways of virus transmission. For this purpose, it is recommended to use the other most variable genes, such as M and H.

References

1. World Health Organization. Measles. [Online]; Available: https://www.who.int/news-room/fact sheets/detail/1#:~:text=1%20vaccination%20averted%2056%20million,the%20age%20of%205%20years [Accessed: September 5, 2023]
2. Russian Statistical Yearbook, 2023. Federal State Statistics Service; 2023. [Online]; Available: https://rosstat.gov.ru/storage/mediabank/Ejegodnik_2023.pdf [Accessed: July 5, 2024] (In Russ.).
3. Global Measles Outbreaks. Centers for Disease Control and Prevention. [Online]; Available: https://www.cdc.gov/global-health/1/data/global-1-outbreaks.html [Accessed: July 5, 2024]
4. Dixon MG, Ferrari M, Antoni S. Li X, Portnoy A, Lambert B, et al. Progress towards regional meats elimination — worldwide, 2000-2020. Morb Mortal Wkly Rep. 2021;70(45):1563. https://doi.org/10.15585/mmwr.mm7045a1
5. Bedford H., Elliman D., Measles rates are rising again, BMJ 2024;384:q259. https://doi.org/10.1136/bmj.q259
6. World Health Organization. Measles. [Online]; Available: https://www.who.int/europe/ru/publications/m/item/1-and-rubella-monthly-update-who-european-region-june-2024 [Accessed: July 5, 2024]
7. Measles incidence in Russia in 2023 was a 30-year record. [Online]; Available: https://medvestnik.ru/content/news/Zabolevaemost-koru-v-Rossii-v-2023-godu-okazalas-rekordnoi-za-30-let.html [Accessed: July 5, 2024] (In Russ.).
8. RIA News. [Online]; Available: https://ria.ru/20230420/kor-1866513301.html [Accessed: July 5, 2024] (In Russ.).
9. Refugees from Ukraine recorded by country. [Online]; Available: https://data.unhcr.org/en/situations/ukraine. [Accessed: July 5, 2024]
10. The World Health Organization. 1 — number of reported cases. [Online]; Available: www.who.int/data/gho/data/indicators/indicator-details/GHO/1--number-of-reported-cases. [Accessed: July 15, 2023]
11. Bryantseva E., Matnazarova G., Tursunov D. and Saidkasimova N. Epidemiological features of 1 infection during an outbreak in Tashkent city. EBWFF 2023 — International Scientific Conference Ecological and Biological Well-Being of Flora and Fauna (Part 1). 2023; Volume 420. https://doi.org/10.1051/e3sconf/202342005014
12. Erokhov DV, Zherdeva PE, Rubalskaya TS, Frolov RA, Tikhonova NT. Global genetic diversity of measles, rubella, and mumps viruses in 2019-2022. *Modern problems of epidemiology, microbiology and hygiene*.2022;108-111(In Russ.). EDN: PBRIWH
13. Nosova A.O., Bogoslovskaya E.V., Shipulin G.A. Modern approaches and prospects for the development of laboratory diagnostics of measles. Clinical microbiology and antimicrobial chemotherapy.2023; 25 (1) (In Russ.). https://doi.org/10.36488/cmac.2023.1.4-12
14. Schulz H., Hiebert J., Frost J., McLachlan E., Severini A. Optimisation of methodology for whole genome sequencing of 1 Virus directly from patient specimens. Journal of Virological Methods, 2022; Volume 299. https://doi.org/10.1016/j.jviromet.2021.114348
15. Benson DA, Cavanaugh M, Clark K, Karsch-Mizrachi I, Lipman DJ, Ostell J, Sayers EW. GenBank. Nucleic Acids Res.

2013 Jan; 41(Database issue):D36-42. https://doi.org/10.1093/nar/gks1195
16. Bankevich A, Nurk S, Antipov D, Gurevich AA, Dvorkin M, Kulikov AS, et al. SPAdes: A New Genome Assembly Algorithm and Its Applications to Single-Cell Sequencing. Journal of Computational Biology. 2012 May;19(5):455–77. https://doi.org/10.1089/cmb.2012.0021
17. Katoh K, Standley DM. MAFFT Multiple Sequence Alignment Software Version 7: Improvements in Performance and Usability. Molecular Biology and Evolution. 2013 Apr 1;30(4):772–80. https://doi.org/10.1093/molbev/mst010
18. Price MN, Dehal PS, Arkin AP (2010) FastTree 2 — Approximately Maximum-Likelihood Trees for Large Alignments. *Plos one* 5(3): e9490. https://doi.org/10.1371/journal.pone.0009490
19. Chekhlyaeva T.S., Erokhov D.V., Zherdeva P.E., Tikhonova N.T. Measles virus genotypes in the Russian Federation and their diversity in 2018-2020. Epidemiologic surveillance of current infections: new threats and challenges. 2021;327–9 (In Russ.). https://doi.org/10.21145/978-5-6046124-2-2_2021
20. Nextstrain. Real-time tracking of pathogen evolution [cited 2024 Aug. 12]; [Онлайн]; Доступно: https://nextstrain.org/1/. [Accessed: July 5, 2024]
21. Kuzmenkov M.V., Spirenkova A.E., Akhmerova R.R., Rvachev V.S. Current epidemiologic features of measles on the territory of the Astrakhan region in 2013-2023. International Research Journal.2024;141(3). https://doi.org/10.23670/IRJ.2024.141.68

Authors' contributions. All the authors confirm that they meet the ICMJE criteria for authorship. The most significant contributions were as follows: Ekaterina N. Chernyaeva — study design, data collection, data processing, results visualization, writing; Kirill V. Morozov — study design, data collection, data processing, results visualization, editing; Alina D. Matsvay — study design, data collection, data processing, editing; Maria S. Guskova — experimental data processing, editing; Andrey Y. Nekrasov — experimental data processing, editing; Ivan F. Stetsenko — data curation, experiment setup; Anastasiya O. Nosova — data curation, experiment setup; Olga G. Kurskaya — study concept and design, collection and primary analysis of biomaterial; Alexander M. Shestopalov — study concept and design, collection and primary analysis of biomaterial; German A. Shipulin — study concept and design, editing, general supervision.

AUTHORS

Ekaterina N. Chernyaeva, Cand. Sci. (Biol.)
https://orcid.org/0000-0002-8306-3466
echernya@gmail.com

Kirill V. Morozov
https://orcid.org/0000-0003-4657-0634
morozov.kv15@physics.msu.ru

Alina D. Matsvay, Cand. Sci. (Biol.)
https://orcid.org/0000-0002-6301-9169
AMatsvay@cspfmba.ru

Maria S. Guskova, Cand. Sci. (Phys.-Math.)
https://orcid.org/0000-0001-9129-3109
MGuskova@cspmz.ru

Andrey Y. Nekrasov
https://orcid.org/0000-0002-8229-7260
ANekrasov1@cspfmba.ru

Ivan F. Stetsenko
https://orcid.org/0000-0003-0979-3409
IStecenko@cspmz.ru

Anastasiya O. Nosova
https://orcid.org/0000-0002-1934-9857
anosova.o@gmail.com

Olga G. Kurskaya, Cand. Sci. (Med.)
https://orcid.org/0000-0002-1931-2026
kurskaya_og@mail.ru

Alexander M. Shestopalov, Doc. Sci. (Biol.)
https://orcid.org/0000-0002-9734-0620
shestopalov2@mail.ru

German A. Shipulin, Cand. Sci. (Med.)
https://orcid.org/0000-0002-9734-0620
shipulin@cspfmba.ru

https://doi.org/10.47183/mes.2024-26-3-51-56

ASSESSMENT OF SOLUBLE sST2 AND NT-proBNP CARDIAC MARKERS DURING END-TO-END STIMULATION OF SPACE FLIGHT STAGES ON A LONG RADIUS CENTRIFUGE

Anna G. Goncharova[1], Kirill S. Kireev[2]✉, Ludmila Ch. Pastushkova[1], Daria N. Kashirina[1], Igor N. Goncharov[1], Irina M. Larina[1]

[1] Institute for Biomedical Problems of the Russian Academy of Sciences, Moscow, Russia

[2] Gagarin Research and Test Cosmonaut Training Center, Zvyozdny Gorodok, Russia

Introduction. Considering the risks of cardiovascular events during all phases of spaceflight (SF), it is relevant to evaluate the levels of cardiac markers sST2 and NT-proBNP in ground-based simulations of exposure to adverse SF factors.

Objective. To identify the levels of sST2 and NT-proBNP as risk criteria for the development of cardiovascular changes following end-to-end simulation of SF stages on the CF-18 centrifuge.

Materials and methods. The levels of cardiac markers sST2 and NT-proBNP were assessed during exposure to chest-to-back overloads of up to 4.5 units and simulated vestibular sensory conflict on a CF-18 centrifuge for 60 min in six healthy male subjects. The sST2 levels were assessed by solid-phase enzyme-linked immunosorbent assay (ELISA). NT-proBNP concentration was measured by immunofluorescence method on a Finecare TM FIA FS-113 analyzer (from Guangzhou Wondfo Biotech).

Results. During the end-to-end simulation of SF stages, the response of the subjects' cardiovascular system was adequate to the loads imposed. The levels of the cardiac markers sST2 and NT-proBNP in venous blood of the subjects did not significantly increase after spinning on the centrifuge.

Conclusions. In the present study, no significant changes indicative of biochemical signs of pathologic overstretching or myocardial damage were observed during rotation on the CF-18. Assessment of individual sST2 levels prior to exposure and in dynamics can be used to probabilistically predict individual sensitivity and adaptation reserves of the heart to unfavorable CP factors.

Keywords: space flight; proteome; cardio marker; ST2; overloads; centrifuge

For citation: Goncharova A.G., Kireev K.S., Pastushkova L.H., Kashirina D.N., Goncharov I.N., Larina I.M. Assessment of soluble sST2 and NT-proBNP cardiac markers during end-to-end stimulation of space flight stages on a long radius centrifuge. *Extreme Medicine*. 2024;26(3):51–56. https://doi.org/10.47183/mes.2024-26-3-51-56

Funding: the study was performed within the framework of the RAS basic theme FMFR-2024-0032.

Compliance with ethics principles: the study was approved by the Biomedical Ethics Commission of the Gagarin Research and Test Cosmonaut Training Center (Zvyozdny Gorodok) (protocol No. 1 of 02/27/2023). All participants signed voluntary informed consent for the study.

Potential conflict of interest: the authors declare no conflict of interest.

✉ Kirill S. Kireev k.kireyev@gctc.ru

Received: 22 July 2024 **Revised:** 27 Aug. 2024 **Accepted:** 29 Aug. 2024

ОЦЕНКА УРОВНЯ КАРДИОМАРКЕРОВ РАСТВОРИМОГО sST2 И NT-proBNP ПРИ СКВОЗНОМ МОДЕЛИРОВАНИИ ЭТАПОВ КОСМИЧЕСКОГО ПОЛЕТА НА ЦЕНТРИФУГЕ ДЛИННОГО РАДИУСА

А.Г. Гончарова[1], К.С. Киреев[2]✉, Л.Х. Пастушкова[1], Д.Н. Каширина[1], И.Н. Гончаров[1], И.М. Ларина[1]

[1] Государственный научный центр Российской Федерации, Институт медико-биологических проблем Российской академии наук, Москва, Россия

[2] Научно-исследовательский испытательный центр подготовки космонавтов имени Ю.А. Гагарина, Звездный городок, Россия

Введение. Оценка уровня кардиомаркеров sST2 и NT-proBNP при наземном моделировании воздействия неблагоприятных факторов КП является актуальной для учета рисков сердечно-сосудистых событий на всех этапах космического полета (КП).

Цель. Определение уровней sST2 и NT-proBNP как критериев риска развития сердечно-сосудистых изменений после сквозного моделирования этапов КП на центрифуге ЦФ-18.

Материалы и методы. Проведена оценка уровней кардиомаркеров sST2 и NT-proBNP при воздействии перегрузок в направлении грудь–спина величиной до 4,5 ед. и моделированного вестибулосенсорного конфликта на центрифуге ЦФ-18 в течение 60 минут с участием 6 практически здоровых испытуемых. Оценку уровня sST2 проводили методом твердофазного иммуноферментного анализа (ELISA). Измерение концентрации NT-proBNP проводили иммунофлуоресцентным методом на анализаторе Finecare TM FIA FS-113 (от Guangzhou Wondfo Biotech).

Результаты. Во время сквозного моделирования этапов КП реакция сердечно-сосудистой системы испытуемых была адекватной предъявляемым нагрузкам. Уровень кардиомаркеров sST2 и NT-proBNP в венозной крови испытуемых достоверно не увеличивался после вращения на центрифуге.

Выводы. В данной работе не выявлено значимых изменений, свидетельствующих о биохимических признаках патологического перерастяжения или повреждения миокарда при вращении на ЦФ-18. Оценка индивидуального уровня sST2 до воздействия и в динамике может использоваться для вероятностного прогноза индивидуальной чувствительности и адаптационных резервов сердца к неблагоприятным факторам КП.

Ключевые слова: космический полет; протеом; кардиомаркеры; sST2; перегрузки; центрифуга

Для цитирования: Гончарова А.Г., Киреев К.С., Пастушкова Л.Х., Каширина Д.Н., Гончаров И.Н., Ларина И.М. Оценка уровня кардиомаркеров растворимого sST2 и NT-proBNP при сквозном моделировании этапов космического полета на центрифуге длинного радиуса. *Медицина экстремальных ситуаций.* 2024;26(3):51–56. https://doi.org/10.47183/mes.2024-26-3-51-56

Финансирование: работа выполнена в рамках базовой тематики РАН FMFR-2024-0032.

Соответствие принципам этики: исследование одобрено комиссией по биомедицинской этике ФГБУ «НИИ ЦПК имени Ю.А. Гагарина» (Звездный городок) (протокол № 1 от 27.02.2023). Все участники подписали добровольное информированное согласие на исследование.

Потенциальный конфликт интересов: авторы заявляют об отсутствии конфликта интересов.

✉ Киреев Кирилл Сергеевич k.kireyev@gctc.ru

Статья поступила: 22.07.2024 **После доработки:** 27.08.2024 **Принята к публикации:** 29.08.2024.

INTRODUCTION

Ensuring the medical safety of space flights and medical control of health status is a priority task in space medicine. A comprehensive health status assessment for predicting the risks of acute and remote cardiovascular events involves the application of highly informative clinical and laboratory techniques. Soluble growth stimulators are known to be expressed by gene 2 (sST2) in cardiomyocytes in response to their overstretching or damage [1]. Unlike other cardiac markers, sST2 levels change rapidly in response to the subject's cardiovascular status but are independent of age, sex, body mass index, and renal function [2, 3]. SST2 has been shown to be the most significant marker for predicting the development and outcome of heart failure [4].

sST2 levels were evaluated during parabolic flights in the context of aerospace physiology. Significantly decreased serum sST2 levels compared to values at baseline and 1 h after parabolic flight were observed to remain unchanged 1 h after parabolic flight [5]. In earlier studies, we analyzed the effects of long-duration space flight (SF) and landing on sST2 protein levels. In the study of venous blood samples of nine astronauts before and after SF to the International Space Station, all subjects showed a significant increase in sST2 level on the first day after the flight. On the 7th day of the recovery period, the sST2 content in plasma decreased to approach the background value. The obtained results indicated transient myocardial overstretching during landing and increased risk of cardiofibrosis over the long term following SF [6].

Another standard cardiac marker of cardiac volume overload and risk of heart failure and cardiac rhythm disturbances is the N-terminal propeptide of natriuretic hormone (B-type) NT-proBNP [7]. However, NT-proBNP is dependent on age, sex, body mass index, daily hormone balance, renal status, and other factors [8]. Considering gravitational features of NT-proBNP regulation, we note that individual astronauts showed a decrease in natriuretic peptide signaling while in space [9]. As shown in Frings-Meuthen P, et al. [10], NT-proBNP concentrations respond to changes in sodium intake under SF conditions, but have lower levels relative to preflight values. This appears to occur due to decreased blood volume in the thoracic cavity provided that impedance measurements are not distorted by changes in chest air content.

We were interested in whether short-term overload and vestibular sensory changes simulated on a CF-18 centrifuge would influence pathologic myocardial extensibility and increase the risk of cardiac fibrosis. Thus, the purpose of the present study was to determine the levels of sST2 and NT-proBNP in relation to the risk of cardiovascular changes in vestibular sensory changes following end-to-end simulation of SF stages on a CF-18 centrifuge.

MATERIALS AND METHODS

Experimental investigations (EI) were carried out at the Gagarin Research and Test Cosmonaut Training Center in 2023 according to the method described earlier [11]. The study involved six practically healthy male subjects aged 45 to 53 years (mean age 50.3 ± 3.3 years, height 175.7 ± 4.7 cm, body mass 86.8 ± 6.7 kg). All subjects were medically cleared for EI and had a valid medical and flight commission report.

A medical examination of the subjects with registration of cardiovascular system functional parameters (blood pressure BP, heart rate HR) and body temperature was carried out by a physician before and after the EI. Prior to the study, the subjects had not been exposed to other influences that could affect their functional state and postural reactions (physical activity, acceleration, negative or excessive pressure on the lower half of the body, hypoxia). Studies were conducted no earlier than 1.5 h after a meal. All subjects received detailed instructions for all stages of the study.

The EIs were performed on a CF-18 centrifuge for physiological studies with a cabin installed in a 3-stage controlled gimbal. The radius of the centrifuge console from the rotation axis of the main engine to the center of intersection of the gimbal frames axes is 18 m. The studies were conducted using the standard seat of the centrifuge CF-18. Under these conditions, the overload acts in the chest-back direction. During the ascent and descent phases, the inclination angle of the seat back to the direction of the overload vector was +78°. Following simulation of the 3rd stage engine separation, the subject's chair was moved to a position at 105° from the direction of the overload vector (anti-orthostasis –15°) and the orbital space flight stage was simulated. Rotations were performed without stopping the centrifuge.

During the rotation on the CF-18, a tacho-oscillographic method was used to monitor the electrocardiogram (ECG) in three standard leads, as well as HR and BP in the brachial artery.

Figure 1 shows a typical profile of overloads influencing the cosmonaut during the Soyuz ascent into Earth orbit ("ascent schedule"), while Figure 2 shows a typical profile of overloads during the Soyuz descent to Earth ("descent schedule"). The overload is stated in multiple units of gravity acceleration (g). The maximum overload during rotation according to the "descent schedule" is 4.0 units; the total rotation time is about 9 min. The overload during the "descent schedule" rotation includes two sections with a maximum overload of 4.5 units (peak 1) and 3.2 units (peak 2) involving a total rotation time of about 6 min. Simulation of the orbital flight stage for 40 min was performed using a special program [11], which provides simultaneous changes in hemodynamics and impact on the vestibular apparatus of the tester. The total duration of rotation was 60 min.

While ECG was recorded in three standard leads in the centrifuge cabin before, during and after rotation, brachial artery BP was performed using tacho-oscillographic method. During centrifuge rotation, ECG was recorded continuously. At the same time, BP was recorded at the 10th, 20th, 30th and 40th minutes of rotation.

To determine the concentration of sST2 and NT-proBNP, venous blood was sampled from the ulnar vein of the subjects immediately before and after rotation. Blood samples of 3 mL were collected before and at the end of rotation into Vacuette® tubes containing K3 EDTA preservative. Following storage in blood tubes at +4°C for no more than 2 h, plasma was obtained by centrifugation at 2000 g

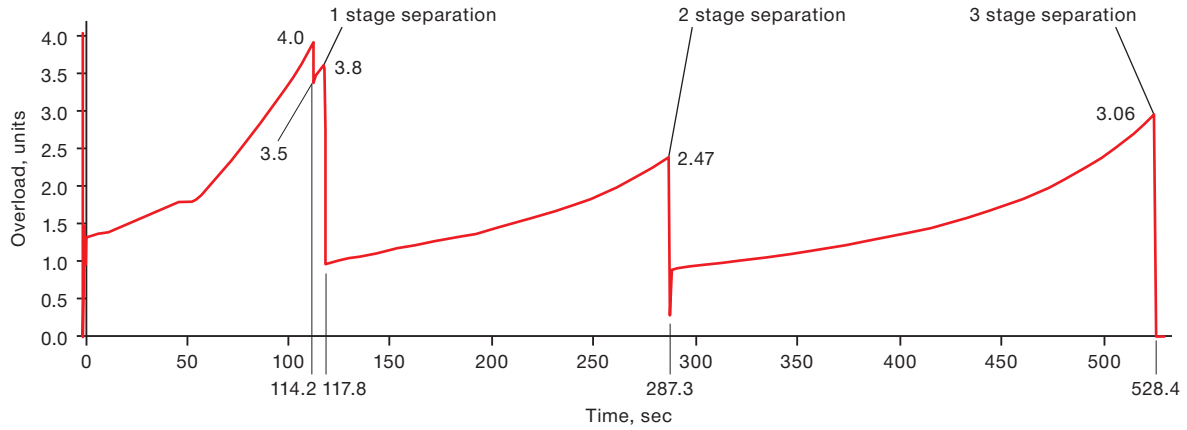

Figure prepared by the authors using their own data

Fig. 1. Typical overload profile during the Soyuz ascent

for 15 min on an MPW-350R centrifuge (Poland); plasma aliquots were sampled using the Eppendorf (Germany) interchangeable volume pipettes. Plasma aliquots were frozen at –80°C.

The sST2 level in blood plasma was assessed by solid-phase enzyme-linked immunosorbent assay (ELISA) using commercial kits of "Critical Diagnostics Presage® ST2 Assay" (USA) and ST2-reader "Critical Diagnostics Presage® ST2 Assay". The results of sST2 level measurement were expressed in ng/mL. NT-proBNP concentration was measured according to the immunofluorescence method on a FinecareTM FIA FS-113 analyzer (from Guangzhou Wondfo Biotech). Statistical processing of the experimental data was carried out using the Statistica 13 software package based on Friedman's analysis of variance criterion and the Wilcoxon test for nonparametric data (p-value < 0.05).

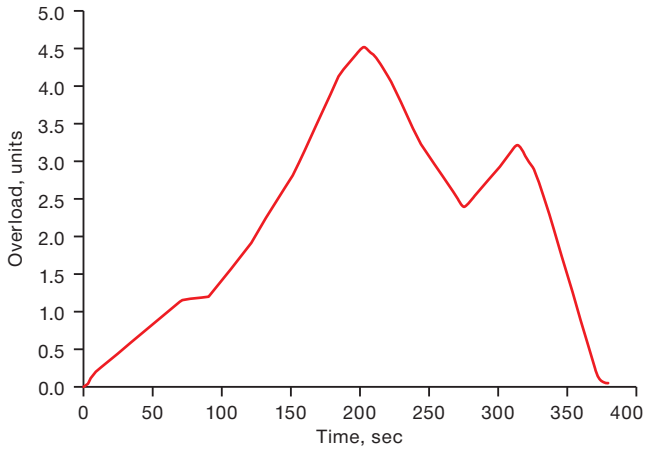

Figure prepared by the authors using their own data

Fig. 2. Typical overload profile during the Soyuz descent

RESULTS

During the medical examination of the subjects before the EI, the mean values of systolic BP were 138.9 ± 11.2 mmHg, diastolic BP was 85.0 ± 9.9 mmHg, mean HR was 74.8 ± 16.9 beats/min, body temperature in all subjects was within the physiologic norm. All subjects were admitted to the EI.

From the first min of orbital flight stage modeling and transfer to the anti-orthostatic position during periodic questioning while rotating, all six subjects subjectively noted blood rush to the head, four reported the sensation of facial swelling and heaviness in the temporal region of the head, three mentioned nasal congestion, two described cold feet, and one reported heavy eyelids. During rotation under video observation, mild hyperemia of the facial skin and swelling of neck veins were objectively observed in all test subjects. The severity of all phenomena rose with increasing duration of rotation to reach a maximum by 20 min and remained unchanged thereafter.

The dynamics of changes in cardiovascular system parameters are presented in Figure 3 and Figure 4.

The response of the cardiovascular system was adequate to the loads imposed. The maximum registered values of HR and BP corresponded to the maximum overloads at each simulated stage of space flight.

When analyzing the ECG during the simulation of the orbital flight section, in most cases the subjects registered an increase in the end part of the ventricular QRS complex and in the amplitude of the T tooth; at the same time, the RST interval was slightly shortened. In isolated cases, a slowing of intraventricular conduction was detected, as expressed in "broadening" of the ventricular complex. These changes, which were functional in nature, disappeared after stopping the TF. Sinus tachycardia was noted during rotations according to the "withdrawal schedule" and "descent schedule"; there were no rhythm or conduction disturbances.

A medical examination following the EI did not reveal any deviations in the state of health. No subjects had any complaints; their general well-being remained positive. Hemodynamic parameters did not significantly differ from background. Average values of systolic BP were 143.2 ± 14.1 mmHg, diastolic BP was 82.6 ± 19.3 mmHg, mean values of HR were 71.7 ± 15.9 beats/min, while body temperature remained within normal limits.

As can be seen from Figure 5, sST2 levels did not exceed the reference values in any test subject. Variability of sST2 levels was noted in all subjects both prior to the modeling and following its completion. When analyzing the group-average sST2 levels, its increase following rotation on the TF was noted (Fig. 6). However, the level of group-average values after exposure to overloads also fell within the reference values (variant of physiological norm up to 35 ng/mL). The obtained data indicate the absence of risks of

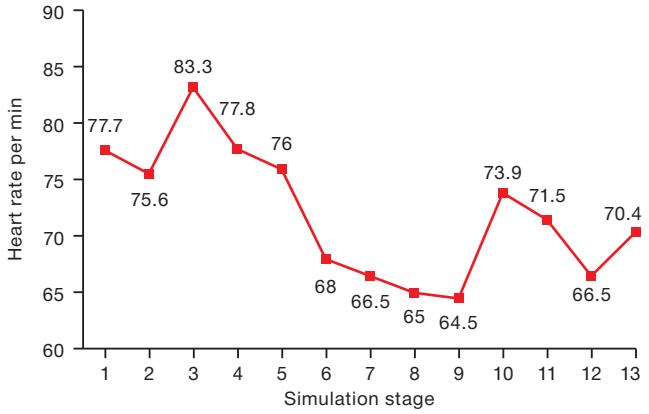

Figure prepared by the authors using their own data

Fig. 3. Heart rate dynamics during simulation of the space flight stages: 1 — baseline before simulation; 2 — beginning simulation; 3 — 1st stage separation; 4 — 2nd stage separation; 5 — 3d stage separation; 6 — 10th min of orbital flight; 7 — 20th min of orbital flight; 8 — 30th min of orbital flight; 9 — 40th min of orbital flight; 10 — 1st overload peak during Soyuz landing; 11 — 2nd overload peak during the Soyuz landing; 12 — end of simulation; 13 — 5 min after end of simulation

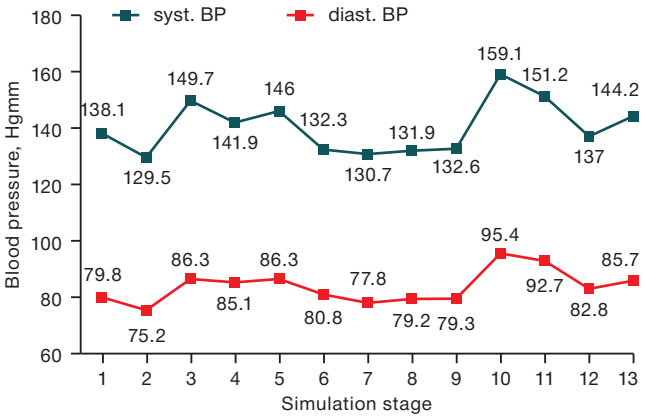

Figure prepared by the authors using their own data

Fig. 4. Blood pressure dynamics during simulation of the space flight stages: 1 — baseline before simulation; 2 — beginning simulation; 3 — 1st stage separation; 4 — 2nd stage separation; 5 — 3d stage separation; 6 — 10th min of orbital flight; 7 — 20th min of orbital flight; 8 — 30th min of orbital flight; 9 — 40th min of orbital flight; 10 — 1st overloads peak during Soyuz landing; 11 — 2nd overloads peak during the Soyuz landing; 12 — end of simulation; 13 — 5 min after end of simulation

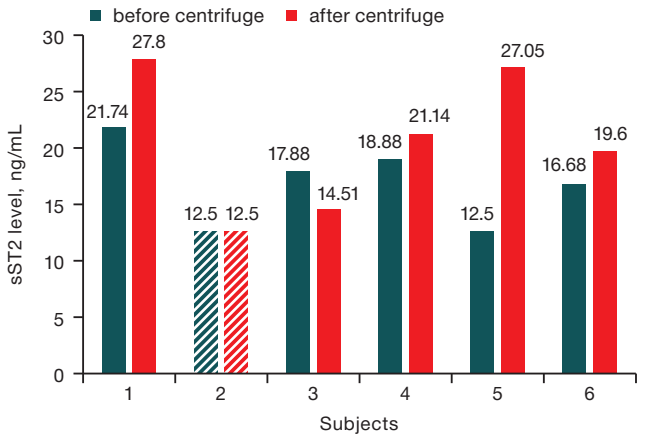

Figure prepared by the authors using their own data

Fig. 5. Individual sST2 levels before and after simulation of the space flight stages. Note: sST2 levels below the sensitivity of the method (<12,5 ng/mL) are marked with a dash

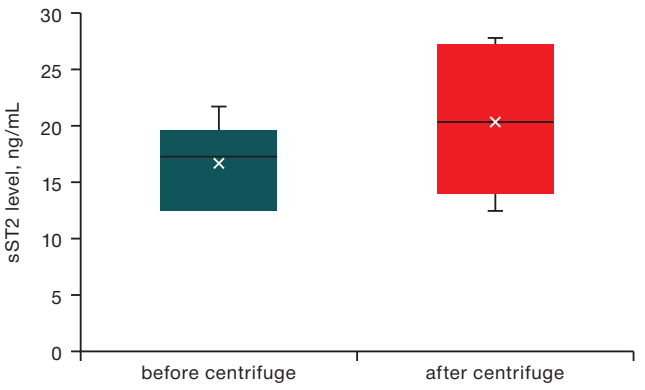

Figure prepared by the authors using their own data

Fig. 6. Mean group sST2 levels before and after simulation of the space flight stages

heart failure and cardiofibrosis under the described study conditions.

As shown in Figure 7, the variability of NT-proBNP before and after modeling remains low. Individual variability is higher than the group average (Figures 7 and 8). NT-proBNP levels remained within the normal range at all investigated points in all test subjects.

When comparing individual and mean group graphs of response of cardiac markers sST2 and NT-proBNP to this type of exposure, attention was paid to unidirectional increase of sST2 and NT-proBNP levels after exposure in 4 out of 6 subjects. However, the NT-proBNP level increased less than sST2.

DISCUSSION

From the analysis of the obtained data, the dynamics of heart rate and blood pressure level was seen to correspond to the applied loads. Maximal registered values of HR and BP observed at maximal impacting overloads at each simulated SF stage did not exceed physiological values of variability of responses of cardiovascular system of a healthy person to the impact of simulated extreme factors of SF. The in-depth study of cardiomyocyte response to the effect of moderate longitudinal overloads on the myocardium of practically healthy subjects showed a unidirectional increase in the levels of cardiac markers sST2 and NT-proBNP, which confirms the high diagnostic sensitivity of these proteins with respect to even short-term effects causing volumetric overstretching of myocardium. Analysis of individual data showed a more pronounced and variable response to overload exposure of the selective cardiac marker sST2 as compared with NT-proBNP. Multimarker models comprised of several biomarkers, including NT-proBNP and sST2, have greater prognostic significance for risk stratification of cardiovascular events [12–14]. Thus, changes in sST2 and NT-proBNP can objectively characterize the response of cardiomyocytes to the effect of overload both at active sites of SF according to ascent and descent schedules and at modeling of redistribution of body fluid media in microgravity conditions. Based on estimation of individual background levels of sST2 and NT-proBNP, it

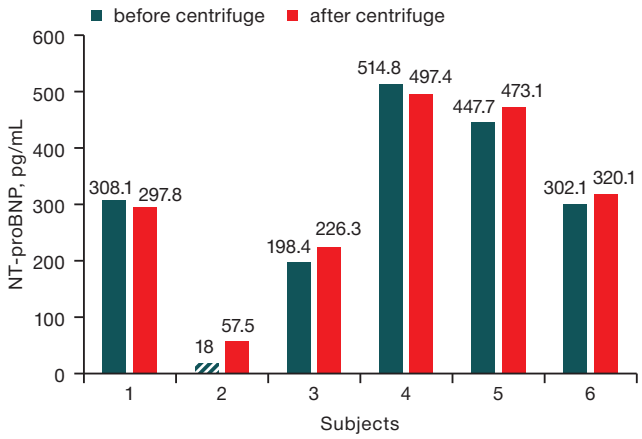

Figure prepared by the authors using their own data

Fig. 7. Individual NT-proBNP levels before and after simulation of the space flight stages. Note: NT-proBNP levels below the sensitivity of the method (<18 pg/mL) are marked with a dash

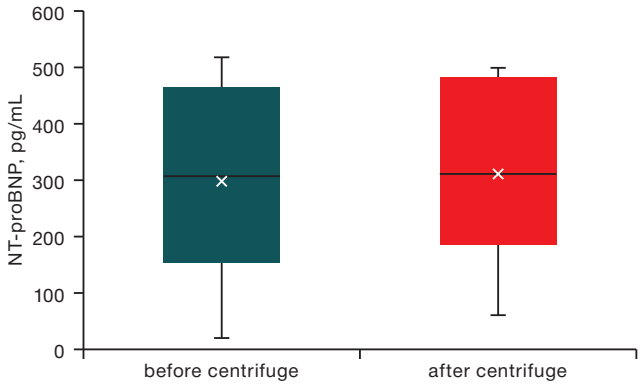

Figure prepared by the authors using their own data

Fig. 8. Mean group NT-proBNP levels before and after simulation of the space flight stages

is also possible to personalize probabilistic prognosis of the effect of the complex of SF factors at the stage of orbital insertion and descent in order to estimate the risk of cardiofibrosis development in remote periods after SF.

In contrast to earlier studies of sST2 level after completion of prolonged SF [6], the present study did not reveal a clinically significant increase in the level of this cardiac marker following completion of space flight stage simulation on a CF-18. The obtained data indicate that isolated exposure of the myocardium of practically healthy subjects to moderate longitudinal overload without prior exposure to prolonged microgravity does not cause pathologic overstretching of cardiomyocytes. The increase in sST2 level following prolonged SF can be explained by the effect of overloads during the descent vehicle return to the Earth on myocardia that are already adapted to the prolonged influence of extreme SF factors [15].

CONCLUSIONS

1. Isolated exposure of short-term moderate longitudinal overloads on the myocardium of practically healthy subjects without prior exposure to prolonged microgravity did not cause pathologic overstretching of cardiomyocytes.

2. Dynamics of heart rate and blood pressure level, which corresponded to the applied loads, did not exceed physiological values of variability of responses of cardiovascular system of a healthy person to the impact of modeled extreme factors of SF.

3. It is promising to continue studies on the influence of isolated unfavorable factors of SF on the levels of cardiac markers in healthy test subjects.

References

1. Weinberg E, Shimpo M, de Keulenaer G. W, MacGillivray C, Tominaga S, Solomon S. D, et al. Expression and regulation of ST2, an interleukin-1 receptor family member, in cardiomyocytes and myocardial infarction. *Circulation*. 2002;106(23):2961–6. https://doi.org/10.1161/01.cir.0000038705.69871.d9
2. Uchasova EG, Gruzdeva OV, Dileva YuA, Karetnikova VN. Interleukin 33 and fibrosis: pathogenesis updated. Medical Immunology. 2018;20(4):477–84 (In Russ.). https://doi.org/10.15789/1563-0625-2018-4-477-484
3. Dudek M, Kałużna-Oleksy M, Migaj J, Straburzyńska-Migaj E. Clinical value of soluble ST2 in cardiology. *Adv Clin Exp Med*. 2020;29(10):1205–10. https://doi.org/10.17219/acem/126049
4. Rehman S, Mueller T, Januzzi JL. Characteristics of the novel interleukin family biomarker ST2 in patients with acute heart failure. *J Am Coll Cardiol*. 2008;52(18):1458–65. https://doi.org/10.1016/j.jacc.2008.07.042
5. Jirak P, Wernly B, Lichtenauer M, Paar V, Franz M, Knost T, et al. Dynamic Changes of Heart Failure Biomarkers in Response to Parabolic Flight. *Int J Mol Sci*. 2020;21(10):3467. https://doi.org/10.3390/ijms21103467
6. Goncharova AG, Pastushkova LKh, Kireev KS, Kashirina DN, Goncharov IN, Koloteva MI, Larina IM. Influence of the Factors of Long-Duration Space Flights and Landing on the Levels of Cardiac Failure Biomarker and sST2 Fibrosis Development Risk. Manned Spaceflight. 2023;46(1):96–103 (In Russ.). https://doi.org/10.18127/j15604136-202301-06
7. Cao Z, Jia Y, Zhu B. BNP and NT-proBNP as Diagnostic Biomarkers for Cardiac Dysfunction in Both Clinical and Forensic Medicine. *Int J Mol Sci*. 2019;20(8):1820. https://doi.org/10.3390/ijms20081820
8. Maries L, Manitiu I. Diagnostic and prognostic values of B-type natriuretic peptides (BNP) and N-terminal fragment brain natriuretic peptides (NT-pro-BNP). *Cardiovasc J Afr*. 2013;7:286–9. https://doi.org/10.5830/CVJA-2013-055
9. Rössler A, Noskov V, László Z, Polyakow VV, Hinghofer-Szalkay HG. Permanent depression of plasma cGMP during long-term space flight. *Physiol Res*. 2001;50:83–90. https://doi.org/10.33549/physiolres.930000.50.83
10. Frings-Meuthen P, Luchitskaya E, Jordan J, Tank J, Lichtinghagen R, Smith SM, et al. Natriuretic Peptide Resetting in Astronauts. *Circulation*. 2020;141(19):1593–5. https://doi.org/10.1161/CIRCULATIONAHA.119.044203
11. Kireev KS, Zaveryukha AS, Vlasova NV, Minyaylo YaYu, Gavrik IN, Bulgakov AV, Dubinin VI. The study of cosmonauts' functional status during the end-to-end simulation of spaceflight phases on the centrifuge TSF-18. Manned Spaceflight. 2024;51(2):63–78 (In Russ.). EDN: AFLTPG
12. Gaggin HK, Truong QA, Gandhi PU, Motiwala SR, Belcher AM, Weiner RB, et al. Systematic evaluation of endothelin 1 measurement relative to traditional and modern biomarkers for clinical assessment and prognosis in patients with chronic systolic heart

failure: serial measurement and multimarker testing. *Am J Clin Pathol*. 2017;147(5):461–72. https://doi.org/10.1093/ajcp/aqx014
13. Ky B, French B, Levy WC, Sweitzer NK, Fang JC, Wu AH, et al. Multiple biomarkers for risk prediction in chronic heart failure. *Circ Heart Fail*. 2012;5(2):183–90. https://doi.org/10.1161/CIRCHEARTFAILURE.111.965020
14. Lupon J, de Antonio M, Vila J, Penafiel J, Galan A, Zamora E, et al. Development of a novel heart failure risk tool: the Barcelona bio-heart failure risk calculator (BCN bio-HF calculator). *PLoS One*. 2014;9(1):e85466. https://doi.org/10.1371/journal.pone.0085466
15. Sy MR, Keefe JA, Sutton JP, Wehrens XHT. Cardiac function, structural, and electrical remodeling by microgravity exposure. *Am J Physiol Heart Circ Physiol*. 2023;324(1):H1–H13. https://doi.org/10.1152/ajpheart.00611.2022

Authors' contributions. All the authors confirm that they meet the ICMJE criteria for authorship. The most significant contributions were as follows. Anna G. Goncharova — drafted the manuscript, analysed data; Kirill S. Kireev — drafted the manuscript, collected and analysed data; Ludmila Ch. Pastushkova — drafted the manuscript, analysed and interpreted data; Daria N. Kashirina — collected, analysed, and interpreted data; Igor N. Goncharov — analysed and interpreted data; Irina M. Larina — drafted the manuscript, analysed data.

AUTHORS

Anna G. Goncharova, Dr. Sci. (Med.), Associated Professor
https://orcid.org/0000-0001-9523-5635
goncharova.anna@gmail.com

Kirill S. Kireev, Cand. Sci. (Med.)
https://orcid.org/0000-0002-0381-9164
k.kireyev@gctc.ru

Ludmila Ch. Pastushkova, Cand. Sci. (Biol.)
https://orcid.org/0000-0002-2071-0443
lpastushkova@mail.ru

Daria N. Kashirina, Cand. Sci. (Biol.)
https://orcid.org/0000-0002-9646-7275
daryakudryavtseva@mail.ru

Igor N. Goncharov
https://orcid.org/0000-0002-4513-6476
igorgoncharov@gmail.com

Irina M. Larina, Dr. Sci. (Med.), Professor
https://orcid.org/0000-0001-6783-4200
irina.larina@gmail.com

https://doi.org/10.47183/mes.2024-26-3-57-64

THE PSYCHOPHYSIOLOGICAL STATE OF A PERSON IN ALTERED MAGNETIC CONDITIONS

Gennady V. Kovrov, Olga V. Popova✉, Anna G. Chernikova, Oleg I. Orlov

Institute for Biomedical Problems of the Russian Academy of Sciences, Moscow, Russia

Introduction. Due to the fact that manned space flights beyond Earth orbit are planned in the near future, it becomes relevant to study the effects of the Earth's reduced magnetic field on humans.

Objective. To evaluate the features of sensorimotor reactions, quality of night sleep (nocturnal sleep) and the development of daytime sleepiness during a 24-hour stay under hypomagnetic conditions (HMC).

Materials and methods. Experimental studies with the participation of 6 male volunteers aged 26 to 37 years were conducted in 2023. In total, four experimental series were carried out, lasting 24 hours each. The subjects were exposed to hypomagnetic conditions in three groups (the average value was between 0.05–0.14 μT). There was no exposure to such conditions in the placebo group.

The research methods included questionnaires regarding the quality and characteristics of night sleep, daytime wakefulness, as well as the study of sensorimotor functions. Statistical processing was carried out by the Statistica 13.0 software package.

Results. Daytime sleepiness was found to increase under hypomagnetic conditions in 66% of observations as compared to 33% of cases in the placebo series ($p = 0.003$). Immediately following the cessation of experimental exposure, a rapid activation of the central nervous system was observed, which was expressed in a statistically significant decrease in the total visual-motor reaction time.

Conclusions. Under hypomagnetic conditions, the work of brain sleep mechanisms is preserved. Daytime drowsiness that develops under hypomagnetic conditions indicates the possibility of changes in circadian rhythmicity in brain activating systems. The rapid activation of the central nervous system reported immediately following the termination of hypomagnetic conditions has a compensatory character. The revealed features of hypomagnetic conditions influence on the sleep-wake cycle and sensorimotor functions suggest further studies of daytime sleepiness using additional subjective and objective methods of wakefulness level and activity of the central nervous system assessment.

Keywords: sensorimotor functions; hypomagnetic conditions; simple visual-motor reaction; questionnaire self-assessment; night sleep; daytime drowsiness

For citation: Kovrov G.V., Popova O.V., Chernikova A.G., Orlov O.I. The psychophysiological state of a person in altered magnetic conditions. *Extreme Medicine.* 2024;26(3):57–64. https://doi.org/10.47183/mes.2024-26-3-57-64

Funding: the study was conducted within the framework of the RAS basic theme FMFR-2024-0042.

Compliance with ethical principles: all studies were conducted in accordance with the principles of biomedical ethics formulated in the 1964 Declaration of Helsinki and its subsequent updates and approved by the Bioethics Commission of the Federal State Budgetary Institution of Science of the State Scientific Center of the Russian Federation — Institute of Medical and Biological Problems of the Russian Academy of Sciences (Moscow) (Protocol No.641 of 14.06.2023). Each participant in the study provided voluntary written informed consent signed by him/her after being informed of the potential risks and benefits, as well as the nature of the forthcoming study.

Potential conflict of interest: authors declare no conflict of interest.

✉ Olga V. Popova olya.popovaolga2710@yandex.ru

Received: 27 May 2024 **Revised:** 2 Sep. 2024 **Accepted:** 7 Sep. 2024

ПСИХОФИЗИОЛОГИЧЕСКОЕ СОСТОЯНИЕ ЧЕЛОВЕКА В ИЗМЕНЕННЫХ МАГНИТНЫХ УСЛОВИЯХ

Г.В. Ковров, О.В. Попова✉, А.Г. Черникова, О.И. Орлов

Государственный научный центр Российской Федерации — Институт медико-биологических проблем Российской академии наук, Москва, Россия

Введение. В связи с тем что в ближайшем будущем планируются космические полеты за пределы околоземной орбиты, становится актуальным изучение воздействия сниженного магнитного поля Земли на человека.

Цель. Оценка особенностей сенсомоторных реакций, качества ночного сна и развития дневной сонливости при 24-часовом пребывании в гипомагнитных условиях.

Материалы и методы. Экспериментальные исследования проведены в 2023 г. с участием 6 мужчин-добровольцев в возрасте от 26 до 37 лет. Были проведены 4 экспериментальные серии длительностью 24 ч каждая. В трех группах испытуемые подвергались воздействию гипомагнитных условий (в пределах 0,05–0,14 мкТл), в группе плацебо не было воздействия. В качестве методов исследования применялись анкетирование (по качеству и особенностям ночного сна и дневного бодрствования) и оценка особенностей сенсомоторных функций.

Результаты. Установлено, что в гипомагнитных условиях усиливается дневная сонливость в 66% наблюдений по сравнению с 33% случаев в серии с плацебо ($p = 0,003$). Сразу после прекращения экспериментального воздействия наблюдалась быстрая активация центральной нервной системы, что выражалось в статистически значимом снижении общего времени зрительно-моторной реакции.

Выводы. В гипомагнитных условиях сохраняется работа мозговых механизмов сна. В дневное время в гипомагнитных условиях развивается сонливость, что указывает на возможность изменения циркадианной ритмики в активирующих системах головного мозга. Сразу после прекращения действия гипомагнитных условий происходит быстрая активация центральной нервной системы, имеющая компенсаторный характер. Выявленные особенности влияния гипомагнитных условий на цикл сна–бодрствования и сенсомоторные функции предполагают проведение дальнейших исследований дневной сонливости с использованием дополнительных субъективных и объективных методов оценки уровня бодрствования и активности центральной нервной системы.

Ключевые слова: сенсомоторные функции; гипомагнитные условия; простая зрительно-моторная реакция; анкетная самооценка; ночной сон; дневная сонливость

Для цитирования: Ковров Г.В., Попова О.В., Черникова А.Г., Орлов О.И. Психофизиологическое состояние человека в измененных магнитных условиях. *Медицина экстремальных ситуаций.* 2024;26(3):57–64. https://doi.org/10.47183/mes.2024-26-3-57-64

Финансирование: работа была выполнена в рамках базовой тематики РАН FMFR-2024–0042.

Соответствие принципам этики: Все исследования проведены в соответствии с принципами биомедицинской этики, сформулированными в Хельсинкской декларации 1964 г. и ее последующих обновлениях, и одобрены биоэтической комиссией федерального государственного бюджетного учреждения науки «Государственный научный центр Российской Федерации — Институт медико-биологических проблем» РАН (Москва) (протокол № 641 от 14.06.2023). Каждый участник исследования представил добровольное письменное информированное согласие, подписанное им после разъяснения ему потенциальных рисков и преимуществ, а также характера предстоящего исследования.

Потенциальный конфликт интересов: авторы заявляют об отсутствии конфликта интересов.

✉ Попова Ольга Владимировна olya.popovaolga2710@yandex.ru

Статья поступила: 27.05.2024 **После доработки:** 02.09.2024 **Принята к публикации:** 07.09.2024

INTRODUCTION

Hypomagnetic conditions (HMC) of outer space, as well as of the Moon and Mars, represent a potentially critical problem for astronauts' health and performance during long interplanetary missions. Experiments devoted to the studies of HMC effects on humans have shown a decrease in body reserves due health problems such as sleep disorders, metabolic changes, and the appearance of neurological disorders [1]. The formation of a labor and rest regime in accordance with a person's physiological capabilities under HMC will allow to increase the adaptation efficiency and fulfillment of the tasks assigned to him/her.

Despite the abundance and diversity of empirical data, the mechanisms underlying magnetoreception are yet to fully identified. As of today, there are many hypotheses — for example, the radical pair model and the magnetoreception model with magnetite (iron oxide) as the key component. Any weakening of the magnetic field represents a stress factor for biological organisms, with the nervous system performing the most important regulatory function in the formation of the organismal stress response [2]. It has been suggested that two types of human nervous system response to the Earth's magnetic field are the stressor response and sedative effect of slow magnetic oscillations. When studying the reactions of the nervous system when exposed to electromagnetic fields, a nonspecific reaction of brain cells accompanied by inhibition of conditioned reflex activity, including learning and memory processes, was found. It is worth mentioning that the cellular reaction resembled Selye's stress syndrome [3].

Due to bioethical issues, most experimental studies of HMC effects are carried out on animals. It has been shown that prolonged absence of a magnetic field significantly reduces the ability to adapt [4]. Exposure to HMC significantly impairs neurogenesis and cognitive function in the hippocampus of adult mice by reducing endogenous levels of aminophenyl butyric acid (ABA) in neural stem cells [5]. HMC exposure also produced impairment of noradrenergic activity in the brainstem of golden hamsters, with both the noradrenaline content and the density of noradrenaline-immunopositive neurons significantly decreasing following prolonged exposure to near-zero magnetic environment [6]. Studies of long-term exposure to HMC have shown that animals spend relatively more time learning a new object and its location in space, Zhang B.F. et al. suggest that exposure to HMC impairs spatial and cognitive memory of mice [5]. In addition, leukopenia, low metabolic rate, increased mortality and disruption of circadian rhythms have been found due to the lack of natural magnetic conditions [7]. Changes in circadian rhythm and melatonin secretion are also known to lead to negative consequences in the form of decreased antioxidant capacity of the organism [8].

The HMC effect on humans is less studied. In particular, the ability to solve cognitive tests in humans deteriorates already at 40 min under HMC [9], and the biological effects of HMC depend on the complexity of the task. The maximum effects were observed when performing complex cognitive tests, where the increase in the number of errors ranged from 5.1 ± 1.6% to 7.4 ± 2.5% [10]. The results of the study by Binga V.N. et al. [11] revealed significant changes in cognitive and sensorimotor tests results: a slower reaction speed, increased number of errors and decreased short-term memory of men who were in the "zero magnetic field". The experiment of Sarimov R.M. et al. [12] in two modes of exposure ("placebo" and "zero magnetic field") lasting 1 h 17 min with an interval of 40–60 days between series revealed that "zero magnetic field" causes an increase in the number of errors and an increase in the time of task performance in cognitive tests, while the results of cognitive tests under conditions of "zero magnetic field" decreased in 25 out of 40 subjects.

The autonomic regulation of cardiac activity also changed already in the first 8 h of stay in the HMC, mainly due to deviations in the activity of the parasympathetic nervous system [13]. The effects of HMC influence on the development of general asthenia, fatigue, drowsiness, affective reactions and other possible negative psychophysiological states, which pose a threat in terms of emergency situations arising in the course of operator activity, contribute to the disruption of interaction in small groups and complicate their activity, thus reducing the efficiency of space flight target tasks, have not been practically studied.

In 1976, Nakagawa described the occurrence of numerous clinical and subclinical symptoms associated with the weakening of the effect of the Earth's natural geomagnetic field on humans, which later became known as "magnetic field deficiency syndrome". In magnetic field deficiency syndrome, loss of work capacity, increased sleepiness, and nighttime sleep disturbances are noted [14]. It can be assumed that HMCs can contribute to the appearance of daytime sleepiness as a condition associated with cognitive deficit and change the quality of night sleep, especially its restorative function, changing the physiological basis for optimal functioning in the sleep-wake cycle.

Quantitative assessment of weak magnetic fields effect on the human body is one of the most debated issues in contemporary magneto- and heliobiology. Since changes in the magnetic field often do not lead to a visible reaction of the organism or significant changes in physiological processes during short-term experiments, the more urgent problem here consists in the assessment of the long-term effect of magnetic field variations.

The aim of the present study was to evaluate the peculiarities of sensorimotor reactions, quality of night sleep, and development of daytime sleepiness during a 24-hour stay in hypomagnetic conditions.

MATERIALS AND METHODS

HMC modeling was carried out in a limited volume by the method of compensation of the Earth's natural magnetic field by a system of windings with current (Helmholtz rings), whose total magnetic field vector is directed in the opposite direction of the Earth's geomagnetic field ("Arfa" unit, (IMBP)).

The Arfa facility is designed for modeling of HMC based on the method of compensation of the natural geomagnetic field (GMF), in which the total MF-vector of Helmholtz rings is directed in the opposite direction to the Earth's magnetic field. A magnetic field uniformly distributed in value and direction is created according to the specially selected diameter of the rings and their location inside the chamber. The system makes it possible to compensate for changes in the magnetic field along the vertical component parallel to the maximum size of the exposure unit.

As a result, the magnetic field induction in the working volume of the movable box of the exposure unit can reach zero and negative values (reverse direction of the GMF-vector). The magnetic field indices are monitored using a three-component FL3-100 sensor (Stefan Mayer Instruments, Germany) [13].

Six healthy male volunteers aged 26 to 37 years (BMI 24.77 ± 2.99) participated in the experiment. All participants underwent medical examination prior to the start of the experiment, were recognized as healthy and had no contraindications for participation in the experiment. All studies were conducted in accordance with the principles of biomedical ethics formulated in the 1964 Helsinki Declaration and its subsequent updates and approved by the Bioethics Commission of the Federal State Budgetary Institution of Science of the State Scientific Center of the Russian Federation — Institute of Medical and Biological Problems of the Russian Academy of Sciences (Moscow) (Protocol No. 641 of 14.06.2023). Each study participant provided a voluntary written informed consent signed by him/her following an explanation of the potential risks and benefits, as well as the nature of the upcoming study. The experiment was a randomized double-blind placebo-controlled study. Each subject participated in 4 experimental series, where one had no exposure to HMC while the other three created HMC with reduced natural magnetic field (mean 0.05–0.14 μT). Thus, 2 experimental groups were distinguished: "Placebo" (n = 6) and "HMC" (n = 18). Each experimental series included 3 sessions (Table 1).

Sensorimotor response studies were performed outside the experimental setup in the first 10 min after the end of session 3.

The study methods included:

1. To identify the features of sleep and wakefulness, an original structured questionnaire developed earlier was used; the subjects answered questions related to the sleep-wake cycle. A full description of the questionnaire was previously published [15]. In this study, answers to the following questions were analyzed: occurrence of daytime sleepiness (yes/no), occurrence of daytime sleep (yes/no, how many times per day); bedtime and wake-up time (astronomical time, hour) duration of falling asleep (min), number and duration of night awakenings (min).

2. Visual motor integration (VMI) test to assess hand-eye coordination within 10 minutes after the 3rd (afternoon) session with HMC outside the experimental setup. The test was conducted on a hardware-software complex developed at the Institute of Medical and Biological Problems. The test consisted of 11 presentations on the monitor screen of a stimulus in the form of a circle with a diameter of about 2.5 cm. While waiting for the stimulus to appear, the test subject was required to hold the cursor in another area of the monitor screen bounded by a square with a side also about 2.5 cm. When the stimulus appeared, the subject was had to move the cursor as quickly as possible from its location to the area of the circle and click the left mouse button. The results of 11 reactions to the stimulus were used to calculate the mean and standard deviation of the time from the onset of the stimulus to the onset of cursor movement (t1, the sensory component of the response), from the onset of cursor movement to placing the cursor in the circle (t2, the motor component of the response), and from the onset of the stimulus to clicking inside the circle (t3, the total reaction time).

Statistical processing was performed with the help of Statistica 13.0 software package using the nonparametric Mann-Whitney criterion, summary tables (banner tables), sign criterion and analysis of variance. The values of quantitative indicators are given as mean values and errors of mean. The peculiarity of the study was that with a sufficient number of indicators, the number of testers

Table 1. Experimental sessions (8 hours) in a series of studies

Experimental sessions and research therein					
1st session (afternoon) in the ARFA unit 12:00-20:00	Break, outside of the ARFA unit 20:00–23:00	2nd session (night) in the ARFA unit 23:00–7:00	Break, outside of the ARFA unit 7:00–10:00	3rd session (afternoon) at the pilot plant 10:00–18:00	After the end of the session outside of the ARFA unit 18:00–18:10
	Questionnaire (n = 24)			Questionnaire (n = 24)	ПЗМР (n = 24)

Table prepared by the authors using their own data

was limited by the peculiarities of its organization (n = 6). Statistical methods acceptable for small samples were used in the study [16].

STUDY RESULTS

Sleep quality. Analysis of the latent period of sleep (the rate of nocturnal falling asleep) revealed no significant pathological deviations in either experimental group. Prolongation of falling asleep time more than one hour was found in 1 case in 6 nights under placebo conditions and in two cases in 18 nights under HMC exposure. Falling asleep duration from 15 to 30 min under the HMC condition was found in 6 cases over 18 nights; in the placebo condition, this occurred in one case over 6 nights (Table 2).

These results indicate similar responses of sleep duration under both placebo and HMC conditions. At the same time, the relative representation of cases of longer sleep duration (more than 15 min) was slightly higher in the HMC group (Figure 1), although the differences did not reach the level of statistical significance.

During the period of nocturnal sleep under HMC exposure, one case of awakening for 18 nights was noted, while under placebo conditions a similar pattern was registered for 6 nights, which also indicates that there were no differences in the experimental groups in terms of the representation of nocturnal sleep disturbances.

Thus, no pathologic abnormalities were found for the duration of falling asleep and the number of nocturnal awakenings during exposure to HMC.

Daytime sleepiness. When comparing the frequency of daytime sleepiness episodes and/or its absence in the HMC and placebo exposure, an increase in the level of daytime sleepiness under the influence of HMC was revealed in 72% of observations (p = 0.003, according to the criterion of signs) as compared to the placebo group. The corresponding data are presented in Figure 2.

The increase in daytime sleepiness was characterized by the occurrence of daytime sleep in both experimental groups. However, the increase in daytime sleepiness under HMC exposure was not accompanied by an increase in the frequency of daytime sleep episodes as compared to placebo conditions. The data are presented in Table 3.

Single daytime naps were observed in 4 cases in the HMC group and once in the placebo group; double daytime naps were recorded 11 times in the HMC group and 4 times in the placebo condition. In both experimental groups, no daytime drowsiness or daytime sleep was noted in 59% of observations.

Hand-eye coordination after expose of HMC

When evaluating the effect of the end of HMC exposure on pand-eye coordination in the VMI-test, it was found that reaction times t1, t2, and t3 in the placebo group were 342.4 ± 52.9 ms, 455.1 ± 82.5 ms, and 632.5 ± 104.6 ms, respectively, and 336.2 ± 44.1 ms, 433.9 ± 64.1 ms, and 596.0 ± 86.8 ms after the end of HMC exposure.

Examination of VMI-test performance dynamics (Figure 3) revealed that after being in HMC, the values of

Table 2. Duration of falling asleep in experimental groups

Conditions	Falling asleep for less than 15 minutes	Falling asleep for 15–30 minutes	Falling asleep for more than an hour	In total
	Number of cases			
Placebo	4	1	1	6
HMC	10	6	2	18
All series	14	7	3	24

Table prepared by the authors using their own data

Table 3. Episodes of daytime sleep under Placebo and HMC conditions

Frequency of sleep disturbances (drowsiness) per day	Study groups	
	Placebo	HMC
Absent	7	21
Once	1	4
Twice	4	11
Total number of observations	12	36

Table prepared by the authors using their own data

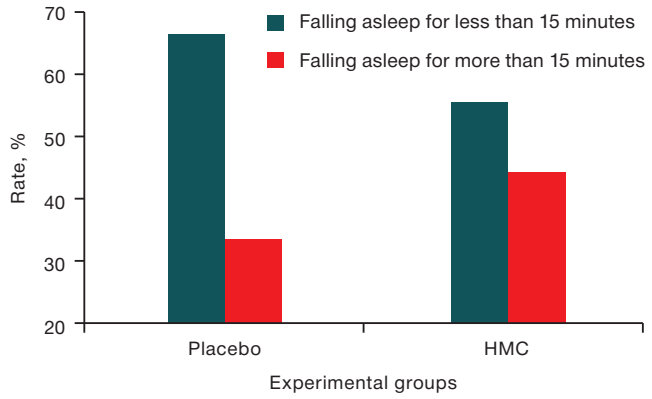

The figure is prepared by the authors using their own data

Fig. 1. Distribution of falling asleep duration values in the experimental groups

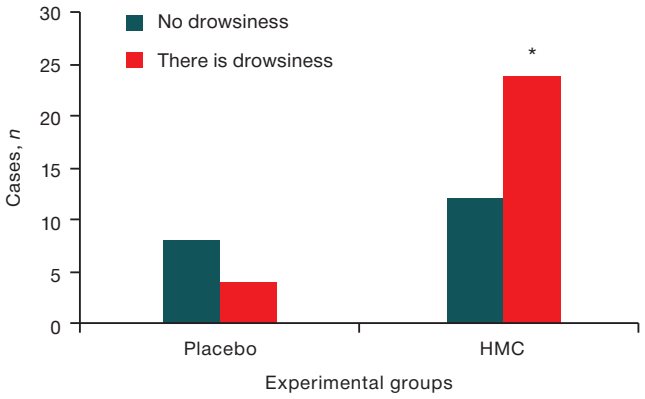

Figure prepared by the authors using their own data

Fig. 2. The presence of daytime sleepiness in Placebo and HMC.
Note: * — p = 0.003

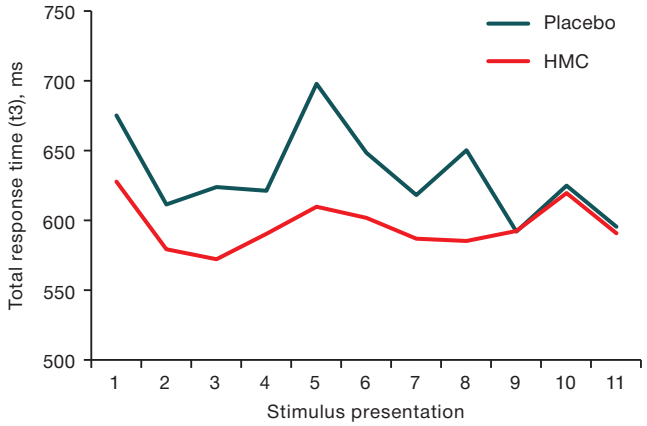

Figure prepared by the authors using their own data

Fig. 3. Time of visual-motor reaction with sequential presentation of stimuli after the end of HMC sessions and Placebo sessions

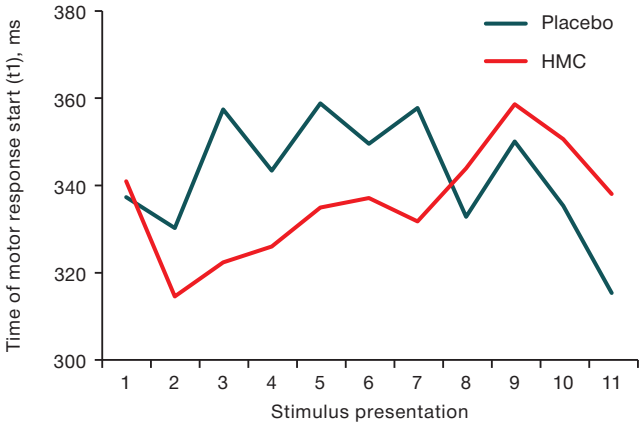

Figure prepared by the authors using their own data

Fig. 4. The time of onset of the motor reaction (t1) with successive presentation of stimuli after the end of the HMC session and Placebo sessions

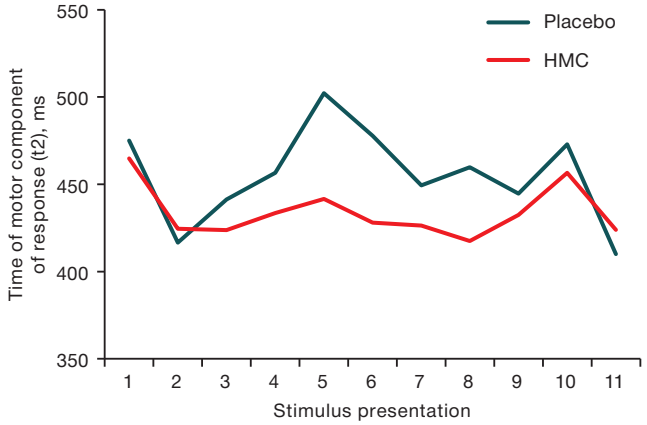

Figure prepared by the authors using their own data

Fig. 5. Cursor movement time to the stimulus (t2) with sequential presentation of stimuli after HMC sessions and placebo sessions

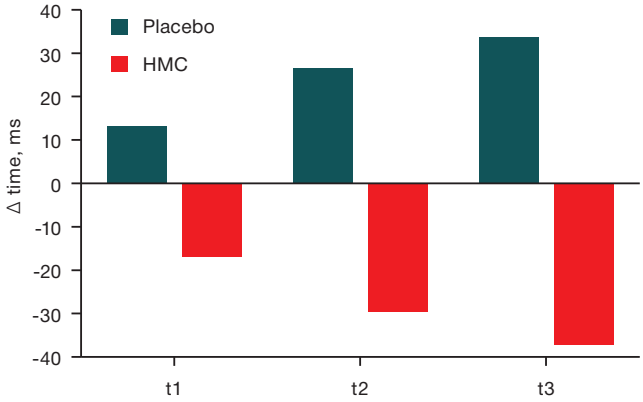

Figure prepared by the authors using their own data

Fig. 6. Sensorimotor functions in groups with and without daytime sleepiness after placebo and HMC conditions
Note: Δ — difference between the values after a session without daytime sleepiness and with daytime sleepiness

total task completion time (t3) (except for the 9th presentation) in the HMC exposure group were statistically significantly lower according to the sign criterion M = 590.5 ms (Q25 = 585.7 ms, Q75 = 607.8 ms) vs. M = 644.0 ms (Q25 = 618.8; Q75 = 649.7) after placebo.

The time to move the cursor from the square to the stimulus–motor component of the response (t2) from the 3rd response to the 10th response in the HMC exposure group was lower M = 430.3 ms (Q25 = 425.7 ms, Q75 = 435.5 ms) in comparison with the analogous index of the placebo group M = 458,1 ms (Q25 = 448.2 ms, Q75 = 474.1 ms) and at statistical processing of the data using the criterion of signs the acceleration of reaction time in 9 out of 11 presentations was noted ($p < 0.05$). The data are presented in Figure 5.

Daytime sleepiness under HMC and sensorimotor functions upon discontinuation

Taking into account the more frequent occurrence of daytime sleepiness in HMC conditions, we compared the reaction time when performing VMI-test in cases where episodes of daytime sleepiness were registered in the past session and where they were not. Analysis was performed using the nonparametric Mann–Whitney criterion. Subjects with identified daytime sleepiness following exposure to HMC had shorter reaction times than subjects exposed to HMC who did not have episodes of sleepiness recorded. In contrast, after placebo sessions, subjects with identified daytime sleepiness had longer VMI-test times than subjects in the placebo group who did not experience sleepiness. The data are presented in Figure 6.

Analysis of variance ($F = 22.6$, $p < 0.05$) was performed to assess changes in t1, t2, t3 for the group with reported sleepiness following exposure to HMC and placebo. Figure 7 shows a statistically significant decrease in sensorimotor reaction time immediately after the end of being in the experimental setup in the HMC exposure series compared to placebo.

Analysis of variance ($F = 22.6$, $p < 0.05$) was performed to assess changes in t1, t2, t3 for the group with reported sleepiness after exposure to HMC and placebo. Figure 7 shows a statistically significant decrease in sensorimotor reaction time immediately after the end of being in the experimental setup in the HMC exposure series compared to placebo.

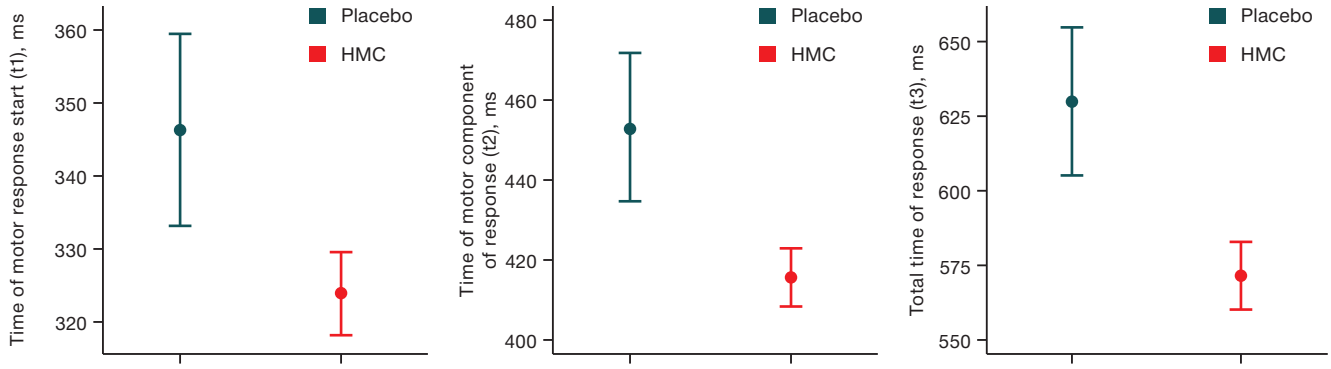

Figure prepared by the authors using their own data

Fig. 7. Results of the variance analysis of VMI-test for the group with daytime sleepiness under placebo and HMC conditions

DISCUSSION

In our study, the detection of daytime sleepiness was based on self-reporting by healthy volunteers who assessed the presence of sleepiness retrospectively after the end of the experimental sessions. This informative approach confirmed the exacerbation of subjective daytime sleepiness under HMC conditions as compared to placebo. The main causes of daytime sleepiness in healthy individuals in most cases are lack of previous nighttime sleep and fatigue state [17]. The appearance of daytime sleepiness and somnolence combined with a reduction in the duration of nocturnal sleep is characteristic of isolation conditions and antiorthostatic tilt [18, 19], which also simulate the effect of some spaceflight factors. In studies by Kukanov V. Yu et al. based on changes in the ratios of the sums of delta and theta bands to the sum of alpha and beta bands of the electroencephalogram, a shift in brain activity toward inhibition processes was noted, possibly constituting evidence of the development of fatigue [13]. In turn, we did not detect a reduction in the duration of the preceding night's sleep, increase in the time taken to fall asleep or an increase in the frequency of night awakenings — i.e., a decrease in its quality, which probably indicates other causes of daytime sleepiness, in particular, the hypnogenic effect of the reduced magnetic field.

The complex symptom of daytime sleepiness, comprised of a feeling of desire to sleep, manifestations of reduced physical and mental activity, ultimately creates additional risks of accident development. It is important to note that sleepiness, which is not a stationary state, can be pronounced or barely noticeable, appear and disappear depending on various external and internal factors, as well as occasionally leading to unexpected falling asleep. The mechanisms of daytime sleepiness development in hypomagnetic conditions are insufficiently studied. Based on the previously revealed drop in the level of norepinephrine in animals under conditions of exposure to HMC [6], we can assume that the neurochemical basis for the development of somnolence in HMC in humans includes a decrease in the level of norepinephrine, acetylcholine, serotonin, dopamine, and other neurotransmitters, whose activity is closely related to the sleep–wake cycle.

The occurrence of daytime sleep and drowsy states may reflect the degree of severity of drowsiness and fatigue and lead to errors in operator activity [17, 20]. Our study showed that under the HMC, the subjects had significantly more frequent drowsy states than in the placebo series, while episodes of daytime sleep were observed only during the development of drowsiness, which indicates not only a more frequent but also a more significant disruption of the sleep-wake cycle [21,22] than in subjects with HMC [21,22] than in subjects in the placebo group. Taking into account that daytime falling asleep is an independent medical problem associated with neurochemical changes in orexin production, it can be assumed that the orexin system of wakefulness maintenance is likely to be affected under HMC [23].

In the conducted study the human state was shown to be more active that immediately after the end of a session of HMC exposure than after a placebo session. Already in the first minutes after resuming the action of the geomagnetic field, there is a decrease in the reaction time when performing the VMI-test, which is an interesting phenomenon reflecting the ability of brain systems to rapidly increase neurotransmitter activity [23]. The biological effects of restoring natural geomagnetic field levels are poorly understood. In animal studies [24], it was shown that an 8-day stay of animals in a hypomagnetic environment (30 min per day) resulted in activation of adrenal function one hour after cessation of HMC. The results of our study may reflect these changes, since enhanced adrenal hormone production is directly related to improved function of central nervous system (CNS) and faster reaction times. At the same time, a 30-day stay in the HMC led to a decrease in adrenal function, so the question of the stimulating effect of restoration of the natural magnetic field remains open and requires further study.

It is possible that a person being in a drowsy state plays the role of a kind of "fuse" in the adaptation of the nervous system to the effects of HMC; thus, the restoration of the magnetic field allows the brain to quickly switch to an active state. If this hypothesis is confirmed, then the HMC conditions can be considered as a way of transferring the organism to the level of functioning that is borderline between sleep and wakefulness, where a decrease in cognitive abilities is a protective reaction. In

this situation, it is necessary to investigate and develop safe work and rest regimes for individuals in hypomagnetic conditions. Magnetic field reduction can also be considered as an auxiliary means of providing "hibernation" of brain activity, which can be used during flights to deep space. Under terrestrial conditions, hypomagnetic installations can be used in the practice of neuroreanimation when it is necessary to reduce brain activity or in rehabilitation after stressful influences. Restoration of the natural magnetic field, contributing to a rapid increase in brain activity, can be considered as a natural stimulant of cognitive activity.

CONCLUSIONS

1. During the nocturnal sleep period, the subjective rate of falling asleep and the frequency of nocturnal awakenings do not change under the influence of HMC, suggesting that brain mechanisms of sleep are preserved in operation.

2. Further studies using larger samples, an expanded set of methods, the study of delayed aftereffects of HMC and "fast" effects of restoration of the normal magnetic field are likely to help evaluate the possibilities of using HMC in the therapy and prevention of neurodegenerative and post-stress disorders.

References

1. Xue X, Ali YF, Luo W, Liu C, Zhou G, Liu NA. Biological Effects of Space Hypomagnetic Environment on Circadian Rhythm. *Front. Physiol*. 2021;12:643943. https://doi.org/10.3389/fphys.2021.643943
2. Nikitina EA, Vasilyeva SA, Shchegolev BF, Savvateeva-Popova EV. Weak static magnetic field: Effects on the nervous system. *Journal of Higher Nervous Activity*. 2022;72(6):783–99 (In Russ.). https://doi.org/10.31857/S0044467722060077
3. Karpin VA, Kostyukova NK. The influence of weak magnetic fields on higher nervous activity. *Baikal Medical Journal.* 2004. 46(5):7–11 (In Russ.).
4. Tian L, Luo Y, Zhan A, Ren J, Qin H, Yongxin Pan. Hypomagnetic Field Induces the Production of Reactive Oxygen Species and Cognitive Deficits in Mice Hippocampus. *Int J Mol Sci*. 2022;23(7):3622. https://doi.org/10.3390/ijms23073622
5. Zhang BF, Wang L, Zhan AS, Wang M, Tian LX, Guo WX, Pan YX. Long-term exposure to a hypomagnetic field attenuates adult hippocampal neurogenesis and cognition. *Nat. Commun.* 2021;(12):1174. https://doi.org/10.1038/s41467-021-21468-x
6. Zhang X, Li J F, Wu Q J, Li B, Jiang JC. Effects of hypomagnetic field on noradrenergic activities in the brainstem of golden hamster. *Bioelectromagnetics.* 2007;(28):155–8. https://doi.org/10.1002/bem.20290
7. Wang X, Jing C, Selby C P, Chiou Y Y, Yang Y, Wu W et al. Comparative properties and functions of type 2 and type 4 pigeon cryptochromes. *Cell Mol. Life Sci*. 2018;(75):4629–41. https://doi.org/10.1007/s00018-018-2920-y
8. Jia B, Xie L, Zheng Q, Yang PF, Zhang WJ, Ding C, et al. A hypomagnetic field aggravates bone loss induced by hindlimb unloading in rat femurs. *PLoS One*. 2014;(9):e105604. https://doi.org/10.1371/journal.pone.0105604
9. Sarimov RM, Binhi VN, Milyaev, VA. The influence of geomagnetic field compensation on human cognitive processes. *Biophysics*. 2008;53(5):433–41. https://doi.org/10.1134/S0006350908050205
10. Binhi VN, Sarimov RM. Zero Magnetic Field Effect Observed in Human Cognitive Processes. *Electromagnetic Biology and Medicine*. 2009;28(3):310–5. https://doi.org/10.3109/15368370903167246
11. Bingi VN, Milyaev VA, Salimov RM, Zarutsky AA. The influence of electrostatic and "zero" magnetic fields on the psychophysiological state of a person. *Biomedical technologies and radio electronics.* 2006;8(9): 48–58 (In Russ.). EDN: HVNYQN
12. Sarimov RM, Binhi VN, Milyaev VA The Influence of Geomagnetic Field Compensation on Human Cognitive Processes. *Biofizika*. 2008;53(5):856–66. https://doi.org/10.1134/S0006350908050205
13. Kukanov VYu, Vasin AL, Demin AV, Schastlivtseva DV, Bubeev YuA, Suvorov AV et al. Effect of Simulated Hypomagnetic Conditions on Some Physiological Paremeters under 8-Hour Exposure. Experiment Arfa-19. *Hum Physiol*. 2023;(49):138–46 (In Russ.). https://doi.org/10.31857/S0131164622600343
14. Nakagawa K. Magnetic Field Deficiency Syndrome and Magnetic Treatment. *Japan Medical Journal*. 1976; 2745
15. Kovrov GV, Vlasova AV, Popova OV, Chernikova AG. Changes in the pattern of sleep disorders in healthy people under conditions of 21-day antiorthostatic hypokinesia *ActaBiomedica Scientifica*. 2023;8(6):241–8 (In Russ.). https://doi.org/10.29413/ABS.2023-8.6.24
16. Nosovsky AM, Popova OV, Smirnov Yul. Modern technologies of statistical analysis of medical data and methods of their graphical representation. Aerospace and environmental medicine. 2023;57(5):149–154 (In Russ.). https://doi.org/10.21687/0233-528X-2023-57-5-149-154
17. Roehrs T., Carskadon M.A., Dement W.C., Roth T. Daytime Sleepiness and Alertness, Principles and Practice of Sleep Medicine. *Elsevier*. 2017;4:39–48. https://doi.org/10.1016/s0149-7634(87)80016-7
18. Vane AM, Ponomareva IP, Yeligulashvili T, Levin YaI, Kovrov GV, Filimonov MI. Features of the sleep-wake cycle during prolonged isolation. *Aerospace and environmental medicine*. 1997;31(4):36–41 (In Russ.).
19. Dorokhov VB. Analysis of the psychophysiological mechanisms of impaired activity during somnolent changes in consciousness. *Bulletin of the RGNF*. 2003;1(4):137–44 (In Russ.).
20. Putilov AA, Donskaya OG, Verevkin EG, Arsen'ev GN, Puchkova AN, Dorokhov VB, et al. Overlap between individual variation in personality traits and sleep-wake behavior. *Current Psychology*. 2021. https://doi.org/10.1007/s12144-021-01495-z
21. Shevtsova KV, Nodel MR, Kachanovsky MS, Kovrov GV, Yakhno NN. Multifactorial daytime sleepiness in Parkinson's disease. Bulletin of the National Society for the Study of Parkinson's *Disease and Movement Disorders*. 2022;(2):223–6 (In Russ.). https://doi.org/10.24412/2226-079X-2022-12473
22. Nodel MR, Shevtsova KV, Kovrov GV, Yakhno NN. Unexpected falling asleep in patients with Parkinson's disease. *Russian Neurological Journal*. 2022;27(1):62–8 (In Russ.). https://doi.org/10.30629/2658-7947-2022-27-1-62-68
23. Kovalzon VM. A modern view on the serotonin theory of depression. *Russian Neurological Journal*. 2020;25(3):40–4 (In Russ.). https://doi.org/10.30629/2658-7947-2020-25-3-40-44
24. Shust IV, Kostin IM. Reactions of the adrenal cortex of animals to the effects of strong constant MP and hypomagnetic medium. *Problems of endocrinology*. 1976;22(2):86–91.

Authors' contributions. All the authors confirm that they meet the ICMJE criteria for authorship. The most significant contributions were as follows. Gennady V. Kovrov — writing an article, data analysis, Olga V. Popova –writing an article, data collection, Anna G. Chernikova — writing an article, data analysis, Oleg I. Orlov — scientific supervisor of the experiment

AUTHORS

Gennady V. Kovrov, Dr. Sci. (Med.), Professor
https://orcid.org/0000-0002-3564-6798
kgv2006@yandex.ru

Olga V. Popova
https://orcid.org/0009-0002-3749-588X
olya.popovaolga2710@yandex.ru

Anna G. Chernikova, Cand. Sci. (Biol.)
https://orcid.org/0000-0002-2596-8929
anna.impb@mail.ru

Oleg I. Orlov, Dr. Sci. (Med.), Acad. of the RAS
https://orcid.org/0000-0002-2174-3183
orlov@imbp.ru

https://doi.org/10.47183/mes.2024-26-3-65-70

PATHOBIOCHEMICAL ASPECTS OF DIVERS BARODENTALGIA

Ilyas R. Klenkov, Artyom S. Krivonos✉, Roman A. Grashin, Alina V. Pototskaya, Vladimir A. Zheleznyak, Inna S. Maday

Kirov Military Medical Academy of the Ministry of Defense of the Russian Federation, Saint-Petersburg, Russia

Introduction. During their descent under water, divers may suffer from acute toothache attacks (barodentalgia), creating an emergency that leads to the termination of diving descent. Barodentalgia can be caused by hypoxic process in the pulp of filled teeth under increased intrapulpal pressure.

Objective. To reveal the peculiarities of hypoxic processes in the pulp of filled teeth under hyperbaric exposure basing on oximetry and fluorescence change parameters.

Materials and methods. The study involved 34 male divers who underwent a dental examination at the first stage to select individuals for the second stage of the experiment. 24 subjects were selected for the second stage and evaluated for oximetric (mixed blood saturation) and fluorescent (reduced coenzyme NADH, oxidized coenzyme FAD, fluorescent oxygen consumption index — FOCI) indices of filled teeth. The evaluation was performed by optical tissue oximetry (OTO) and laser-induced fluorescence (LIF) methods before and after immersion in a barocamera at pressure of 0.4 MPa while breathing air.

Results. Following exposure to increased pressure of the gas medium as compared to the initial values in the filled teeth, the following phenomena were observed: decrease in pulp saturation by 33.7% ($p<0.05$); increase in NADH by 14.4%; decrease in FAD by 22.9%; increase in FOD by 73.4% ($p<0.05$).

Conclusions. The revealed changes in the indicators of mixed blood saturation, NADH, FAD and FOCI confirm the presence of hypoxic process in the pulp of filled teeth under hyperbaric exposure.

Keywords: toothache; dentistry; barodentalgia; divers; hypoxia; saturation; filled teeth

For citation: Klenkov I.R., Krivonos A.S., Grashin R.A., Pototskaya A.V., Zheleznyak V.A., Madai I.S. Pathobiochemical aspects of divers barodentalgia. *Extreme Medicine*. 2024;26(3):65–70. https://doi.org/10.47183/mes.2024-26-3-65-70

Funding: the study was performed without external funding.

Acknowledgements: the authors would like to express their gratitude to Professor Eleonora G. Borisova and Associate Professor Alexander M. Kovalevsky from Military Medical Academy for their constructive comments on an earlier version of the article.

Compliance with ethical principles: the study was approved by a meeting of the independent ethical committee in Kirov Military Medical Academy (extract from protocol No. 286 of 19.12.2023). All participants signed voluntary informed consent for the study.

Potential conflict of interest: authors declare no conflict of interest.

✉ Artyom S. Krivonos artemkriwonos@yandex.ru

Received: 7 July 2024 **Revised:** 27 Aug. 2024 **Accepted:** 29 Aug. 2024

ПАТОБИОХИМИЧЕСКИЕ АСПЕКТЫ ВОЗНИКНОВЕНИЯ БАРОДЕНТАЛГИИ У ВОДОЛАЗОВ

И.Р. Кленков, А.С. Кривонос✉, Р.А. Грашин, А.В. Потоцкая, В.А. Железняк, И.С. Мадай

Военно-медицинская академия имени С.М. Кирова Министерства обороны Российской Федерации, Санкт-Петербург, Россия

Введение. У водолазов при спуске под воду могут возникать приступы острой зубной боли (бародонталгии), которая создает аварийную ситуацию и ведет к прекращению водолазного спуска. Бародонталгия может быть обусловлена гипоксическим процессом в пульпе пломбированных зубов и повышением внутрипульпарного давления.

Цель. На основании изменений показателей (оксиметрии и флуоресценции) выявить особенности протекания гипоксических процессов в пульпе пломбированных зубов при гипербарическом воздействии.

Материалы и методы. В исследовании приняли участие 34 водолаза из числа лиц мужского пола. На первом этапе было проведено их стоматологическое обследование с целью отбора претендентов на второй этап эксперимента. На второй этап отобрано 24 испытуемых, у которых проведена оценка оксиметрических (сатурация смешанной крови) и флуоресцентных (восстановленный кофермент НАДН, окисленный кофермент ФАД, флуоресцентный показатель потребления кислорода — ФПК) показателей пломбированных зубов. Оценку проводили методами оптической тканевой оксиметрии (ОТО) и лазерной флуоресцентной диагностики (ЛДФ) до и после погружения в барокамере при давлении 0,4 МПа при дыхании воздухом.

Результаты. После воздействия повышенного давления газовой среды по сравнению с исходными значениями в пломбированных зубах наблюдалось: снижение сатурации пульпы на 33,7% ($p < 0,05$); увеличение НАДН на 14,4%; снижение ФАД на 22,9%; повышение ФПК на 73,4% ($p < 0,05$).

Выводы. Выявленные изменения показателей сатурации смешанной крови, НАДН, ФАД и ФПК подтверждают наличие гипоксического процесса в пульпе пломбированных зубов при гипербарическом воздействии.

Ключевые слова: зубная боль; стоматология; бародонталгия; водолазы; гипоксия; сатурация; пломбированные зубы

Для цитирования: Кленков И.Р., Кривонос А.С., Грашин Р.А., Потоцкая А.В., Железняк В.А., Мадай И.С. Патобиохимические аспекты возникновения бародонталгии у водолазов. *Медицина экстремальных ситуаций*. 2024;26(3):65–70. https://doi.org/10.47183/mes.2024-26-3-65-70

Финансирование: работа выполнена без спонсорской поддержки.

Благодарности: профессору Борисовой Элеоноре Геннадиевне и доценту Ковалевскому Александру Мечиславовичу из Военно-медицинской академии за ценные критические замечания.

Соответствие принципам этики: исследование одобрено на заседании независимого этического комитета при Военно-медицинской академии имени С.М. Кирова (выписка из протокола № 286 от 19.12.2023). Все участники подписали добровольное информированное согласие на исследование.

Потенциальный конфликт интересов: авторы заявляют об отсутствии конфликта интересов.

✉ Кривонос Артем Сергеевич artemkriwonos@yandex.ru

Статья поступила: 07.07.2024 **После доработки:** 27.08.2024 **Принята к публикации:** 29.08.2024

INTRODUCTION

When diving under water, a person is affected by numerous factors of increased environmental pressure (the value of the total pressure and its variations, increased partial pressure of gases, high density of the gas mixture, frequency and duration of period under pressure, increased heat capacity and thermal conductivity of water, mechanical impact of equipment, etc.), forming specific conditions of diving labor and causing changes in the state of the human body some of which may be pathological [1].

Such pathological manifestations can significantly reduce professional efficiency of a diver and create an emergency situation, which inevitably entails reduction of professional longevity. One such pathological condition is barodentalgia, a syndrome arising under conditions of altered environmental pressure characterized by attacks of acute or aching toothache, as well as painful sensations in the dental row area [2].

According to research [2], one of the risk factors for barodentalgia in divers is the presence of filled teeth. In the pathogenesis of barodentalgia, an important role may be played by the hypoxic process, which develops in the pulp chamber of filled teeth as a result of impaired microcirculation. Hypoxic processes occur as a result of peripheral pulp vessels narrowing under the impact of increased environmental pressure and reduction of the pulp chamber in volume due to the formation of replacement dentin — a plastic process of the pulp that occurs in response to the consequence of damage to the hard tissues of the tooth (carious lesion).

Various methods are currently used to perform a quantitative assessment of metabolic processes occurring in human tissues — in particular, in the dental pulp [3–4]. In the present context, the most accessible techniques include optical tissue oximetry (OTO) and laser-induced fluorescence (LIF) [5]. These techniques allow to assess not only tissue parameters in general, but also changes in cellular metabolism characteristic of the hypoxic process in the dental pulp.

The purpose of the study is to identify the peculiarities of hypoxic processes in the pulp of intact and filled teeth under hyperbaric exposure on the basis of changes in the oximetry and fluorescence parameters.

MATERIALS AND METHODS

Under the auspices of the Military Medical Academy, we conducted a study with the participation of the Northern Fleet divers (n = 34), who were selected for the presence of barodentalgia in the anamnesis revealed via questioning using a questionnaire developed by us, as well as those referred for health reasons. The age of the experimental subjects ranged from 24 to 47 years. All subjects were male. The study was carried out in two stages.

At the first stage of the study, 34 individuals were selected based on oral examination data and analysis of cone beam computed tomograms (hereinafter referred to as CBCTs). The main selection criterion for participation in the study was the presence of a pair of symmetrical teeth (one morphofunctional group) in which one tooth was affected by barodentalgia and the second tooth was intact. 24 testers were selected for the second stage.

At the second stage of the study, we evaluated oximetric and fluorescent indices of intact and filled teeth of 24 subjects by the method of oxidative metabolism diagnostics using the LASMA-D apparatus (Russia) before and after immersion in the flow-decompression chamber KVD-1600 (Russia) for a duration of 125 minutes at a pressure of 0.4 MPa under a special decompression mode with air breathing.

The following parameters were measured: mixed blood (arterial and venous) saturation using the technique of optical tissue oximetry (OTO), fluorescence emission amplitude of reduced coenzyme NADH and oxidized coenzyme FAD using the technique of laser-induced fluorescence (LIF).

Based on the fluorescence spectra obtained under excitation by external radiation, we calculated the fluorescence oxygen consumption index (FOCI), which reflects the redox potential in intracellular mitochondria, according to the formula [5]:

$$FOCI = \frac{ANADH}{AFAD}, \quad (1)$$

where FOCI — fluorescent indicator of oxygen consumption; ANADH — amplitude of fluorescence emission of the reduced nicotinamide adenine dinucleotide coenzyme; AFAD — amplitude of fluorescence emission of oxidized flavoproteins.

Mathematical data processing was carried out on a personal computer using the software package “StatSoft STATISTICA 10”. Quantitative data were checked for compliance with the theoretical Gauss-Laplace distribution law using the Shapiro-Wilk criterion. The groups were compared using the Mann-Whitney U-criterion.

STUDY RESULTS

During the collection of anamnesis data, the tooth subjected to barodentalgia was identified. It was also determined that barodentalgia occurred in filled teeth with clinically complete fillings, in carious teeth with different localization of the carious process and in teeth with caries recurrence. Based on the results of the dental examination, 24 individuals were selected, each having a pair of symmetrical teeth (of the same morphofunctional group), in which one tooth was barodontalgic while the other was intact. Filled teeth with clinically complete fillings and without signs of caries recurrence, in which the filling material was located within the peri-pulpal dentin, were selected for the study.

The incidence of filled teeth was significantly higher in the masseter group of the jaws than in the anterior group. Figure 1 shows an example of a CBCT of an experimental subject who met the selection criteria for participation in the study.

At the second stage, to evaluate oximetric and fluorescent parameters, we examined the molar groups of teeth

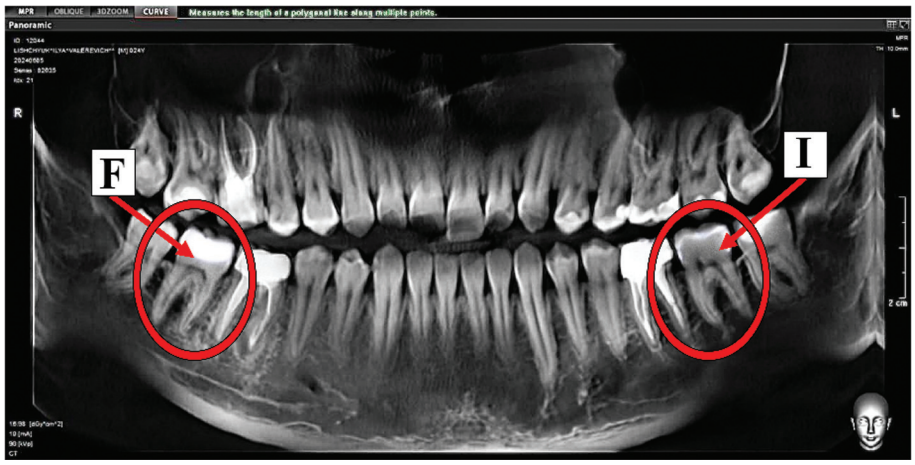

The figure was prepared by the authors using their own data

Fig. 1. Panoramic section of the cone-beam computed tomogram of diver V. (P is a filled tooth, and E is an intact tooth)

of the upper and lower jaws due to the high frequency of occurrence ($p < 0.05$) of filled teeth in this localization compared to other groups.

The results of oximetric and fluorescence diagnostics are presented in Table 1.

Figure 2 shows the results of OTO. Following exposure to elevated pressure, the mixed blood saturation level in intact teeth increased by 19.4%, while in filled teeth it decreased by 33.7% compared to baseline, which is a statistically significant change ($p < 0.05$).

While a decrease in the mixed blood saturation level in the filled teeth following hyperbaric exposure indicates the presence of a hypoxic process in the pulp, our tasks were, firstly, to identify the cause of this process, and secondly, to determine the changing vector in the metabolic processes of intact and sealed teeth at the tissue level, forming the basis for an extended LIF-used diagnostics of pulp.

The results of the LIF are presented in the table. The initial value of the fluorescence emission amplitude of the

Table 1. Oximetric and fluorescence diagnostic results

Indicator	Tooth condition	Descent period	Me [Q25;Q75]	Degree of change, %
Oximetric indicators (GRT)				
Saturation	intact	before hyperbaric exposure	38.1[28.9;49.3]	19.40
		after hyperbaric exposure	45.5[38.5;56.6]	
	filled	before hyperbaric exposure	19.6[11.9;35.3]	–33.70*
		after hyperbaric exposure	13.0[5.7;23.0]	
Fluorescent indicators (LIF)				
NADH	intact	before hyperbaric exposure	1.16[0.87;1.22]	–15.50
		after hyperbaric exposure	0.98[0.82;1.16]	
	filled	before hyperbaric exposure	1.11[0.92;1.20]	14.40
		after hyperbaric exposure	1.27[1.17;1.38]	
FAD	intact	before hyperbaric exposure	1.13[0.88;1.28]	–34.50
		after hyperbaric exposure	0.74[0.62;0.98]	
	filled	before hyperbaric exposure	1.18[0.965;1.31]	–22.90
		after hyperbaric exposure	0.91[0.685;1.16]	
FOCI	intact	before hyperbaric exposure	1.02[0.83;1.42]	23.50
		after hyperbaric exposure	1.26[0.92;1.43]	
	filled	before hyperbaric exposure	0.94[0.77;1.23]	73.40*
		after hyperbaric exposure	1.63[1.33;1.84]	

The table was prepared by the authors using their own data

Note: * — $p < 0.05$

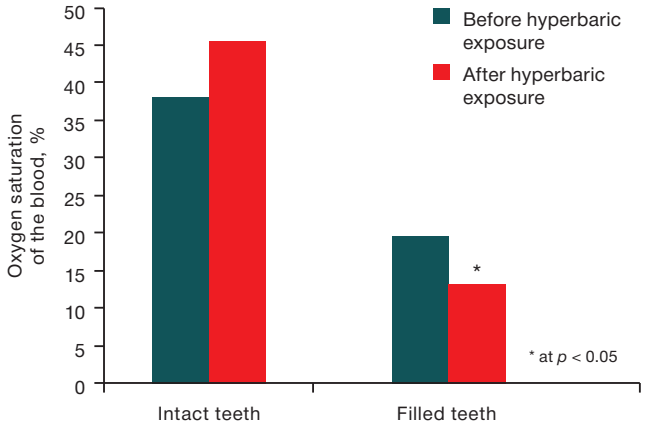

The figure was prepared by the authors using their own data

Fig. 2. Change in the oximetric indices of mixed blood saturation ($p < 0.05$)

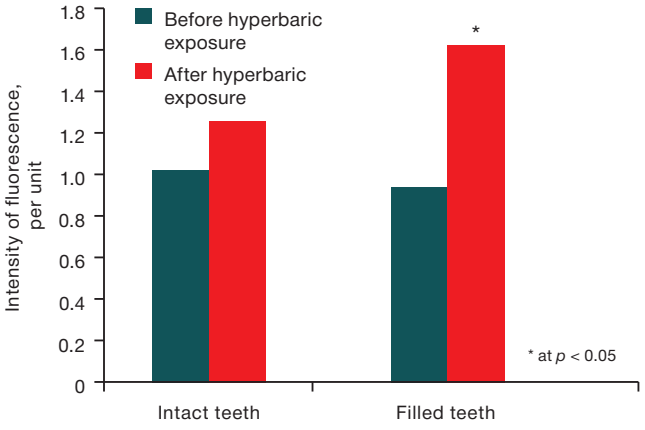

The figure is prepared by the authors using their own data

Fig. 3. Change in fluorescence index of oxygen consumption ($p < 0.05$)

reduced NADH coenzyme in intact teeth was 15.5% higher than after hyperbaric exposure. The initial NADH level in the filled teeth turned out to be 14.4% lower on average than after hyperbaric exposure. The data of the NADH indicator are not statistically strong.

The initial values of the fluorescence emission amplitude of the oxidized coenzyme FAD in intact teeth turned out to be significantly higher than those after exposure to increased pressure by an average of 34.5%. The initial values of the same indicator for the filled teeth were higher than after exposure to increased pressure by an average of 22.9%. The data of the FAD indicator are not statistically expressed.

The results of calculating the fluorescent indicator of oxygen consumption are shown in Figure 3. Under normobaric conditions, the FPC in intact teeth was 23.5% lower than after hyperbaric exposure. The initial values of FPC in the filled teeth were statistically significantly lower than after hyperbaric exposure by an average of 73.4% ($p < 0.05$).

Thus, changes in saturation and FPC indicators reveal a hypoxic process in sealed teeth that occur under conditions of increased gas pressure, whereas in intact teeth a change in this indicator is a sign of a slight decrease in the activity of metabolic processes.

DISCUSSION OF THE RESULTS

The calculated FPC indicator, which is based on determining the activity of intracellular mitochondria, indirectly reflects the level of oxygen metabolism in cells; however, in our study this indicator turned out to be very informative, since it allowed us to determine the presence of a hypoxic process in the pulp of filled teeth.

According to C.M. Math et al. (2017), centralization of blood flow under conditions of increased environmental pressure is followed by the development of a compensatory adaptive reaction in the form of narrowing of peripheral vessels against the background of a systemic increase in blood pressure [2]. In the pulp of the filled teeth, which are reduced in volume due to the formation of substitutive (tertiary) dentin, vasoconstriction leads to a significant decrease in microcirculation and perfusion.

With insufficient perfusion of the filled tooth tissues, an energy deficit occurs due to the participation of oxygen as a substrate of cytochrome oxidase in aerobic energy formation reactions. Lack of oxygen leads to a change in the enzyme complexes activity of the respiratory chain and a decrease in the level of adenosine triphosphate (ATP). This has a detrimental effect on energy-dependent cellular reactions, e.g., the formation of membrane potential, ion transport, electrogenic cell function, etc. [6–7].

A partial blockade of the respiratory chain also leads rapidly to an excessive concentration of reduced coenzymes such as NADH and $FADH_2$, which spontaneously dissociate with the release of protons to increase intramitochondrial hypoxia. This stage is characterized by an even greater slowdown in the oxidation of substrates in the tricarboxylic acid cycle and oxidative decarboxylation of pyruvic acid, increasing the accumulation of lactic acid (lactate) due to glycolysis under these conditions becoming the main energy process in the pulp cells of sealed teeth, while a high level of lactate contributes to an increase in the concentration of pyruvic acid and/or NADH [8–9].

The hypoxic process causing the development of an energy deficit of pulp cells triggers the release of biologically active substances such as bradykinin, serotonin, neuroactive peptides, etc., which, acting on the microvessels of the pulp, lead to vasodilation and increased vascular permeability, which entails an increase in intrapulpal pressure.

Why does barodentalgia occur? It may be caused by an increase in intrapulpal pressure, leading to irritation of nerve endings, since the pulp chamber of the filled tooth is reduced in volume due to the formed replacement dentin [10–11] and constant pressure of the filling material on the tooth pulp [12–13]. In intact teeth, the volume of the pulp chamber is of normal size, which does not cause an increase in intrapulpal pressure. At the stage of energy deficiency in the filled teeth, it is also worth noting the increase in the concentration of lactic acid in the intercellular space that contains a large number of nerve endings, which may

in all likelihood exacerbate the development of barodentalgia [14]. Biologically active substances such as bradykinin, serotonin, etc. can additionally increase the intensity of barodentalgia [15].

CONCLUSIONS

1. Following exposure to altered environmental pressure, there was a statistically significant decrease in mixed blood saturation in pulp vessels by an average of 33.7%, an increase in the fluorescence intensity of reduced NADH coenzymes by 14.4%, and a decrease in the fluorescence intensity of oxidized FAD coenzymes by 22.9% as compared with intact teeth.

2. The calculated index of the FPC of the filled teeth after exposure to increased environmental pressure significantly increased by 73.4% as compared with the identical index in intact teeth. The above changes in the studied indicators confirm the fact of the presence of a hypoxic process in the pulp of sealed teeth in divers under conditions of increased environmental pressure as compared with intact teeth. The exact mechanism by which a number of pathophysiological and biochemical changes trigger the development of barodentalgia due to the hypoxic process requires further research.

References

1. Zverev DP, Klenkov IR, Myasnikov AA, Shitov AYu, Fisun AV, Starkov AV, et al. The human body's resistance to the action of high partial pressures of nitrogen and methodological aspects of its assessment. *Marine medicine*. 2020;(4):44–53 (In Russ.). https://doi.org/10.22328/2413-5747-2020-6-4-44-53
2. Pototskaya AV, Krivonos AS, Polikarpochkin AN, Klenkov IR, Poplaukhin TS, Klenkova DA. The effect of increased pressure of the gaseous medium on the microcirculation of teeth. *Doctor*. 2023;(3):66–9 (In Russ.). https://doi.org/10.29296/25877305-2023-03-14
3. Loginova NK, Ermolyev SN, Shiryaev AP Reactive changes in capillary blood flow in dental pulp in dental caries and the development of pulpitis. *Endodontics Today*. 2011;(2):20–2 (In Russ.). EDN: OFYWBD
4. Loginova NK, Troitskaya TV. Laser Doppler flowmetry of tooth pulp (literature review) (Part I). *Institute of Dentistry*. 2007;(1):110–1 (In Russ.). EDN: MWGUPJ
5. Moskvin SV, Antipov EV, Zarubina EG, Ryazanova EA. Efficiency of oxygen metabolism after the application of laserophoresis of various gels based on hyaluronic acid. *Bulletin of Aesthetic Medicine*. 2011;(3):48–55 (In Russ.). EDN: RABTEX
6. Skvortsov VV, Skvortsova EM, Bangarov RYu. Lactate acidosis in the practice of an anesthesiologist-resuscitator. *Bulletin of Anesthesiology and Intensive Care*. 2020;(3):95–100 (In Russ.). https://doi.org/10.21292/2078-5658-2020-17-3-95-100
7. Kraut JA, Madias NE. Lactic acidosis. N Engl J Med. 2014; 371(24):2309–19. https://doi.org/10.1056/NEJMra1309483
8. Robergs RA, Ghiasvand F, Parker D. Biochemistry of exercise-induced metabolic acidosis. *Am J Physiol Regul Integr Comp Physiol*. 2004;287(3):R502–16. https://doi.org/10.1152/ajpregu.00114.2004
9. Windpessl M, Wallner M. Lactic acidosis. *N Engl J Med*. 2015;372(11):1077. https://doi.org/10.1056/NEJMc1500327
10. Choung HW, Lee DS, Lee JH, Shon WJ, Lee JH, Ku Y, Park JC. Tertiary Dentin Formation after Indirect Pulp Capping Using Protein CPNE7. *J Dent Res*. 2016;95(8):906–12. https://doi.org/10.1177/0022034516639919
11. Lee M, Lee YS, Shon WJ, Park JC. Physiologic dentin regeneration: its past, present, and future perspectives. *Front Physiol*. 2023;14:1313927. https://doi.org/10.3389/fphys.2023.1313927
12. Kamalak H, Kamalak A, Taghizadehghalehjoughi A. Cytotoxic effects of new-generation bulk-fill composites on human dental pulp stem cells. *Cell Mol Biol (Noisy-le-grand)*. 2018;64(3):62–71. https://doi.org/10.14715/cmb/2018.64.3.11
13. Costa CA, Giro EM, do Nascimento AB, Teixeira HM, Hebling J. Short-term evaluation of the pulpo-dentin complex response to a resin-modified glass-ionomer cement and a bonding agent applied in deep cavities. *Dent Mater*. 2003;19(8):739–46. https://doi.org/10.1016/s0109-5641(03)00021-6
14. Jha MK, Song GJ, Lee MG, Jeoung NH, Go Y, Harris RA, Park DH, Kook H, Lee IK, Suk K. Metabolic Connection of Inflammatory Pain: Pivotal Role of a Pyruvate Dehydrogenase Kinase-Pyruvate Dehydrogenase-Lactic Acid Axis. *J Neurosci*. 2015;35(42):14353–69. https://doi.org/10.1523/JNEUROSCI.1910-15.2015
15. McHugh JM, McHugh WB. Pain: neuroanatomy, chemical mediators, and clinical implications. *AACN Clin Issues*. 2000;11(2):168–78. https://doi.org/10.1097/00044067-200005000-00003

Authors' contributions. All the authors confirm that they meet the ICMJE criteria for authorship. The most significant contributions were as follows: Ilyas R. Klenkov — development of the concept and design of the study, general management; Artyom S. Krivonos — conducting research, writing the manuscript; Roman A. Grashin — verification of critical intellectual content; Alina V. Pototskaya — data collection, statistical model development, data processing; Vladimir A. Zheleznyak — manuscript editing, approval of the final version of the manuscript for publication; Inna S. Maday — manuscript editing.

AUTHORS

Ilyas R. Klenkov, Cand. Sci. (Med.)
https://orcid.org/0000-0002-1465-1539
klen.ir@mail.ru

Artyom S. Krivonos
https://orcid.org/0000-0001-5515-9770
artemkriwonos@yandex.ru

Roman A. Grashin, Dr. Sci. (Med.), Professor
https://orcid.org/0000-0002-8698-5124
grashin62@mail.ru

Alina V. Pototskaya, Cand. Sci. (Med.)
https://orcid.org/0000-0001-8747-1363
alina3377@rambler.ru

Vladimir A. Zheleznyak, Cand. Sci. (Med.), Associated Professor
https://orcid.org/0000-0002-6597-4450
zhva73@yandex.ru

Inna S. Maday, Cand. Sci. (Ped.), Associated Professor
https://orcid.org/0009-0000-3610-976X
ismaday@mail.ru

https://doi.org/10.47183/mes.2024-26-3-71-76

HYPERBARIC OXYGENATION FOR ASSISTING RECOVERY OF ATHLETES INCLUDING THOSE AFFECTED BY COVID-19 UNDER MEDIUM-ALTITUDE CONDITIONS

Gukas N. Ter-Akopov, Yulia V. Koryagina✉, Sabina M. Abutalimova, Sergey V. Nopin, Yulia V. Kushnareva

North-Caucasian Federal Research-Clinical Center, Essentuki, Russia

Introduction. Modern scientific studies demonstrate the effectiveness of hyperbaric oxygenation in assisting recovery following physical exertion including those affected by COVID-19 infection.

Objective. The study sets out to identify the beneficial effects of hyperbaric oxygenation therapy in assisting the recovery of athletes under medium-altitude conditions, including those who have previously undergone COVID-19, by examining respiratory and circulatory systems.

Materials and methods. The study was performed on 39 highly qualified athletes during a period of training in mountainous areas. The athletes' heart rate variability, central hemodynamics, saturation and external respiration were determined prior to hyperbaric oxygenation, as well as immediately following the procedure, 10 min after the procedure, and following a course of 7 procedures.

Results. According to heart rate variability indices in women who underwent COVID-19, there was a tendency to decrease heart rate 10 min after hyperbaric oxygenation and very a slow wave power index after the course of (before — 665.65 (592.54; 921.07) ms^2; after — 541.47 (371.01; 840.89) ms^2, $p < 0.05$). After the first session there was a decrease in systolic blood pressure (before — 117 (111; 120) mm Hg; after — 109 (104; 115) mm Hg, $p < 0.03$), as well as in the index of volumetric airflow velocity at the moment of exhalation of 50% of forced vital capacity of lungs. A comparison of men's parameters revealed a decrease in peripheral vascular resistance and blood pressure. In women and men who had previously suffered COVID-19 infection, the index of impaired oxygen uptake from the microcirculation system decreased under the influence of hyperbaric oxygenation.

Conclusions. Hyperbaric oxygenation therapy is a safe and effective method for assisting the recovery of athletes under medium-altitude conditions, including those who have previously suffered COVID-19 infection. The observed improvements in functional state are manifested over the course of application (7 sessions).

Keywords: athletes; functional status; cardiovascular system; respiratory system; mid- mountain; hyperbaric oxygenation therapy; COVID-19

For citation: Ter-Akopov G.N., Koryagina Y.V., Abutalimova S.M., Nopin S.V., Kushnareva Y.V. Hyperbaric oxygenation for assisting recovery of athletes including those affected by COVID-19 under medium-altitude conditions. *Extreme Medicine*. 2024;26(3):71–76. https://doi.org/10.47183/mes.2024-26-3-71-76

Funding: the study was performed in accordance with the state assignment of North-Caucasian Federal Research-Clinical Center No. 48.001.22.800 from January 01, 2022, for the performance of the research "Development and scientific substantiation of the system of recovery and rehabilitation measures for athletes who suffered COVID-19 with the use of factors of hypo- and hyperoxia in the medium-altitude conditions", cipher: "COVID medium-altitude 22/24".

Compliance with ethical principles: the study was approved by the Local Ethical Committee for Expert Review of Biomedical Research of North-Caucasian Federal Research-Clinical Center, protocol #1 of 20.01.2022. All participants gave informed consent to participate in the study in accordance with the World Medical Association Declaration of Helsinki (WMA Declaration of Helsinki — Ethical Principles for Medical Research Involving Human Subjects, 2013), as well as permission to process personal data.

Potential conflict of interest: the authors declare no conflict of interest.

✉ Yulia V. Koryagina nauka@skfmba.ru

Received: 20 June 2024 **Revised:** 18 Oct. 2024 **Accepted:** 24 Oct. 2024

ПРИМЕНЕНИЕ ГИПЕРБАРИЧЕСКОЙ ОКСИГЕНАЦИИ ДЛЯ ВОССТАНОВЛЕНИЯ СПОРТСМЕНОВ, В ТОМ ЧИСЛЕ РАНЕЕ ПЕРЕНЕСШИХ COVID-19, В УСЛОВИЯХ СРЕДНЕГОРЬЯ

Г.Н. Тер-Акопов, Ю.В. Корягина✉, С.М. Абуталимова, С.В. Нопин, Ю.В. Кушнарева

Северо-Кавказский федеральный научно-клинический центр Федерального медико-биологического агентства, Ессентуки, Россия

Введение. В современных научных работах имеются данные, показывающие эффективность применения гипербарической оксигенации для восстановления после COVID-19, а также восстановления спортсменов после физических нагрузок.

Цель. Выявление эффектов применения гипербарической оксигенации для восстановления спортсменов, в том числе ранее перенесших COVID-19, в условиях среднегорья по данным исследования систем дыхания и кровообращения.

Материал и методы. Исследование проходило в период подготовки в среднегорье у 39 спортсменов высокой квалификации. До гипербарической оксигенации, сразу после, через 10 мин после, после курса из 7 процедур у спортсменов определялись показатели вариабельности сердечного ритма, центральной гемодинамики, сатурации и внешнего дыхания.

Результаты. Согласно показателям вариабельности сердечного ритма у женщин, перенесших COVID-19, имелась тенденция к снижению частоты сердечного ритма через 10 мин после гипербарической оксигенации и показателя мощности очень медленных волн после курса (до — 665,65 (592,54; 921,07) мс^2; после — 541,47 (371,01; 840,89) мс^2, $p < 0,05$). После первого сеанса выявлено снижение систолического артериального давления (до — 117 (111; 120) мм рт. ст.; после — 109 (104; 115) мм рт. ст., $p < 0,03$), а также показателя объемной скорости воздушного потока в момент выдоха 50% форсированной жизненной емкости легких. Сравнение показателей мужчин выявило снижение периферического сосудистого сопротивления и артериального давления. У женщин и мужчин, ранее болевших COVID-19, под действием гипербарической оксигенации снижался показатель нарушения поглощения кислорода из системы микроциркуляции.

Выводы. Гипербарическая оксигенация — безопасный и эффективный метод восстановления организма спортсменов в условиях среднегорья, в том числе у ранее перенесших COVID-19. Выраженные улучшения функционального состояния, проявляются при курсовом применении (7 сеансов).

Ключевые слова: спортсмены; функциональное состояние; сердечно-сосудистая система; дыхательная система; среднегорье; гипербарическая оксигенация; COVID-19

Для цитирования: Тер-Акопов Г.Н., Корягина Ю.В., Абуталимова С.М., Нопин С.В., Кушнарева Ю.В. Применение гипербарической оксигенации для восстановления спортсменов, в том числе ранее перенесших COVID-19, в условиях среднегорья. *Медицина экстремальных ситуаций*. 2024;26(3):71–76. https://doi.org/10.47183/mes.2024-26-3-71-76

Финансирование: работа выполнена в соответствии с государственным заданием ФГБУ СКФНКЦ ФМБА России № 48.001.22.800 от 1 января 2022 г. на выполнение НИР «Разработка и научное обоснование системы восстановительных и реабилитационных мероприятий для спортсменов, перенесших COVID-19, с использованием факторов гипо- и гипероксии в условиях среднегорья», шифр: «COVID среднегорье 22/24».

Соответствие принципам этики: исследование было одобрено локальным этическим комитетом по экспертизе биомедицинских исследований ФГБУ СКФНКЦ ФМБА России, протокол № 1 от 20.01.2022. Все участники дали информированное согласие на участие в исследовании в соответствии с Хельсинкской декларацией Всемирной медицинской ассоциации (WMA Declaration of Helsinki — Ethical Principles for Medical Research Involving Human Subjects, 2013), а также разрешение на обработку персональных данных.

Потенциальный конфликт интересов: авторы заявляют об отсутствии конфликта интересов.

✉ Корягина Юлия Владиславовна nauka@skfmba.ru

Статья поступила: 20.06.2024 **После доработки:** 18.10.2024 **Принята к публикации:** 24.10.2024

INTRODUCTION

Hyperbaric oxygen therapy (HBOT) provides an artificial increase in blood oxygen capacity due to additional dissolution of oxygen in plasma as a result of increase in the partial pressure of oxygen in the inhaled gas mixture related to the total barometric pressure of the external environment [1, 2]. When subjected to HBOT in suboptimal or optimal doses, the human organism switches to a qualitatively new state characterized by economy (hypofunction) of physiological systems [3, 4].

Due to the onset of the novel coronavirus COVID-19 pandemic, a need arose for the use of methods to ameliorate complications associated with this disease manifesting as hypoxia and requiring supplemental oxygen support [5]. Thus, the issue of ensuring the safety of HBOT therapy in patients with COVID-19 becomes relevant. The inclusion of daily HBOT sessions (at least 4) in “soft” modes (1.4–1.6 atm.) as part of complex therapy for COVID-19 has demonstrated its safety and a preliminary positive effect on the subjective state of the examined patients and blood oxygen saturation dynamics [6].

According to A.G. Shchurov’s studies, HBOT can be used in various sports to quickly eliminate fatigue resulting from the performed load. This may serve as a preliminary stimulation of performance before training or competitions, as well as for the prevention and elimination of organ and system dysfunctions due to excessive physical overstrain [8]. Published data demonstrate the effectiveness of HBOT for the recovery of patients after COVID-19, as well as for the recovery of athletes after physical exertion. However, no data on the use of HBOT for the recovery of athletes training under hypobaric hypoxia (medium-altitude) conditions, or athletes who have previously suffered COVID-19 infection under such conditions, were found in the available sources.

The study set out to reveal the beneficial effects of hyperbaric oxygenation therapy in the recovery of athletes, including those who had previously contacted COVID-19, under medium-altitude conditions according to the study of respiratory and circulatory systems.

MATERIALS AND METHODS

The study of HBOT effects during training of athletes in the medium-altitude conditions was carried out during training camps at an altitude of 1240 meters in Russia on 39 highly qualified athletes (mean age — 21.5 (18; 25) years; sports qualification — Candidates Masters of Sports and Masters of Sports; mixed groups in sports: sambo, ski racing, figure skating, handball), including 27 women (main group (MG) — 16; control group (CG) –11), and 12 men (7 MG and 5 CG).

As our earlier studies showed, athletes may experience strain of adaptation mechanisms during training in the middle mountains without the use of special means of recovery (HBOT). The observed strain, as manifested in increased sympathetic activity and central hemodynamics, was especially pronounced in athletes who had previously experienced COVID-19 [11, 12]. Due to the fact that these data have already been published, the division into MG and CG was based only on the presence of COVID-19 in the anamnesis in the present study. Consequently, athletes with a history of COVID-19 were categorized as MG and those without COVID-19 were categorized as CG. All athletes participating in the study were administered HBOT treatment.

Inclusion criteria: high qualification of athletes, high training loads under medium-altitude conditions. Exclusion criteria: refusal to participate in the study, acute illnesses and injuries, contraindications to HBOT (history of epilepsy, claustrophobia, hyperthermia, uncontrolled arterial hypertension, hypotension, sinusitis, impaired patency of the eustachian tubes and channels connecting the sinuses with the external environment, hypersensitivity to oxygen).

The course of HBOT procedures was carried out in a “BaroOx 1.0” barocamera using a “Covidien LLC” (USA) mask according to a preset program having the following parameters: overpressure — 30 kPa; oxygen content — 93±2 %; air flow rate — 45 L/min; compression/decompression rate — 6 kPa/min; duration of one procedure — 30 min; course — at least 7 procedures (1 procedure per day); body position — half-lying.

The study of central hemodynamics, heart rate variability (HRV) and oxygen parameters (impaired oxygen uptake from the microcirculation system and blood saturation) was performed using the ESTECK System Complex device (LD Technology, USA). The spirometric indices of the athletes were determined using a “Carefusion MicroLab Mk8” spirometer (South Wales, UK).

Statistical processing of the data was performed using the “Statistica 13.0” computer program. A comparison of indicators between the main and control groups was carried out using the Mann-Whitney criterion; indicators of

the main and control groups when HBOT was applied to them in dynamics were compared using the nonparametric Wilcoxon criterion. The indicators are presented in the form of medians and quartiles.

RESULTS

When analyzing the data of the HBOT effect, the indicators of athletes before HBOT (baseline), immediately following HBOT administration, 10 min after HBOT, as well as after a course of 7 HBOT sessions, were compared. The baseline MG and CG parameters did not differ statistically significantly. Although the dynamics of heart rate (HR) did not reveal statistically significant changes according to the HRV parameters in women, all women (COVID-19 infected and non-infected) displayed a tendency to decrease HR 10 min after HBOT as compared to the baseline level (Fig. 1A).

The same positive trend was observed for the power index of fast high-frequency (HF) waves, which increased 10 min after administration of HBOT in female athletes who had not previously had COVID-19 (before — 758.38 (585.11; 1015.1) ms^2; 10 min after — 1734.57 (998.57; 2086.71) ms^2).

The low-frequency (LF) wave power index in female athletes with no previous COVID-19 infection tended to decrease after the HBOT course (before — 731.07 (505.87; 984.3) ms^2; immediately after the 1st session — 711.66 (441.24; 894.39) ms^2; 10 min after the 1st session — 808.8 (619.2; 1086.15) ms^2; after the course — 426.23 (265.4; 940.66) ms^2).

The power index of very low frequency waves (VLF) reflecting the work of the slowest level of regulation (suprasegmental or energetic metabolic) in female athletes who had previously undergone COVID-19 decreased by the end of the course (before the course — 665.65 (592.54; 921.07) ms^2; after the course — 541.47 (371.01; 840.89) ms^2, $p < 0.05$). In female athletes who had not previously had COVID-19, there was also a tendency for this index to decrease following the HBOT course, but to increase after the 1st session (up to — 665.24 (618.97; 848.75) ms^2; immediately after the 1st session — 695.94 (639.81; 992.72) ms^2; 10 min after the 1st session — 1219.29 (577.34; 1759.04) ms^2; after the course — 620.17 (414; 712.03) ms^2). In women who had not previously been infected with COVID-19, there is an additional tendency towards decreased stress index (SI) immediately after the 1st HBOT session (before — 100.3 (73.8; 128.2) conventional units; immediately after the 1st session — 81.55 (39.7; 111.5) conventional units; 10 min after the 1st session — 48.35 (44.9; 113.35) conventional units; after the course — 107.3 (65.1; 149.4) conventional units).

When analyzing the central hemodynamic parameters in women who had previously had COVID-19, a decrease in systolic blood pressure was revealed after the first session (before — 117 (111; 120) mmHg; immediately after the 1st session — 109 (104; 115) mmHg, $p < 0.03$; 10 minutes after the 1st session — 114 (107; 117) mmHg, $p < 0.05$; after the course — 114 (108; 122.5) mmHg) (Fig. 1B). The index of impaired oxygen absorption from the microcirculation system VO2 decreased (before — 320 (310; 320) mL/min/m^2; immediately after the 1st session — 130 (130; 180) mL/min/m^2, $p < 0.001$; 10 minutes after the 1st session — 130 (130; 130) mL/min/m^2, $p < 0.001$; after the course — 320 (310; 330) mL/min/m^2).

In women without a history of COVID-19, a decrease in the stiffness index, which characterizes blood pressure in large arteries, was observed both after one session and after a course of HBOT procedures (before — 6.22 (5.26; 6.86) m/s; immediately after the 1st session — 6.02 (5.27; 6.29) m/s, $p < 0.05$; 10 minutes after the 1st session — 6.15 (6.02; 6.62) m/s; after the course — 5.94 (5.24; 6.56) m/s, $p < 0.05$). After the first session, the same group showed a decrease in the PSS (before — 1207.6 (1132.9; 1243.8) MPa*s/m^3; immediately after the 1st session — 1180.3 (975.5; 1243.5) MPa*s/m^3, $p < 0.05$; 10 minutes after the 1st session — 1062.9 (823.15; 1330.2) MPa*s/m^3, $p < 0.05$; after the course — 1156.6 (1074.3; 1342.5) MPa*s/m^3 (Fig. 34)) and diastolic blood (arterial) pressure (DBP)

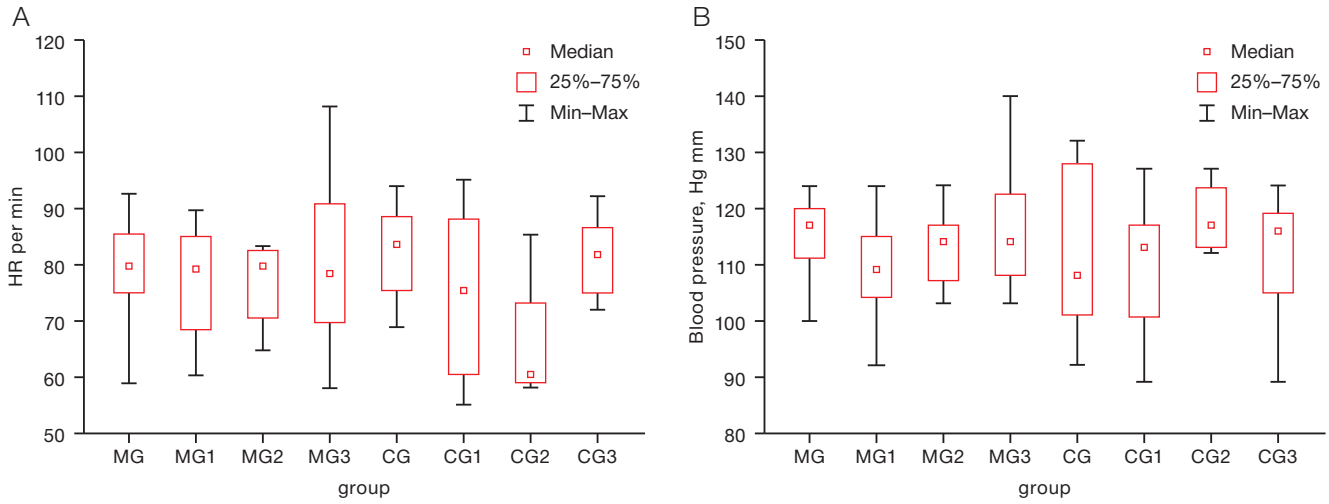

Figure prepared by the authors using their own data

Fig. 1. HRV (A) and Systolic blood pressure (SBP) (B) in highly qualified female athletes with and without COVID-19 under the influence of HBOT: MG — before HBOT sessions; MG1 — immediately after HBOT; MG2 — 10th min after HBOT; MG3 — after HBOT course; CG — before HBOT sessions; CG1 — immediately after HBOT; CG2 — 10th min after HBOT; CG3 — 3 after HBOT course

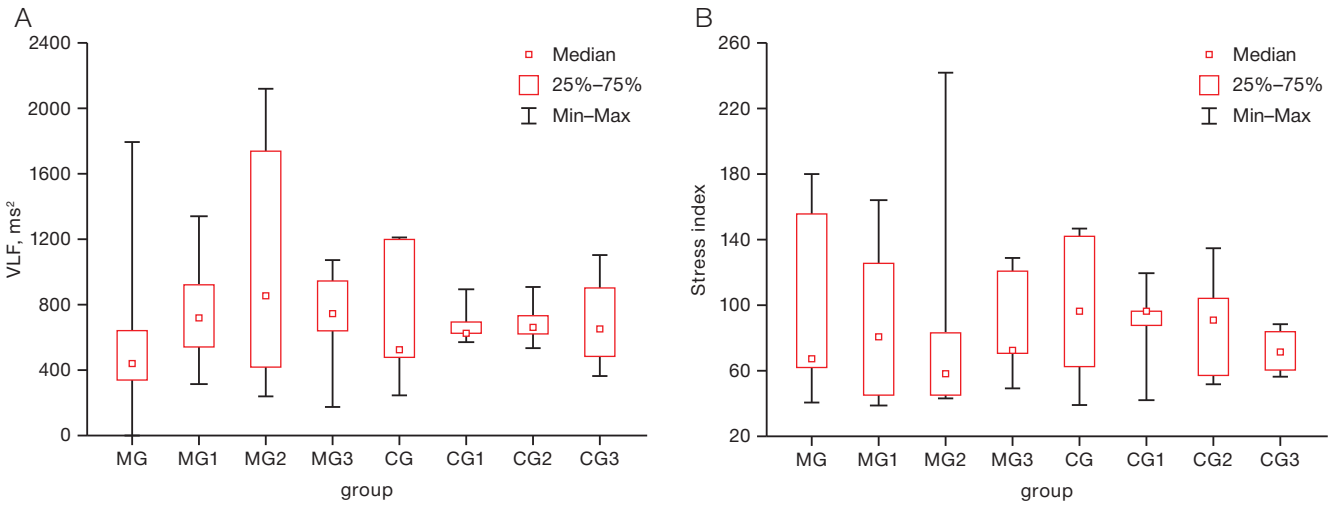

Figures prepared by the authors using their own data

Fig. 2. VLF (A) and stress index (B) indicators in male athletes with and without COVID-19, under the influence of HBOT: MG — before HBOT, MG1 — immediately after HBOT, MG2 — 10th minute after HBOT, MG3 — after the HBOT course, CG — before HBOT sessions, CG1 — immediately after HBOT, CG2 — 10th minute after HBOT, CG3 — 3 after the HBOT course

(before — 67 (64; 74) mmHg, $p < 0.05$; immediately after the 1st session — 64 (59.5; 69.5) mmHg, $p < 0.05$; 10 minutes after the 1st session — 65.5 (61.5; 70) mmHg; after the course — 64 (61; 69)) mmHg.

In terms of external respiratory function in women who had previously undergone COVID-19, no significant changes were observed during HBOT application apart from MEF_{50} (maximal expiratory flow at 50% of forced vital capacity), which significantly decreased (before — 4.99 (4.42; 5.83) L; immediately after — 4.66 (4.09; 5.62) L, $p < 0.01$), apparently due to relaxation of respiratory muscles. In women with no previous history of COVID-19, forced vital capacity of lungs (FVC) decreased statistically significantly after the HBOT course (before — 4.25 (4; 4.77) L; after the course — 4.13 (3.85; 4.53) L, $p < 0.02$).

A comparison of HRV indices during HBOT sessions in COVID-19 male athletes with previous COVID-19 revealed a statistically significant increase in the power of very low frequency (VLF) waves ($p < 0.05$) (Fig. 2A). In male athletes who had not previously had COVID-19, there was a tendency towards decreased stress index after a course of HBOT (up to — 96.2 (61.5; 141.1) conventional units; immediately after the 1st session — 95.6 (86.6; 95.8) conventional units; 10 min after the 1st session — 90.2 (56.3; 103) conventional units; after the course — 70.45 (59.2; 82.8) conventional units (Fig. 2B).

According to the central hemodynamic parameters (Table 1), the peripheral vascular resistance decreased immediately after the first HBOT session ($p < 0.05$); however, following the course, this parameter returned to the initial values. There was also a tendency towards decreased systolic and diastolic blood pressure. Male athletes who had previously contacted COVID-19 also exhibited statistically significantly decreased impaired oxygen uptake indicator from the VO_2 microcirculation system under the influence of HBOT. Both in men who had previously had COVID-19 and those who did not have a history of COVID-19, spirometry parameters did not change statistically significantly. In male athletes who had not previously had COVID-19, statistically significant differences in heart rate variability (HRV)

Table 1. Indices of central hemodynamics and impaired oxygen uptake from the microcirculation system in male athletes who previously underwent COVID-19 during HBOT application, Me (Q1; Q3), $n = 7$

Indices	MG	MG 1	MG 2	MG 3	*P*
SVR, MPa*s/m³	1020.3 (857.9; 1232.5)	970.3 (822.6; 1247.2)	972.6 (823.1; 1036.6)	1045.15 (995.3; 1086.5)	MG-MG1 < 0.05
CO, L/min	7.3 (6.6; 8.4)	7.5 (6.6; 8.5)	7.7 (6.8; 8.7)	7 (6.7; 7.1)	-
CI, L/min/m²	3.4 (3.3; 3.9)	3.9 (3.2; 3.9)	3.9 (3.4; 4.2)	3.55 (3.2; 3.9)	-
Average blood pressure, mmHg	92 (90; 95.3)	87.7 (83; 103)	90 (83; 103)	90.65 (87.3; 93)	-
VO_2, mL/min/m²	320 (320; 320)	180 (130; 320)	190 (130; 320)	315 (310; 320)	MG-MG2, MG-MG3 < 0.05
SBP, mmHg	127 (120; 136)	122 (115; 133)	122 (115; 133)	123 (120; 129)	-
DBP, mmHg	75 (73; 78)	69 (67; 88)	73 (67; 88)	74.5 (71; 78)	-

Table prepared by the authors using their own data

Note: VO_2 — index of oxygen uptake disturbance from the microcirculation system, SVR — peripheral (systemic) vascular resistance, CO — cardiac output, CI — cardiac index or index of volumetric blood flow velocity, MG — before HBOT, MG1 — immediately after HBOT, MG2 — 10 min after HBOT, MG3 — after HBOT course.

and central hemodynamic parameters were not revealed during the session or over the course of HBOT.

DISCUSSION

Researchers have previously noted not only accelerated recovery of the body as a result of HBOT therapy, but also an expansion of physiological reserves [8]. Significant differences between the groups using HBOT and normobaric oxygenation were observed in blood saturation and tissue saturation indexes [13]. Data in foreign literature describing not always effective use of HBOT for restoring the performance of athletes and recovery from sports injuries [14, 15] may be due to the different protocols of the procedures followed.

In our study carried out under medium-altitude conditions, it was found that the use of HBOT does not have an unambiguously positive effect on increasing the functional capabilities of the body, but rather promotes relaxation. Saturation indicators following HBOT did not change (before and after were within normal limits); however, after the 1st session, the indicator of impaired oxygen absorption from the microcirculation system decreases, indicating a beneficial effect and the necessary saturation of tissues with oxygen. The more pronounced positive effects of HBOT in women were particularly evident in the form of increased parasympathetic activity following the entire course. The general condition caused by the increased tone of the parasympathetic division of the autonomic nervous system (ANS) in women manifested itself in a relaxing effect, including on the respiratory muscles.

Currently, the following models of training at different altitudes are known. The classic approach is the "Live high — train high" model, when athletes live and train at the same altitude in mountainous terrain [12, 16]. There is also a model of mountain training using hyperoxia, "Live high — train low with additional oxygen". In this case, athletes train in the mid-altitude zone, but simulate sea level using additional oxygen inhalation [17]. As part of developing the directions of mountain training for athletes based on the obtained data, we propose a new training model designated as "Live high — train high — recover with HBOT".

CONCLUSION

The use of HBOT in medium-altitude conditions has proven to be a safe and effective method of restoring the body, including in athletes who have previously had COVID-19. However, the use of one session does not have an immediately positive effect in terms of increasing the functionality of the circulatory and respiratory systems; rather, this method is effective when used over the course of at least 7 sessions. Following the first HBOT session, the dynamics of functional indicators in athletes (both those who had been infected with COVID-19 and those who had not) under the influence of HBOT under medium-altitude training conditions was manifested by decreased vascular tone and blood pressure producing a hyperadaptive response. The positive effects of an entire course of HBOT, which were manifested in the form of increased parasympathetic activity, were more pronounced in women, leading to a relaxing effect, including on the respiratory muscles. All athletes experienced improved tissue oxygen saturation. In general, this method is recommended for general recovery of the body following a training day, as well as micro- and mesocycles and during the off-season preparation period. However, the method is not recommended immediately before training sessions and competitions.

References

1. Branco B.H., Fukuda D.H., Andreato L.V., Santos J.F., Esteves J.V., Franchini E. The Effects of Hyperbaric Oxygen Therapy on PostTraining Recovery in Jiu-Jitsu Athletes. *PLoS ONE*. 2016;11(3):e0150517. https://doi.org/10.1371/journal.pone.0150517
2. Pustovoit V.I., Nikonov R.V. Hyperbaric oxygenation in clinical and sports practice. *Kremlin Medicine Journal*. 2022;(1):78–86 (In Russ.). https://doi.org/10.26269/1jtg-0435
3. Baidin S.A., Gramenitsky A.B., Rubinchik B.A. A Guide to Hyperbaric Medicine. Moscow: *Medicine*; 2008 (In Russ.). EDN: QLRMML
4. Polikarpochkin A.N., Levshin I.V. Hyperbaric oxygenation in physical rehabilitation after recovery from "COVID-19" infection. *Actual problems of physical and special training of law enforcement agencies.* 2021;(1):225–30 (In Russ.). EDN: VNHKQQ
5. Levina O.A., Evseev A.K., Shabanov A.K., Kulabukhov V.V., Kutrovskaya N.Y., Goroncharovskaya I.V., et al. The Safety of Hyperbaric Oxygen Therapy in the Treatment of Covid-19. *Russian Sklifosovsky Journal "Emergency Medical Care"*. 2020;9(3):314–20 (In Russ.). https://doi.org/10.23934/2223-9022-2020-9-3-314-320
6. Chernyak A.V., Neklyudova G.V., Naumenko Zh.K., Pashkova T.L. Lung function in athletes involved in skiing and speed skating. *Pulmonology*. 2019;29(1):62–9 (in Russ.). https://doi.org/10.18093/0869-0189-2019-29-1-62-69
7. Shchurov A.G., Dmitriyev G.G., Yendaltsev B.V. Dinamika vosstanovleniya funktsional'nogo sostoyaniya sportsmenov posle fizicheskoy nagruzki v usloviyakh giperbaricheskoy oksigenatsii. *Teoriya i praktika fizicheskoy kultury*. 2016;(2):37–9 (In Russ.). EDN: VOLNWX
8. Sperlich B, Zinner C, Hauser A, Holmberg HC, Wegrzyk J. The impact of hyperoxia on human performance and recovery. *Sports Med*. 2017;47(3):429–38. https://doi.org/10.1007/s40279-016-0590-1
9. Ishihara, A. Mild hyperbaric oxygen: mechanisms and effects. *J Physiol Sci*. 2019;69(4):573–80. https://doi.org/10.1007/s12576-019-00678-5
10. Koryagina Yu.V., Nopin S.V., Abutalimova S.M., Ter-Akopov G.N. Vegetative regulation of the heart rate of highly qualified ski racers in the conditions of training in the middle mountains. *Problems of Balneology, Physiotherapy and Exercise Therapy*. 2021;98(3–2):98 (In Russ.). https://doi.org/10.17116/kurort20219803221
11. Ter-Akopov G.N., Koryagina Yu.V., Nopin S.V., Abutalimova S.M. Morphofunctional state of athletes with a history of covid-19 in the conditions of the middle mountains. *Theory and practiceof physical culture.* 2022;(12):33–5 (In Russ.). EDN: JDPFMX
12. Sperlich PF, Holmberg HC, Reed JL, Zinner C, Mester J, Sperlich B. Individual versus Standardized Running Protocols in the Determination of VO2max. *J Sports Sci Med*. 2015;14(2):386–93. PMCID: PMC4424469
13. Bennett MH, Lehm JP, Jepson N. Hyperbaric oxygen therapy for acute coronary syndrome. *Cochrane Database of Systematic Reviews*. 2015;23(7):CD004818. https://doi.org/10.1002/14651858.cd004818.pub4

14. Branco BH, Fukuda DH, Andreato LV, Santos JF, Esteves JV, Franchini E. The Effects of Hyperbaric Oxygen Therapy on PostTraining Recovery in Jiu-Jitsu Athletes. *PLoS ONE*. 2016;11(3):e0150517. https://doi.org/10.1371/journal.pone.0150517
15. Sharma AP. Factors Affecting Sea-Level Performance Following Altitude Training in Elite Athletes. *Journal of Science in Sport and Exercise*. 2022;4(2):315–30. https://doi.org/10.1007/s42978-022-00198-6
16. Park HY, Hwang H, Park J, Lee S, Lim K. The effects of altitude/hypoxic training on oxygen delivery capacity of the blood and aerobic exercise capacity in elite athletes — a meta-analysis. *J Exerc Nutrition Biochem*. 2016;20(1):15–22. https://doi.org/10.20463/jenb.2016.03.20.1.3

Authors' contributions. All authors confirm that their authorship meets ICMJE criteria. The largest contribution is distributed as follows: Gukas N. Ter-Akopov — development of the idea and design of the study, analysis of the final results; Yulia V. Koryagina — data analysis, the text of the article; Sabina M. Abutalimova — collection of material and compilation of initial tables; Sergey V. Nopin — statistical processing and data analysis; Yulia V. Kushnareva — collection of material and compilation of initial tables.

AUTHORS

Gukas N. Ter-Akopov, Cand. Sci. (Econ.)
https://orcid.org/0000-0002-7432-8987
sk@fmbamail.ru

Yulia V. Koryagina, Dr. Sci. (Biol.)
https://orcid.org/0000-0001-5468-0636
science@skfmba.ru

Sabina M. Abutalimova, Cand. Sci. (Med.)
https://orcid.org/0000-0003-1722-0774
sabina190989@yandex.ru

Sergey V. Nopin, Cand. Sci. (Tech.)
https://orcid.org/0000-0001-9406-4504
work800@yandex.ru

Yulia V. Kushnareva, Cand. Sci. (Med.)
https://orcid.org/0000-0002-7343-4622
july_83-83@mail.ru

https://doi.org/10.47183/mes.2024-26-3-77-86

PESTICIDES: CURRENT TRENDS IN THE USE AND EPIDEMIOLOGY OF ACUTE POISONING

Pavel G. Rozhkov[1]✉, Zulfira M. Gasimova[1], Yuri Y. Bukharin[1], Tatiana A. Sokolova[1], Vsevolod V. Severtsev[1], Natalia F. Lezhenina[1,2]

[1] Research Institute of Physical Chemical Medicine, Moscow, Russia

[2] Russian Medical Academy of Continuous Professional Education, Moscow, Russia

Introduction. The widespread use of pesticides, which ensures the sustainable development of agriculture and global economic growth, necessitates the constant monitoring of their harmful effects on human health and the environment.

Objective. To analyze and systemically review scientific publications on the prevalence of acute pesticide poisoning and trends in their use in order to identify the causes and structure of acute pesticide poisoning at the present time.

Materials and methods. A search of the scientific literature is carried out in electronic bibliographic databases in the Russian (eLibrary, CyberLeninka) and English (Web of Science, Scopus, PubMed, Google Scholar, Cochrane Library) languages.

Results. The risks of pesticide poisoning remain high in many countries of the world among both adults and children. In the structure of acute pesticide poisoning, household and suicidal poisoning with organophosphate and halogenated insecticides, anticoagulant rodenticides and pyrethroids are prevalent. Poisonings that occur at mass-, group- and family levels often have fatal outcomes, whether among agricultural workers or urban residents. The problem of acute poisoning with extremely dangerous limited-use substances based on aluminum or zinc phosphide is relevant not only in industrial agriculture, but also under domestic conditions and when working in personal subsidiary farms.

Conclusions. Strengthening controls and ensuring strict compliance with sanitary and hygienic standards of individual and public safety in the storage, use and disposal of pesticides, as well as combating their illegal trafficking, will minimize the risks of acute poisoning involving pesticides under industrial and domestic conditions.

Keywords: epidemiology; pesticides; acute poisoning; toxic effect

For citation: Rozhkov P.G., Gasimova Z.M., Bukharin Y.Y., Sokolova T.A., Severtsev V.V., Lezhenina N.F. Pesticides: current trends in the use and epidemiology of acute poisoning (literature review). *Extreme Medicine*. 2024;26(3):77–86. https://doi.org/10.47183/mes.2024-26-3-77-86

Funding: the work was carried out within the framework of the state assignment of the FMBA of Russia “Development of scientifically based approaches for the preparation of clinical recommendations and standards of medical care for acute toxic effects of pesticides (ICD:T60)”. R&D Reg. No.122020500016-3.

Potential conflict of interest: the authors declare no conflict of interest.

✉ Pavel G. Rozhkov rtiac@mail.ru

Received: 28 June 2024 **Revised:** 21 Oct. 2024 **Accepted:** 23 Oct. 2024

ПЕСТИЦИДЫ: СОВРЕМЕННЫЕ ТЕНДЕНЦИИ ПРИМЕНЕНИЯ И ЭПИДЕМИОЛОГИЯ ОСТРЫХ ОТРАВЛЕНИЙ

П.Г. Рожков[1]✉, З.М. Гасимова[1], Ю.Ю. Бухарин[1], Т.А. Соколова[1], В.В. Северцев[1], Н.Ф. Леженина[1,2]

[1] Федеральный научно-клинический центр физико-химической медицины имени академика Ю.М. Лопухина Федерального медико-биологического агентства, Москва, Россия

[2] Российская медицинская академия непрерывного профессионального образования Министерства здравоохранения Российской Федерации, Москва, Россия

Введение. Широкомасштабное применение пестицидов, обеспечивающее устойчивое развитие сельского хозяйства и рост мировой экономики, обусловливает необходимость постоянного мониторинга их вредного воздействия на здоровье человека и окружающую среду.

Цель. Проведение систематического обзора и анализа литературных данных для выявления характера распространенности, причин развития и структуры острых отравлений пестицидами на современном этапе.

Материалы и методы. Поиск научной литературы выполнен в электронных библиографических базах данных на русском (eLibrary, CyberLeninka) и английском (Web of Science, Scopus, PubMed, Google Scholar, Cochrane Library) языках.

Результаты. Риски развития отравлений пестицидами остаются высокими во многих странах мира как среди взрослого, так и детского населения. В структуре острых отравлений пестицидами превалируют бытовые и суицидальные отравления фосфорорганическими и галогенированными инсектицидами, родентицидами антикоагулянтного действия, пиретроидами. Отмечаются массовые, групповые и семейные отравления, нередко с летальными исходами, как у аграрных работников, так и у городских жителей. Актуальной является проблема острых отравлений чрезвычайно опасными препаратами ограниченного применения на основе фосфида алюминия или цинка не только в производственных, но и бытовых условиях и при работе в личных подсобных хозяйствах.

Выводы. Усиление контроля и строгое выполнение санитарно-гигиенических норм индивидуальной и общественной безопасности при хранении, применении и утилизации пестицидов, борьба с их незаконным оборотом позволят минимизировать риски острых отравлений пестицидами в производственных и бытовых условиях.

Ключевые слова: эпидемиология; пестициды; острое отравление; токсическое действие

Для цитирования: Рожков П.Г., Гасимова З.М., Бухарин Ю.Ю., Соколова Т.А., Северцев В.В., Леженина Н.Ф. Пестициды: современные тенденции применения и эпидемиология острых отравлений (обзор литературы). *Медицина экстремальных ситуаций*. 2024;26(3):77–86. https://doi.org/10.47183/mes.2024-26-3-77-86

Финансирование: работа проведена в рамках государственного задания ФМБА России «Разработка научно обоснованных подходов для подготовки клинических рекомендаций и стандартов медицинской помощи при остром токсическом действии пестицидов (Код по МКБ — Т60)». Рег. № НИОКТР 122020500016-3

Потенциальный конфликт интересов: авторы заявляют об отсутствии конфликта интересов.

✉ Рожков Павел Геннадьевич rtiac@mail.ru

Статья поступила: 28.06.2024 **После доработки:** 21.10.2024 **Принята к публикации:** 23.10.2024

INTRODUCTION

Pesticides (Latin *pestis* for “taint” and *caedo* for “to kill”) are chemicals or biochemicals used to control pests and diseases of plants, including weeds. Such substances are used in agricultural and forestry production processes, as well as their storage, transportation or trade. Pesticides are also used to control harmful organisms in residential buildings and public places, including vectors of human or animal diseases. Similar substances are also used for plant growth regulation, pre-harvest leaf removal (defoliants) and drying of plants (desiccants), thinning or preventing premature fruit fall. Pesticides may be used in the form of various formulations that include the active ingredient of the pesticide itself or a mixture of active ingredients and excipients (solvents, emulsifiers, surfactants, adjuvants, etc.). The active agent is a biologically active part of a pesticide preparation that directly provides a toxic effect on a harmful organism or on the growth and development of plants. The active principle of a biological preparation of a pesticide (biopesticide) is a microorganism or a product of its vital activity, a chemical is a substance of chemical synthesis [1].

Current trends in the use of pesticides are also associated with the development of new formulations containing nanoscale particles of active substances and a nanocomposite component as an adjuvant for delivery to the target object [4]. While bio- and nanopesticides are considered as an alternative to chemicals as a new generation of effective and safe pesticides, safety criteria for regulating their use have not been sufficiently developed. There are many concerns about the potential risks of toxic effects of pesticides on the environment, as well as on human and animal health [2]. In the near future, despite the growing global market for bio- and nanopesticides, the widespread use of chemical pesticides will continue to dominate [3]. Although making significant contributions to solving hunger problems and preventing of various diseases, pesticides have a negative impact on public health and can lead to the risk of acute poisoning with severe health and even fatal outcomes both under industrial and domestic conditions [4].

The purpose of the study is to carry out a systematic review and analysis of literature data to identify the nature of the prevalence, causes of development and structure of acute pesticide poisoning at the present stage.

MATERIALS AND METHODS

A search for scientific literature was carried out in electronic bibliographic databases in the Russian (eLibrary, CyberLeninka) and English (Web of Science, Scopus, PubMed, Google Scholar, Cochrane Library) languages.

RESULTS

Current trends in the use of pesticides

Despite restrictions imposed in some countries and a reduction in the use of highly hazardous pesticides, the global pesticide market has been growing in recent decades. So, while in 1960, about 100 active substances of pesticides were recognized globally, by 2020 there were already about 600 active pesticide substances. Meanwhile, the volume of pesticide used in the equivalent of active substances doubled from 1.5 million tons in the 1980 to 3 million tons in 2020. The leaders in terms of annual pesticide use for the period from 2010 to 2020 were China, the USA and Argentina — about 1.8 million tons, 386,000 tons and 265,000 tons, respectively. In Russia, the pesticide market has quadrupled over this period; by 2020, their use amounted to 187,900 tons [5]. The number of substances included the State Catalog of Pesticides and Agrochemicals Approved for use in the territory of the Russian Federation increased by more than 70% over the period 2010–2015 to comprise around 1800 preparative forms of pesticides as of 2021 [6]. According to analytical studies, the volume of the global pesticide market will reach about 200 billion US dollars by 2031 from 85.12 billion in 2022 [5]. The projected global growth of the pesticide market at the present stage is explained by the need to increase agricultural production due to the growth of the Earth’s population as well as tackling phytosanitary risks in agriculture and forestry associated with the introduction, penetration, spread and acclimatization of new insect pest species, pathogens and weeds alien to certain geographical areas occurring as a result of global climate change [5, 7]. In addition, the need to systematically expand and increase the range of constantly updated drugs, the use of mixtures of pesticides with various active substances and the search for new pesticide formulas arises due to the increased resistance of harmful organisms to pesticides, which is universal regardless of the class and type of active substance used [8].

The creation of new forms of pesticides and introduction of technologies for their use often outstrip studies into the effects of their use on human health. Moreover, risks of acute toxic effects of pesticides on humans when used under industrial and household conditions often exceed the prognostic risk estimates of their active substances obtained from experimental animal models [3]. Some authors expect the problem of toxicity of new forms of pesticides to increase in the near future resulting in higher costs associated with their creation [8].

A growing global problem in the international market is the expanded supply of generic pesticides against a background of declining sales of developed and patented substances [8, 9]. In recent years, the proportion of counterfeit pesticide products on the global market has increased by about 25%. Such practices are typically implemented on small farms and the segment of private producers of agricultural products [10]. Counterfeit pesticides, whose composition can be changed both qualitatively and quantitatively, seldom correspond in identity and quality with the active substances and additional components used in officially approved pesticides. Disruption of technological processes during the production of generic pesticides in

clandestine industries significantly increases the risks of acute poisoning when used [3]. In this connection, it may be noted that around 85–90% of all counterfeit pesticides are imported from China and India [10].

The potential hazard presented by pesticides to humans and wildlife is associated with their deliberate introduction into the environment to destroy targeted living objects (pests), which may be spread over vast territories, resulting in their circulation in ecosystems and food chains along with the risk of toxic effects on large segments of non-target wildlife populations [11]. For many years, cases of intentional and unintentional mass poisoning of domestic and wild animals have been reported in almost all countries of the world, including Russia, as a result of inhalation or ingestion of pesticide preparations, including absorption through the skin and transmission through food chains. Toxic effects on animals of banned pesticides and their mixtures used on arable lands in many countries of the world are the rule than the exception, thus necessitating a legal study of this issue and the imposition of criminal and administrative liability for the import, production and use of prohibited pesticides, as well as regulatory violations in the use of permitted pesticides [11, 12].

In recent years, the range of pesticides used has been significantly updated. Mercury-containing, chlorine-containing, highly hazardous organophosphate pesticides, aluminum and zinc phosphides, methyl bromide and other pesticides leading to severe industrial and household poisoning were widely used in the global agro-industrial sector until the end of the 1980s. Thus, in 1971–72 in Iraq, one of the largest mass poisonings of farmers and their family members (6530 were affected, 459 of them fatally) occurred as a result of eating homemade bread made from methylmercury-etched seed grains [13]. In 1967, one of the first cases of poisoning of sailors on a dry cargo ship with methyl bromide used in the practice of quarantine fumigation to kill ticks, nematodes, rodents, pathogens of fungal diseases, was registered. In 1983, the number of reported deaths from poisoning with this fumigant exceeded 950 cases. Methyl bromide was widely used as an agricultural fumigant from the 1930s until the decision to limit its use was approved by the Montreal Protocol on Substances that Deplete the Ozone Layer in 1987. Although the complete prohibition of methyl bromide was planned to apply by 2010, even today it remains one of the main means for fumigation of cargo holds and quarantine treatment of imported products, which can lead to severe cases of poisoning with fatal outcomes [14]. When processing transported goods in containers by sea and storing grain in granaries, extremely toxic aluminum phosphide and magnesium phosphides are used along with other pesticides not included in the State Catalog of Pesticides Approved for Use in Russia, sulfuryl fluoride, formaldehyde, ethylene oxide, 1,2-dichloroethane, dichloromethane (chloromethane), chloropicrin [15, 16].

In industrialized countries, the use of low- and moderately toxic substances has increased, contributing to a decrease in the number of fatal and severe poisonings. However, despite the 2006 decision of the Food and Agriculture Organization of the United Nations to consistently ban the use of especially dangerous pesticides, more than 200 active substances of especially dangerous pesticides are used in many developing countries despite being prohibited for use in European countries and the United States [17]. According to Donley N et al. [18], in the period 2015–2019 unregistered pesticide products containing 26 different highly hazardous organophosphate or carbamate insecticides were produced in the United States for export to 53 countries. At the same time, the US Environmental Protection Agency (EPA) does not provide guaranteed notifications to importing countries (as required by law) about the export of a pesticide recognized as harmful to human health or for which a standard safety assessment has not been conducted. According to some authors, in 72% of the countries importing unregistered pesticides from the United States, acute pesticide poisoning was observed in more than a third of agricultural workers [18].

The problem of acute poisoning with extremely dangerous pesticides approved for use in almost all countries of the world (aluminum phosphide, metal bromide, anticoagulant rodenticides), as well as moderately and low-hazard organophosphorus, carbamate, halogenated pesticides, pyrethroids, rodenticides, glyphosates, neonicotinoids and other groups of pesticides, remains relevant [18]. Thus, in 2018 on a dry cargo ship transporting grain treated with aluminum phosphide from Kazakhstan to Azerbaijan across the Caspian Sea, 12 crew members were seriously poisoned with phosphine, three of them fatally. The cause of poisoning of sailors with phosphine released by aluminum phosphide was non-compliance with safety requirements on the ship, as well as the general dilapidation of the vessel in terms of leaky holds etc. [19]. Cases of mass poisoning with anticoagulant rodenticides (vitamin K antagonists) were reported in the USA in 2018 and 2021 [20], as well as in Israel in 2021–22 [21]. Poisoning occurred due to inhalation of synthetic cannabinoids contaminated with these pesticides. As a result of these poisonings, 450 people were injured in the United States, 13 of them fatally, while 98 people were poisoned in Israel, three of them fatally. In Russia in 2019, poisoning with anticoagulant rodenticides as a result of eating sunflower oil made at home from pickled seeds was registered in 80 people, three of whom died [22]. In Uganda, a case of criminal poisoning has been described in seven people with three fatal outcomes as a result of eating bread made from flour contaminated with malathion [23].

According to the data published in a systematic analysis by Boedeker W et al. [4] of the results of 157 scientific studies for the period 2006–2018, the annual number of acute unintentional poisoning in 58 countries amounted to a total of 740,000 cases, including 7446 deaths. According to WHO-registered data from 83 countries for the period 2011–2015, an average of 835 fatal cases of unintentional

poisoning were observed annually, 139 of them in children under 15 years of age. The largest number of unintentional fatal cases of pesticide poisoning recorded by WHO in this period were in Guatemala, Mexico, Japan; in Egypt, Iran, and Mexico affecting children; in Mexico, Brazil, and Japan among farmers [4].

Table 1 shows the countries with the highest number of cases of unintentional fatal pesticide poisoning reported in adults and children in general and separately in children and farmers (industrial poisoning).

According to Table 1, the structure of unintentional fatal pesticide poisoning in the countries that provided information was dominated by domestic poisoning cases, including among farmers. The number of deaths from industrial poisoning among farmers was 8% in Brazil, 7% in Mexico, 3% in Japan, and 0.3% in Guatemala [4]. At the same time, the practice of incomplete accounting and registration of deaths, injuries and occupational diseases among agricultural workers, which is widespread in many countries of the world, is highly dangerous for the life and health of workers in industries both in industrialized and developing countries [24].

Extrapolating the results of a systematic analysis of scientific research data and information on mortality registered in WHO acute pesticide poisoning to the world community, Boedeker W et al. [4] concluded that about 385 million cases of unintentional pesticide poisoning occur annually at the global level with 11,000 deaths — i.e., about 44% of farmers are exposed to the toxic effects of pesticides annually. According to the Environmental Protection Agency, from 10,000 to 20,000 confirmed cases of acute pesticide poisoning affecting agricultural workers are registered annually in the United States. When taking into account cases of non-treatment of victims for medical care and undiagnosed cases of poisoning, the real number may exceed 300,000 per year.

The majority of fatal cases of acute pesticide poisoning occur when substances are taken orally or parenterally administered for suicidal purposes. About 14 million people died from suicidal pesticide poisoning between 1940 and 1980 during the “green revolution” in developing countries — agrarian transformations that included the use of highly toxic pesticides. At the same time, about 50% of fatal suicide poisonings registered in the world during this period were reported in China [25].

The measures taken to prevent suicidal pesticide poisoning in China have significantly contributed to the global decrease in fatal cases of suicidal pesticide poisoning observed since the 1990s, which nevertheless continue to be a serious public health problem [26]. According to WHO [27], currently more than 700,000 people worldwide commit suicide every year. At the same time, pesticide poisoning is one of the most common methods of suicide: one in five suicides is caused by pesticide poisoning. Most of them are observed in rural areas of South Asian countries, mainly involving pesticides based on organophosphate compounds and aluminum phosphide. This is due to the fact that in developing countries, whose economies are based on agriculture, pesticides are a cheap product and are not limited in sale, which contributes to a high risk of fatal poisoning in domestic conditions, including suicidal actions in the presence of crisis or conflict situations. In this regard, the prevention of suicidal pesticide poisoning should be aimed at limiting public access to particularly dangerous pesticides [28]. The reduction in the use and restriction of sales of especially dangerous pesticides (paraquat, metaphosphate, methyl bromide, aluminum phosphide, etc.) led to a significant decrease in the number of all deaths from pesticide poisoning in Japan, Denmark, Republic of Korea, the United Kingdom, the United States, and Taiwan. Thus, in Japan in 2019, 221 fatal cases of pesticide poisoning were registered, which is a 92% reduction from 1986. At the same time,

Table 1. Countries with the highest number of cases of unintentional fatal pesticide poisoning reported to WHO for the period 2011–2015

Countries	Study period	Total number of fatal poisoning cases during the study period			Average annual number of fatal poisoning cases		
		total	children	farmers	total	children	farmers
Brazil	2011–2015	236	29	19	47.2	5.8	3.8
Guatemala	2011–2015	687	43	2	137.4	8.6	0.4
Egypt	2011–2015	366	177	–	73.2	35.4	–
Iran	2013–2015	154	61	–	51.3	20.3	–
Mexico	2011–2015	573	91	40	114.6	18.2	8
South Africa	2011–2015	83	49	–	16.6	9.8	–
Republic of Korea	2011–2015	181	1	–	36.2	0.2	–
Japan	2011–2015	396	0	11	79.2	0	2.2

Table prepared by the authors according to the source [4]

Note: “–” the number of fatal cases of poisoning among farmers is unknown

the number of deaths from unintentional pesticide poisoning decreased by 83.8%. This decrease was due to a decrease in sales of both insecticides based on organophosphates and carbamates, as well as herbicides based on paraquat and diquat [29].

A need arises to limit use of the new insecticide chlorfenapyr, which, according to the WHO classification, belongs to moderately dangerous pesticides and is used to destroy insects resistant to organophosphorus insecticides. The effect of this drug is similar to bipyridine herbicides (in particular paraquat), which cause a high mortality rate, especially in suicidal poisoning [30].

Currently, 2,4-Dinitrophenol (DNP), which is used sparingly in industry and agriculture due to its pronounced herbicidal, fungicidal and insecticidal effects, has become a serious threat to human health in many industrialized countries. Due to the effective "fat-burning" action of DNP in the USA in the 1930s, biologically active additives for weight loss began to be used on its basis. In 1938, their use was banned due to a number of acute poisoning incidents having fatal outcomes. Since the 2000s, there has been a resurgence in the use of DNP as an illegal drug for weight correction or muscle building in the United States and other countries of the world. The growth of online sales and distribution of this drug has led to an increase in the number of cases of both accidental and intentional fatal poisoning [31].

Epidemiology of acute pesticide poisoning in post-soviet countries

Since the 1990s, traditional forms of farming in post-Soviet countries have radically changed due to the liquidation of state and collective agricultural farms. The reform of the agricultural sector and the creation of small and large farms was accompanied by a significant reduction in the financing of measures to ensure production safety and labor protection, imperfection of regulatory documentation on regulating the activities of the agro-industrial complex, insufficient awareness of agricultural workers and the public about the risks of toxic effects of applied pesticides, as well as an expansion of the list of insecticides, fungicides, herbicides allowed for free sale on the markets, rodenticides and their active use in everyday life and individual household farms [32, 33]. These consequences of reforming the market economy have largely determined the causes and patterns of acute pesticide poisoning.

According to Prodanchuk et al. [32], the creation of unfavorable working conditions on farms in Ukraine was due to the imperfection of the technological processes, the widespread use of outdated equipment and machinery, low-mechanized labor operations, and the predominance of manual labor, especially in the cultivation of sugar beet, orchards and vineyards, as well as the inadequate provision of workers with personal protective equipment. An analysis of the etiology and structure of 647 cases of acute pesticide poisoning in agricultural workers over a 25-year follow-up period revealed 522 cases (80.7%) of acute poisoning with herbicides based on 2,4–dichlorophenoxyacetic acid, 60 cases (9.3%) of poisoning with organophosphorus insecticides, 36 cases (5.7%) with herbicides based on sulfonylurea, 14 cases (2.2%) — synthetic pyrethroids and 15 isolated cases of poisoning with aluminum phosphide, dithiocarbamates (active ingredients carboxin and thiram), and fipronil (chemical class of pyrazolines). Among the victims, beet growers (76.1% of cases) and (11.6%) winegrowers (11.6%) prevailed; less often, gardeners and workers of warehouses for the storage of pesticides [35]. Registered mass and group poisonings with pesticides accounted for 14.7–43.6% of the total structure of occupational pathology in rural areas. In 90% of cases, poisoning developed as a result of wind-borne distributions of pesticide preparations from neighboring treated areas; less often, in violation of current sanitary rules and hygienic standards.

A retrospective analysis of 287 cases of acute household pesticide poisoning among the adult population of Kiev over the period 1993–2013 revealed a decrease in the number of cases of severe poisoning, among which organophosphate poisoning prevailed (80% of cases). Mortality rates for severe pesticide poisoning remained high and tended to increase. The average annual number of severe pesticide poisoning ranged from 0.25–1.5% in the structure of all severe poisoning of chemical etiology. In contrast to poisoning in rural areas, an increase in the number of severe oral poisonings with synthetic pyrethroids and neonicotinoids, mainly of a suicidal character, was noted in urban conditions. Acute fungicide poisoning during the research period was noted with the use of carbamates, cyprodinils, and copper hydroxide [33].

In the Republic of Moldova, 919 registered non-industrial cases of pesticide poisoning with 58 deaths were detected in the period 2011–2016. At the same time, there was a trend of annual increase in the number of poisoning cases: 2011 — 95 cases (10 of them fatal); 2012 — 118 (9 fatal); 2013 — 173 (15 fatal); 2014 — 199 (13 fatal); 2015 — 122 (5 fatal); 2016 — 212 (6 fatal) [34]. Among the child population in the Republic of Moldova for the period 2014–2018, 231 cases of pesticide poisoning were registered, two of them massive: inhalation poisoning with organophosphorus insecticide Bi-58 affected 58 schoolchildren; a preparation based on aluminum phosphide when used in a subsidiary farm in poisoned people, three of them fatally [35].

An increase in cases of pesticide poisoning was also observed in Georgia from 74 cases reported in 2017 to 236 cases identified in 2019 [36].

In the Republic of Azerbaijan during the period 2009–2016, the number of acute pesticide poisonings amounted to 806 cases with a mortality rate of 4.22%, of which 436 cases involved organophosphorus insecticides (mortality rate of 5.05%), while 330 cases were connected with rodenticides (mortality rate of 3.64%). At the same time, in the adolescent age group of people aged 15–19,

pesticide poisoning occupied a leading place in the structure of mortality from acute chemical poisoning, amounting to 30.43±9.59% of cases in the children's age group (0–14 years) In second place, 15.63±6.42% involved poisoning by snake venom [40]. In the structure of pesticide poisoning in children, 237 cases of poisoning (5 of them fatal) with organophosphorus compounds accounted for 46.8%, while rodenticide poisonings amounted to 39.2%. All fatal pesticide poisonings in children were caused by ingestion of organophosphate insecticides. The most common organophosphorus pesticides that provoked the development of acute chemical poisoning were neocidol, BI-58 (dimethoate), dichlorvos, metaphos, chlorpyrifos, malathion, and ethoprophos [38].

In Uzbekistan from 2002 to 2019, the number of acute pesticide poisonings accounted for 2.8% of the total structure of chemical injury. At the same time, there was a twofold increase in the number of hospitalized patients with acute chemical poisoning, from 6670 cases reported in 2002 to 13,255 cases reported in 2019, of which poisonings about 30% were diagnosed in children [39].

In the Republic of Belarus, the share of acute pesticide poisoning in the total structure of chemical poisoning was 2% in 2014 and 1% in 2015 and 2016 [33]. In the structure of chemical poisoning with fatal outcome for the period 2016–2018, the total number of cases amounted to 6910, while the proportion of poisoning with the use of agricultural poisons was 0.17% (12 cases, 1 of them in a child), and that of organophosphorus compounds — 0.09% (6 cases) [40].

Epidemiology of acute poisoning in the Russian Federation

While strict hygienic and toxicological assessment of the safety of pesticide use in the Russian Federation [41] has significantly contributed to a reduction the number of acute poisonings, the risks of their development remain high; cases of severe and acute poisonings are still registered annually. Of around 500 active pesticide substances permitted for use in Russia, about 200 have become widespread. The official document containing the list of pesticides and agrochemicals permitted for circulation in agriculture, forestry, communal and personal subsidiary farms and presenting the main regulations for their use is the "State Catalog of Pesticides and Agrochemicals allowed for use on the territory of the Russian Federation" [15].

Pesticides are one of the major production risk factors affecting the health of agricultural workers. Depending on the type of work performed, the a priori occupational health risk of employees in the hygienic assessment of working conditions is estimated in categories from medium to high; the prognostic probability of developing adverse health effects is 50–80% [42]. According to the indicators of acute toxicity (oral, dermal, inhalation) in the the Russian hygienic classification, pesticides are classified into 4 classes according to the degree of danger: 1 — extremely dangerous; 2 — highly dangerous; 3 — moderately dangerous; 4 — low-hazard. Currently, 17 extremely dangerous commercial pesticide preparations are used: rodenticide preparations based on brodifacoum (Ratticum) and bromadiolone (Bromine-BD, concentrate); insecticide and acaricide preparations based on carbofuran (Hinufur, suspension concentrate); oxalic acid dinitrile (oxalic acid dinitrile, oxalonitrile, cyanogen); methyl bromide (Metabrom-RFO); preparations based on aluminum phosphide (8 preparations) and magnesium phosphide (4 preparations) [15].

When monitoring the causes of acute poisoning of chemical etiology or analyzing the structure and dynamics of acute poisoning, detailed statistical data on cases of pesticide poisoning are generally lacking. Instead, researchers are usually referred to the general group of other or other monitored toxicants, which also includes organic solvents, halogen derivatives of aliphatic and aromatic hydrocarbons, as well as corrosive substances, metals, carbon monoxide, etc. [43]. This omission hinders comprehensive toxicological monitoring of acute pesticide poisoning. However, generalized analysis of published data on the dynamics and structure of acute pesticide poisoning in certain Russian regions permits a rough assessment the epidemiological situation of this incidence and its nosological forms.

Thus, the mortality rate in acute pesticide poisoning of 20.0±0.8% in Omsk in 2002 was the leading category in the structure of acute chemical injury; moreover, every fifth case of acute pesticide poisoning was fatal. The significant decrease in mortality by 7.6 times from 2002–2011 is associated with the disappearance of highly toxic insecticides based on organophosphorus and organochlorine compounds from household circulation. Deaths in subsequent years were recorded mainly as a result of acute poisoning with veratrin-based insecticides [44].

During the period 1999–2018, 197 adult patients (0.8% of the total number of hospitalized with acute chemical poisoning) with a mortality rate of 2.1% were treated at the Irkutsk Toxicological Center [45]. The appearance of unusual forms of poisoning was noted, which were characterized by refractoriness to specific therapy and long-term accumulation of a toxic agent.

In the Rostov region during the period 2008–2015, 2261 cases of acute poisoning with pesticides (fumitox, carbophos, rat poison, dichlorophos, chlorophos, hellebore tincture, etc.) were registered, accounting for 7.6% of the total structure of chemical poisoning [46].

Pesticide poisoning in children was registered in St. Petersburg 86 cases for the period 2010–2022 [47]; in Kazan, 15 cases of rat poison poisoning (10 of them children aged 0–3 years) occurred over the period 2018–2021 [48]. In Irkutsk during the period 1999–2018, 191 children were hospitalized with acute pesticide poisoning (the smallest number of hospitalized children (1 case) was

noted in 2003, while the largest (28 patients) occurred in 2018 [48]. The problem of children poisonings with rat poison is currently relevant in Donbas [49].

The number of appeals for the period 2019–2021 to the information and advisory toxicological department of the Golikov Research Center of Toxicology [50] on acute pesticide poisonings amounted to 541 cases (2.3% in the total structure of appeals). The purpose of the appeals in 30% of cases were issues of diagnosis and tactics of treatment of poisoning with organophosphorus insecticides: in 9% of cases — halogenated insecticides; 29% — other insecticides; 7% — herbicides and fungicides; 8% — rodenticides. Unintentional poisoning was observed in 481 (89%) cases (12 industrial and 469 domestic).

Industrial poisoning has been caused by the toxic effects of organophosphorus insecticides, rodenticides, pyrethroids and aluminum phosphide. The general circumstances of accidental poisonings were household (household) work and accidental ingestion (less often). Intentional poisoning was detected in 26 (5%) cases, of which 23 were suicidal (mainly with rodenticides and organophosphorus insecticides, as well as copper chloride, dinitrophenol, permethrin) and one was criminal (oral administration of dichlorvos), while two cases were for the purpose of intoxication (inhalation of dichlorvos). In 34 (6%) of cases, the circumstances of poisoning are unknown. The condition of patients at the time of consultation was satisfactory in 338 (62%) cases; in 111 (21%) — of moderate severity; in 13 (2%) — severe; in 79 (15%) — objectively undetermined. The cause of severe cases of poisoning was oral administration of rat poison (three cases), fenthion (two cases), diazinon, chlorpyriphos, an insecticide of an unspecified class (in one case), as well as inhalation exposure to an insecticide from bedbugs and an unspecified class (in two people), organophosphorus insecticide (in one case).

At the same time, four mass-, five group- and 10 family poisoning cases were registered. In the structure of mass poisoning, about 80 people suffered as a result of eating sunflower oil produced at home from seeds etched with anticoagulant rodenticide; 15 people suffered from inhalation effects of an organophosphorus insecticide and a pesticide of an unspecified class, six from malathion, and five from an insecticide of an unspecified group. The main cause of family poisoning was inhalation exposure to insecticides from cockroaches, bedbugs and insecticides of unspecified groups. There have also been isolated cases of accidental inhalation poisoning with aluminum phosphide and glyphosates, as well as four cases of oral poisoning with dinitrophenol taken in order to reduce weight.

CONCLUSIONS

The widespread use of pesticides in industrial and household conditions, in which circumstances food, drinking water, and air can become potential sources of toxic effects, leads to serious consequences for the health of the entire planetary population. This increases the risk of acute pesticide poisoning, which has become a priority global public health problem. No part of the human population is completely protected from the adverse effects of pesticides. An analysis of current trends in the use of pesticides and the epidemiology of acute poisoning has revealed global problems of mass death of wild and domestic animals due to intentional and unintentional acute poisoning with permitted and prohibited pesticides and the increased use of counterfeit drugs that increase the risks of acute poisoning. In developing countries, the toxic effects of pesticides are a serious health problem, reaching epidemic proportions in some countries. There are growth trends in cases of pesticide poisoning in Ukraine, Moldova, Georgia, Azerbaijan, and Uzbekistan.

Although strict toxicological assessment of pesticide safety in the Russian Federation has contributed significantly to reducing the number of acute poisonings, the risks of their occurrence remain high. Annually registered cases of severe acute poisoning with pesticides, some having fatal outcomes, mainly involve organophosphate insecticides, rodenticides, veratrines, and aluminum phosphide. Analyzing the causes and structure of poisoning contributes to the optimization of a set of preventive measures to strengthen sanitary control and compliance with hygienic standards of individual and public safety during the storage and use of pesticides.

References

1. FAO. The international Code of Conduct for the sustainable use and management of fertilizers. 2019. https://doi.org/10.4060/CA5253EN
2. Khamidullina HH, Ryabikova D N. Green pesticides (advantages and problems of implementation). *Toxicological Review.* 2020;3(162):53–6 (In Russ.). https://doi.org/10.36946/0869-7922-2020-3-53-56
3. Kumar S, Nehra M, Dilbaghi N, Marrazza G, Hassan AA, Kim KH. Nano-based smart pesticide formulations: Emerging opportunities for agriculture. *J Control Release.* 2019;294:131–53. https://doi.org/10.1016/j.jconrel.2018.12.012
4. Boedeker W, Watts M, Clausing P, Marquez E. The global distribution of acute unintentional pesticide poisoning: estimations based on a systematic review. *BMC Public Health.* 2020;20(1):1875. https://doi.org/10.1186/s12889-020-09939-0
5. Tareev AI, Bereznov AV, Smirnov VV, Tareeva A, Kislaya SS. The world market of chemical plant protection products: potential crop losses, trends and prospects of pesticide production for the Russian economy. *Food production equipment and technology.* 2024;54 (2):310–29 (In Russ.). https://doi.org/10.21603/2074-9414-2024-2-250

6. Dolzhenko VI, Laptiev AB. Modern range of plant protection products: biological efficiency and safety. Fertility. 2021;3(120):71–5 (In Russ.). https://doi.org/10.25680/S19948603.2021.120.13
7. PPC Secretariat. Scientific review of the impact of climate change on plant pests — A global challenge to prevent and mitigate plant pest risks in agriculture, forestry and ecosystems. Rome. 2021. FAO on behalf of the IPPC Secretariat. https://doi.org/10.4060/cb4769en
8. Benbrook CM. Why Regulators Lost Track and Control of Pesticide Risks: Lessons From the Case of Glyphosate-Based Herbicides and Genetically Engineered-Crop Technology. *Curr Environ Health Rep*. 2018;5(3):387–95. https://doi.org/ 10.1007/s40572-018-0207-y
9. Weisner O, Frische T, Liebmann L, Reemtsma T, Ro-Nickoll M, Schäfer RB, et.al. Risk from pesticide mixtures — The gap between risk assessment and reality. *Sci Total Environ.* 2021;796:149017. https://doi.org/10.1016/j.scitotenv.2021.149017
10. Boyko OA, Ivanov SL. Tariffication in counterfeit and counterfeit plant protection products: determinants and counteraction measures. *Citizen and law.* 2021;1:42–51 (In Russ.). EDN: FRKNGD
11. Valverde I, Espín S, Gómez-Ramírez P, Sánchez-Virosta P, García-Fernández AJ, Berny P. Developing a European network of analytical laboratories and government institutions to prevent poisoning of raptors. *Environ Monit Assess*. 2022;194(2):113. https://doi.org/10.1007/s10661-021-09719-2
12. Matishov GG, Staheev VV, Savitsky RM. Application of rodenticides and the mass death of animals in the south of Russia. *Science of the South of Russia*. 2024;20(1):77–84 (In Russ.). https://doi.org/10.7868/25000640240110
13. Bakir F, Rustam H, Tikriti S, Al-Damluji SF, Shihristani H. Clinical and epidemiological aspects of methylmercury poisoning. *Postgrad Med J.* 1980;56(651):1–10. https://doi.org/10.1136/pgmj.56.651.1
14. Afandiyev INO. Mass Occupational Phosphine Poisoning of a Dry-Cargo Ship Crew: A Case Report. *Iran J Public Health.* 2022 Jun;51(6):1428–31. https://doi.org/10.18502/ijph.v51i6.9700
15. The State catalog of pesticides and agrochemicals approved for use in the territory of the Russian Federation. Part I. Pesticides. M.;2024 (In Russ.).
16. Golovan TV, Tonkonog VV, Arestova YuA. Security problems of customs officials during the inspection of containers treated with fumigants. *Problems of social hygiene, health care and the history of medicine.* 2022; 30(4):592–599 (In Russ.). https://doi.org/ 10.32687/0869-866X-2022-30-4-592-599
17. Parra-Arroyo L, González-González RB, Castillo-Zacarías C, Melchor Martínez EM, Sosa-Hernández JE, Bilal M, Iqbal HMN et. al Highly hazardous pesticides and related pollutants: Toxicological, regulatory, and analytical aspects. *Sci Total Environ.* 2022;807(3):151879. https://doi.org/ 10.1016/j.scitotenv.2021.151879
18. Donley N, Bullard RD, Economos J, Figueroa I, Lee J, Liebman AK et.al. Pesticides and environmental injustice in the USA: root causes, current regulatory reinforcement and a path forward. *BMC Public Health*. 2022;22(1):708. https://doi.org/10.1186/s12889-022-13057-4
19. Afandiyev INO. Mass Occupational Phosphine Poisoning of a Dry-Cargo Ship Crew: A Case Report. *Iran J Public Health.* 2022 Jun;51(6):1428–31. https://doi.org/10.18502/ijph.v51i6.9700
20. Feinstein DL, Hafner J, van Breemen R, Rubinstein I. Inhaled synthetic cannabinoids laced with long-acting anticoagulant rodenticides: A clear and present worldwide danger. *Toxicol Commun*. 2022;6(1):28–9. https://doi.org/10.1080/24734306.2022.2025690
21. Bar N, Lopez-Alonso R, Merhav G, Naaman E, Leiderman M, Ilivitzki A, et.al. Radiological findings in poisoning by synthetic cannabinoids adulterated with brodifacoum. *Eur Radiol*. 2024;34(7):4540-9. https://doi.org/10.1007/s00330-023-10496-4
22. Galstyan GM, Davydkin IL, Nikolaeva AS, Vekhova NI, Pavlova ZE, Ponomarenko IS, Klebanova EE, Savchenko VG. Outbreak of mass poisoning with anticoagulant rodenticides. *Russian journal of hematology and transfusiology*. 2020;65(2):174–89 (In Russ.). https://doi.org/10.35754/0234-5730-2020-65-2-174-189
23. Kwesiga B, Ario AR, Bulage L, Harris J, Zhu BP. Fatal cases associated with eating chapatti contaminated with organophosphate in Tororo District, Eastern Uganda, 2015: case series. *BMC Public Health.* 2019;19(1):767. https://doi.org/10.1186/s12889-019-7143-0
24. Rakitskiy VN. Prognostic risk of toxic effects of pesticides on the health of workers. *Occupational medicine and industrial ecology.* 2015;(10):5–7 (In Russ.). EDN: UMUIOF
25. Karunarathne A, Gunnell D, Konradsen F, Eddleston M. How many premature deaths from pesticide suicide have occurred since the agricultural green revolution? *Clin Toxicol (Phila)* 2020;58(4):227–32. https://doi.org/10.1080/15563650.2019.1662433
26. Preventing suicide: a resource for pesticide registrars and regulators (who.int)
27. Preventing suicide: a resource for media professionals. https://www.who.int/publications/i/item/9789240076846
28. Gunnell D, Knipe D, Chang SS, Pearson M, Konradsen F, Lee WJ, Eddleston M. Prevention of suicide with regulations aimed at restricting access to highly hazardous pesticides: a systematic review of the international evidence. *Lancet Glob Health*. 2017;5(10):e1026-e1037. https://doi.org/10.1016/S2214-109X(17)30299-1
29. Eddleston M, Nagami H, Lin CY, Davis ML, Chang SS. Pesticide use, agricultural outputs, and pesticide poisoning deaths in Japan. *Clin Toxicol (Phila)*. 2022;60(8):933–41. https://doi.org/10.1080/15563650.2022.2064868
30. Cheng J, Chen Y, Wang W, Zhu X, Jiang Z, Liu P, Du L. Chlorfenapyr poisoning: mechanisms, clinical presentations, and treatment strategies. *World J Emerg Med*. 2024;15(3):214–19. https://doi.org/10.5847/wjem.j.1920-8642.2024.046
31. Holborow A, Purnell RM, Wong JF. Beware the yellow slimming pill: fatal 2,4-dinitrophenol overdose. *BMJ Case Rep*. 2017;(1):1–4. https://doi.org/ 10.1136/bcr-2016-214689

32. Prodanchuk MH, Balan GM, Bubalo NM, Zhminko PH, Kharchenko OA, Bahlei YA. The problem of acute pesticide poisonings of agricultural workers in ukraine under the conditions of the new business patterns. *Wiad Lek*. 2019;72(5 cz 2):1083–6. EDN: BQKECL
33. Kurdil NV, Zozulya IS, Ivashchenko OV. Features of acute pesticide poisoning in urban conditions. *Emergency medicine.* 2015;3(66):37–42 (In Russ.). EDN: UAUBSZ
34. Mancheva TS. Pynzaru YuV, Sandulyak EV. Analysis of acute unprofessional pesticide poisoning in the Republic of Moldova in the period 2011-2016 Proceedings of the Republican scientific and practical conference with international participation. Health and the Environment. Minsk; 2017 (In Russ.). EDN: YRFTHI
35. Mancheva TS. Acute poisoning in children in the Republic of Moldova. Proceedings of the international scientific and practical conference. Health and the Environment. Minsk; 2019 (In Russ.). EDN: SHLMTU
36. Kobidze TS, Gerzmava OX, Kereselidze MT, Tsetskhladze N. Chemical trauma. Some features of the provision of specialized toxicological care to the population of Georgia. Conference proceedings of the scientific and practical conference Janelidze Readings. St. Petersburg; 2021 (In Russ.). EDN: KPDYIP
37. Efendiev IN, Bunyatov M O, Akhundova MT. Lethal poisoning in Azerbaijan: epidemiology, risk factors and possible ways of prevention. *Eurasian journal of clinical sciences.* 2019;2(2):1–9 (In Russ.). https://doi.org/10.28942/ejcs.v2i2.82
38. Efendiev IN. Poisoning with substances of anticholinesterase action. *Eurasian Journal of Clinical Sciences.* 2021;3(1):1–8 (In Russ.). https://doi.org/10.28942/ejcs.v3i1.98
39. Khadjibaev AM, Alakaev AA, Stopnitsky RN. Clinical toxicology in the Republic of Uzbekistan. Twenty years of experience working as part of the emergency medical care system. Emergency medical care. Proceedings of the 20th All-Russian Congress. St. Petersburg;2021 (In Russ.). EDN: KYCJHB
40. Borisevitch S, Grishenkova L, Bohdan A, Borovikova L. Structure and dynamics of acute poisoningswith lethal outcome in the republic of Belarus in 2016–2018. *Laboratory Diagnostics. Eastern Europe.* 2020;9(4):375–87. https://doi.org/10.34883/PI.2020.9.4.003
41. Rakitskii VN, Tereshkova LP, Chkhvirkiya EG, Epishina TM. Fundamentals of ensuring the safe application of pesticides. *Health Care of the Russian Federation*. 2020;64(1):45–50 (In Russ.). https://doi.org/10.18821/0044-197X-2020-64-1-45-50
42. National report. On the state of sanitary and epidemiological well-being of the population in the Russian Federation in 2020. Moscow: Federal Service for the Oversight of Consumer Protection and Welfare; 2021. 256 p. (In Russ.).
43. Litvinova OS, Kalinovskaya MV. Toxicological monitoring of the causes of acute poisoning of chemical etiology in the Russian Federation. *Toxicological Review.* 2017;1(142):5–9 (In Russ.). https://doi.org/10.36946/0869-7922-2017-1-5-9
44. Sabaev AV. Mortality dynamics according to the data of the Center for acute poisoning in Omsk for 2002–2011. *Siberian Medical Journal*. 2013;18(3):79–81 (In Russ.). EDN: QIWPWV
45. Zobnin YuV, Tretyakov AB, Nemtsova AA, Perfiliev DV, Dragunov MA. Acute poisoning in adults and children in Irkutsk in 1999–2018. *Baikal Medical Journal.*2019;159(4):46-55 (In Russ.). https://doi.org/10.34673/isma.2019.36.86.011
46. Aydinov GT, Marchenko BI, Sinelnikova YuA. Acute chemical poisonings as an index of the system of socio-hygienic monitoring in the Rostov region. *Hygiene and Sanitation*. 2018;97(3): 279–85 (In Russ.). https://doi.org/10.18821/0016-9900-2018-97-3-279-285
47. Udaltsov MA, Pshenisnov KV, Aleksandrovich YuS, Kaziakhmedov VA, Ironosov VE. Epidemiology of acute poisoning in pediatric practice. *Russian Journal of Anesthesiology and Reanimatology*. 2024;(2):58–66 (In Russ.). https://doi.org/10.17116/anaesthesiology202402158
48. Kamalova AA, Gorina GA, Kadyrova YuA, Nizamova RA, Zainetdinova MSh, Kvitko EM. Acute poisoning in children: a retrospective analysis of cases. *Toxicological bulletin.* 2022;30(6):351–8 (In Russ.). https://doi.org/10.47470/0869-7922-2022-30-6-351-358
49. Ostrovsky IM, Naletov AV, Lennart TV. Modern features of poisoning in children of Donbass. *Bulletin of Emergency and Reconstructive Surgery.* 2020;5(2):126–9 (In Russ.). EDN: IUXIWF
50. Rozhkov PG, Gasimova ZM, Bukharin YY. Retrospective analysis of requests for information and advisory toxicological assistance on issues of acute pesticide poisoning for the period 2019–2021. Proceedings of the International University Scientific Forum. Practice Oriented Science UAE–RUSSIA–INDIA. 2024.

Authors' contribution: All authors confirm that their authorship meets the ICMJE criteria. The greatest contribution is distributed as follows: P.G. Rozhkov — development of the concept and design of the study, general guidance, approval of the final version of the manuscript for publication; Z.M. Gasimova — collecting information, writing the text of the manuscript; Yu.Yu. Bukharin checking critical intellectual content, editing the manuscript; T.A. Sokolova — collecting information, making a list of references: V.V. Severtsev — information collection, analysis and interpretation of data; N.F. Lezhenina — collecting information, editing the manuscript.

AUTHORS

Pavel G. Rozhkov
https://orcid.org/0000-0003-4157-9015
rtiac@mail.ru

Zulfira M. Gasimova, Cand. Sci. (Biol.)
https://orcid.org/0000-0002-3531-9981
zulfiram@mail.ru

Yuri Y. Bukharin
https://orcid.org/0000-0002-0318-1922
doc-62@mail.ru

Tatiana A. Sokolova
https://orcid.org/0000-0003-2117-4563
tanyaasokolova66@mail.ru

Vsevolod V. Severtsev, Cand. Sci. (Med.)
https://orcid.org/0000-0001-8712-3561
severtsevmed@gmail.com

Natalia F. Lezhenina, Cand. Sci. (Med.), Associate Professor
https://orcid.org/0000-0002-3520-0075
natalilezhenina@rambler.ru

https://doi.org/10.47183/mes.2024-26-3-87-91

EFFECT OF BOVINE PROSTATE EXTRACT ON THE CONTRACTILE ACTIVITY OF LYMPHATIC VESSELS IN RATS

Olga V. Nechaykina[1]✉, Denis S. Laptev[1], Sergei G. Petunov[1], Dmitry V. Bobkov[1], Tatyana A. Kudryavtseva[2]

[1] Research Institute of Hygiene, Occupational Pathology and Human Ecology, Leningrad Region, Russia

[2] Institute of Experimental Medicine, Saint-Petersburg, Russia

Introduction. A comprehensive approach to treatment of chronic prostatitis, representing a widespread and poorly treatable disease, includes the use of antibacterial, anti-inflammatory medicines, etc. In this context, a promising approach to the treatment of chronic prostatitis involves the use of bioregulatory peptides isolated from bovine prostate tissue.

Objective. To study the effect of cattle prostate extract containing bioregulatory peptides on the functional activity of lymphatic vessels.

Materials and methods. The study was performed on isolated lymphatic vessels of rats. The range of studied concentrations of the substance was 2–10 μg/mL (in terms of water-soluble peptides).

Results. Bioregulatory peptides included into the prostate extract impacts the vasomotor activity of lymphatic vessels. In the range of studied concentrations (2–10 μg/mL), the substance has a stimulating effect on lymphangion motility. This is realized by increasing the rate of lymphatic vessel contractions, which effect is most pronounced at the concentration of 5 μg/mL as a 37.6% ($p \leq 0.05$) of base level. The obtained stimulating effect is stable during 30-min "washing" of lymphatic vessels with physiological solution.

Conclusions. Water-soluble bioregulatory peptides contained in the extract of cattle prostate and having organotropic action on the prostate gland may contribute to the reduction of tissue edema by activating the motility of pelvic lymphatic vessels.

Keywords: bovine prostate extract; isolated lymphatic vessels; chronotropic effect

For citation: Nechaykina O.V., Laptev D.S., Petunov S.G., Bobkov D.V., Kudryavtseva T. A. Effect of bovine prostate extract on the contractile activity of lymphatic vessels in rats. *Extreme Medicine.* 2024;26(3):87–91. https://doi.org/10.47183/mes.2024-26-3-87-91

Funding: the study was performed within the framework of R&D No. 594/23 with funding from AO MBNPK "Cytomed".

Compliance with the principles of ethics: the study was performed in compliance with the rules of bioethics approved by the European Convention for the Protection of Vertebrate Animals Used for Experimental and Other Purposes. The animals were kept in accordance with GOST 33215-2014 "Guidelines for the maintenance and care of laboratory animals" from 2016. The experiments were approved by the Bioethics Commission of the Federal State Unitary Enterprise Research Institute "GPECH" FMBA of Russia (Minutes No. 5 of 16.12.2022).

Potential conflict of interest: the authors declare that there is no conflict of interest.

✉ Nechaykina Olga Valeryevna olga2278@mail.ru

Article received: 05 June 2024 **Revised:** 04 Sep. 2024 **Accepted:** 07 Sep. 2024

ВЛИЯНИЕ ЭКСТРАКТА ПРОСТАТЫ БЫКА НА СОКРАТИТЕЛЬНУЮ АКТИВНОСТЬ ЛИМФАТИЧЕСКИХ СОСУДОВ КРЫСЫ

О.В. Нечайкина[1]✉, Д.С. Лаптев[1], С.Г. Петунов[1], Д.В. Бобков[1], Т.А. Кудрявцева[2]

[1] Научно-исследовательский институт гигиены, профпатологии и экологии человека Федерального медико-биологического агентства, г.п. Кузьмоловский, Ленинградская область, Россия

[2] Институт экспериментальной медицины, Санкт-Петербург, Россия

Введение. Хронический простатит — распространенное и плохо поддающееся терапии заболевание, комплексный подход к лечению которого включает применение антибактериальных, противовоспалительных средств и др. Перспективным подходом в лечении хронического простатита является использование биорегуляторных пептидов, выделенных из ткани предстательной железы крупного рогатого скота.

Цель. Изучить влияние экстракта простаты крупного рогатого скота, содержащей биорегуляторные пептиды, на функциональную активность лимфатических сосудов.

Материалы и методы. Работа выполнена на изолированных лимфатических сосудах крыс. Диапазон изучаемых концентраций субстанции — 2–10 мкг/мл (в пересчете на водорастворимые пептиды).

Результаты. Биорегуляторные пептиды, входящие в состав экстракта простаты, обладают вазомоторной активностью в отношении лимфатических сосудов. В диапазоне концентраций 2–10 мкг/мл изучаемая субстанция оказывает стимулирующее влияние на моторику лимфангионов, которое реализуется за счет увеличения частоты сокращений лимфатических сосудов, наиболее выраженное в концентрации 5 мкг/мл на уровне 37,6% ($p \leq 0,05$) от фона. Полученный стимулирующий эффект устойчив в течение 30-минутного «отмывания» лимфатических сосудов физиологическим раствором.

Выводы. Водорастворимые биорегуляторные пептиды, входящие в состав экстракта простаты КРС и обладающие органотропным действием на предстательную железу, могут способствовать снижению отека ткани путем активации моторики лимфатических сосудов органов малого таза.

Ключевые слова: экстракт простаты КРС; изолированные лимфатические сосуды; хронотропное действие

Для цитирования: Нечайкина О.В., Лаптев Д.С., Петунов С.Г., Бобков Д.В., Кудрявцева Т.А. Влияние экстракта простаты быка на сократительную активность лимфатических сосудов крысы. *Медицина экстремальных ситуаций.* 2024;26(3):87–91. https://doi.org/10.47183/mes.2024-26-3-87-91

Финансирование: работа выполнена в рамках НИР № 594/23 при финансировании АО МБНПК «Цитомед».

Соответствие принципам этики: исследование выполнено с соблюдением правил биоэтики, утвержденных Европейской конвенцией о защите позвоночных животных, используемых для экспериментальных и других целей. Содержание животных осуществлялось в соответствии с ГОСТ 33215-2014 «Руководство по содержанию и уходу за лабораторными животными» от 2016 г. Эксперименты были одобрены комиссией по биоэтике ФГУП «Научно-исследовательский институт гигиены, профпатологии и экологии человека» Федерального медико-биологического агентства (протокол № 5 от 16.12.2022).

Потенциальный конфликт интересов: авторы заявляют об отсутствии конфликта интересов.

✉ Нечайкина Ольга Валерьевна olga2278@mail.ru

Статья поступила: 05.06.2024 **После доработки:** 04.09.2024 **Принята к публикации:** 07.09.2024

INTRODUCTION

Chronic prostatitis is one of the most common and at the same time among the most understudied and poorly treated diseases. The main target patient population is predominantly of reproductive age. The course of chronic prostatitis is often complicated by impaired copulatory and generative functions [1]. Recently, the disease is increasingly detected in elderly men, sometimes in combination with benign prostatic hyperplasia [2]. Thus, in men under 50 years of age, the incidence of confirmed prostatitis is only twice as high as in patients over 50 years of age [3].

The prostate gland has a well-developed intra-organ vasculature, including blood and lymphatic capillaries and postcapillaries. Blood and lymphatic microvessel beds form microvascular-muscular complexes with bundles of smooth myocytes in the anterior parts of the prostate gland and microvascular-glandular complexes with prostatic glands in the posterior and lateral parts of the prostate gland [4]. The leading place in the pathogenesis of chronic prostatitis is occupied by the disruption of lymphatic outflow into the vascular bed and congestion in glandular structures.

Due to the polyetiological and multifactorial nature of pathogenesis, the treatment of chronic prostatitis implies a comprehensive approach, including antibacterial and anti-inflammatory therapies, physiotherapeutic procedures, and other effects. A promising approach in the treatment of chronic prostatitis involves the use of bioregulatory peptides isolated from bovine prostate tissue [2]. The biological effect of prostatic peptides isolated from the bovine prostate gland was first revealed in the mid-1980s. Under experimental conditions it was revealed that polypeptides from the prostate gland possessing tropism to blood vessels increase the antiaggregatory activity of vascular walls [5]. Prostatic peptides, which along with other regulatory peptides are characterized by a lack of species specificity, also have a pronounced tropism to prostate tissues, permitting their consideration as a target organ.

The pharmaceutical market offers a large number of medicines having bovine prostate extract as an active ingredient. Active pharmaceutical substances included in the State Register of Medicinal Products are used for the production of these medicines. However, the features of their composition and strength of their biological effect are significantly determined by their widely varying production technology [6]. Substance-mixture Prostatilen® produced by AO MBNPK “Cytomed” obtained by tangential ultrafiltration technology is an active pharmaceutical substance used in the manufacture of the peptide drug Prostatilen®.

One of the formulations of Prostatilen® is rectal suppository. Its active ingredient is a complex of water-soluble peptides obtained from the prostate tissue of sexually mature bulls with addition of glycine. The ability of Prostatilen® to restore blood rheological properties and improve microcirculation in target organs leads to hemodynamic normalization and provides treatment of inflammatory diseases of the prostate gland [7]. The high bioavailability of Prostatilen® is provided by the low molecular weight of its peptide fraction components and realized by passive transport of drug through enterocytes of rectal mucosa. Peptides are absorbed by the rectal vessels and exert their effect through the system of anastomoses on the pelvic organs, including the prostate gland located in anatomical proximity to the injection site [8]. The outflow of interstitial fluid containing regulatory peptides is ensured by adequate contractile activity of lymphatic vessels sensitive to the action of various vasoactive substances, including endogenous modulators of functional state [9–11].

Isolated lymphatic vessels with spontaneous rhythmic contractile activity are the one of available and informative experimental models used to study the effect of vasoactive substances on the transport function of lymphatic system. In this regard, the evaluation of the peptide complex (active substance of Prostatilen® drug) effect on the contractile activity of lymphatic vessels is an urgent problem, whose solution can be used in the development and optimization of therapeutic methods for treating chronic prostatitis.

The aim of the study was to investigate the effect of the substance-mixture Prostatilen® (hereinafter referred to as Prostatilen®) on the functional activity of lymphatic vessels as a potential target of the therapeutic effect of the studied extract.

MATERIALS AND METHODS

The study was performed on isolated segments of the anterior mesenteric lymphatic duct of sexually mature male nonlinear white rats weighing 250–300 g. The samples were obtained from the branch of SIC “Kurchatov Institute” PIAR — “Nursery of laboratory animals ‘Rappolovo’ (Leningrad region) — PIAR — “Rappolovo Laboratory Animal Nursery” (Leningrad Region). The maintenance and feeding of laboratory animals were performed in accordance with GOST 33215-2014 “Guidelines for the maintenance and care of laboratory animals” from 2016. Healthy sexually mature animals that underwent a 14-day quarantine were used for the studies. Microclimate parameters (temperature, relative humidity, air exchange rate parameters), as well as the quality of feed and bedding material were controlled in the vivarium premises. The animals were fed a standard diet in the form of pelleted feed. In the rooms where experimental animals were kept, a lighting regime of 12 h day/12 h night was established.

The experimental study was conducted in accordance with the European Convention for the Protection of Animals Used in Experimentation (Directive 86/609/EEC) and approved by the Bioethics Commission (protocol #5 of 16.12.2022).

The experimental study of the Prostatilen® effect on the functional parameters of isolated lymphatic vessels of rats ex vivo was carried out using a multi-channel myograph Multi Wire Myograph System DMT 620M (DMT, Denmark) according to the previously described method [12]. The parameters of contractile activity of lymphatic vessels, including the level of tonic tension, amplitude and phasic contraction rate (CR), were recorded using a PowerLab Data acquisition system 8/30 (ADInstruments, USA) with subsequent processing in the LabChartProUpgrade 7.0 software package.

The test object is a mixture-substance Prostatilen®, as well as a Prostatilen® solution with a content of 11.7% water-soluble peptides (according to the manufacturer's passport). Prostatilen® was used in concentrations (based on the content of water-soluble peptides) of 1 μg/mL, 2 μg/mL, 5 μg/mL, and 10 μg/mL was added to perfusate to research the reactivity of lymphatic vessels. The exposure time of each concentration was 20 min. A Krebs-Henseleit saline solution with the same exposure time was used as a control.

Statistical processing of the data was carried out using methods of descriptive and analytical statistics using the GraphPad Prism 5.04 software package. The critical level of significance was taken to be $p \leq 0.05$. The median value was used to describe the central tendency; the first (Q1) and third (Q3) quartiles were used as a measure of dispersion. Data were analyzed using the Wilcoxon T-test for related samples. The Mann-Whitney U-test was used to detect intergroup differences.

RESULTS

Like any biological object, the parameters of lymphatic vessels phase activity are characterized by a certain variability (Table 1). Therefore, when analyzing the obtained results, we used relative units characterizing the change of parameters under the action of the drug compared to the base values, which were taken as 100%. When performing the work, data collection was carried out in parallel (simultaneously) in all experimental groups.

The results of experiments evaluating the effect of Prostatilen® on isolated lymphatic vessels are summarized in Table 2.

It was found that Prostatilen® application in the minimum studied concentration (1 μg/mL) during 20-minute period had no effect on the contractile activity of lymphangions. At a 20-minute exposure with concentrations of 2 μg/mL, 5 μg/mL and 10 μg/mL, Prostatilen® caused an increase in CR from background values by 23.7% ($p \leq 0.05$), 37.6% ($p \leq 0.05$) and 26.8% ($p \leq 0.05$), respectively. In all studied concentrations, the contraction amplitude and tonus of lymphatic vessels under the influence of substance-mixture were registered at the level of background values and did not differ statistically significantly from the control.

In addition to bioregulatory peptides, the composition of Prostatilen® includes the amino acid glycine. Being an integral part of the mitochondrial respiratory chain, glycine is actively involved in the process of cell renewal and oxygenation, in the synthesis of proteins (in particular, glutathione tripeptide), and in detoxification reactions. It has a wide range of anti-inflammatory, cytoprotective and immunomodulatory properties [13]. According to the literature, glycine also has an effect on the blood and lymphatic vessels that make up the cardiovascular system [14–16]. In order to exclude the intrinsic effect of glycine on mesenteric lymphatic vessels, experiments were conducted with Prostatilen® solution used for the manufacture of the liquid formulation of Prostatilen® medicine (solution for intramuscular administration) and not containing glycine. A minimum effective concentration of 2 μg/mL (based on the content of water-soluble peptides) was selected.

As follows from the data shown in Table 2, a Prostatilen® solution at a concentration of 2 μg/mL resulted in a 29.6% ($p \leq 0.05$) increase in CR of lymphangions as compared to background. At the same time the amplitude of contractions and tonic tension were registered at the level of background values. The obtained results are comparable with the results obtained when studying the effect of Prostatilen® substance-mixture on lymphatic vessels, which demonstrates

Table 1. Background indices of contractile activity of rat lymphatic vessels in the experimental groups. Absolute data are presented as Me (0.25; 0.75)

Indicators	Saline solution, *n* = 12	Substance-mixture Prostatilen®			
		1 μg/mL, *n* = 11	2 μg/mL, *n* = 11	5 μg/mL, *n* = 11	10 μg/mL, *n* = 13
CR, min^{-1}	4.55 (3.28; 6.95)	3.00 (2.60; 6.25)	5.70 (2.35; 6.65)	5.20 (2.85; 7.10)	5.60 (4.15; 8.50)
Amplitude, mN	0.62 (0.49; 0.83)	0.45 (0.34; 0.70)	0.80 (0.31; 0.90)	0.73 (0.42; 1.03)	0.65 (0.40; 0.97)
Tonus, mN	1.38 (1.29; 0.75)	1.69 (1.38; 2.15)	1.72 (1.16; 2.15)	1.82 (1.55; 2.54)	1.49 (1.11; 1.76)

Table prepared by the authors using their own data

Table 2. Parameters of contractile activity of rat lymphatic vessels under the influence of Prostatilen®. Relative data in percentages are presented as Me (0.25; 0.75)

Investigated substance	*n*	FC	Amplitude	Tonus
Saline solution	12	103.6 (98.5; 109.1)	100.6 (96.9; 104.8)	98.5 (97.5; 100.4)
substance-mixture Prostatilen®, 1 μg/mL	11	106.6 (101.7; 108.7)	104.0 (94.6; 106.6	99.3 (97.9; 103.9)
substance-mixture Prostatilen®, 2 μg/mL	11	123.7 (111.9; 130.6)*	100.4 (97.7; 104.5)	99.8 (97.2; 101.7)
substance-mixture Prostatilen®, 5 μg/mL	11	137.6 (129.9; 158.3)*	99.0 (94.0; 101.8)	99.9 (97.4; 100.9)
substance-mixture Prostatilen®, 10 μg/mL	13	126.8 (114.7; 129.8)*	97.6 (94.6; 100.7)	100.7 (99.1; 104.7)
solution of Prostatilen® 2 μg/mL (without glycine)	12	129.6 (112.8; 144.0)*	100.8 (97.9; 107.7)	99.6 (97.8; 101.0)

Table prepared by the authors using their own data

Note: * — statistically significant difference from background values at $p < 0.05$

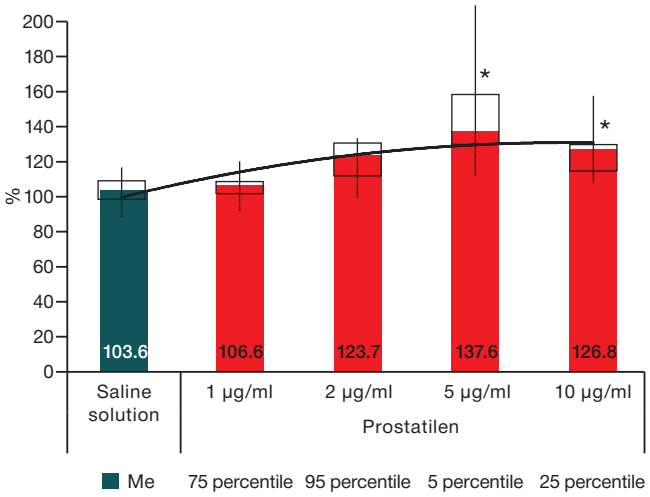

Figure prepared by the authors using their own data

Fig. 1. Changes in the rate of lymphatic vessels contractions when exposed to Prostatilen®. Exposure duration 20 min. Data presented as a percentage relative to the background in the form of Me. * — statistically significant difference from saline solution at $p < 0.05$.

the mechanism of the chronotropic effect of Prostatilen® due to the action of bioregulatory peptides.

RESULTS AND DISCUSSION

Initial changes in the phasic contractions rate occurred as an effect of substance-mixture Prostatilen® at a concentration of 2 μg/mL. The effect increased with increasing concentration of Prostatilen®. The maximum increase in CR was observed as effect of Prostatilen® in concentration of 5 μg/mL. When the concentration of the substance was increased up to 10 kg/mL, the positive chronotropic effect on lymphatic vessels was maintained. Although the increase in CR was slightly lower than at the previous concentration, this increase was also statistically significantly different from the control ($p \leq 0.05$). Thus, Prostatilen® has a positive chronotropic effect on lymphatic vessels. Dynamics of changes in the CR of lymphangions under Prostatilen® exposure in all concentrations is presented in Figure 1.

CR is well known to be associated with the spontaneous generation frequency of action potentials in smooth muscle pacemaker cells where the basis for the occurrence of action potentials is spontaneous short-term depolarization (Spontaneous Transitory Depolarization), which occurs due to the opening of Ca^{2+}-dependent Cl-channels during intracellular release of Ca^{2+} ions from inositol-1,4,5-triphosphate-sensitive depot [17]. It can be assumed that Prostatilen® promotes the release of Ca^{2+} ions from intracellular depot, which, in turn, leads to increased CR.

To study the stability of the obtained stimulating effect of Prostatilen®, we analyzed the change of CR during a "washing" period, when the working chamber of the myograph was perfused with Krebs-Henseleit solution without the active substance. After a 30-min washout period after the expose of Prostatilen® at a concentration of 10 μg/mL, the phasic contractile activity exceeded the background values by 30.1% ($p \leq 0.05$) indicating the prolonged action of the drug. Such an effect of the aftereffect of bioregulatory peptides can be explained in terms of I.P. Ashmarin's theory of the functional and regulatory continuum of the system of regulatory peptides [18]. Intracellular processes following peptide receptions are associated with the action of the latter on secondary messenger systems, which in turn trigger an intracellular cascade of sequential enzyme activation that ultimately manifests itself as a change in metabolic processes in the cell and determines the physiological response. It is fundamentally important that bioregulatory peptides are capable of triggering a number of processes at all levels of the metabolic hierarchy of cells following interaction with a receptor — from the membrane to the genome — with different durations — from minutes (or fractions thereof) to hours. This makes possible the existence of cascade effects in the organism caused by the introduction or release of a particular bioregulatory peptide [19].

CONCLUSIONS

1. As a result of this study, it has been shown for the first time that the substance-mixture Prostatilen® demonstrates a vasoactive effect on lymphatic vessels. Across the concentration range between 2 and 10 μg/mL, Prostatilen® stimulates the motility of lymphangions, thus providing a basis to consider isolated lymphatic vessels as an adequate physiological model for the study of vasoactive properties of the medicine.

2. Water-soluble bioregulatory peptides included in the composition of the Prostatilen® medicine can be assumed not only to have a directed (organotropic) effect on the prostate gland and organs of the urogenital system, but also making a contribution to the reduction of tissue edema by activating the motility of lymphatic vessels of the pelvic organs, once again confirming the feasibility of regulatory peptides in the treatment of diseases associated with inflammatory and congestive phenomena.

References

1. Beliy LE. Prostatic peptides for the correction of pathospermia in patients with chronic bacterial prostatitis. *Meditsinsky Sovet*. 2018;21:178–82 (In Russ.). https://doi.org/10.21518/2079-701X-2018-21-178-182
2. Gorilovsky LM., Dobrokhotov MM. Chronic prostatitis. *Medical advice.* 2010;(7–8):72–7 (In Russ.). EDN: MVYXVD
3. Uchvatkin GV, Tatarintseva MB. Prostatic peptides in the treatment of prostate diseases. *Urological reports*. 2017;7(3):44–8 (In Russ.). https://doi.org/10.17816/uroved7344-48
4. Petrenko VM. Vascular bed of the prostate. *International Journal of Experimental Education*. 2010;7:48–9 (In Russ.). EDN: RAJOOF
5. Khavinson VH., Morozov VG., Kuznik BI, et al. Effect of polypeptides from the prostate on the hemostasis system. *Pharmacology and toxicology*. 1985;48(5):69–71 (In Russ.). EDN: OXGGLQ
6. Savel'ev SA., Dorosh MY., Lagereva IA, et al. Influence of manufacturing technology on the properties of active pharmaceuti-

cal ingredients of prostate extract. Pharmaceutical Chemistry Journal. 2022;56(3): 50–8 (In Russ.). https://doi.org/10.30906/0023-1134-2022-56-3-50-58
7. Kuzmin IV, Borovets SYU, Gorbachev AG, Al-Shukri SKH. Prostatic bioregulatory polypeptide prostatilen: pharmacological properties and 30-year experience of clinical application in urology. *Urology Reports.* 2020;10(3):243–58 (In Russ.). https://doi.org/10.17816/uroved42472
8. https://cytomed.ru/wp-content/uploads/2023/11/ohlp_prostatilen-3-mg.pdf
9. Razavi MS, Dixon JB, Gleason RL. Characterization of rat-tail lymphatic contractility and biomechanics: incorporating nitric oxide-mediated vasoregulation. *JR Soc Interface.* 2020;17(170):20200598. https://doi.org/10.1098/rsif.2020.0598
10. Johnston MG., Gordon JL. Regulation of lymphatic contractility by arachidonate metabolites. *Nature.* 1981;293:294–7. https://doi.org/10.1038/293294a0
11. Lobov GI, Unt DV. Glucocorticoids stimulate the contractile activity of lymphatic vessels and lymph nodes. *Regional blood circulation and microcirculation.* 2017; 4(64):73–9 (In Russ.). https://doi.org/10.24884/1682-6655-2017-16-4-73-79
12. Nechaykina OV, Laptev DS, et al. Effect of Unsymmetrical Dimethylhydrazine on Isolated Heart and Lymphatic Vessels. *Bull Exp Biol Med.* 2021;172(9): 283–6 (In Russ.). https://doi.org/10.1007/s10517-022-05380-y
13. Pérez-Torres I. Zuniga-Munoz A. M., Guarner-Lans V. Beneficial Effects of the Amino Acid Glycine. *Mini Rev Med Chem.* 2017;17(1);15–32. https://doi.org/10.2174/1389557516666160609081602
14. Stalberg HP, Hahn RG, Hjelmqvist H, Ullman J, Rundgren M, Stalberg HP. Haemodynamics and fluid balance after intravenous infusion of 1.5% glycine in sheep. *Acta Anaesthesiol Scand.* 1993;37(3):281–7. https://doi.org/10.1111/j.1399-6576.1993.tb03716.x
15. Podoprigora GI, Nartsissov YR. Effect of glycine on the microcirculation in rat mesenteric vessels. *Bull Exp Biol Med.* 2009;147(3):308–11. https://doi.org/10.1007/s10517-009-0498-y
16. Sawada M, McAdoo DJ, Ichinose M, Price CH. Influences of glycine and neuron R14 on contraction of the anterior aorta of Aplysia. *Jpn J Physiol.* 1984;34(4):747–67. https://doi.org/10.2170/jjphysiol.34.747
17. Von der Weid PY, Rahman M, et al. Spontaneous transient depolarizations in lymphatic vessels of the guinea pig mesentery: Pharmacology and implication for spontaneous contractility. *Am J Physiol Heart Circ Physiol.* 2008;295:1989–2000. https://doi.org/10.1152/ajpheart.00007.2008
18. Ashmarin IP, Obukhova MF. Sovremennoe sostoianie gipotezy o funktsional'nom kontinuume reguliatornykh peptidov [Current state of the hypothesis on functional continuum of regulatory peptides]. *Vestn Ross Akad Med Nauk.* 1994;10:28–34 (In Russ.). PMID: 7534535.
19. Ashmarin IP, Obukhova MF. Regulatory peptides: functionally continuous integrity. *Biochemistry.* 1986;51(4):531–45 (In Russ.).

Authors' contributions. All the authors confirm that they meet the ICMJE criteria for authorship. The most significant contributions were as follows. Olga V. Nechaykina — research concept and design, information collection, data processing, text writing;Denis S. Laptev — research concept and design, information collection, data processing, editing; Sergei G. Petunov — data processing and interpretation, general guidance;Dmitry V. Bobkov — data processing, editing; Tatyana A. Kudryavtseva — the concept and design of the study, editing.

AUTHORS

Olga V. Nechaykina
https://orcid.org/0000-0001-7151-7240
olga2278@mail.ru

Denis S. Laptev, Cand. Sci. (Biol.)
https://orcid.org/0000-0002-3960-3058
lapden@mail.ru

Sergei G. Petunov, Cand. Sci. (Med.), Associated Professor
https://orcid.org/0000-0001-6781-8315
sergey-petunov@mail.ru

Dmitry V. Bobkov
https://orcid.org/0000-0002-1823-4361
bdv21@yandex.ru

Tatyana A. Kudryavtseva, Cand. Sci. (Biol.)
https://orcid.org/0000-0003-4997-9830
tatjana_ku@inbox.ru

https://doi.org/10.47183/mes.2024-26-3-92-97

A MODERN APPROACH TO THE DIFFERENTIAL DIAGNOSIS OF HUMAN BETAHERPESVIRUS INFECTION 6A/V IN CHILDREN

Natalia S. Tian[1]✉, Irina V. Babachenko[1,2], Olga V. Goleva[1], Lyudmila I. Zhelezova[1], Elena V. Baziyan[1], Oleg S. Glotov[1]

[1] Children's Scientific and Clinical Center for Infectious Diseases of the Federal Medical and Biological Agency, St. Petersburg, Russia

[2] St. Petersburg State Pediatric Medical University, St. Petersburg, Russia

Introduction. Herpesvirus infections — in particular, those caused by human betaherpesvirus 6A/B (HHV-6A/C), are a serious problem at the present time due to their ubiquity, polymorphism of manifestations, lifelong persistence in the body with the possibility of reactivation, and need for comprehensive diagnostics to the form of infection. Herpesvirus infections are especially serious when occurring in children with recurrent respiratory diseases.

Objective. To propose a modern method of differential diagnosis (DD) of active and latent forms of HHV-6A/B infection in children to optimize patient management tactics.

Materials and methods. To build a discriminant model, 152 patients aged 1 month to 17 years inclusive were included in the study, 112 of them making up a training sample, while 40 comprised a test sample. A dichotomous variable was taken as a response variable: 1 — latent form of HHV-6A/B infection (n = 89), 2 — active (n = 23). 27 potential predictors were considered. The test sample consisted of 40 children. Statistical processing was performed using Microsoft Excel and StatSoft Statistica 7.0

Results. The developed prognostic model of DD of active and latent forms of HHV-6A/B infection in children, which takes into account the severity of fever, the presence of cough, the absolute neutrophil count and the value of threshold cycles of HHV-6A/B DNA, is characterized by its high sensitivity (91.3%) and specificity (94.4%). The presented example reflects the step-by-step use of the model.

Conclusions. The prognostic model can be used in practice for identifying DD forms of HHV-6A/B infection in the presence of lymphoproliferative and respiratory syndromes in children, for the detection of HHV-6A/B DNA in the blood, and to substantiate indications for immunotropic therapy.

Keywords: human betaherpesvirus infection 6A/B; active form; latent form; recurrent respiratory diseases; diagnosis; children

For citation: Tyan N.S., Babachenko I.V., Goleva O.V., Zheleznova L.I., Baziyan E.V., Glotov O.S. A modern approach to the differential diagnosis of human betaherpesvirus infection 6A/V in children. *Extreme Medicine*. 2024;26(3):92–97. https://doi.org/10.47183/mes.2024-26-3-92-97

Funding: the study was performed without external funding.

Acknowledgements: the authors would like to express their gratitude to Academician of the RAS, Dr. Sci. (Med.), prof. Yuri V. Lobzin, Honored Scientist, corresponding member of the RAS, Dr. Sci. (Med.), prof. Konstantin V. Zhdanov, Honored Scientist, Dr. Sci. (Med.), and prof. Natalia V. Skripchenko for their comprehensive support and the opportunity to perform research. We also thank Dr. Sci. (Med.) prof. Stepan G. Grigoriev, Senior Research Officer and patent specialist Nelly A. Dobroskok for their assistance in obtaining a patent for an invention.

Compliance with the principles of ethics: the study was conducted in accordance with the principles of the Helsinki Declaration and approved by the Local Ethics Committee of the Federal State Budgetary Institution "Children's Scientific and Clinical Center for Infectious Diseases of the Federal Medical and Biological Agency" (Protocol No. 160 dated 09/27/2022). Clinical and laboratory examination of patients was carried out after familiarization of their legal representatives with the stages of the study set out in the brochure and signing of informed consent, consent to the use of personal data.

Potential conflict of interest: the authors declare no conflict of interest.

✉ Natalia S. Tian tiannatalia94@yandex.ru

Received: 10 Sep. 2024 **Revised:** 18 Oct. 2024 **Accepted:** 21 Oct. 2024

СОВРЕМЕННЫЙ ПОДХОД К ДИФФЕРЕНЦИАЛЬНОЙ ДИАГНОСТИКЕ БЕТА-ГЕРПЕСВИРУСНОЙ ИНФЕКЦИИ ЧЕЛОВЕКА 6А/В У ДЕТЕЙ

Н.С. Тян[1]✉, И.В. Бабаченко[1,2], О.В. Голева[1], Л.И. Железова[1], Е.В. Базиян[1], О.С. Глотов[1]

[1] Детский научно-клинический центр инфекционных болезней Федерального медико-биологического агентства, Санкт-Петербург, Россия

[2] Санкт-Петербургский государственный педиатрический медицинский университет, Санкт-Петербург, Россия

Введение. Герпесвирусные инфекции, вызванные, в частности, бетагерпесвирусом человека 6А/В (ВГЧ-6А/В), являются важной проблемой современности ввиду повсеместной распространенности, полиморфизма проявлений, пожизненной персистенции в организме с возможностью реактивации, необходимости комплексной диагностики для установления формы инфекции, особенно у детей с рекуррентными респираторными заболеваниями.

Цель. Предложить современный способ дифференциальной диагностики (ДД) активной и латентной форм ВГЧ-6А/В инфекции у детей для оптимизации тактики ведения пациентов.

Материалы и методы. Для построения дискриминантной модели в исследование включили 152 пациента в возрасте от 1 месяца до 17 лет включительно, из них 112 — это тренировочная выборка, а 40 — тестовая. В качестве переменной отклика взята дихотомическая переменная: 1 — латентная форма ВГЧ-6А/В инфекции (n = 89), 2 — активная (n = 23). Рассмотрено 27 потенциальных предикторов. Тестовую выборку составили 40 детей. Статистическая обработка выполнена с использованием Microsoft Excel, StatSoft Statistica 7.0

Результаты. Разработанная прогностическая модель ДД активной и латентной форм ВГЧ-6А/В инфекции у детей учитывает выраженность лихорадки, наличие кашля, абсолютное число нейтрофилов и значение пороговых циклов ДНК ВГЧ-6А/В и характеризуется высокими показателями чувствительности (91,3%) и специфичности (94,4%). Представлен пример, отражающий пошаговое использование модели.

Выводы. Прогностическая модель может использоваться в практике для ДД форм ВГЧ-6А/В инфекции при наличии у детей лимфопролиферативного, респираторного синдромов и выявлении ДНК ВГЧ-6А/В в крови и для обоснования показаний к проведению иммунотропной терапии.

Ключевые слова: бета-герпесвирусная инфекция человека 6А/В; активная форма; латентная форма; рекуррентные респираторные заболевания; диагностика; дети

Для цитирования: Тян Н.С., Бабаченко И.В., Голева О.В., Железова Л.И., Базиян Е.В., Глотов О.С. Современный подход к дифференциальной диагностике бета-герпесвирусной инфекции человека 6A/B у детей. *Медицина экстремальных ситуаций*. 2024;26(3):92–97. https://doi.org/10.47183/mes.2024-26-3-92-97

Финансирование: работа выполнена без спонсорской поддержки.

Благодарности: академику РАН, д-ру мед. наук, профессору Лобзину Юрию Владимировичу, президенту ФГБУ «Детский научно-клинический центр инфекционных болезней» Федерального медико-биологического агентства, заслуженному деятелю науки Российской Федерации, член-корреспонденту Академии РАН, д-ру мед. наук, профессору Жданову Константину Валерьевичу, исполняющему обязанности директора ФГБУ «Детский научно-клинический центр инфекционных болезней» Федерального медико-биологического агентства, заслуженному деятелю науки Российской Федерации, д-ру мед. наук, профессору Скрипченко Наталье Викторовне, заместителю директора по научной работе ФГБУ «Детский научно-клинический центр инфекционных болезней» Федерального медико-биологического агентства, за всестороннюю поддержку и предоставленную возможность выполнить исследование в стенах Центра; д-ру мед. наук, профессору Григорьеву Степану Григорьевичу, старшему научному сотруднику отдела организации медицинской помощи ФГБУ «Детский научно-клинический центр инфекционных болезней» Федерального медико-биологического агентства Доброскок Нелли Александровне, патентоведу ФГБУ «Детский научно-клинический центр инфекционных болезней» Федерального медико-биологического агентства, за помощь в оформлении патента на изобретение.

Соответствие принципам этики: Исследование проведено в соответствии с принципами Хельсинкской декларации и одобрено Локальным этическим комитетом ФГБУ «Детский научно-клинический центр инфекционных болезней» Федерального медико-биологического агентства (протокол № 160 от 27.09.2022). Клинико-лабораторное обследование пациентов осуществлялось после ознакомления их законных представителей с этапами исследования, изложенными в брошюре, и подписания информированного согласия, согласия на использование персональных данных.

Потенциальный конфликт интересов: авторы заявляют об отсутствии конфликта интересов.

✉ Тян Наталья Сергеевна tiannatalia94@yandex.ru

Статья поступила: 10.09.2024 **После доработки:** 18.10.2024 **Принята к публикации:** 21.10.2024

INTRODUCTION

Herpesvirus infections are a serious problem at the present time due to their ubiquity, high infection rate of the population, and the possibility of their reactivation in the development of immunodeficiency conditions having a high risk of adverse outcomes [1–3]. In recent years, increasing attention has been paid to herpesviruses due to the increasing case numbers of active herpesvirus infections, including human betaherpesviruses 6A/B, in people with infectious diseases caused by the SARS-CoV-2 virus (COVID-19) [4–6], as well as in children with recurrent respiratory diseases (RRD). Although human betaherpesvirus 6A/B (HHV-6A/B) was first detected in 1985 in immunocompromised patients [7], it is currently known as one of the most common herpesviruses with the level of seropositive individuals to HHV-6A, HHV-6B or both types in the adult population reaching 95% [8]. Like other representatives of the family, HHV-6A/B is characterized by polymorphism of clinical manifestations and acts as a trigger of autoimmune and lymphoproliferative diseases [9–13].

The high level of infection with HHV-6A/B leads to the frequent detection of markers of betaherpesvirus HHV-6A/B infection, difficulties in differential diagnosis (DD) of active and latent forms, especially in children with lymphoproliferative and catarrhal syndromes, as well as RRD, overdiagnosis of active forms of infection and subsequent administration of immunotropic therapy with antiviral purpose [8, 14–16].

The aim of our study is to propose a modern DD method for active and latent forms of HHV–6A/B infection in children as a means of optimizing patient management tactics.

MATERIALS AND METHODS

The study, carried out in the Children's Scientific and Clinical Center for Infectious Diseases of the Federal Medical and Biological Agency of Russia from 2021 to 2023, included 152 patients aged 1 month to 17 years 11 months and 29 days, 112 of whom made up a training sample for training the classifier, while 40 comprised a test sample for validating the classifier. Inclusion criterion for the training sample: detection of HHV-6A/B DNA in whole blood by qualitative polymerase chain reaction (PCR) with subsequent assessment of the levels of threshold amplification cycles (cycle threshold, Ct). Exclusion criteria: disagreement of legal guardians of patients to participate in the study; severe somatic diseases in the decompensation stage; detection of SARS-CoV-2 RNA in the upper respiratory tract by PCR.

Depending on the severity of the condition, The patients were admitted to a 24-hour or day hospital. Upon admission, anamnestic data was collected, including the data of medical documentation of the outpatient stage (history of the child's development — form No. 112/U or an extract from it). During the examination, special attention was paid to assessing the presence and severity of lymphoproliferative syndromes typical of herpesvirus infection, namely: adenoiditis, tonsillitis, lymphadenopathy, hepatosplenomegaly.

On the first day of hospitalization, clinical and biochemical blood tests were performed to assess the level of C-reactive protein (CRP). To interpret the results of the laboratory examination, reference values of manufacturers of test systems were used, taking into account age characteristics. All patients underwent a whole blood examination using high-quality real-time PCR to detect HHV-6A/B DNA with an assessment of Ct level (kits "AmpliSens EBV/CMV/HHV6-screen-FL" (Central Research Institute of Epidemiology, Russia). The Ct level is the value at which the threshold line intersects the S-shaped signal accumulation curves in the test samples and control samples. Thus, this indicator indicates the number of amplification cycles required to start

detecting the virus DNA in the sample. A low Ct value indicates a significant amount of isolated viral DNA in the sample, which indicates a high viral load, while a high Ct value indicates a low viral load [17].

Statistical processing was carried out using Microsoft Excel modules, the StatSoft Statistica 7.0 software package. Using a training sample, a model was built for the dependence of the patient's belonging to one of two groups according to the value of factors in various combinations, where 1 is the latent form of HHV-6A/B infection (n = 89), 2 is the active form of HHV-6A/B infection (n = 23). The group of active infection included children with sudden exanthema caused by laboratory-confirmed HHV-6A/V [18–20]. 27 anamnestic, clinical and paraclinical signs were considered as potential predictors in the initial training model. The discriminant model was constructed using the step-by-step inclusion of predictors using the Fisher F-criterion (the value of the F–criterion is 4.0, the lower limit of tolerance is 0.01). The significance level $p < 0.05$ was used for all types of statistical analysis.

RESULTS OF THE STUDY

In order to improve the accuracy and timeliness of diagnosis based on a comprehensive clinical and laboratory examination, including a PCR study, a predictive model using discriminant analysis was developed. Of the 27 studied features, 4 parameters were identified as demonstrating the greatest statistically significant differences between the groups — $p < 0.001$ (Table 1).

The obtained model of DD of latent and active forms of HHV-6A/B infection in children demonstrated high statistical significance ($p < 0.001$) and classificatory ability at the level of 93.75%. The model, which takes into account such parameters as severity of fever, the presence of a cough, the absolute number of neutrophils and the Ct DNA level of HHV-6A/B, has high sensitivity (91.3%) and specificity (94.4%).

On this basis, a diagnosis can be carried out as follows. When seeking medical help for a child with a suspected active form of HHV-6A/ B infection (fever, catarrhal and lymphoproliferative syndromes, clinical manifestations of infectious mononucleosis, the presence of RRD), a clinical blood test is performed on an automated hematology analyzer with an assessment of the absolute value of neutrophils, a whole blood study by PCR with Ct DNA determination of HHV-6A/V. The obtained data of predictor features are used for calculations using formulas (1, 2) of the linear discriminant function (LDF):

LDF1 (the latent form of HHV-6A/B infection): (1)

$$42.7 \times X1 - 49.2 \times X2 - 6.2 \times X3 + 5.2 \times X4 - 865,$$

LDF2 (the active form of HHV-6A/B infection): (2)

$$45.1 \times X1 - 53 \times X2 - 6.7 \times X3 + 4.7 \times X4 - 940,$$

where X1 — the maximum severity of fever, °C;
X2 — the presence of a cough: no — 0, yes — 1;
X3 — absolute neutrophil count, $\times 10^9$/L;
X4 — threshold cycle of HHV-6A/B DNA amplification.

The obtained values of LDF1 and LDF2 are compared as follows: if LDF1 is greater than LDF2, the latent form of HHV-6A /B infection is diagnosed; with LDF2 more than LDF1, the active form is diagnosed.

A classification of the test sample (n = 40) was performed. Discriminant analysis successfully identified 8 out of 10 cases of the active form of HHV-6A/B infection and 29 out of 30 cases of latent infection. The total percentage of correct diagnoses was 92.5%, which is comparable to the results in the training sample. The patent for invention No. 2817089 dated 09/04/2024 was obtained [21].

For a better understanding of the proposed model, we present our own clinical observation.

Clinical case No. 1

The girl Ksenia, 8 years and 2 months old, was admitted to the Children's Scientific and Clinical Center for Infectious Diseases of the Federal Medical and Biological Agency on a planned basis due to RRD accompanied by febrile fever, for examination and selection of therapy. The child has a history of Schinz disease, atopic dermatitis. The epidemiological history is not burdened. Upon admission, condition satisfactory, body temperature falling within the normal range (the value of the predictor X1 is "36.5"). Skin of normal color, moist, without an infectious rash. Rhinitis and cough absent (the value of the predictor X2 is "0"). Pharynx calm, tonsils not enlarged, no plaque. Peripheral lymph nodes not enlarged. Heart tones clear, rhythmic. Vesicular breathing carried out in all parts of the lungs; no wheezing heard. Abdomen soft, painless; liver and spleen not enlarged. Diuresis preserved. Following a clinical blood test, all parameters within the reference values (the value of the predictor X3 (absolute neutrophil count) is "3.35"). No

Table 1. List of predictors, coefficient values and their significance level

No.	Name and gradation of predictors	Code	LDF1 (latent form of HHV-6A/B infection)	LDF2 (active form of HHV-6A/B infection)	*p* value
1	The maximum severity of fever, °C	X1	42.7	45.1	<0.001
2	The presence of a cough: 0 — no; 1 — yes	X2	-49.2	-53	<0.001
3	Absolute neutrophil count, *10^9/L	X3	-6.2	-6.7	<0.001
4	Threshold cycle of HHV-6A/B DNA amplification	X4	5.2	4.7	<0.001
5	Constant	-	-865	-940	-

Table prepared by the authors using their own data

inflammatory changes detected in the general urine analysis. An increase in normobiota was observed in the crops of the discharge from the nasopharynx and oropharynx to the microflora. Taking into account the anamnestic data, in order to exclude reactivation of herpesviruses, high-quality whole blood PCR for HHV-6A/B DNA, Epstein-Barr virus and cytomegalovirus was performed by PCR: HHV-6A/B DNA was detected, Ct value (predictor X4) — 31. When examining blood by ELISA for specific antibodies of the IgM class, IgG to herpesviruses, the following results were obtained: IgG to cytomegalovirus (CMV) detected. IgM antibodies to CMV, IgG antibodies to the nuclear and capsid antigens of EBV, HHV-6A/B not detected. Given the positive result of PCR on HHV-6A/B DNA, final clinical diagnosis was interpreted as persistent HHV-6A/B infection in the activation stage. The child was prescribed immunotropic therapy with antiviral action consisting of meglumine acridonacetate according to the manufacturer's instructions in a course of 23 days.

The calculation was performed retrospectively using the formulas:

$$LDF1 = 42.7\times36.5 - 49.2\times0 - 6.2\times3.35 + 5.2\times31 - 865 = 834.98$$

$$LDF2 = 45.1\times36.5 - 53\times0 - 6.7\times3.35+4.7\times31 - 940 = 829.41$$

Since LDF1 > LDF2, a 94.4% probability of a latent form of HHV-6A/B infection was pronounced.

This case demonstrates that, according to the proposed discriminant model, the probability of an active form of HHV-6A/B infection was extremely low (5.6%); on this basis, it was possible to avoid a long course of immunotropic therapy.

DISCUSSION

The existing problem of overdiagnosis of the active form of HHV-6A/B infection is related to the interpretation of the results of high-quality PCR of whole blood without taking into account the possible latency of the virus in mononuclear cells. Despite their unsuitability in most cases, the detection of HHV-6A/B DNA generally leads to the prescription of long-term repeated courses of immunotropic therapy. Thus, the developed prognostic model using discriminant analysis based on a comprehensive assessment of clinical and laboratory parameters solves the problem of DD of active and latent forms of HHV-6A/B infection in children with lymphoproliferative and respiratory syndromes.

Utkin et al. proposed a method for identifying infectious mononucleosis associated with human betaherpesvirus 6A/B. The invention takes into account such biomarkers as AVEN mRNA, CHUK transcript 2, CIRBP transcript 2, TRAF3 transcript 2 and IRAK4 transcript 10. Although the method is extremely interesting from the point of view of studying the molecular mechanisms of pathogenesis, its disadvantages include the assessment of infection activity in relation to only one nosological form (infectious mononucleosis), inaccessibility of implementation in practical healthcare with a large flow of patients, lack of technical equipment of laboratories and trained personnel necessary for the study of genes and transcripts, as well as high financial costs and difficulty in interpreting the obtained results [22].

As a solution of this problem, Melekhina et al. developed a method for identifying the indications for antiherpetic therapy of HHV-6A/B infection in children with acute respiratory diseases. The active form of infection, which requires the prescription of antiviral therapy, is established when more than 100 copies of the of HHV-6A/B DNA/10^5 cells are detected in the blood by quantitative PCR. The proposed method is characterized by its speed of execution and adequate approach to the obtained results taking into account different levels of viral load, as well as its convenience in the presence of quantitative PCR — which, however, is not an affordable diagnostic method at all levels of medical care [23].

It is possible to use reverse transcription PCR to differentiate the active and latent forms of HHV-6A/B infection. This method is characterized by its higher sensitivity and specificity than culture-based studies. The determination of the form of infection depends on the detected matrix RNA of viral proteins: the open reading frames U42, U22, U38, U100 indicate an active form of infection, while U94, conversely, indicates a latent infection [20]. Thus, the method is promising, but currently unavailable in practice.

Our described model offers additional advantages such as simplicity, accessibility, speed of execution, as well as the possibility of providing DD of active and latent forms of HHV-6A/B infection without involving additional financial costs for expensive laboratory tests. The uniqueness of the method is confirmed by the patent for the invention.

CONCLUSIONS

The developed prognostic model can be applied in clinical practice for the diagnosis of active and latent forms of HHV-6A/B infection in children with catarrhal, lymphoproliferative syndromes when HHV-6A/B DNA is detected in whole blood, as well as to justify the appointment of immunotropic therapy with antiviral action. When establishing the latent form of HHV-6A/B infection, it is necessary to conduct a further diagnostic search to exclude autoinflammatory diseases accompanied by an appropriate symptom complex or the active form of infectious mononucleosis of mono– and combined herpesvirus etiology along with lesions of organs and systems associated with viral infection.

References

1. Melekhina EV, Gorelov AV. Infection caused by human herpesvirus 6a/b in children (clinical and pathogenetic aspects, diagnosis and therapy). M.: «Dynasty», 2023 (in Russ.). EDN: DIEEDC
2. Efremov DO, Gerasimova OA, Kozlov KV, Gabdrakhmanov IA, Zhdanov KV. Cytomegalovirus infection in patients after orthotopic liver transplantation (clinical report). *Journal Infectology*. 2019;11(4):148–52 (In Russ.). https://doi.org/10.22625/2072-6732-2019-11-4-148-152
3. Antonova TV, Pobegalova OE, Gorchakova OV, Zubarovskaya LS, Yudinceva OS, Lioznov DA. Reactivation of cytomegalovirus, human herpes virus, and Epstein-Barr virus infections after hematopoietic stem cell transplantation in children. *Journal Infectology*. 2023;15(4):62–9 (In Russ.). https://doi.org/10.22625/2072-6732-2023-15-4-62-69
4. National report. On the state of sanitary and epidemiological well-being of the population in the Russian Federation in 2023. Moscow: Federal Service for the Oversight of Consumer Protection and Welfare; 2024 (In Russ.)
5. Savenkova MS, Sotnikov IA, Afanas'eva AA, Afanas'eva YaV, Dushkin RV. Savenkova MS, Sotnikov IA, Afanasieva AA, et al. Importance of herpes viruses in children with post-COVID conditions. *Russian Journal of Woman and Child Health*. 2023;6(1):39–44 (in Russ.). https://doi.org/10.32364/2618-8430-2023-6-1-39-44
6. Melekhina EV, Muzyka AD, Ponezheva ZhB, Gorelov AV. Herpesvirus infections in the works of the Clinical Department of Infectious Pathology, Central Research Institute of Epidemiology, Russian Federal Service for Supervision of Consumer Rights Protection and Human Well-Being. *Epidemiology and Infectious Diseases. Current Items*. 2023;13(2):45–50 (In Russ.). https://doi.org/10.18565/epidem.2023.13.2.45-50
7. Salahuddin SZ, Ablashi DV, Markham PD, Josephs SF, Sturzenegger S, Kaplan M, et al. Isolation of a new virus, HBLV, in patients with lymphoproliferative disorders. *Science*. 1986;234(4776):596–601. https://doi.org/10.1126/science.2876520
8. King O, Khalili YAI. Herpes Virus Type 6 [*Internet*]. *StatPearls*. 2023 [cited 2024 Jun 17].
9. Balakrishna JP, Bhavsar T, Nicolae A, Raffled M, Jaffe ES, Pittaluga S. Human Herpes Virus 6 (HHV-6)-associated Lymphadenitis: Pitfalls in Diagnosis in Benign and Malignant Settings. *The American Journal of Surgical Pathology*. 2018;42(10):1402–8. https://doi.org/10.1097/pas.0000000000001121
10. Chen X, Li H, Wu C, Zhang Y. Epstein–Barr virus and human herpesvirus 6 infection in patients with systemic lupus erythematosus. *Virology Journal*. 2023;20(1):e29. https://doi.org/10.1186/s12985-023-01987-3
11. Eliassen E, Krueger G, Luppi M, Ablashi D. Lymphoproliferative Syndromes Associated with Human Herpesvirus-6A and Human Herpesvirus-6B. *Mediterranean Journal of Hematology and Infectious Diseases*. 2018;10(1):e2018035. https://doi.org/10.4084/mjhid.2018.035
12. Sultanova A, Cistjakovs M, Sokolovska L, Cunskis E, Murovska M. Investigation of the Involvement of HHV-6 Encoded Viral Chemokine Receptors in Autoimmune Thyroiditis Development. *Microbiology Spectrum*. 2022;10(3):e0236921. https://doi.org/10.1128/spectrum.02369-21
13. Weider T, Genoni A, Broccolo F, Paulsen TH, Dahl-Jorgensen A, Tonioli A, et al. High Prevalence of Common Human Viruses in Thyroid Tissue. *Frontiers in Endocrinology*. 2022;13:e938633. https://doi.org/10.3389/fendo.2022.938633
14. Al-Sadeq DW, Zedan HT, Aldewik N, Elkhider A, Hicazi A, Younes A et al. Human herpes simplex virus-6 (HHV-6) detection and seroprevalence among Qatari nationals and immigrants residing in Qatar. *International journal of infectious diseases regions*. 2022;2:90–5. https://doi.org/10.1016/j.ijregi.2021.12.005
15. Isakov VA, Isakov DV, Stukolkina NE Vozmozhnosti terapii respiratornykh infektsiy u chasto boleyushchikh patsientov. *Clinical pharmacology and therapy*. 2018;2:56–63 (In Russ.). EDN: XYLEBF
16. Levina AS, Babachenko IV. Persistent infection in frequent and prolonged ill children, possibilities of etiopathogenetic therapy. *Children infections*. 2014;13(4):41–5 (In Russ.). EDN: TDUUIJ
17. Instructions for the use of a set of reagents for the detection and quantification of herpes virus type 6 (HHV6) DNA in clinical material by polymerase chain reaction (PCR) with hybridization-fluorescence detection "AmpliSens-HHV6-screen-titer-FL". Approved by the order №2352-Pr/12 of Roszdravnadzor from 05/15/2012 [Internet] [cited 2024 Jun 17]. Available from: https://www.amplisens.ru/upload/iblock/6c8/HHV6-skrin-titr-FL.pdf/ (In Russ.).
18. Bonnafous P, Marlet J, Bouvet D, Salame E, Tellier A-C, Guyetant S, et al. Fatal outcome after reactivation of inherited chromosomally integrated HHV-6A (iciHHV-6A) transmitted through liver transplantation. *American Journal of Transplantation*. 2018;18(6):1548–51. https://doi.org/10.1111/ajt.14657
19. Petit V, Bonnafous P, Fages V, Gautheret-Dejean A, Engelmann I, Baras A et al. Donor-to-recipient transmission and reactivation in a kidney transplant recipient of an inherited chromosomally integrated HHV-6A: Evidence and outcomes. *American Journal of Transplantation*. 2020;20(12):3667–72. https://doi.org/10.1111/ajt.16067
20. Realegeno S, Pandey U. Human Herpesvirus 6 Infection and Diagnostics. *Clinical Microbiology Newsletter*. 2022;44(9):83–90. https://doi.org/10.1016/j.clinmicnews.2022.04.005
21. Tian NS, Babachenko IV, Goleva OV, Skripchenko NV, Grigorev SG. A method for differential diagnosis of latent and active forms of HCV-6 infection in children. Patent of Russian Federation № 2817089. 2024 (In Russ.). EDN: BLXOKL
22. Utkin OV, Filatova EN, Sakharnov NA., Knyazev DI. A method for identifying infectious mononucleosis associated with human herpes virus type 6. Patent of Russian Federation № 2729413.2019 (In Russ.). EDN: OSLTPN
23. Melekhina EV, Muzyka AD, Petukhova EV, Chugunova OL, Gorelov AV, Shipulina OYu. Sposob opredeleniya pokazaniy k provedeniyu protivogerpeticheskoy terapii pri infektsii VGCh-6 u detey s ostrymi respiratornymi zabolevaniyami. Patent of the Russian Federation № 2641609. 2017 (In Russ.). EDN: FHNKDX

Authors' contributions. All the authors confirm that they meet the ICMJE criteria for authorship. The most significant contributions were as follows: Natalia S. Tian — formation of an idea, participation in scientific design, collection of clinical and anamnestic, paraclinical data, creation of a database, drafting of a manuscript, statistical data processing, approval of the final version; Irina V. Babachenko — formation of the idea, research objectives, development of methodology, approval of the final version; Olga V. Goleva — formation of the idea, research objectives, development of methodology, laboratory research, approval of the final version; Lyudmila I. Zhelezova — development of methodology, laboratory research, approval of the final version; Elena V. Baziyan — provision of biomaterials of patients, laboratory tests, approval of the final version; Oleg S. Glotov — formation of the idea, research objectives, development of methodology, approval of the final version.

AUTHORS

Natalia S. Tian
https://orcid.org/0000-0002-9799-5280
tiannatalia94@yandex.ru

Irina V. Babachenko, Dr. Sci. (Med.), prof.
https://orcid.org/0000-0002-1159-0515
babachenko-doc@mail.ru

Olga V. Goleva, Cand. Sci. (Biol.)
https://orcid.org/0000-0003-3285-9699
golev.ao@mail.ru

Lyudmila I. Zhelezova, Cand. Sci. (Med.)
https://orcid.org/0000-0001-8071-3243
Ludabac@list.ru

Elena V. Baziyan
https://orcid.org/0000-0001-7837-3315
waz2107gen@yandex.ru

Oleg S. Glotov, Dr. Sci. (Biol.),
https://orcid.org/0000-0002-0091-2224
olglotov@mail.ru

https://doi.org/10.47183/mes.2024-26-3-98-105

A MODERN APPROACH TO MICROSURGICAL ELIMINATION OF TONGUE DEFECTS USING COMPUTER DIGITAL PLANNING

Arbak A. Khachatryan[1]✉, David N. Nazarian[1], Mikhail M. Chernenkiy[1], Victoria O. Dzhuganova[1], Alexander V. Fedosov[1], Georgiy K. Zakharov[1], Maksim B. Potapov[1], Olga I. Danishuk[2], Ekaterina V. Osipenko[1], Eugenia I. Micheeva[1]

[1] National Medical Research Center for Otolaryngology of the Federal Medical Biological Agency, Moscow, Russia

[2] Federal Clinical Center for High Medical Technologies of the Federal Medical Biological Agency, Moscow, Russia

Introduction. The treatment of malignant neoplasms of the oral mucosa implies a combined treatment, whose first stage generally involves surgery. However, the most common non-personalized surgical methods are based on resection of the tongue, often affecting more than half of the organ, which can lead to significant functional deficiency and disability of patients.

Objective. To demonstrate the possibility of tongue defect reconstruction using preoperative computer 3D planning through clinical cases.

Materials and methods. From 2021 to 2024, four patients with primary cancer of the lateral surface of the tongue were operated on using this methodology at the Maxillofacial Surgery Department of the NMICO FMBA of Russia. All patients underwent hemiglossectomy and preventive cervical lymphadenectomy on the affected side, with simultaneous reconstruction of the tongue using a radial forearm flap. The average age of the patients was 53 years; males outnumbered females by a ratio of 3:1. Patients presented with stages rT1-rT4; histological examination revealed no regional lymph node involvement (N0) in any patient. Preoperative instrumental examinations included: magnetic resonance imaging (MRI) of the soft tissues of the maxillofacial area with contrast enhancement; multislice computed tomography (MSCT) of the maxillofacial area with contrast enhancement; MSCT of the donor area (forearm) with contrast enhancement; Doppler ultrasound of the brachiocephalic trunk vessels and donor area vessels; transnasal endoscopic laryngoscopy with swallowing tests (three-swallow test) with video recording. All patients were surveyed preoperatively and postoperatively using EORT QLQ — H&N35, EORT QLQ — C30, FACT — H&N, MD Anderson, and VHI-10 questionnaires. Patients with abundant hair in the donor area underwent laser hair removal prior to hospitalization. After performing computer simulation of the surgical intervention using Slicer and Blender software, templates were printed on a Elegoo Saturn 2 printer. Assessment of speech and swallowing functions was carried out by a speech therapist specializing in these areas using the Pokrovsky protocol and Vospector-DSI software at both preoperative and postoperative stages. The attending physician performed anthropophotometry and video recording of patient complaints and speech at all stages of care. The postoperative period was without complications; nasogastric tubes were removed on the 12th day; the average hospital stay was 14 days.

Results. The flap survival rate was 100% across the entire series of observations. Oncological radicality was achieved at R0 for all patients. The average duration of the surgical intervention was 288 minutes. In three patients, the acoustic parameters of speech were within normal limits (in one patient, this parameter could not be assessed due to systemic speech underdevelopment caused by hearing impairment). The average syllable intelligibility coefficient according to Pokrovsky was 88%. All patients adapted to their usual diet and continued their professional activities. According to the results of the EORT QLQ — H&N35, EORT QLQ — C30, and FACT — H&N questionnaires, patients rated their quality of life as good in one case and excellent in three cases.

Conclusions. The developed algorithm for preoperative computer planning is promising. The use of surgical templates allowed for adequate oncological radicality, synchronized the simultaneous work of two surgical teams, reduced the duration of anesthetic assistance (with an average surgical intervention time of 288 minutes), and achieved good functional and aesthetic results. However, this methodology requires further refinement in a larger group of patients.

Keywords: tongue cancer; hemiglossectomy; microsurgery; radial flap; free flap; 3D reconstruction; tongue reconstruction; 3D printer

For citation: Khachatryan A.A., Nazaryan D.N., Chernenky M.M., Dzhuganova V.O., Fedosov A.V., Zakharov G.K., Potapov M.B., Danischuk O.I., Osipenko E.V., Mikheeva E.I. Modern approach in microsurgical elimination of tongue defects using computerized digital planning. *Extreme Medicine*. 2024;26(3):98–105. https://doi.org/10.47183/mes.2024-26-3-98-105

Funding: the study was performed without any sponsor support.

Compliance with ethical principles: the study was conducted in accordance with the Declaration of Helsinki "Ethical Principles of Medical Research Involving Human Subjects" of 1964 (ed. 2008). All patients signed a voluntary informed consent for the study.

Potential conflict of interest: the authors declare no conflict of interest.

✉ Arbak A. Khachatryan drarbak@yandex.ru

Received: 6 Aug. 2024 **Revised:** 3 Oct. 2024 **Accepted:** 3 Oct. 2024

СОВРЕМЕННЫЙ ПОДХОД В МИКРОХИРУРГИЧЕСКОМ УСТРАНЕНИИ ДЕФЕКТОВ ЯЗЫКА С ПРИМЕНЕНИЕМ КОМПЬЮТЕРНОГО ЦИФРОВОГО ПЛАНИРОВАНИЯ

А.А. Хачатрян[1]✉, Д.Н. Назарян[1], М.М. Черненький[1], В.О. Джуганова[1], А.В. Федосов[1], Г.К. Захаров[1], М.Б. Потапов[1], О.И. Данищук[2], Е.В. Осипенко[1], Е.И. Михеева[1]

[1] Национальный медицинский исследовательский центр оториноларингологии Федерального медико-биологического агентства, Москва, Россия

[2] Федеральный клинический центр высоких медицинских технологий Федерального медико-биологического агентства, Москва, Россия

Введение. Принцип лечения злокачественных новообразований слизистой оболочки ротовой полости подразумевает комбинированное лечение, первым этапом которого является хирургический метод. Большинство хирургических методов не являются персонализированными и основаны на резекции языка, затрагивающей больше половины органа, что приводит к существенному функциональному дефициту и инвалидизации пациентов.

Цель. На серии клинических случаев продемонстрировать возможность устранения дефектов языка с применением предоперационного компьютерного 3D-планирования.

Материалы и методы. За период с 2021 по 2024 г. в условиях отделения ЧЛХ ФГБУ НМИЦО ФМБА России с применением компьютерного цифрового 3D-планирования были прооперированы 4 пациента (3 мужчин и 1 женщина) с первичным раком боковой поверхности языка. Средний возраст больных составил 53 года. Средний период наблюдения 14 мес, за период наблюдения ни у одного пациента не было отмечено продол-

женного роста или рецидива новообразования. Пациенты были представлены со стадиями pT1–pT4, без поражения регионарных лимфатических узлов (N0). Пациентам на предоперационном этапе проведены инструментальные и клинико-лабораторные исследования по стандартизированному протоколу. Для оценки эффективности лечения и качества жизни все пациенты на предоперационном и постоперационном этапах были анкетированы по опросникам Европейской организации по исследованию и лечению рака головы и шеи.
Компьютерное моделирование оперативного вмешательства осуществлялось в программах Slicer и Blender, печать шаблонов выполнялась на 3D-принтере Elegoo Saturn 2. Произведена оценка функций речи и глотания с использованием протокола Покровского и программного обеспечения Vospector-DSI на предоперационном и постоперационном этапах. Лечащим врачом проводились антропофотометрия и видеофиксация речи пациентов и их жалоб на всех этапах курации.
Результаты. Всем пациентам была выполнена гемиглоссэктомия и профилактическая шейная лимфодиссекция на стороне поражения с одномоментной реконструкцией языка лучевым лоскутом предплечья с использованием предоперационного компьютерного 3D-планирования. Выживаемость лоскутов составила 100% во всей серии наблюдений. Онкологическая радикальность у всех пациентов была обеспечена R0. Среднее время оперативного вмешательства составило 288 мин. Постоперационный период проходил без осложнений, средний период пребывания пациентов в стационаре составил 14 сут, отдаленный период наблюдения — от 6 до 20 мес. У всех пациентов достигнут хороший эстетический результат, акустические параметры речи в пределах нормальных значений, средний коэффициент слоговой разборчивости речи по Покровскому составил 88%. Все пациенты были адаптированы к своей привычной диете и профессиональной деятельности без ограничений. По результатам опросников Европейской организации по исследованию и лечению рака головы и шеи (European organization for research and treatment of cancer (EORTC) quality of life questionnaires for head and neck module (QLQ-H&N35), European Organization for Research and Treatment of Cancer Quality of Life Questionnaire) пациенты оценили качество своей жизни после оперативного лечения как хорошее в трех случаях и отличное в одном случае.
Выводы. Использованный нами алгоритм предоперационного компьютерного 3D-планирования является перспективным. Применение операционных шаблонов позволило достичь адекватной онкологической радикальности, синхронизировать работу двух хирургических бригад, сократить время анестезиологического пособия (среднее время оперативного вмешательства 288 мин) и достичь оптимальных функциональных и эстетических результатов. Ввиду подвижности языка и изменчивости его формы требуется создание новых протоколов предоперационной инструментальной диагностики для стандартизации положения языка в ротовой полости. Данная методика требует дальнейшего совершенствования на большей группе пациентов.

Ключевые слова: рак языка; гемиглоссэктомия; микрохирургия; лучевой лоскут; свободный лоскут; 3D-реконструкция; реконструкция языка; 3D-принтер

Для цитирования: Хачатрян А.А., Назарян Д.Н., Черненький М.М., Джуганова В.О., Федосов А.В., Захаров Г.К., Потапов М.Б., Данищук О.И., Осипенко Е.В., Михеева Е.И. Современный подход в микрохирургическом устранении дефектов языка с применением компьютерного цифрового планирования. *Медицина экстремальных ситуаций*. 2024;26(3):98–105. https://doi.org/10.47183/mes.2024-26-3-98-105

Финансирование: исследование выполнено без спонсорской поддержки.

Соответствие принципам этики: исследование проведено в соответствии с Хельсинкской декларацией «Этические принципы медицинских исследований с участием человека в качестве испытуемого» от 1964 г. (ред. 2008 г.). Всеми пациентами подписано добровольное информированное согласие на исследование.

Потенциальный конфликт интересов: авторы заявляют об отсутствии конфликта интересов.

✉ Хачатрян Арбак Арманович drarbak@yandex.ru

Статья поступила: 06.08.2024 **После доработки:** 03.10.2024 **Принята к публикации:** 03.10.2024

INTRODUCTION

Malignant neoplasms (MN) of the head and neck occupy the sixth place in the structure of general oncologic morbidity; in 90% of cases, MNs are presented by squamous cell cancer. Of cancers in the head and neck region, oral cancer is the most commonly occurring malignant neoplasm. The leading localization of all tumor formations of the oral cavity in 60% of cases is the tongue with the same frequency of lesions of both the right and left halves of the tongue [1-3]. In the structure of oncologic diseases in the period 2013–2020 in Russia, the incidence of oral mucosal tumors amounted to about 1.9% according to different sources [4].

One of the main approaches for the treatment of malignant neoplasms of the oral mucosa at the first stage involves surgery. However, resection of even a part of the tongue significantly affects processes of swallowing and speech formation, resulting in a functional reduction in quality of life [5–10]. The current state of the art in the treatment of patients with tongue defects involves the use of free revascularized flaps on microvascular anastomoses [5, 10, 11].

In 1981, Yang described a method of using radial fasciocutaneous forearm flap to repair defects in various areas of the human body. This method has steadily taken its place in the arsenal of reconstructive surgeons. A flap is a thin plastic material with a permanent vascular anatomy and a long vascular pedicle. In tongue reconstruction, the flap is used for defects that form following hemiglossectomies; in order to increase its volume, it can be provided with an additional amount of adipose tissue harvested from the patient's forearm. Moreover, sensitive reinnervation of the flap can be accomplished at the expense of the forearm cutaneous nerve [12].

Many techniques for cutting a forearm cutaneous fascial flap (bilobed flap) and adapting the flap to the defect edges have been described [13]. However, these methods cannot be called personalized due to the impossibility of subjecting them to mathematical analysis and obtaining adequate information about the required flap parameters. The use of digital technologies in reconstructive surgery of the tongue makes it possible to obtain a predictable and standardized result, contributing to the reduction of the operative time of intervention due to the possibility of simultaneous work of two teams [14].

The use of intraoperatively cut resection 2D-templates, most often on paper, when planning soft tissue autografts, has its disadvantages, including the impossibility of designing the template in advance due to the template's creation following excision of the tumor mass and visualization of the tongue defect based only on the visual control of the surgeon. This moment causes prolongation of anesthesiologic and surgical aids due to the impossibility of simultaneous work of two surgical teams. Another disadvantage of the 2D technique is also due to a lack of information at the preoperative stage about the planned volume of tongue resection and tumor size. This is due to the impossibility of assessing the subsequent loss of tongue volume associated with radiation therapy and/or flap atrophy prior to surgical intervention [15–16]. To solve this problem, we tested the proposed method of tongue defect repair with a soft tissue flap in cancer patients requiring tongue resection. The approach involves one-stage tongue reconstruction based on 3D computer planning and creation of resection templates. Scientific novelty is confirmed by the Russian patent for invention No.2024104882 "Method of tongue defects elimination after partial glossectomy", published on 07/04/2024.

The study purpose was to demonstrate on a series of clinical cases the possibility of tongue defect repair using preoperative computerized 3D planning.

MATERIALS AND METHODS

From 2021 to 2024, 4 patients (three men and one woman) diagnosed with primary cancer of tongue lateral surface were operated on at the Maxillofacial Surgery Department of the "National Medical Research Center for Otorhinolaryngology of the Federal Medical and Biological Agency" using a microsurgical tongue defect repair technique based on 3D computerized digital planning. Patients were presented with stages of tumor process development pT1-pT4a, without regional lymph node involvement (N0), confirmed by the results of histological examination. The average age of the patients was 53 years. All patients underwent hemiglossectomy and preventive lymphodissection on the side of the lesion with one-stage reconstruction of the tongue with a radial forearm flap. The patients' summary data are shown in Table 1.

Instrumental methods of research at the preoperative stage included:

- magnetic resonance imaging of soft tissues of the maxillofacial region with contrast enhancement (MRI of the maxillofacial region with contrast) to clarify the stage of the process according to the T-criterion (international classification of oncological tumors) and assess the spread of the tumor process in the tissues of the tongue;

Table 1. Summary data of patients

Patient data	Patients			
	1	2	3	4
Gender	Male	Male	Male	Female
Age, years	40	50	50	70
Location of tumor	Right lateral surface of the tongue	Left lateral surface of the tongue	Right lateral surface of the tongue, root of the tongue	Right lateral surface of the tongue
Stage of tumor process according to TNM*	pT2N0M0	pT2N0M0	pT4aN0M0	pT1N0M0
Resection feature	Resection of the right lateral surface of the tongue with preservation of the tongue tip and root	Resection of the left lateral surface of the tongue with preservation of the tongue tip and root	Resection of the right lateral surface, tip and root of the tongue	Resection of the right lateral surface of the tongue with preservation of the tongue tip and root
Percentage of resected volume from tongue volume, %	40	40	60	40
Flap dimensions length/width, mm	50/40	57/72	71/65	60/40
The timing of flap collection, min	125	115	90	130
Resection time, min	80	92	97	82
Time of surgical intervention, min	310	270	295	280
Hospitalization time, days in hospital	13	14	15	14
Period of nasogastric tube removal, days	12	12	12	12
Pokrovsky index, %	93	_	73	95
Postoperative complications	Venous stasis of the flap	no	no	no
Observation period, months	21	16	16	6
Oncologic status	Relapse-free course	Relapse-free course	Relapse-free course	Relapse-free course
Patient/s status at the moment of article publication	alive	alive	alive	alive
Self-questionnaire quality of life assessment (1 to 7 points)	6 (good)	6 (good)	6 (good)	7 (excellent)

Table prepared by the authors using their own data

Note: * — TNM (international classification of oncological tumors, where T — tumor, the prevalence of the primary tumor, N (nodus) the presence, absence and advance of metastases in regional lymph nodes, M (detached metastases), the presence or absence of detached metastases.

- multispiral computed tomography of the maxillofacial region with contrast enhancement to select recipient vessels;
- determination of the vascular flow of the external carotid artery basin and exclusion of intravascular pathologies (occlusion, thrombosis);
- multispiral computed tomography of the donor area (forearm) with contrast enhancement (MSCT with contrast enhancement) to take into account the diameter of the main trunk vessels, to detect anomalies of the vascular channel and anatomical features of the vessels;
- Doppler ultrasound of the brachiocephalic trunk vessels and vessels of the donor area.

To select the donor area (upper extremity of the forearm), a clinical assessment of arterial patency and collateral blood supply of the hand by Allen test was performed. To assess swallowing function, transnasal endoscopic laryngoscopy with swallowing tests (three-glottic test) with video recording was performed in all patients.

All patients at the preoperative and postoperative stages were surveyed using quality of life questionnaires recommended by the European Organization for Research and Treatment of Cancer (EORTC) for head and neck module (QLQ-H&N35), (EORTC Quality of Life Questionnaire). The questionnaire additionally included MD Anderson and Voice Handicap Index (VHI-10) scales, which have higher specificity for patients treated for oropharyngeal cancer. The questionnaires were administered at prehospital and at each follow-up visit after 1, 3, 6, and 12 months. Patients with abundant hair in the donor area underwent laser hair removal at the prehospital stage. Speech and swallowing functions were assessed by a staff phoniatrician (speech and swallowing specialist) using the Pokrovsky protocol and Vospector-DSI software at the preoperative and postoperative stages [19]. The attending physician performed anthropophotometry and video recording of patients' speech and complaints at all stages of the curation. Treatment tactics for all patients were determined at the oncologic consilium on the basis of the A.I. Burnazyan Federal Medical Biophysical Center.

Computer modeling of the surgical intervention was performed using Slicer and Blender software; the templates were printed on a Formlab 3 3D printer.

RESULTS

One week before the surgical intervention, computerized preoperative planning was carried out based on the data of the MSCTs of the maxillofacial region upper extremities, as well as the MRI of the maxillofacial region. For this purpose, tongue tissues were contoured slice-by-slice with a step of 5–7 slices.

Further on the basis of mathematical interpolation methods using Slicer and Blender software the selected volume of the formation was determined taking into account the indentation from the tumor borders of 1.5 cm to reach the edges of the resection borders R0. The obtained data were converted to surface area and adapted to the topography of the donor arm by placing the surface of the stencil template over the axial vessels (radial vessels) to incorporate them into the flap. The surface area of the flap was increased by 15% taking into account possible flap shrinkage after radiation therapy. Thus, two templates were made: a resection template for hemiglossectomy and a template for cutting the skin area of the radial flap (Fig. 1).

Following coordination of preoperative planning with the operating surgeons, the digital project in the form of an STL (stereolithographic) model was sent for printing on an Elegoo Saturn 2 3D printer. The average time of template printing was 40–50 min.

Surgical interventions were performed by two teams of surgeons according to the standard protocol. The first team of surgeons performed tongue tumor ablation using a resection template, cervical lymphodissection, and isolation of recipient vessels of the neck (Fig. 2).

Each patient underwent emergency intraoperative edge biopsy (6 preparations) of the resection, in all cases the resection edges were R0 (Fig. 3).

The second team of surgeons simultaneously isolated the radial flap using a template. The average time of the resection stage was 87 min. The average time of flap harvesting was about 115 min. Radial flap isolation in all cases was performed with inclusion of the radial artery and vena comitans, as well as the lateral cutaneous nerve of the forearm (Fig. 4). Following flap isolation, the vascular pedicle of the graft was cut off and the graft was moved into the oral cavity.

After affixing the skin site of the flap to the remaining part of the tongue with guiding sutures, the donor vessels were carried out in a tunnel formed in the soft tissues of the floor of the mouth, after which the microsurgical stage was performed. Anastomosing of the radial artery with the facial artery was performed in all cases according to the type of "end-to-end" anastomosis; similarly, vena comitans were anastomosed with the external jugular vein. At the

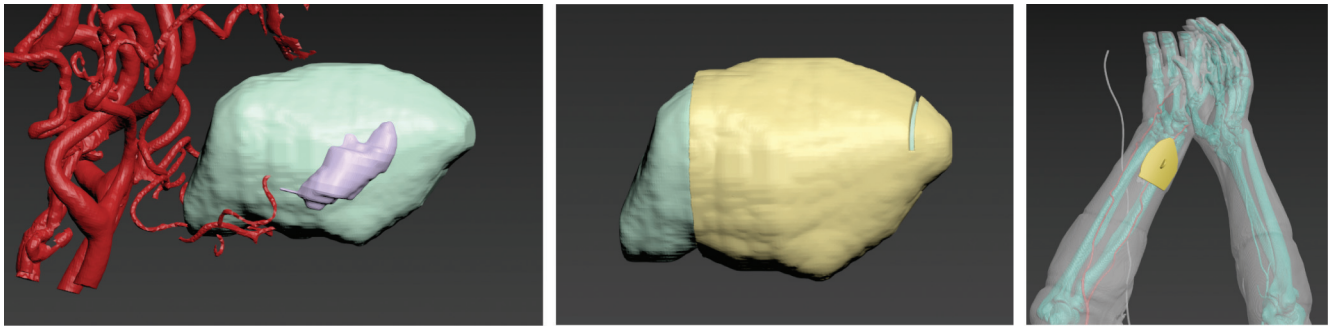

Figure prepared by the authors

Fig. 1. Preoperative 3D computer planning

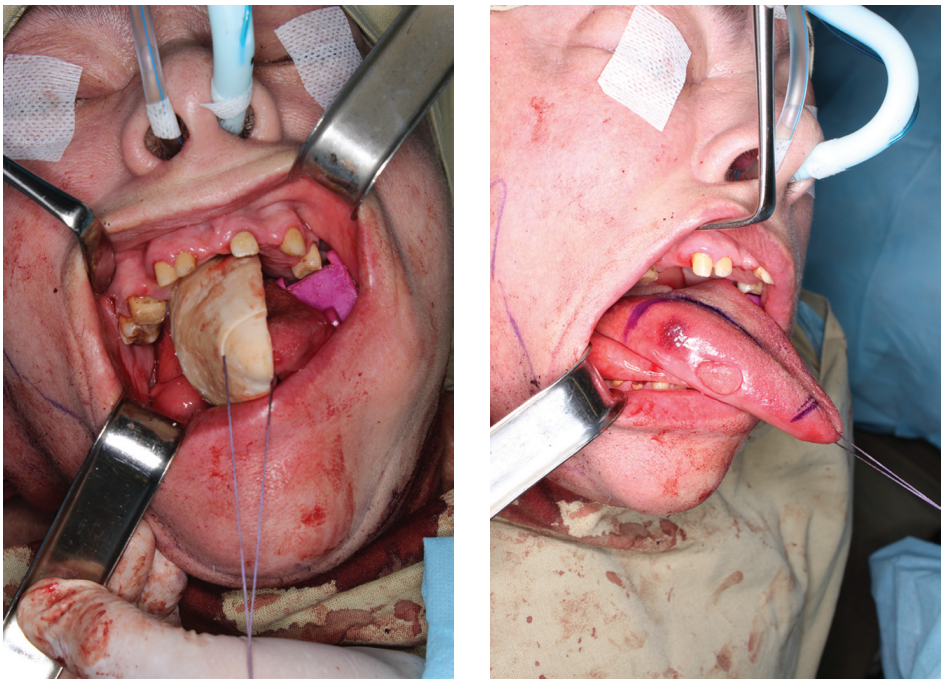

Figure prepared by the authors

Fig. 2. Marking the resection area using a resection template for visualizing a malignant neoplasm of the tongue affecting its lateral surface

final stage, neurorrhaphy of the lateral cutaneous nerve and lingual nerve was performed in two cases, while neurorrhaphy of the hyoid nerve (end-to-side type) was also carried out in two cases. The average time of the microsurgical stage was 45 min. After restarting the blood flow, the filling of the donor vessels was assessed visually and using a portable Doppler Minidop (Bioss). When the flap had been successfully adapted to the remaining part of the tongue with resorbable Vicryl 3.0 thread, layer-by-layer wound closure was performed (Fig. 5).

The postoperative period in most patients was uneventful. Only one patient had venous stasis of the flap 3 hours after the surgical intervention; in this case, a revision surgery with repeated venous anastomoses was performed. The postoperative period passed further in this patient without peculiarities. The nasogastric tube was removed in all patients on the 12th day; the average period of hospitalization was 14 days (Fig. 6).

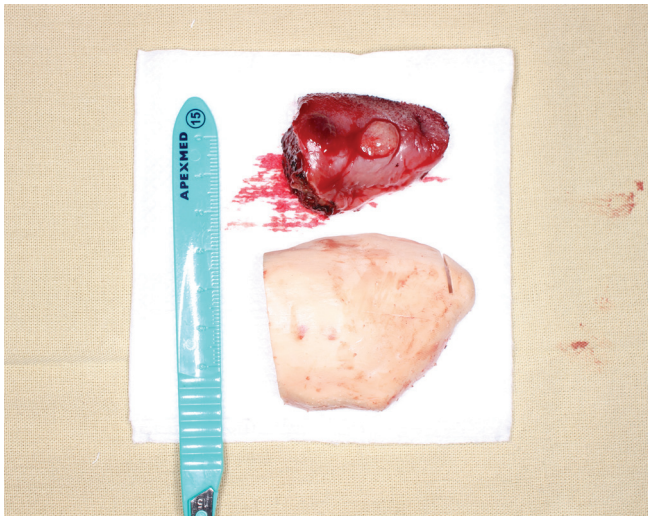

Figure prepared by the authors

Fig. 3. Removed tongue preparation

DISCUSSION

Computer modeling is widely used in reconstructive maxillofacial surgery to eliminate bone defects of the maxillofacial region to facilitate the performance of complex reconstructive surgeries with a predictable result. However, in the elimination of soft tissue defects of the maxillofacial region, the use of surgical templates remains poorly studied. The complexity of applying this technique and planning soft tissue autografts lies in the absence of stable supporting bone elements, as well as the need to not only restore the volume of tissues, but also to ensure their proper mobility [14].

The first use of resection templates — namely, resection 2D-templates in the planning of soft tissue autografts for replacing the deficit of tongue tissues — was first described by R.M. Baskin et al. [15].

It should be noted that the results of the application of computerized planning and template surgery for the elimination of soft tissue defects of the tongue and the floor of the mouth are not described in the Russian scientific literature; in the foreign literature, we found only two original articles covering this issue [16–17].

The closest approach to the one tested by us is that presented by H. Koumoullis, who first proposed a method of using 3D modeling and template surgery to perform tongue reconstruction following glossectomy using Personalized Patient-specific Planning of Soft Tissue Reconstruction (PANSOFOS) [16]. The author noted the possibility of personalized reconstruction of soft tissues of the head and neck with a soft tissue autograft using 3D-planning.

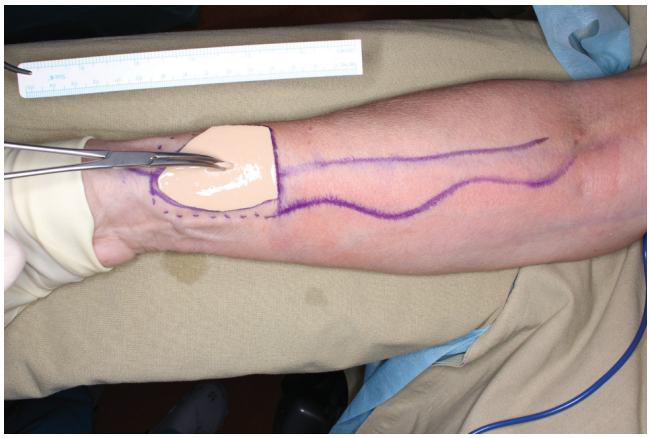

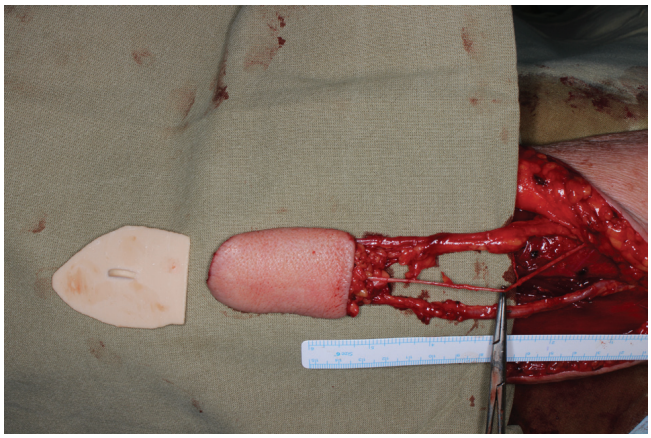

Figure prepared by the authors

Fig. 4. Marking a flap using a template. Radial flap on a vascular pedicle

However, the main disadvantage of his proposed technique consisted in an inability to predict the planned volume of tongue resection at the preoperative stage or to determine the loss of organ volume after radiation therapy and/or flap atrophy.

Lu H, Qin J, Yue R, Liu C et al describe a method of tumor visualization using computed tomography data to perform precision resection of midline tongue tumors without disturbing blood flow through the facial arteries. However, this technique did not involve the use of surgical templates [17].

Sinha P et al proposed a method of tongue tumor visualization by printing a physical model of the patient's tongue on a 3D printer with an alternative color of the tumor at the preoperative stage, allowing surgeons to carry out a better assessment of the extent of tumor spread. However, this approach did not include the fabrication of either resection templates or templates for free flap cutting [18].

In approbation of the above approach (preoperative planning of soft tissue reconstructive autografts), we and a number of authors [19] noted a significant decrease in the time of surgical intervention, which significantly reduces intraoperative risks for the patient and reduces the financial costs of anesthesia care.

The described approach to tongue defect elimination following removal of malignant neoplasm using

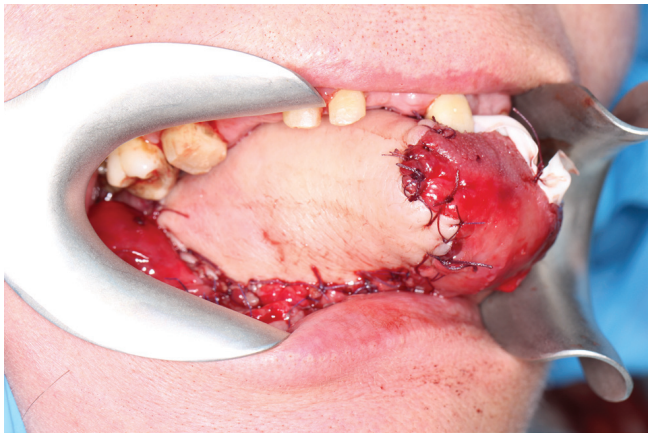

Figure prepared by the authors

Fig. 5. View of the flap after suturing the wound and restarting the blood flow

computer-aided digital planning, which is based on previously performed surgical intervention in the digital field, can be used to accurately (with an error of 0.2 mm) determine the boundaries of the tumor. To ensure the required oncologic radicality (clean margins), the resection template includes a parameter such as an oncologic margin of 1.5 cm from the tumor. The stencil for the cutaneous fascial flap pattern, which takes into account the volume of the resected part of the tongue, has an

Figure prepared by the authors

Fig. 6. Anthropophotometry one month after surgery

increased volume of 15% to level out postoperative scarring and reduce flap volume.

Despite the availability of modern protocols for suppressing artifacts from metal prosthetic restorations during head and neck radiology, not all patients were able to achieve objective visualization of the soft tissues of the tongue and floor of the oral cavity. Most of our patients had metal orthopedic constructions (gold, cobalt-chromium alloy) in the oral cavity at the time of treatment. In order to level out artifacts in radial methods of diagnostics (MRI, MSCT) and following a clinical examination of the oral cavity, the staff dentist-orthopedist removed all metal prosthetic constructions and replaced them with plastic crowns.

The problem of tongue mobility and changes in its volume due to muscle contraction at the stage of radial diagnosis remains a significant problem, whose solution will be presented in subsequent studies. In order to standardize preoperative planning, the need to create specialized protocols for the position of the tongue in the oral cavity at the diagnostic stages seems relevant.

CONCLUSIONS

The proposed 3D computerized planning method has demonstrated its utility in achieving accurate preoperative surgical planning. The use of surgical templates to achieve adequate oncological radicality (due to the pre-planned resection zone), synchronization of the work of two surgical teams, and reduction of the anesthesia time (average time of surgical intervention 288 min) demonstrates good functional and aesthetic results. The resection template provides a means for neoplasm removal in accordance with oncological principles; the template-pencil is used to accurately mark the shape and volume of the free microsurgical flap to in order to eliminate the tongue defect. However, due to the mobility of the tongue and the variability of its shape, new protocols for preoperative instrumental diagnostics are required for standardizing the position of the organ in the oral cavity. Thus, due to the need to develop new reconstructive operations to improve functional and reduce traumatization without compromising oncologic radicality, the presented surgical intervention approach represents a promising direction requiring further refinements and approbation on a larger group of patients.

References

1. Sarode G, Maniyar N, Sarode SC, Jafer M, Patil S, Awan KH. Epidemiologic aspects of oral cancer. *Dis Mon.* 2020,66(12):100988. https://doi.org/10.1016/j.disamonth.2020.100988
2. Kumar M, Nanavati R, Modi TG, Dobariya C. Oral cancer: Etiology and risk factors: A review. *J Cancer Res Ther.* 2016,12(2):458-63. https://doi.org/10.4103/0973-1482.186696
3. Stepan KO, Mazul AL, Larson J, Shah P, Jackson RS, Pipkorn P, et al. Changing Epidemiology of Oral Cavity Cancer in the United States. *Otolaryngol Head Neck Surg.* 2023,168(4):761–8. https://doi.org/10.1177/01945998221098011
4. Rychlevich AA. Total incidence of oral mucosal malignancies in the Russian Federation in 2013–2020. *Current problems of health care and medical statistics.* 2022,4:689–705 (In Russ). https://doi.org/10.24412/2312-2935-2022-4-689-705
5. Yi CR, Jeong WS, Oh TS, Koh KS, Choi JW. Analysis of speech and functional outcomes in tongue reconstruction after hemiglossectomy. *Journal of Reconstructive Microsurgery.* 2020,36:507–13. https://doi.org/10.1055/s-0040-1709493
6. Engel H, Huang JJ, Lin CY, Lam W, Kao HK, Gazyakan E, Cheng MH. A strategic approach for tongue reconstruction to achieve predictable and improved functional and aesthetic outcomes. *Plast Reconstr Surg.* 2010,126(6):1967–77. https://doi.org/10.1097/PRS.0b013e3181f44742
7. Lam L, Samman N. Speech and swallowing following tongue cancer surgery and free flap reconstruction--a systematic review. *Oral Oncol.* 2013,49(6):507–24. https://doi.org/10.1016/j.oraloncology.2013.03.001
8. Chang EI, Yu P, Skoracki RJ, Liu J, Hanasono MM. Comprehensive analysis of functional outcomes and survival after microvascular reconstruction of glossectomy defects. *Ann Surg Oncol.* 2015,22(9):3061–9. https://doi.org/10.1245/s10434-015-4386-6
9. Ihara Y, Tashimo Y, Nozue S, Iizumi Y, Fukunishi Y, Saito Y, Shimane T, Takahashi K. Changes in Oral Function and Quality of Life in Tongue Cancer Patients Based on Resected Area. *Asian Pac J Cancer Prev.* 2021,22(8):2549–57. https://doi.org/10.31557/APJCP.2021.22.8.2549
10. Gilbert RW. Reconstruction of the oral cavity, past, present and future. *Oral Oncol.* 2020,108:104683. https://doi.org/10.1016/j.oraloncology.2020.104683
11. Haughey BH. Tongue reconstruction: concepts and practice. *Laryngoscope.* 1993,103(10):1132–41. https://doi.org/10.1288/00005537-199310000-00010
12. Chepeha DB, Teknos TN, Shargorodsky J, Sacco AG, Lyden T, Prince ME, Bradford CR, Wolf GT. Rectangle tongue template for reconstruction of the hemiglossectomy defect. *Arch Otolaryngol Head Neck Surg.* 2008,134(9):993–8. https://doi.org/10.1001/archotol.134.9.993
13. Absolon KB, Rogers W, Aust JB. Some historical developments of the surgical therapy of tongue cancer from the seventeenth to the nineteenth century. *Am J Surg.* 1962,104:686–91. https://doi.org/10.1016/0002-9610(62)90419-1
14. Jacek B, Maciej P, Tomasz P, Agata B, Wiesław K, Radosław W, et al. 3D printed models in mandibular reconstruction with bony free flaps. *J Mater Sci Mater Med.* 2018,29(3):23–5. https://doi.org/10.1007/s10856-018-6029-5
15. Baskin RM, Seikaly H, Sawhney R, Danan D, Burt M, Idris S, et al. Tongue reconstruction: Rebuilding mobile three-dimensional structures from immobile two-dimensional substrates, a fresh cadaver study. *Head Neck.* 2019,41(10):3693–99. https://doi.org/10.1002/hed.25889
16. Koumoullis H, Burley O, Kyzas P. Patient-specific soft tissue reconstruction: an IDEAL stage I report of hemiglossectomy reconstruction and introduction of the PANSOFOS flap. *Br J Oral Maxillofac Surg.* 2020,58(6):681–6. https://doi.org/10.1016/j.bjoms.2020.04.017
17. Lu H, Qin J, Yue R, Liu C, Li S, Wu D. Application of 3D reconstruction for midline glossectomy in OSA patients. *Eur Arch Otorhinolaryngol.* 2020,277(3):925–31. https://doi.org/10.1007/s00405-020-05783-5
18. Sinha P, Bylapudi BP, Puranik P, Subash A, Rao V. 3D Patient-Specific Biomechanical Model of the Tongue for the Management of Tongue Tumors: Conceptualization to Reality. *Sisli Etfal Hastan Tip Bul.* 2022,56(4):559–63. https://doi.org/10.14744/SEMB.2022.37039
19. McCarty JL, Corey AS, El-Deiry MW, Baddour HM, Cavazuti BM, Hudgins PA. Imaging of Surgical Free Flaps in Head and Neck Reconstruction. *AJNR Am J Neuroradiol.* 2019,40(1):5–13. https://doi.org/10.3174/ajnr.A5776
20. Pokrovskii NB. Raschet i izmerenie razborchivosti rechi. *Svyazizdat.*1962,392 (In Russ).

Authors' contributions. All authors confirm that their authorship meets ICMJE criteria. The largest contribution is distributed as follows: Arbak A. Khachatryan — literature analysis, surgical stage, patient supervision, David N. Nazarian — study planning, surgical stage, Mikhail M. Chernenkiy — preoperative computer planning, Victoria O. Dzhuganova — literature analysis, preparation of a draft manuscript, Alexander V. Fedosov — data collection, surgical stage, Georgiy K. Zakharov — data collection, surgical stage, Maksim B. Potapov — data collection, surgical stage, Olga I. Danishuk — data analysis, Ekaterina V. Osipenko — data analysis, speech therapy rehabilitation, Eugenia I. Micheeva — preparation of a draft manuscript, speech therapy rehabilitation.

AUTHORS

Arbak A. Khachatryan
https://orcid.org/0000-0002-3066-8373
drarbak@yandex.ru

David N. Nazarian, Dr. Sci. (Med.),
https://orcid.org/0000-0001-9423-2221
craniofacial@yandex.ru

Mikhail M. Chernenkiy
https://orcid.org/0000-0002-9583-5291
3d.model@mail.ru

Victoria O. Dzhuganova
https://orcid.org/0000-0002-1823-4361
viktorijadzhuganova@gmail.com

Alexander V. Fedosov
https://orcid.org/0000-0002-0929-7723
dr.fedosov@mail.ru

Georgiy K. Zakharov
https://orcid.org/0000-0002-3406-2088
geza86@mail.ru

Maksim B. Potapov
https://orcid.org/0000-0002-2405-0104
maks_ardent@mail.ru

Olga I. Danishuk
https://orcid.org/0000-0002-0022-4923
danolga@mail.ru

Ekaterina V. Osipenko, Cand. Sci. (Med.)
https://orcid.org/0000-0001-9548-5730
nxhosipenko71@yandex.ru

Eugenia I. Micheeva
https://orcid.org/0000-0001-9306-7818
jenya.skvortsova@gmail.com

https://doi.org/10.47183/mes.2024-26-3-106-112

STUDY OF COMPLICATIONS ASSOCIATED WITH CENTRAL VEIN CATHETERIZATION IN PATIENTS WITH BLOOD DISORDER

Nikolay A. Romanenko✉

Russian Research Institute of Hematology and Transfusiology of the Federal Medical and Biological Agency of the Russian Federation, Saint-Petersburg, Russia

Introduction. Central venous catheter (CVC) provides intensive infusion and transfusion therapy in cancer patients, but catheter placement and operation are often associated with complications.

Objective. To determine the incidence of complications associated with CVC in patients with blood disorders.

Materials and methods. The study involved 3115 patients and 46 bone marrow donors. The right subclavian vein was catheterized in 2600 (82.2%) patients, the left subclavian vein in 552 patients (17.5%), and the internal jugular vein in 9 patients (0.3%). All persons underwent radiologic control; bacteriological blood examination was performed in case of suspected infection.

Results. Early revealed complications were: hematoma in 4.0% of patients; bleeding — in 2.3%; subclavian artery puncture — in 2.7%; pain and paresthesia of the upper limb — in 1.7%; lymphorrhea — in 1.4%; weakness / collapse — in 1.2%; extravasation — in 1.1%; catheter thrombosis — in 1.1%; less frequently, pneumothorax was detected in 0.2% of patients; allergic reaction to anesthetic — in 0.1%. Delayed complications (infiltrate, phlebitis, thrombophlebitis) were diagnosed in 2.7% of patients, bacteremia — in 2.4%, delayed bleeding — 0.4%. Among infections, Gram positive microorganisms were more frequently detected in 61.8% of cases, Gram negative in 29.7% ($p < 0.01$), and rarely fungal pathogens in 8.5% ($p < 0.001$). It was not possible to catheterize the central vein due to anatomical features of the patient in 0.5% of cases.

Conclusions. The analysis of trunk vein catheterization in patients with blood disorders established a high rate of hematomas, bleeding, subclavian artery punctures; among delayed complications, infiltrate, phlebitis, and bacteremia. Infectious complications demonstrated a prevalence of Gram-positive infectious agents.

Keywords: central venous catheter; bacteremia; bleeding; hematoma; infection; arterial puncture; pneumothorax

For citation: Romanenko N.A. Study of complications associated with central vein catheterization in patients with blood disorder. *Extreme Medicine*. 2024;26(3):106–112. https://doi.org/10.47183/mes.2024-26-3-106-112

Funding: the study was performed without external funding.

Compliance with ethical principles: the study and the publication of the article were approved at the meeting of the Local Ethical Committee of the Russian Research Institute of Hematology and Transfusiology of the Federal Medical and Biological Agency of the Russian Federation (protocol No. 7 of 01.02.2024) All patients signed voluntary informed consent for the study.

Potential conflict of interest: the author declares no conflict of interest.

✉ Nikolay A. Romanenko rom-nik@yandex.ru

Received: 19 June 2024 **Revised:** 12 Sep. 2024 **Accepted:** 16 Sep. 2024

ИЗУЧЕНИЕ ЧАСТОТЫ ОСЛОЖНЕНИЙ, АССОЦИИРОВАННЫХ С КАТЕТЕРИЗАЦИЕЙ ЦЕНТРАЛЬНЫХ ВЕН, У ПАЦИЕНТОВ С ЗАБОЛЕВАНИЯМИ СИСТЕМЫ КРОВИ

Н.А. Романенко✉

Российский научно-исследовательский институт гематологии и трансфузиологии Федерального медико-биологического агентства, Санкт-Петербург, Россия

Введение. Центральный венозный катетер (ЦВК) позволяет обеспечить интенсивную инфузионно-трансфузионную терапию у онкологических больных, но постановка и эксплуатация катетера нередко ассоциированы с осложнениями.

Цель. Определить частоту осложнений, ассоциированных с ЦВК, у пациентов с заболеваниями системы крови.

Материалы и методы. Включено 3115 больных и 46 доноров костного мозга. Правая подключичная вена катетеризирована 2600 (82,2%) пациентам, левая — 552 (17,5%), внутренняя яремная — 9 (0,3%). Всем лицам проведен рентгенологический контроль, при подозрении на инфекцию проводилось бактериологическое исследование крови.

Результаты. Выявлены ранние осложнения в виде гематомы у 4,0% больных, кровотечения — у 2,3%, пункции подключичной артерии — у 2,7%, боли и парестезии верхней конечности — у 1,7%, лимфореи — у 1,4%, слабости, коллапса — у 1,2%, экстравазации — у 1,1%, тромбирования катетера — у 1,1%; реже выявлен пневмоторакс — у 0,2%, аллергическая реакция на анестетик — у 0,1%. Отсроченные осложнения в виде инфильтрата, флебита, тромбофлебита диагностированы у 2,7% пациентов, бактериемия — у 2,4%, отсроченное кровотечение — у 0,4%. Среди инфекций чаще выявлялись грамположительные микроорганизмы — в 61,8% случаев, грамотрицательные — в 29,7% ($p < 0,01$), редко грибковые возбудители — в 8,5% ($p < 0,001$). В 0,5% случаев не удалось катетеризировать центральную вену из-за анатомических особенностей пациента.

Выводы. Анализ катетеризации магистральных вен у пациентов с заболеваниями системы крови позволил констатировать среди ранних осложнений большую частоту гематом, кровотечений, пункций подключичной артерии. Среди отсроченных осложнений — инфильтрат, флебит, бактериемию. При инфекционных осложнениях превалировали грамположительные инфекционные агенты.

Ключевые слова: центральный венозный катетер; бактериемия; гематома; кровотечение; инфекция; пункция артерии; пневмоторакс

Для цитирования: Романенко Н.А. Изучение частоты осложнений, ассоциированных с катетеризацией центральных вен, у пациентов с заболеваниями системы крови. *Медицина экстремальных ситуаций*. 2024;26(3):106–112. https://doi.org/10.47183/mes.2024-26-3-106-112

Финансирование: работа выполнена без спонсорской поддержки.

Соответствие принципам этики: исследование и публикация статьи одобрены на заседании Локального этического комитета ФГБУ «Российский научно-исследовательский институт гематологии и трансфузиологии» ФМБА России (протокол № 7 от 01.02.2024). Все пациенты подписали добровольное информированное согласие на исследование.

Потенциальный конфликт интересов: автор заявляет об отсутствии конфликта интересов.

✉ Романенко Николай Александрович rom-nik@yandex.ru

Статья поступила: 19.06.2024 **После доработки:** 12.09.2024 **Принята к публикации:** 16.09.2024

INTRODUCTION

Managing patients with blood disorders at present often requires adequate venous access, which can be provided through the use of central venous catheters (CVCs). The use of CVCs in patients allows the introduction of various infusion media, hemocomponents, chemotherapy drugs directly into the lumen of the central vein. This provides the possibility of administering large volumes of fluid and round-the-clock infusion of drugs, parenteral nutrition, hematopoietic stem cell harvesting, as well as monitoring of central venous pressure and clinical and laboratory parameters. At the same time, administration of chemotherapy drugs into the peripheral vein does not exclude their extravasation into the surrounding soft tissues, with the risk of infiltrate or necrosis development and subsequent scar formation [1].

Provision of central venous access using CVCs in patients in intensive care units has been widespread since the 1970s. This procedure makes possible a quick refilling of circulating blood and plasma volume in case of blood loss and shock, significantly improving the quality of life of patients due to the absence of the need for multiple repeated venipunctures, particularly in patients with low venous pressure and weak peripheral veins [1–2].

The procedure of CVC placement, which refers to surgical interventions, is often associated with the following complications: hematoma, bleeding, arterial puncture, pneumothorax, venous thrombosis, secondary infections up to the bacteremia or sepsis; in some port-systems, placement or even detachment of the implanted catheter with its migration into the right atrium can occur [2–6]. According to some authors [2, 3, 7], the incidence of complications associated with central vein catheterization reaches 15–25%. This depends on the anatomical and topographical features of the vessel structure, the state of the hemostasis system in the patient, as well as the proper technique of CVC placement. In addition, the risk of thrombotic and infectious complications increases with prolonged use of venous catheter especially during the period of antitumor therapy. Therefore, in patients with hemostasis disorders (thrombocytopenia, disseminated intravascular coagulation — DIC), immunodeficiency, neutropenia, compliance with aseptic conditions at all stages of CVC operation, including the use of aseptic technique ANTT (Aseptic Non-Touch Technique) is particularly strictly required [8–10].

This study aims to investigate the incidence of central venous catheter-associated complications in patients with blood disorders.

MATERIALS AND METHODS

A retrospective study was conducted to investigate the incidence of complications associated with CVC placement at RosNIIGT of FMBA in Russia. The study included patients aged 18 years and older with blood disorder who signed an informed voluntary consent for CVC placement. Healthy donors of hematopoietic stem cells were additionally included in the study. Patients were excluded who refused to sign informed consent, persons under the age of 18 years, and those who were not diagnosed with oncohematological diseases or aplastic anemia.

Inpatient records of 3161 patients who underwent central vein catheterization and were treated at the hematology clinic of the institute for the period from 2003 to 2023 were studied. Of these, 3115 patients with blood diseases and 46 bone marrow donors were examined.

The age of the patients was 18–89 years (mean age = 53 years) and donors were 29–57 years (mean age = 41 years). Patients who underwent CVC staging had principal diagnoses of B-cell chronic lymphocytic leukemia (B-CLL), myelodysplastic syndrome (MDS), multiple myeloma (MM), primary myelofibrosis (PMF), and chronic myeloid leukemia (CML) in the blast crisis phase (CML-BC), myelodysplastic syndrome/myeloproliferative neoplasm (MDS/MPN), non-Hodgkin's lymphoma (NHL), acute myeloid leukemia (AML), acute lymphoblastic leukemia (ALL), Hodgkin's lymphoma (HL), and aplastic anemia (AA). The distribution of patients with CVC by relevant nosologies is presented in Figure 1.

As anesthesia, 1% lidocaine solution of 10–15 mL (in 99.1% of patients) or 0.5% novocaine solution of up to 10–15 mL (0.9% of patients) was used. CVC placement was performed in the right subclavian vein in 2,600 (82.2%) patients, in the left subclavian vein in 552 (17.5%), and in only 9 (0.3%) patients in the right internal jugular vein. The left subclavian vein or right internal jugular vein was catheterized in

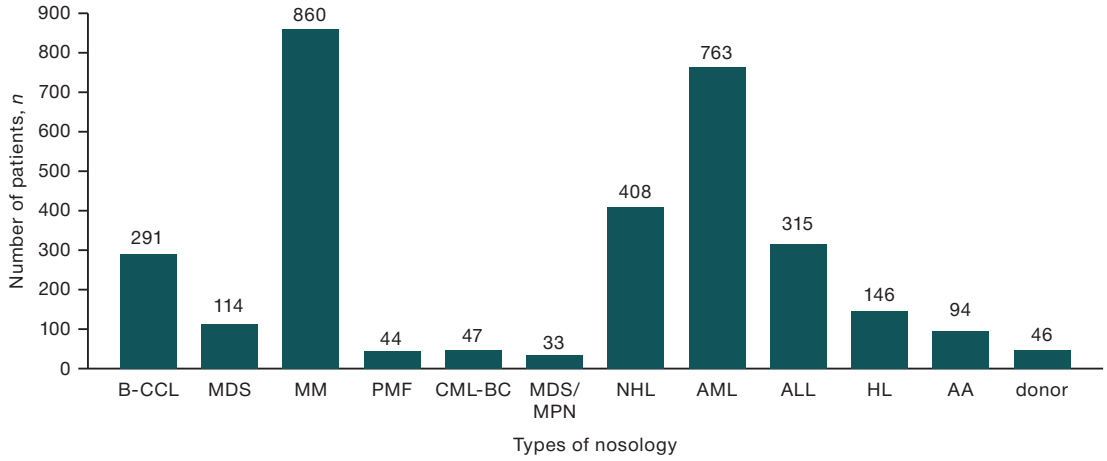

Figure prepared by the author using his own data

Fig. 1. Distribution of patients with established CVC depending on the disease

patients with a history of previous failed attempts at CVC placement or technical difficulties in performing the manipulation at the moment.

The choice of central venous catheter was made taking the choice of further therapies into account: chemotherapy, hemotransfusion, harvesting of peripheral stem cells, or the volume of expected infusions, duration of treatment, etc. B.BRAUN (Germany) Certofix® Duo S 720 for patients with blood disorders and Certofix® Duo RA M 1220 for stem cell donors were used for catheterization of the main veins.

The effectiveness of the central vein catheterization procedure was assessed by retrograde blood flow into the syringe, visual inspection, radiography; if necessary, the procedure was performed under ultrasound data control. The figures show radiographs to visualize the terminal (distal) segment of the catheter location. The normal location of the catheter is shown below (Fig. 2).

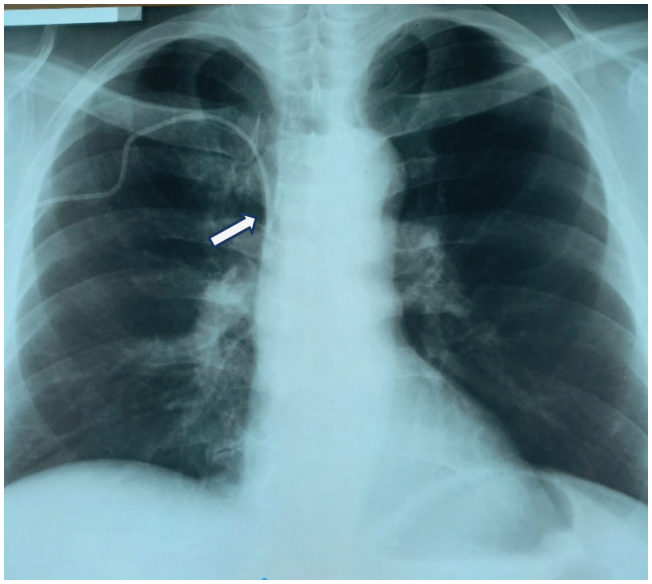

Figure prepared by the author using his own data

Fig. 2. Chest X-ray of the patient after correct catheterization of the right subclavian vein (arrow shows the catheter's distal segment)

Figure prepared by the author using his own data

Fig. 3. X-ray of chest: extravasation of the central venous catheter — outside the subclavian vein (the catheter is localized outside the subclavian vein)

The vertical position of the CVC of the end segment in the internal jugular vein was confirmed radiologically (Fig. 4). If the CVC was upright, it was often retained for short-term therapy. However, if peripheral stem cell procurement was required or high-dose chemotherapy was planned, the CVC was removed and placed on the opposite side due to the risk of phlebitis and thrombosis.

In case of fever (>38°C) or suspicion of infections associated with CVC, blood was effused directly from the patient's vein or catheter with subsequent bacteriological analysis, for which blood was introduced into one or more vials with nutrient medium (for blood — thioglycolate medium; for a biosample from the catheter — sugar broth, Sabouraud's medium, or thioglycolate medium). To identify the pathogen and determine the sensitivity of microorganisms to antibacterial medicines, the biomaterial was transferred to differentiating media. In addition, the level of procalcitonin in blood was studied in order to predict the possible development of bacterial sepsis in the shortest possible time and differentiate the infectious process, depending on the composition of anaerobic and aerobic microflora. If infection associated with CVC was detected, the catheter was removed and antibacterial therapy was performed.

All complications associated with CVC are divided into those directly related to the procedure of catheter placement and delayed complications, i.e., related to catheter care and disorders in the system of hemostasis, immunity.

Statistical processing of the obtained data was performed using Microsoft Office Excel 2010 and SPSS Statistic 22 software packages in the Windows 2016 environment. Samples were tested for normality of distribution

Figure prepared by the author using his own data

Fig. 4. X-ray of the neck and upper chest of the patient after CVC placement from the right subclavian access — vertical placement of the catheter in the internal jugular vein (the arrow shows the distal segment of the catheter)

using the Kolmogorov-Smirnov test of agreement; the level of statistical significance $p > 0.2$ was considered reliable. The mean (*M*), standard deviation (*m*), median (Me) were calculated. Fractions were compared using Fisher's angular transformation (φ). Differences were considered statistically significant at $p < 0.05$.

RESULTS

In 46 healthy bone marrow donors, no clinically significant complications related to central vein catheterization were documented in any case. Only one patient had weakness on anesthetic injection (lidocaine); this symptom was resolved independently 15 min after catheterization. In 46 healthy bone marrow donors, the duration of CVC in the vein was 1.2±0.1 days (1–3 days).

In patients with blood diseases ($n = 3115$), complications directly related to the technique of placement were observed, mainly mechanical or hemostasis disorders (bleeding, hematomas, thrombosis), delayed complications associated with the accession of secondary infection due to defects in the care of CVCs and/or immune system in patients. Among the complications reported at the stage of CVC insertion or after its implementation were arterial punctures, hematomas, bleeding from the catheter passage, pneumothorax, pneumomediastinum, hemoptysis, catheter malposition (extravasation), lymphorrhea, pain, paresthesia on the side of catheterization, vascular (general weakness, collapse), and allergic reaction (urticaria, Quincke's edema) to the anesthetic, as well as infectious-inflammatory — infiltrate, phlebitis, thrombophlebitis, bacteremia, and sepsis. Catheter bending (knot formation), disruption of catheter integrity, and catheter obstruction (thrombosis) are also listed as adverse events. While the latter do not constitute complications for the patient, further infusion through such a catheter is impossible and removal of the CVC is required. In addition, 16 (0.5%) patients failed to place the catheter due to anatomical peculiarities of vessel location in the patient.

The nature and frequency of complications associated with CVC placement depended on the anatomical features of the patient's vascular structure, technique of CVC placement, vascular access, physician's experience, peculiarities of the course of the disease itself (cytopenia, coagulopathy), and catheter care. A total of 702 adverse events were reported, representing 22.5%. Data on complications associated with CVC placement and care are presented in Table 1.

An analysis of the data in Table 1 revealed a low incidence of complications in patients. Attention was drawn to the frequent development of hematomas in 4.0% of cases ($p < 0.01$), bleeding from the catheter site, immediate and delayed bleeding 2.3% ($p < 0.05$) and 0.4%, respectively, registered subclavian artery puncture in 2.7% of cases ($p < 0.01$), development of infiltrate, phlebitis, thrombophlebitis in 2.7% of cases ($p < 0.01$), and bacteremia or sepsis in 2.4% of patients ($p < 0.01$). Other complications were reported significantly less frequently. Such dangerous complications as pneumothorax and pneumomediastinum were detected only in 6 (0.2%) and 1 (0.03%) patients. When diagnosing tension pneumothorax, it is necessary to drain the pleural cavity to evacuate air therefrom.

A radiograph of a 52-year-old patient with bilateral tension pneumothorax is presented. This is a rare but potentially dangerous complication: there is no lung pattern in the upper parts of both sides of the chest (Fig. 5). The patient underwent pleural cavity drainage in the 6th intercostal space along the mid axillary line on both sides for decompression. Full recovery occurred on the 2nd day. The incidence of such complications during CVC placement is less than 1%.

The manifestation of complications in the form of infectious processes was noted by the presence of infiltration with hyperemia at the catheter entry site, sometimes with exudate separated from the wound, soreness at the site of CVC insertion, as well as the appearance of thickening or edema at the site of CVC entry and/or along its length with increasing soreness. In case of deep spread of the infectious process, phlebitis was registered, manifested by erythema, thickening, pain along the course of the vein where the CVC was located, and increased body temperature in the patient. In some patients, phlebitis turned into

Table 1. Complications associated with CVC placement and care ($n = 3115$)

Type of complications	Number of complications ($n = 702$)	Frequency of complications (%)
Puncture (puncture) of the subclavian artery	85	2.7◆
Hematoma	124	4.0◆
Bleeding that occurred immediately after CVC placement	71	2.3*
Delayed bleeding (2 hours more)	12	0.4
Pneumothorax	6	0.2
Pneumomediastinum	1	0.03
Hemoptysis	2	0.06
CVC extravasation	35	1.1
Lymphorrhea	43	1.4
Pain, paresthesia in the upper extremity	53	1.7
Weakness, collapse (reaction to anesthetic)	38	1.2
Allergic reaction to anesthetic	3	0.1
Infiltrate, phlebitis, thrombophlebitis	83	2.7◆
Bacteremia, sepsis	76	2.4◆
Bend of catheter	6	0.2
Defect of catheter integrity (crack, fracture of CVCs)	14	0.4
Catheter obstruction (thrombosis)	34	1.1
Impossibility of CVC placement (anatomical peculiarities)	16	0.5

Table prepared by the author using his own data

Note: ◆ — statistically significant difference from background values at $p < 0.01$
* — statistically significant difference from background values at $p < 0.01$

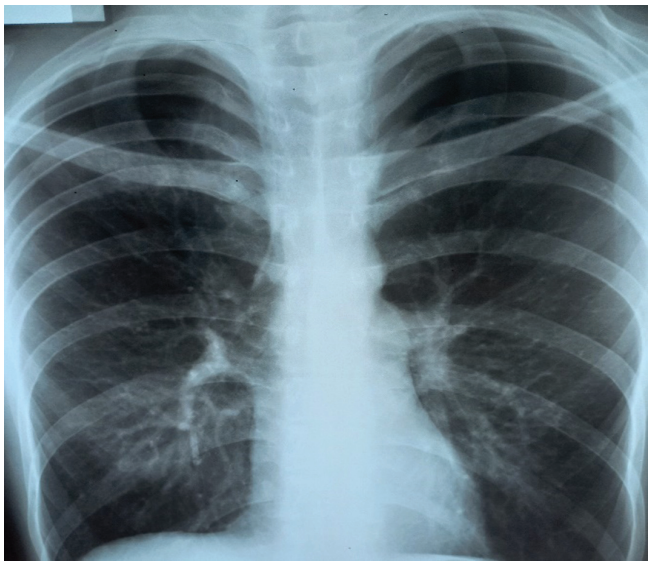

Figure prepared by the author using his own data

Fig. 5. X-ray of patient's chest — bilateral tension pneumothorax

bloodstream infection with the development of bacteremia or sepsis.

Thus, the analysis revealed the development of bloodstream infections in patients 3–7 days after catheterization. These infections were most frequently caused by Gram-positive microflora: either coagulase-negative *Staphylococcus epidermidis*, probably due to a defect in the care of CVCs, or, in later periods coagulase-positive *Staphylococcus aureus*. Infections due to Gram-negative pathogens and fungi (*Escherichia coli, Enterobacter spp.* etc.) were probably caused by penetration into the body during catheter use during infusions, as well as by hematogenous pathway (not related to CVC placement). In 76 patients, it was possible to identify the pathogen by bacteriological examination of blood; the corresponding data are presented in Table 2. At the same time, bacteriological examination in 13 patients allowed the simultaneous isolation of 2–3 pathogens, which in total amounted to 94 cases of positive identification of a microbial culture.

Among the infectious pathogens isolated from hemoculture in patients with complications, Gram-positive microorganisms (*Staph. Epidermidis and Staph. Aureus*, etc.), significantly less frequently in 29.7% of cases ($p < 0.01$) — Gram-negative (*Escherichia coli, Enterobacter spp.*, etc.), in 8.5% of cases ($p < 0.001$) infection was caused by fungal pathogens (*Candida albicans*, etc.). For clarity, the main spectrum of detected microorganisms is presented in Fig. 6.

Thus, in the course of the study, hematomas, bleeding, and subclavian artery puncture were more frequently reported among the immediate complications after CVC placement, while among the delayed ones (after 3–7 days) — infiltrate, phlebitis, thrombophlebitis, and bloodstream infections.

DISCUSSION

The availability of central venous access for the administration of adequate therapy in oncohematological patients is of great importance. This allows the physician to perform daily infusion therapy, administer large volumes of infusion media, high-dose chemotherapy, and parenteral nutrition. However, despite the importance of central vascular access for facilitating the administration of drugs, there is a risk of complications that can occur during the catheterization procedure especially with a prolonged stay of the catheter in the vein. The incidence of particular complications occurring during CVC placement is highly variable, ranging from 2.7% to 8% (mean 4.5%); however, aggregate incidence can even reach up to 15–25% [2, 3, 7, 8, 9]. The incidence of complications is influenced by factors such as the type of CVC (port or with an external segment), puncture access

Table 2. Types of pathogens identified in patients with blood diseases ($n = 76$)

Pathogens		Number of positive tests, *n*	Ratio of positive tests isolated, %
Gram-positive microbes	*Staphylococcus epidermidis*	47	50.0
	Staphylococcus aureus	8	8.5
	Streptococcus viridance	1	1.1
	Enterococcus spp.	1	1.1
	Micrococcus spp.	1	1.1
Gram-negative microbes	*Escherichia coli*	14	14.9
	Enterobacter spp.	9	9.5
	Acinetobacter spp.	1	1.1
	Pseudomonas aeruginosa	2	2.1
	Neisseria spp.	2	2.1
Fungal infections	*Candida. albicans*	5	5.3
	Candida crusei	1	1.1
	Rhodotorula spp.	1	1.1
	Aspergillus spp.	1	1.1

Table prepared by the author using his own data

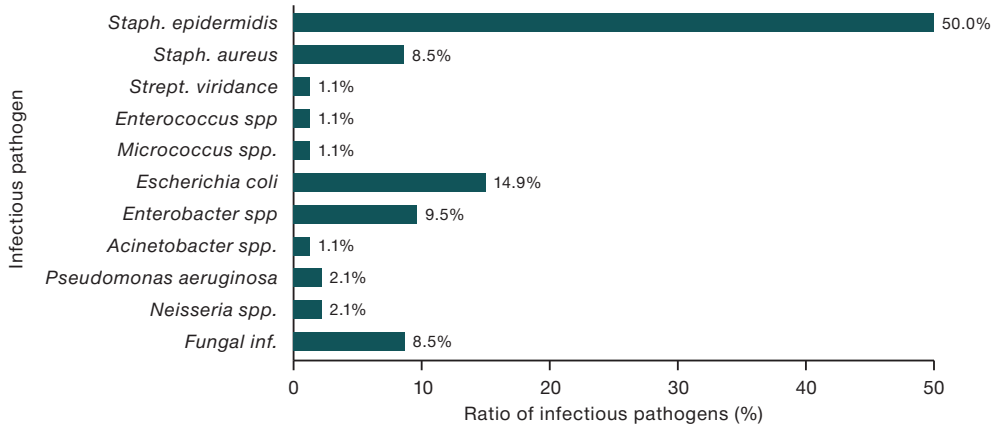

Figure prepared by the author using his own data

Fig. 6. Pathogens associated with central venous catheter-associated infections

(occurs less frequently in subclavian or jugular vein catheterization), prior catheter placement, pathophysiological conditions (immunodeficiency, cytopenia, coagulopathy) and anatomical and topographical features of the structure in the patient, experience of the anesthesiologist or surgeon, and conscientiousness in identifying and documenting the occurrence of the complication [2, 8, 9]. For example, when a port system is used, the cumulative incidence of early complications reaches 3.28% [11]. In addition, there are cases of failure of central vein catheterization; moreover, their frequency increases with each repeated unsuccessful attempt: after the first attempt — by 1.6%; after the second — by 10.2%, after the third and more — by 43.2% [12]. During the study, no catheterization of any subclavian vein could be carried out in 16 (0.5%) of the total number of patients; for these patients, infusion therapy was administered through peripheral veins.

When analyzing the frequency of complications associated directly with the procedure of catheter placement, the occurrence of hematomas was statistically significantly more frequent in 4% of patients, while bleeding from the site of CVC catheterization was slightly less frequent in 2.7% (immediately after the procedure — 2.3%; delayed — 0.4%; 2 hours or more after catheterization, subclavian artery puncture occurred in 2.7% of patients). It is important to emphasize that the occurrence of hematomas and bleeding in patients with blood diseases is more frequently caused by hemostasis disorders: such catheterized patients more often suffer from severe thrombocytopenia (mainly IV or III severity), and less often — from coagulopathy. Arterial puncture as a complication was mainly due to anatomical features in patients "keel-shaped chest", pronounced edema syndrome, obesity, clavicle fractures (in the past), presence of tumors/enlarged lymph nodes in the subclavian and/or supraclavicular region or in the neck region. These complications have generally been resolved without additional surgical interventions. In cases of severe thrombocytopenia, hemostatic therapy and transfusions with platelet concentrate at a therapeutic dose of 200–250×10^9 platelets per 1 m^2 of body surface area (usually 200–300 mL of platelet concentrate per injection) were carried out. In most cases, collapse, lymphorrhea, pain, and paresthesia did not require additional medical interventions and were managed independently. However, if the patient was found to have massive lymphorrhea lasting more than a day, the CVC was removed, followed by a sterile dressing. In case of patency failure (thrombosis), integrity, bending or extravasation, the catheter was removed and, if necessary, reinserted more often from the opposite side or via jugular access.

According to some authors, the frequency of detection of such a formidable complication as pneumothorax can reach 0.3–1.0% of cases [3, 13]. In our study, pneumothorax and pneumomediastinum were diagnosed in 0.2% and 0.06% of cases, respectively, which required additional medical interventions, in particular, drainage of the pleural cavity. Complications associated with CVC placement as manifested by the development of inflammation depend not only on compliance with the rules of asepsis, but also on the immune status of the patient (presence of severe neutropenia), the type of venous catheter. Thus, according to D.G. Maki and co-authors, when using central venous catheters with an open segment, infectious-inflammatory complications amounted to 2.7 per 1000 catheter-days, while the use of port-systems — no more than 0.1 per 1000 catheter-days [14]. In the patients observed in the present study, complications associated with infectious-inflammatory reaction in the form of infiltrate, phlebitis or thrombophlebitis were diagnosed in 2.7% of cases, while bloodstream infection occurred in 2.4% of cases, which amounted to 3.1 per 1000 per catheter-days. This is higher than in non-oncologic patients. However, the studied cohort of patients with oncohematological diseases and aplastic anemia often have a defect of hematopoiesis as manifested by postcytostatic immunosuppression and neutropenia of III-IV severity and a consequently higher risk of infectious complications. Therefore, if an infectious process is suspected, microbiological examination should be performed and empirical antibacterial therapy prescribed. In the case of positive bacteriologic analysis or identification, the catheter should be removed due to the possibility of comprising a source of infection; if necessary, the antibacterial drug sensitive to the identified pathogen should also be changed [1].

CONCLUSIONS

1. The analysis of catheterizations of the main veins established a higher frequency of such early complications

as hematomas, bleeding caused by hemostasis disorders (thrombocytopenia, coagulopathy) in oncohematological patients, as well as punctures of the subclavian artery due to anatomical features of the main vessels due to compression and displacement by tumor mass of lymph nodes and changes in the walls of subclavian veins associated with frequent repeated catheterizations and resulting scars.

2. Infiltrates, phlebitis, bacteremia, or sepsis were more often stated among delayed complications. Among the infectious pathogens isolated during bacteriological examination of hemoculture, Gram-positive pathogens prevailed significantly, which could be due not only to neutropenia in the study subjects, but also to contamination of infections from the environment during the operation and care of the venous catheter.

3. Given the high risk of complications associated with CVCs in the category of oncohematological patients with neutropenia, immunodeficiency requires strict compliance with aseptic conditions and measures to prevent catheter-associated infections at all stages of its operation.

References

1. Abdulkadyrov KM, Shmidt AV. Central venous catheters in hematology: priorities and problems. In the book Hematology: The Newest Handbook. *M.: Publishing House Owl.* 2004:851–89 (In Russ.).
   EDN: YLYRBH
2. Romanenko NA. Central venous catheter in oncohematological practice (Lecture and own data). *Medicine: Theory and Practice.* 2024;9(1):58–73 (In Russ.).
   https://doi.org/10.56871/MTP.2024.70.59.009
3. Sugak AB, Shchukin VV, Konstantinova AN, Feoktistova EV. Complications of central venous catheters insertion and exploitation// *Issues of Hematology/Oncology and Immunopathology in Pediatrics.* 2019;18(1):127–39 (In Russ.).
   https://doi.org/10.24287/1726-1708-2019-18-1-127-139
4. Sumin SA, Kuzkov VV, Gorbachev VI, Shapovalov KG. Catheterization of the subclavian and other central veins. Guidelines. *Bulletin of Intensive Care named after. AI Saltanova*. 2020;1:7–18 (In Russ.).
   https://doi.org/10.21320/1818-474X-2020-1-7-18
5. Klinicheskie rekomendacii. Anesteziologiya-reanimatologiya. M.: GEOTAR-Media, 2016:914–7 (In Russ.).
   EDN: XGHJDL
6. Olkhova IV, Popov VE. Spontaneous Catheter Separation from the Implanted Venous Port and Its Migration to the Venous Heart: Clinical Case. *Onkopediatriya.* 2018;5(2):127–32 (In Russ.).
   https://doi.org/10.15690/onco.v5i2.1915
7. Orlova OA, Semenenko TA, Akimkin VG, Yumtsunova NA. Clinical and epidemiological characteristics of catheter-associated bloodstream infections in patients with hematological profile. *Medicinskiy Alphabit.* 2020;(34):9–12 (In Russ.).
   https://doi.org/10.33667/2078-5631-2020-34-9-12
8. Greene ES. Challenges in reducing the risk of infection when accessing vascular catheters. *J Hosp Infect*. 2021;113:130–44.
   https://doi.org/10.1016/j.jhin.2021.03.005
9. Rickard CM, Flynn J, Larsen E, Mihala G, Playford G, Shaw J, et al. Needleless connector decontamination for prevention of central venous access device infection: a pilot randomized controlled trial. *Am J Infect Control*. 2021;49: 269–73.
   https://doi.org/10.1016/j.ajic.2020.07.026
10. Rowley S, Clare S. Standardizing the critical clinical competency of aseptic, sterile, and clean technique with a single international standard. Aseptic Non Touch Technique (ANTT). *J Assoc Vasc Access*. 2019;24(4):12–7.
    https://doi.org/10.2309/j.java.2019.004.003
11. Smolyar AN, Ginzburg LM, Smirnov MA. Totally implantable central venous port: analysis of complications and their prevention. *Pirogov Journal of Surgary*, 2019;(12):13–7 (In Russ.).
    https://doi.org/10.17116/hirurgia201912113
12. Di Carlo I, Pulvireni E, Mannino M, Toro A. Increased use of percutaneous technique for totally implantable venous access devices. Is it real progress? A 27-year comprehensive review on early complications. *Ann. Surg. Oncol*. 2010;17(6):1649–56.
    https://doi.org/10.1245/s10434-010-1005-4
13. Romanenko NA. Central vein catheterization in oncohematology patients: complication, associated with procedure and care. *HemaSphere.* 2022;6(3):1487–8.
    https://doi.org/10.1097/01.HS9.0000849280.98974.58
14. Maki DG, Kluger DM, Crnich CJ. The risk of bloodstream infection in adults with different intravascular devices: a systematic review of 200 published prospective studies. *Mayo Clinic Proc.* 2006;81(9):1159–71.
    https://doi.org/10.4065/81.9.1159

Authors' contributions. The author confirms that he meets the ICMJE criteria for authorship. The author's contribution is as follows: Nikolay A. Romanenko — research concept and design, information collection, data processing, interpretation of results, text writing, editing.

AUTHOR

Nikolay A. Romanenko, Dr. Sci. (Med.), Associate Professor
https://orcid.org/0000-0002-7602-9382
rom-nik@yandex.ru

https://doi.org/10.47183/mes.2024-26-3-113-121

MORBIDITY, MORTALITY, AND LETHALITY OF THE RUSSIAN POPULATION DUE TO RESPIRATORY DISEASES FOR 2016–2021 AND COVID-19 FOR 2020–2021

Tatiana N. Bilichenko✉, Elena V. Bystritskaya, Viktor M. Misharin

Federal Pulmonology Research Institute, Moscow, Russia

Introduction. The impact of the epidemic circulation of the novel coronavirus respiratory infection on the Russian population in terms of morbidity, mortality and lethality from respiratory diseases (RD) and consequent social damage requires an in-depth study.

Objective. The study set out to compare the morbidity, mortality and lethality dynamics of the total population of the Russian Federation due to respiratory diseases (RD) in 2016–2021 and COVID-19 in 2020–2021.

Materials and methods. The study was based on official statistical information provided by the Ministry of Health of the Russian Federation, Russian Federal State Statistics Service and Russian Federal Service for the Oversight of Consumer Protection and Welfare on the morbidity and mortality of the population due to RD (codes J00-J98 in accordance with the International Statistical Classification of Diseases and Related Health Problems, 10th edition (ICD-10). The data for 2020–2021 are compared with the average morbidity and mortality rates of the Russian population for 2016–2019. Statistical data processing was carried out using Statistica software, version 10, and Epi5 (WHO), version 7. When comparing the indicators, the relative risk, 95% confidence interval, and Matel-Hansel2 were calculated. The differences were considered to be significant at $p < 0.05$.

Results. The primary and general morbidity and mortality from RD in the Russian population in 2020–2021 exceeded the average levels of similar indicators for 2016–2019. The increase in indicators was associated with a larger number of patients presenting with pneumonia, as well as interstitial and suppurative lung diseases. This was accompanied by an increase in hospital mortality and lethality due to RD and COVID-19 in 2020–2021.

Conclusions. The epidemic circulation of the new coronavirus infection was accompanied by a significant increase in the morbidity and mortality of the population from RD.

Keywords: respiratory diseases; COVID-19; morbidity; mortality; lethality

For citation: Bilichenko T.N., Bystritskaya E.V., Misharin V.M. Morbidity, mortality, and lethality of the Russian population due to respiratory diseases for 2016–2021 and COVID-19 for 2020–2021. *Extreme Medicine.* 2024;26(3):113–121. https://doi.org/10.47183/mes.2024-26-3-113-121

Funding: the study was carried out without sponsorship.

Potential conflict of interest: the authors declare no conflict of interest.

✉ Bilichenko Tatyana N., tbilichenko@yandex.ru

Received: 28 June 2024 **Revised:** 8 Oct. 2024 **Accepted:** 11 Oct. 2024

ЗАБОЛЕВАЕМОСТЬ, ЛЕТАЛЬНОСТЬ И СМЕРТНОСТЬ НАСЕЛЕНИЯ РОССИИ ПО ПРИЧИНЕ БОЛЕЗНЕЙ ОРГАНОВ ДЫХАНИЯ ЗА 2016–2021 гг. И COVID-19 ЗА 2020–2021 гг.

Т.Н. Биличенко✉, Е.В. Быстрицкая, В.М. Мишарин

Научно-исследовательский институт пульмонологии Федерального медико-биологического агентства, Москва, Россия

Введение. Влияние эпидемической циркуляции новой респираторной коронавирусной инфекции на заболеваемость и смертность населения России от болезней органов дыхания (БОД) в связи с нанесенным социальным ущербом нуждается в углубленном изучении.

Цель. Изучить динамику показателей заболеваемости, летальности и смертности всего населения Российской Федерации по причине БОД за 2016–2021 гг. и COVID-19 за 2020–2021 гг.

Материалы и методы. Использована официальная статистическая информация Минздрава России, Росстата и Роспотребнадзора о заболеваемости и смертности населения по причине БОД (коды J00–J98 в соответствии с Международной статистической классификацией болезней и проблем, связанных со здоровьем, 10-го пересмотра (МКБ-10)). Данные за 2020–2021 гг. сопоставлены со средними показателями заболеваемости и смертности населения России за 2016–2019 гг. Статистическая обработка данных проведена с помощью программ Statistica, версия 10; Epi5 (WHO), версия 7. При сравнении показателей рассчитывали относительный риск, 95% доверительный интервал, Мэтел-Хэнсзел χ^2. Различия считали достоверными при уровне значимости $p < 0,05$.

Результаты. Первичная и общая заболеваемость и смертность от БОД населения России в 2020–2021 гг. превышала средние уровни аналогичных показателей за 2016–2019 гг. Прирост показателей был связан с увеличением числа пациентов с пневмонией, а также с интерстициальными и нагноительными болезнями легких. Это сопровождалось увеличением госпитальной летальности и смертности по причине БОД и COVID-19 в 2020–2021 гг.

Выводы. Эпидемическая циркуляция новой коронавирусной инфекции сопровождалась значительным приростом заболеваемости и смертности населения от БОД.

Ключевые слова: болезни органов дыхания; COVID-19; заболеваемость; летальность; смертность

Для цитирования: Биличенко Т.Н., Быстрицкая Е.В., Мишарин В.М. Заболеваемость, летальность и смертность населения России по причине болезней органов дыхания за 2016–2021 гг. и COVID-19 за 2020–2021 гг. *Медицина экстремальных ситуаций.* 2024;26(3):113–121. https://doi.org/10.47183/mes.2024-26-3-113-121

Финансирование: исследование выполнено без спонсорской поддержки.

Потенциальный конфликт интересов: авторы заявляют об отсутствии конфликта интересов.

✉ Биличенко Татьяна Николаевна tbilichenko@yandex.ru

Статья поступила: 28.06.2024 **После доработки:** 08.10.2024 **Принята к публикации:** 11.10.2024

INTRODUCTION

Respiratory diseases (RD) represent a widespread group of diseases affecting the Russian population, whose increasing incidence and differs significantly in the territories of cold and southern climatic zones having a different gender and age structure and population density [1]. The epidemic circulation of the new coronaviral infection COVID-19 had a great impact on the morbidity and mortality of the Russian RD population in 2020-2021, the significance of which requires in-depth study [2].

OBJECTIVE

To study the dynamics of morbidity, mortality and lethality rates of the total population of the Russian Federation due to respiratory diseases (RD) in 2016–2021 and COVID-19 in 2020–2021.

MATERIALS AND METHODS

We present an analysis of statistical data provided by the Ministry of Health of the Russian Federation and Russian Federal State Statistics Service on primary and total morbidity and mortality of the total population of the Russian Federation due to RD (class X J00-J99, according to the International Statistical Classification of Diseases and Related Health Problems, 10th edition (ICD-10) for 2016–2021 and morbidity COVID-19 (code U07.1, U07.2) [3–6]. The state statistical reporting forms No. 12 and No. 14 for 2019–2021 were used for the analysis. The data analysis was carried out using the statistical programs Statistica v.10, and Epi5 (WHO), v.7. The average indicators of overall incidence for 2016–2019 and the hazard ratio (HR) in 2020 and 2021 were calculated compared with the average value for previous years. When comparing the indicators, the difference $p < 0.05$ was considered significant. The data analysis was carried out by the following Federal Districts (FD) of Russia: Central (CFD); Northwestern (NWFD); Southern (SFD), North Caucasus (NCFD), Volga (VFD), Ural (UFD), Siberian (SFD), Far Eastern (FEFD), and the Crimean Federal District (which existed from 2014–2016).

RESULTS

According to the data of the Ministry of Health of the Russian Federation, a total of 59,731,931 cases of RD were registered in 2019, including 52,277,647 primary cases (87.5% of all RD) and 769,691 cases of secondary pneumonia (1.47% of all RD). By way of comparison, in 2020, these indicators increased to total RD 61,312,356 (+2.65%), 54,273,331 cases of primary infection (+3.82%) and 1,989,498 cases of pneumonia (+158.48%), while, in 2021, total RD amounted to 66,596,584 cases (+11.49%), including 59,381,887 cases of primary infection (13.59%) and 1,997,536 cases of pneumonia (+159.52%).

In 2021, the morbidity of the total population due to RD amounted to 45,560.7 cases per 100,000 of the total population, ahead of cardiovascular system diseases (24,792.3 cases), musculoskeletal system (12,087.0 cases), genitourinary system (10,591.0 cases), digestive system (10,332.9 cases).

Although the RD morbidity of the Russian total population has tended to increase since 2016, a significant increase in cases of diseases occurred in 2021. In terms of dynamics over the years since 2016, RD morbidity increased by 1% in 2017 (HR = 1.01; 95% CI 1.01–1.02; $p < 0.001$), by 3% in 2018 (HR = 1.03; 95% CI 1.02–1.03; $p < 0.001$), and by 2% in 2019 (HR = 1.02; 95% CI 1.01–1.02; $p < 0.001$). The average RD morbidity of the total population for 2016–2019 was 40,516.5 per 100,000. In 2020, the RD morbidity of the total population exceeded the 4-year average level to reach 41,862.9 and HR = 1.03; 95% CI 1.03–1.04; $p < 0.001$; in 2021 — 45,560.7 per 100,000 and HR = 1.12; 95% CI 1.12–1.13; $p < 0.001$ (Fig. 1). Morbidity of the total population in 2021 increased in all federal districts as compared with the levels of 2016–2019 with a maximum value in the Northwestern Federal District (Table 1). The excess of the average level of RD morbidity in Russia in 2021 was noted in 4 federal districts: SFD — 48,059.9 (HR = 1.05; 95% CI 1.05–1.06; $p < 0.001$); VFD — 49,837.3 (HR = 1.09; 95% CI 1.09–1.10; $p < 0.001$); UFD — 51 497.4 (HR = 1.13; 95% CI 1.13–1.13; $p < 0.001$); and NWFD — 55,680.9 (HR = 1.22; 95% CI 1.22–1.23; $p < 0.001$).

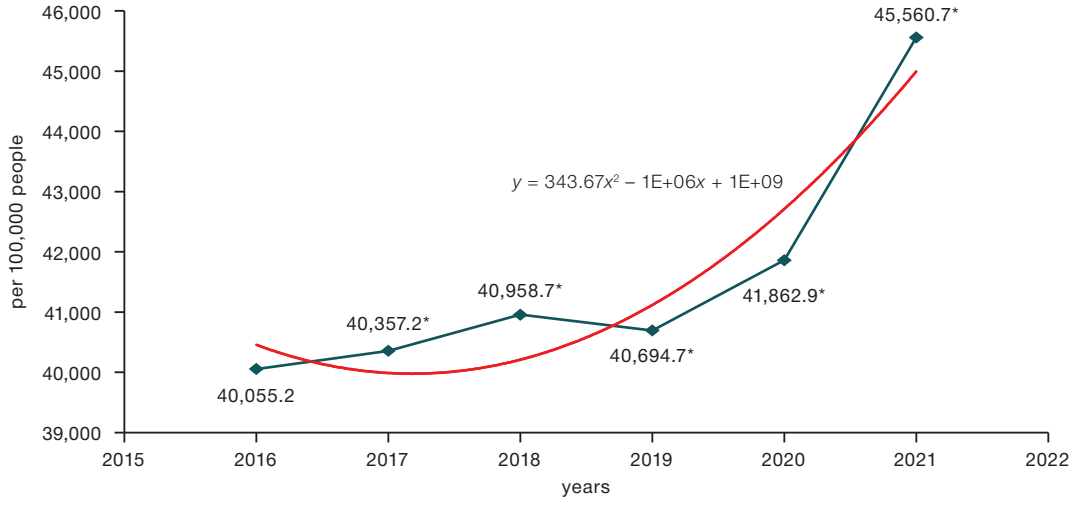

Figure prepared by the authors

Fig. 1. Dynamics of the general incidence of respiratory diseases in the total population in 2016–2021. (polynomial trend line. * — $p < 0.05$)

Table 1. Total incidence of respiratory diseases of the total population of the Russian Federation in 2016–2021

Territory	Total RD incidence (per 100,000 people)					
	Years					
	2016	2017	2018	2019	2020	2021
RUSSIA	40,055.2	40,357.2	40,958.7	40,694.7	41,862.9	45,560.7
CFD	37,784.6	37,658.0	38,352.1	38,142.3	38,836.9	42,282.2
NWFD	50,180.9	50,547.9	51,659.9	50,224.1	49,599.5	55,680.9
SFD	33,226.2	33,260.5	33,611.4	34,363.1	34,518.4	37,185.5
NCFD	30,420.8	30,699.6	29,334.1	30,423.9	32,300.6	33,292.3
VFD	43,762.0	43,968.1	44,783.2	43,866.8	46,756.2	49,837.3
UFD	41,861.3	42,623.3	44,326.8	44,460.8	46,504.5	51,497.4
SFD	40,086.0	41,222.4	41,866.4	41,434.4	42,976.2	48,059.9
FEFD	41,285.9	41,930.9	41,527.1	41,586.9	41,299.0	44,988.8

Table prepared by the authors

Among the subjects of the Russian Federation in 2021, the highest rates of RD were observed in the Nenets Autonomous District of the Northwestern Federal District (68,330.0 per 100,000 of the total population), the Chukotka Autonomous District of the Far Eastern Federal District (67,133.1), the Oryol Region of the Central Federal District (63,035.6), the Altai Territory of the SFD (64,924.9), the Vladimir Region of the Central Federal District (62,978.7), and the Republic of Sakha (Yakutia) of the Far Eastern Federal District (62,861,4).

Below-average RD morbidity for Russia in 2021 was experienced in the North Caucasus Federal District (33,292.3), Southern Federal District (37,185.5), Central Federal District (42,282.2), and Far Eastern Federal District (44,988.8). The lowest RD morbidity in the subjects of the Russian Federation in the North Caucasus Federal District was in the Chechen Republic (21,600.4 cases per 100,000 of the total population), the Kabardino-Balkarian Republic (24,874.5), and the Republic of Ingushetia (28,692.5).

The RD primary incidence rate (PIR) in the total population in 2016–2019 tended to increase: 2016 — 35,161.2; 2017 — 35,356.6 (HR = 1.01; 95% CI 1.00–1.01; $p = 0.004$); 2018 — 35,982,0 (HR = 1.02; 95% CI 1.02–1.03; $p < 0.001$); 2019 — 35,616.2 per 100,000 of the total population (HR = 1.01; 95% CI 1.01–1.02; $p < 0.001$). The average 4-year RD rate was 35,529.0 per 100,000 of the total population. In 2020, the RD index increased to 37,056.8 (HR = 1.04; 95% CI 1.04–1.05; $p < 0.001$); in 2021, to 40,624.9 per 100,000 of the total population (HR = 1.14; 95% CI 1.14–1.15; $p < 0.001$). In 2021, a higher than the average Russian indicator of the total population (40,624.9 per 100,000 of the total population) was registered in the NWFD — 49,744.0 (HR = 1.22; 95% CI 1.21–1.24; $p < 0.001$), UFD — 46,756.1 (HR = 1.15; 95%CI 1.14–1.16; $p < 0.001$), VFD — 44 786.8 (HR = 1.10; 95% CI 1.09–1.11; $p < 0.001$), SFD — 41 831.9 (HR = 1.03; 95% CI 1.02–1.04; $p < 0.001$). In 2021, the highest RD rates were recorded in the Nenets Autonomous District of the Northwestern Federal District (65,189.6), the Chukotka Autonomous District of the Far Eastern Federal District (63,589.6), the Vladimir Region of the Central Federal District (59,023.3), the Oryol Region of the Central Federal District (59,010.5 per 100,000 of the total population). The lowest RD rates were recorded in the Kabardino-Balkarian Republic (21,714.9 per 100,000 of the total population), the Republic of Ingushetia of the North Caucasus Federal District (20,131.4), the Chechen Republic of the North Caucasus Federal District (16,528.7).

In 2020, the COVID-19 disease of the total Russian population in terms of access to medical institutions was registered at the level of 3391.1 cases per 100,000 of the total population (4,966,644 people) with a 2.4–fold increase in the disease in 2021 — 8,085.7 cases per 100,000 of the total population (11,818,983 people). In 2021 The highest rates of COVID-19 were detected in the Northwestern Federal District (10,625.6), UFD (9,684.2), and Central Federal District (8,969.4 cases per 100,000 of the total population). In the Southern Federal District, the incidence of COVID-19 increased by 3.5 times: from 1835.3 in 2020 to 6386.3 cases per 100,000 of the total population in 2021. The highest incidence of COVID-19 in 2021 was registered in St. Petersburg (NWFD) at 13814.5 per 100,000 of the total population (74 3820 people), representing a 2.4-times increase compared to 2020 (5856.8 per 100,000 of the total population — 315 751 people). In Moscow (CFD), the incidence of COVID-19 was higher than the national average, but lower than in St. Petersburg: 2020 — 6191.0 cases per 100,000 (784,192 people); 2021 — 8976.0 cases per 100,000 of the total population (1,135,919 people), respectively.

COVID-19 incidences in the total population are below the national average in 2021. They were registered in the North Caucasus Federal District (3975.9), Southern Federal District (6386.3), Far Eastern Federal District (7295.3), VFD (7635.8), SFD (7913.3 cases per 100,000 of the total population). In terms of Russian Federal Subjects, the lowest rates of COVID-19 were detected in 2021 in the Chechen Republic of the North Caucasus Federal District at 1170.1 cases per 100,000 of the total population.

As well as pneumonia, acute laryngitis and tracheitis occupied a leading place in the structure of separate RD morbidity of the total population in 2021. Compared with the average level for 2016–2019 (2387.6 per 100,000 of the total population), the incidence of acute laryngitis and tracheitis of the total population in 2020 decreased to 2309.2 (HR = 0.97; 95%CI 0.95–0.98; $p < 0.001$) and in 2021 — 2215.2 (HR = 0.93; 95%CI 0.91–0.94; $p < 0.001$).

The incidence of pneumonia in the total population hardly differed 2016 and 2017, while in 2018 and 2019, an increase occurred: 2016 — 462.5 per 100,000 of the

Table 2. Incidence of pneumonia of the total population of the Russian Federation in 2016–2021

Territory	Total incidence of pneumonia (per 100,000 people)					
	Years					
	2016	2017	2018	2019	2020	2021
RUSSIA	462.5	457.7	514.6	524.4	1358.4	1366.6
CFD	375.7	382.1	430.8	414.2	1190.0	1336.8
NWFD	470.7	471.9	514.9	452.7	1071.2	1358.4
SFD	483.3	448.6	492.5	479.5	1119.7	1551.9
NCFD	380.0	423.4	419.2	465.2	1535.2	1377.8
VFD	509.3	529.7	579.7	575.2	1829.2	1391.8
UFD	503.7	459.8	567.9	660.1	1178.2	1130.6
SFD	520.4	484.4	557.8	609.6	1447.6	1336.9
FEFD	558.4	526.3	647.7	749.2	1286.1	1418.9

Table prepared by the authors

total population; 2017 — 457.7 (p = 0.49); 2018 — 514.6 (HR = 1.11; 95% CI 1.08–1.14; $p < 0.001$); 2019 — 524.4 (HR = 1.13; 95% CI 1.10-1.17; $p < 0.001$) (Table 2). Compared with the average level for 2016–2019 (489.7 per 100,000 of the total population), the incidence of pneumonia in 2020 and 2021 increased 2.8 times: 1358.4 (HR = 2.77; 95% CI 2.69–2.86; $p < 0.001$) and 1366.6 (HR = 2.79; 95% CI 2.70–2.88; $p < 0.001$), respectively. An increase in the incidence of pneumonia in 2020–2021 was noted in all territories of the Russian Federation with a maximum increase in the incidence of pneumonia in 2021 in the Southern Federal District, North Caucasus Federal District, VFD, and the Far Eastern Federal District.

Compared with the average level for 2016–2019 (1156.6 per 100,000 population), there was a decrease in 2020 and 2021 of chronic and unspecified bronchitis and lung emphysema in the total population (1092.1; HR = 0.74; 95% CI 0.72–0.75; $p < 0.001$) and 1055.3 cases (HR = 0.97; 95% CI 0.94–0.99; p = 0.008), respectively.

The average level of the total population for 2016–2019 of bronchial asthma (BA) was 1058.3; this did not significantly change in 2020 (1059.4; p = 0.936) and in 2021 (1073.1; p = 0.320).

Compared with the average level of chronic obstructive pulmonary disease (COPD) in the total population for 2016–2019. (562.3 per 100,000 of the total population) in 2020, the morbidity index decreased to 542.3 (HR = 0.96; 95% CI 0.94–0.99; p = 0.004) and did not change in 2021 — 529.3 (p = 0.065)

The average level of the total population for 2016–2019 with other interstitial pulmonary diseases, purulent and necrotic conditions of the lower respiratory tract, and other pleural diseases was 24.7 and did not change in 2020 (27.7 cases; p = 0.127), but increased in 2021 — 39.5 respectively (HR = 1.43; 95% CI 1.26–1.62; $p < 0.001$).

According to the data of statistical forms No. 14, in 2019, inpatient treatment for RD (J00-J98 ICD-10) was carried out in only 1,541,339 adult patients aged 18 and over, among whom 24,816 people died (1.6%). 252,105 people were treated in hospital for acute respiratory infections (ARI) of the upper respiratory tract (URT) (J00-J06 ICD-10); among these, 38 people died (0.02%); with lower respiratory tract infections (LRT) (J20-J22 ICD-10), 63,829 people were affected, of whom 7 people died (0.1%); pneumonia (J12-J18 ICD-10) — 439,901 people, 10,510 people died (2.39%).

Although in 2020, the number of patients aged 18 and over who received inpatient treatment for RD decreased, the lethality increased by 3 times. A total of 1,348,122 adult patients were discharged from hospitals, of whom 65,997 died (4.9%; $p < 0.001$): URT ARI– 172,366 people, 28 people died (0.02%) and LRT ARI– 45,333 people, 205 people died (0.45%; $p < 0.001$), pneumonia — 646,444 people, 47,939 people died (7.42%; $p < 0.001$).

In 2021, the number of patients aged 18 and over who received inpatient treatment for RD continued to decrease, but lethality among them increased mainly due to pneumonia. A total of 1,008,875 adult patients were discharged from hospitals, 64,909 people died (6.43%; $p < 0.001$), among whom URT ARI– 128,922 cases, 40 people died (0.03%) and LRT ARI — 45,333 cases, 205 people died (0.45%; $p < 0.001$); pneumonia — 378,715 cases, 48,711 died people (12.86 %; $p < 0.001$).

In connection with COVID-19 (U07.1-U07.2 ICD-10) in 2020, 1,902,903 people were discharged from hospitals at the age of 18 or more, among whom 1,154,77 people died (6.07%), 3,588,017 people were discharged in 2021, 458,529 people died (12.78%; $p < 0.001$).

Among children 0–17 years old in 2019, only 18,098 people were discharged from hospitals in connection with RD, 334 people (0.02%) died, including 779,103 people with ARI, 12 people (0.002%) died and LRT — 492,981 people, 10 people (0.002%) died; with pneumonia — 272,339 people, 226 people died (0.080%).

In 2020, there were only 1,095,976 children aged 0–17 in hospitals for RD, 313 people died (0.029%), among whom URT ARI– 469,594 people, 13 people died (0.003%) and LRT ARI — 314,116 people, 5 people died (0.002%); with pneumonia — 143,627 people, 213 people died (0.148%; $p < 0.001$).

In 2021, among children 0–17 years old, only 1,170,033 people were discharged from hospitals for RD. 339 people died (0.029%), among whom URT ARI — 508,705 people, 10 people died (0.002%) and LRT ARI — 333,031 people, 16 people died (0.005%; $p < 0.001$), 139,279 people died with pneumonia, 239 people died (0.171%; $p < 0.001$).

In connection with COVID-19 (U07.1–U07.2 ICD-10), 44,964 children were discharged from hospitals in 2020,

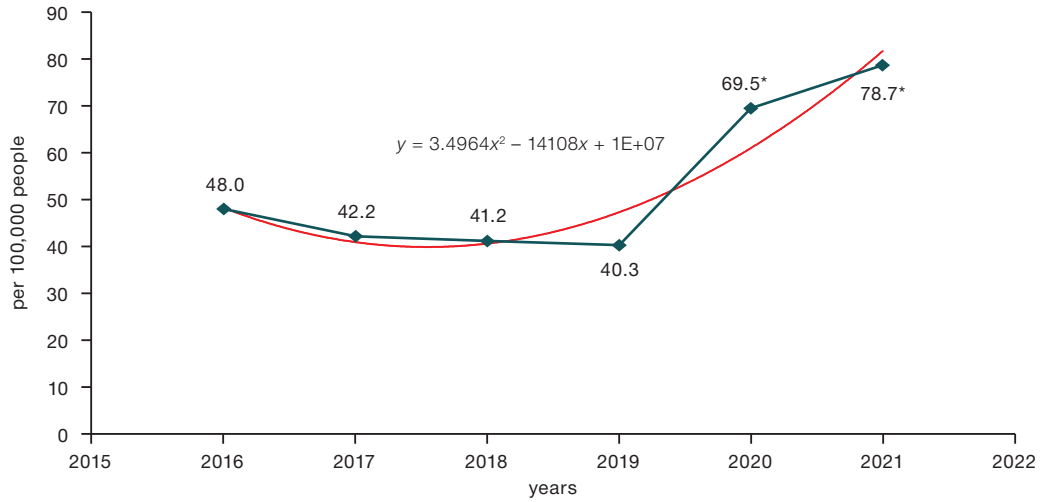

Figure prepared by the authors

Figure 2. Dynamics of mortality rates from respiratory diseases of the total population of the Russian Federation in 2016-2021. (Polynomial trend line. * — reliability of differences in indicators ($p < 0.001$)

of which 40 died — 0.090%. In 2021, 85,838 children were discharged, that is, 1.9 times more, of which 164 died (0.191%; $p < 0.001$).

Thus, the total number of RD patients discharged from hospitals in 2019 was only 3,341,437, 25,150 people died (0.75%), in 2020 — only 2,444,098 people, 66,310 people died (2.71%; $p < 0.001$), in 2021 — only 2,178,908 people, 65,248 people died (2.99%; $p < 0.001$).

In 2020, only 1,947,867 people with COVID-19 were discharged from hospitals, including 115,517 people (5.93%) died, in 2021 — only 3,673,855 people, 458,693 people died (12.48%; $p < 0.001$).

According to Russian Federal State Statistics Service, in the structure of mortality rates from all causes per 100,000 population in 2021 (1,673.9 cases) RD ranked 5th (78.7 cases — 4.7% of all cases) after diseases of the cardiovascular system (640.3 cases — 38.3% of all cases), mortality from COVID-19 (319.1 cases — 19.1% of all cases), neoplasms (194.1 cases — 11.6% of all cases), external causes (95.1 — 5.7% of all cases) [7].

If in the period 2016–2019 there was a decrease in RD mortality from 48.0 to 40.3 per 100,000 population ($p < 0.001$), then in the period 2020-2021 there was an increase in RD mortality of the total population of the Russian Federation (Fig. 2) [7–9].

The increase in RD mortality in 2020 compared to 2019 (40.3 cases per 100,000 of the total population) amounted to 72.46% (69.5%; $p < 0.001$); in 2021, the corresponding figure was 95.3% (78.7%; $p < 0.001$). An increase in the RD mortality of the population in 2020 and 2021 was noted in all territories of Russia, but above the average Russian level in 2021. Mortality was registered in the Volga Federal District (102.7 per 100,000 population), Far Eastern Federal District (111.0), SFD (93.1), and Southern Federal District (88.4 cases) (Table 3).

Below the average Russian level, the respiratory disease mortality rate was registered in the UFD (49.1), NWFD (55.8), Central Federal District (64.5), and North Caucasus Federal District (65.9 per 100,000 population). Among the subjects of the Russian Federation, the highest respiratory disease mortality rate in 2021 was recorded among the population of the Bryansk region of the Central Federal District (261.7 per 100,000 population). High respiratory disease mortality rates in 2021 were registered in the subjects of the Volga Federal District: the Kirov Region (256.3 per 100,000 population), the Republic of Mari El (231.8),

Table 3. Mortality rates from the respiratory diseases of the total population in the federal districts of the Russian Federation in 2016–2021

	Total respiratory diseases mortality rate (per 100,000 people)					
	Years					
Territory	2016	2017	2018	2019	2020	2021
RUSSIA	48.0	42.2	41.6	40,3	**65.9**	**78.7**
CFD	**50.5**	42.1	41.3	37.7	55.5	64.5
NWFD	46.5	42.0	37.8	36.3	45.5	55.8
SFD	36.6	32.0	33.6	35.7	59.1	**88.4**
NCFD	32.5	30.7	27.7	28.0	**72.9**	65.9
VFD	**49.3**	**44.0**	**44.7**	**43.7**	**84.1**	**102.7**
UFD	44.7	39.8	34.8	30.2	52.2	49.1
SFD	**59.7**	**55.6**	**55.4**	**54.7**	**81.9**	**93.1**
FEFD	**52.7**	**44.0**	**53.2**	**57.0**	**78.8**	**111.0**

Table prepared by the authors

the Republic of Bashkortostan (222.1), and in the Republic of Mordovia (114.5 per 100,000 population). The lowest respiratory disease mortality rate was registered in 2021 in Moscow Central Federal District (21.7), St. Petersburg NWFD (23.9), and Yamal-Nenets Autonomous District of the UFD (24.2 per 100,000 population).

The respiratory disease mortality rate had a direct relationship with age. In 2021, the respiratory disease mortality rate of the total population of the Russian Federation at the age of 0-17 years was 2.2; of the able–bodied population — 27.2; over the working age — 254.7 per 100,000 of the population of the corresponding age. The highest respiratory disease mortality rates were registered in the age group of 85 and older: in 2020 — 561.1, in 2021 — 713.0 per 100,000 population (the ratio of the level of 2021 to 2020 was 127.1%).

Among individual federal districts, the highest respiratory diseases mortality rate in 2021 were recorded in the Far Eastern Federal District: at the age of 0–17 years — 4.5; working–age population — 41.3; older than working age — 407.4 per 100,000 population of the corresponding age.

Among the subjects of the Russian Federation, the highest respiratory disease mortality rates are registered in the Republic of Bashkortostan of the Volga Federal District: 0–17 years old — 5.6; able–bodied population — 56.0; older than working age — 800.1 per 100,000 population of the corresponding age. The lowest mortality rates were registered in the Central Federal District of Moscow: among the total working-age population (6.4), older than the working age (66.6 of the corresponding age).

Among all men in 2020, the respiratory disease mortality rate was 84.5 per 100,000 male population (58,968 people); in 2021, it increased to 91.4 (64,155 people — +8.2%); $p < 0.001$. Among all women, the respiratory disease mortality rate in 2020 was 2.83 times lower than that of men, amounting to 29.9 (37,571 people), $p < 0.001$; in 2021, it was 2.36 times lower — 38.8 per 100,000 female population (50,572 people — +29.8%), $p < 0.001$. In 2021, among men of working age, the respiratory disease mortality rate was 3.2 times higher than among women (40.6 and 12.7, respectively, per 100,000 of the population of the corresponding age and gender; $p < 0.001$); in men older than working age, it was 2.4 times higher (431.2 and 179.4, respectively; $p < 0.001$). In 2021, the respiratory disease mortality rate of men of working age was higher than the average Russian level in the Far Eastern Federal District (59.5), CFD (50.0), VFD (49.9), SFD (43.4 per 100,000 of the corresponding age population). Below-average Russian mortality rates were recorded in the Northwestern Federal District (35.3), Central Federal District (34.0), UFD (27.8), and North Federal District (26.5 per 100,000 of the population of the corresponding age). In 2021, the respiratory disease mortality rate of women of working age above the national average was also registered in the Far Eastern Federal District (20.4), the SFD (16.6), the Volga Federal District (15.1), the Southern Federal District (15.1 per 100,000 population of the appropriate age); below average Russian mortality rates were recorded in the Northwestern Federal District (10.5), Central Federal District (9.8), North Caucasus Federal District (9.4), and UFD (8.3).

In the structure of the total RD mortality, the proportion of pneumonia mortal rate (J12-J16, J18) in 2021 was 65.3%. The levels of mortality rate from pneumonia in 2021 of the total population increased by 3.2 times compared to 2019 (16.3 per 100,000 villages): 2020 — 39.8 ($p < 0.001$); 2021 — 51.3 ($p < 0.001$) (Table 4). The increase in mortality from pneumonia in 2021 compared to 2020 has amounted to 28%. Above-national-average morality rates in 2021 were registered in the Far Eastern Federal District (81.9 per 100,000 population), the SFD (63.9), the VFD (66.5), the Southern Federal District (66.7 per 100,000 population), and the lowest mortality are in the UFD (21.7), Central Federal District (37.9), North Caucasus Federal District (38.6), Northwestern Federal District (41.8). Among the working-age population in 2021 The mortality from pneumonia was 20.3 per 100,000 of the population of the corresponding age. The highest mortality from pneumonia in this age group were recorded in the Far Eastern Federal District (33.9 per 100,000 population of the corresponding age), the SFD (25.6), the VFD (24.5), the Southern Federal District (23.0), while the lowest mortality rates were recorded in the UFD (11.3), the North Caucasus Federal District (12.6), the Central Federal District (15.8), and the Northwestern Federal District (19.8).

Mortality from COPD (J41, J42, J44) of the total population of the Russian Federation ranged from 22.5 in 2016 to 21.4 per 100,000 population in 2021 (p>0.05). In the structure of total RD mortality COPD mortality rate was 26.0%.

Table 4. Mortality rates from pneumonia of the total population in the federal districts of the Russian Federation in 2016-2021

	Total pneumonia mortality rate (per 100,000 people)					
	Years					
Territory	2016	2017	2018	2019	2020	2021
RUSSIA	**21.3**	**17.8**	**17.5**	**16.3**	**39.8**	**51.3**
CFD	**22.2**	17.0	16.9	14.8	31.2	37.9
NWFD	**30.9**	**27.0**	**23.2**	**21.5**	31.2	41.8
SFD	19.3	15.5	16.1	**18.1**	**41.0**	**66.7**
NCFD	6.4	4.7	4.9	5.6	**45.9**	38.6
VFD	17.2	15.1	15.6	12.7	**48.8**	**66.5**
UFD	16.6	13.9	10.5	8.3	25.6	21.7
SFD	**26.8**	**24.4**	**26.5**	**25.4**	**52.0**	**63.9**
FEFD	**34.6**	**28.3**	**26.1**	**29.5**	**49.5**	**81.9**

Table prepared by the authors

The bronchial asthma (J45-J46) mortality rate of the total population of the Russian Federation in 2021, which did not change, ranged from 1.0 per 100,000 population in 2016 to 0.8 in 2021 ($p > 0.05$).

In 2021, the contribution to the overall mortality structure of COVID-19 was 19.1%. Compared with 2020, there was a 3.2-fold increase in mortality rate due to COVID–19 in 2021 — from 98.8 (144,691 people) to 319.1 deaths (465,525 people) per 100,000 population ($p < 0.001$). An increased mortality rate from COVID-19 in 2021 was noted in all eight federal districts in 85 subjects of the Russian Federation. A higher mortality rate from COVID-19 than the average Russian level in 2021 was registered in the Northwestern Federal District (370.5), Central Federal District (367.7), UFD (355.1 deaths per 100,000 population). Among Russian Federal Subjects, the highest mortality rates from COVID-19 in 2021 occurred in the Orenburg region of the Volga Federal District — 472.6; Kursk region of the Central Federal District — 465.7; Oryol region of the Central Federal District — 460.9; Voronezh region of the Central Federal District — 460.4; Omsk region of the SFD — 448.1 per 100,000 population. Below average mortality rates from COVID-19 in 2021 were observed in the North Caucasus Federal District (156.1), Far Eastern Federal District (228.0), SFD (294.0), VFD (312.2), and Southern Federal District (314.9 deaths per 100,000 population). Among the Russian Federal Subjects, the lowest mortality rates from COVID-19 were noted in the Kirov Region of the Far Eastern Federal District — 65.2, the Chukotka Autonomous District of the Far Eastern Federal District — 76.3, the Republic of Tyva of the SFD — 99.6, the Chechen Republic of the North Caucasus Federal District — 103.2, and the Sakhalin Region of the Far Eastern Federal District — 106.4 per 100,000 population.

Compared to 2020, 2021 saw an increase in mortality from COVID-19 in all age groups, both among men and women. The highest mortality rates from COVID-19 were registered in the age group of 85 and older — 867.1 (2020) and 3052.93 deaths (2021) per 100,000 population, respectively.

Compared to 2020, the mortality from COVID-19 increased in 2021 among men by 2.7 times (from 107.3 to 286.1 deaths per 100,000 population, respectively; $p < 0.001$) and among women by 3.8 times (from 91.4 to 347.8 deaths per 100,000 population, respectively; $p < 0.001$). Moreover, if in 2020 mortality was higher in men, then in 2021 a higher mortality was recorded in women.

Among men in 2021, mortality rates due to COVID-19 above the national average (286.1 deaths per 100,000 population) were recorded in the Northwestern Federal District (344.0), Central Federal District (328.0), UFD (320.0), and Southern Federal District (287.9). The highest mortality rates from COVID-19 in men occurred in the Voronezh region of the Central Federal District (404.0 deaths per 100,000 population). Lower than the average Russian mortality rates due to COVID-19 in men were registered in the North Caucasus Federal District (146.4), Far Eastern Federal District (203.5), SFD (263.0), VFD (273.5 deaths per 100,000 population); the lowest mortality rate was recorded in the Kirov region of the VFD (61.5).

Among women in 2021, the mortality rate from COVID-19 was higher than the average in Russia (347.8 deaths per 100,000 population) in the UFD (385.8), Northwestern Federal District (393.2), Central Federal District (401.6). Mortality rates below the average were recorded in the North Caucasus Federal District (164.9), Far Eastern Federal District (251.1), SFD (321.1), Southern Federal District (338.3), and VFD (345.5). The highest mortality due to COVID-19 among women was registered in the Orenburg Region of the Far Eastern Federal District (533.2 deaths per 100,000 population), the Ivanovo Region of the Central Federal District (507.0); the lowest mortality rate from COVID-19 was recorded in the Chukotka Autonomous District of the Far Eastern Federal District (53.1).

DISCUSSION

The presented analysis of official statistics from the Ministry of Health of the Russian Federation and Russian Federal State Statistics Service shows that during the epidemic circulation of the COVID-19 virus infection in 2020–2021, there was a significant increase in morbidity, hospital lethality and mortality of the total Russian population due to RD, in which structure pneumonia occupied a leading place. Compared to 2019, RD increased in the total population by 13.59% in 2021; pneumonia — by 159.52%, and RD — by 11.49%. Due to the conversion of hospitals for the treatment of patients with COVID-19, the number of patients hospitalized for RD decreased in 2020 and 2021; however, the severity increased, which led to a 3.97-fold increase in lethality from these diseases. Thus, the number of patients discharged from hospitals for RD in 2019 amounted to 3,341,437 people (lethality — 0.75%); in 2020 — 2,444,098 people (lethality — 2.71%); in 2021 — 2,178,908 people (lethality — 2.99%). The main contribution to the lethality rate of the population aged 18 and over was made by pneumonia (J12-J18 ICD-10): 2019 — 439,901 people (10,510 people died — 2.39%); 2020 — 646,444 people (47,939 people died — 7.42%); 2021 — 378,715 cases (48,711 people died — 12.86%). A similar situation of increased lethality from pneumonia was noted among children aged 0–17 years: 2019 — 272,339 people (226 people died — 0.08%); 2020 — 143,627 people (213 people died — 0.148%); 2021 — 139,279 people (239 people died — 0.171%).

In 2020, in Russia, the incidence of COVID-19 of the total population in terms of access to medical institutions was registered at the level of 3391.1 cases per 100,000 of the total population (4,966,644 people). This increased by 2.4 times in 2021 — 8,085.7 cases per 100,000 of the total population (11,818,983 people). In 2020 1,947,867 people were discharged from hospitals with COVID-19, which amounted to 39.22% of all patients with COVID-19 (lethality — 5.93%); in 2022, 1.89 times more — 3,673,855 people, that is, 31.08% of all patients with COVID-19 (lethality — 12.48%).

There were significant fluctuations in the levels of morbidity, overall incidence and lethality from RD in the population of different territories of the Russian Federation and age groups. As in the previous period, the highest incidence of RD in the population in 2020–2021 was recorded in the territories of the cold climate zone in the Northwestern Federal District, VFD, UFD, and SFD. The incidence of pneumonia among the population was higher than the national average

in 2021. It was registered in the Southern Federal District, the North Caucasus Federal District, the Far Eastern Federal District and the Far Eastern Federal District.

During the COVID-19 epidemic in 2020-2021, there was an increase in RD mortality compared to 2019 (40.3 cases) by 72.46% in 2020 (69.5 cases), and in 2021 — by 95.3% (78.7 cases per 100,000 of the total population). Above average Russian levels of RD mortality in 2021 were registered in the Far Eastern Federal District (111.0), the Volga Federal District (102.7), the SFD (93.1), the Southern Federal District (88.4 cases per 100,000 population). RD mortality increased with age and was higher among men than among women. In the structure of mortality from all RD, mortality from pneumonia (J12-J16, J18) in 2021 was 65.3%. Mortality from pneumonia in the total population increased 3.2 times from 2019 (16.3) to 2021 (51.3 per 100,000 population). While etiological verification of pneumonia in 2020–2021 involves practical difficulties, given the data on the circulation of a novel coronavirus infection, it can be assumed that a significant part of it is associated with a previous viral infection.

In 2021, the highest incidence rates of COVID-19 were detected in the Northwestern Federal District (10,625.6), UFD (9684.2), Central Federal District (8969.4 cases per 100,000 of the total population) and mortality from COVID-19 in 2021 were also registered in the population of the same territories of the Northwestern Federal District, Central Federal District, UFD.

The problem of the epidemic circulation of the new coronavirus and the long-term course of the consequences of COVID-19 has posed new challenges that remain relevant for the healthcare system and the medical community at the present time. The severe course of COVID-19 is accompanied by multi-systemic manifestations of the disease involving an increase in mortality [2]. In this regard, improving the methods of primary prevention and effective treatment of COVID-19 and other respiratory infections will be of great importance for public health. The development and widespread introduction of a domestic vaccine against the new coronavirus since January 2021 made it possible to stop the epidemic and reduce mortality from COVID-19 in 2022. At the same time, the circulation of the new SARS-CoV-2 coronavirus continues along with other respiratory infections. The study of data on vaccination of Russia against influenza and pneumococcal infection in Moscow confirms the need for wider coverage of these methods of prevention of the population having a high risk of morbidity and mortality from respiratory infections [10]. A study of the risk factors for deaths in the adult population with COVID-19 based on the presented data showed that elderly, male patients had the highest risk. This is consistent with the results of foreign studies conducted on large groups of patients. Data on primary care of the electronic healthcare platform of England (OpenSAFELY), which covered 40% of all patients, were analyzed. Data from 17,278,392 adults were compared with data from 10,926 patients who died from COVID-19. They confirmed that old age increases HR = 1.59 by 10 years (95% CI 1.19–2.13), as well as male gender — HR = 1.59 (95% CI 1.53-1.65), belonging to black peoples — HR = 1.48 (95% CI 1.30–1.69) and South-Asian peoples — HR = 1.44 (95% CI 1.32-1.58) [11]. In older patients, chronic diseases that increase the risk of death are more common: coronary heart disease — HR = 5.16 (95% CI 5.16-8.49), chronic renal failure — HR = 3.69 (95%CI 3.09–4.39), COPD — HR = 3.55 (95% CI 1.88-6.79), obesity with BMI of 40 and above — HR = 1.92 (95% CI 1.72–2.13), diabetes mellitus — HR = 1.92 (95% CI 1.48–2.48), arterial hypertension — HR = 1.09 (95%CI 1.05–1.14) and other diseases [12]. According to the results of a comparative analysis of the data of 12,007 patients (10,761 with favorable and 1,246 with unfavorable COVID–19 outcomes) from 66 hospitals in the Moscow region, it was found that in the absence of comorbid conditions, the death rate was 9.4%; with one comorbid condition — 13.9% ($p < 0.001$); with multimorbidity — 24.8% ($p < 0.001$) [13].

Smoking at the time of the disease also increased the incidence of an adverse outcome (HR = 1.07; 95%CI 0.98-1.18) [12]. The adult population of Russia is characterized by a high prevalence of smoking among both men and women [14]. With the exception of the North Caucasus Federal District, the prevalence of smoking among men in other federal districts of Russia in 2021 exceeded 35.8%. Among women, the prevalence of smoking is higher than the national average (9.2%) registered in the Northwestern Federal District (12.6%), the UFD (11.4%), the SFD (12.7%) and the Far Eastern Federal District (18.9%), whose population is characterized by high incidence of acute and chronic RD.

Representing one of the strategic directions of medical science, pulmonology actively uses innovative methods of diagnosis and treatment in order to preserve the health of the Russian population [13]. The development and implementation of scientifically based RD prevention measures will help reduce morbidity and mortality, increase the duration of socially active life, and reduce the economic burden on the state due to RD.

CONCLUSIONS

1. Compared with 2019, the total RD morbidity of the total population of Russia in 2021 increased by 11.49%, while the RD morbidity of the total population increased by 13.59%, mainly due to the increased incidence of pneumonia. Excesses in the average level of RD morbidity in Russia in 2021 were noted in four federal districts: SFD, VFD, UFD and NWFD.

2. Due to the increase in the number of patients with COVID-19, hospitalization due to RD decreased in 2020 and 2021; however, the severity of infections increased, leading to a 3.97-fold increase in lethality from RD, primarily from pneumonia.

3. In the period 2020–2021, there was an increase in RD mortality compared to 2019 by 72.46% in 2020 (69.5 cases), and in 2021 — by 95.3% (78.7 cases per 100,000 of the total population). Excesses of the average Russian level of RD mortality in 2021 were registered in the Far Eastern Federal District, VFD, CFD, and SFD.

4. RD mortality increased with age and was higher among men than among women; however, in 2021, higher mortality rates among women were recorded. In the structure of mortality from all RD, the share of mortality from pneumonia (J12-J16, J18) in 2021 was 65.3%. Mortality

from pneumonia in the total population increased 3.2 times from 2019 (16.3) to 2021 (51.3 per 100,000 population).

5. The COVID-19 epidemic in 2020–2021, which was caused by the novel coronavirus SARS-CoV-2, had a significant impact on the morbidity and lethality of the Russian population from RD.

6. The incidence of COVID-19 increased from 3,391.1 cases per 100,000 of the total population (4,966,644 people) in 2020 to 8,085.7 cases (11,818,983 people) in 2021, exceeding the national average in the UFD, Central Federal District, and Northwestern Federal District.

7. An increase in mortality from COVID-19 in 2020–2021 was registered in all Federal districts of the Russian Federation; moreover, if in 2020 the mortality of men was higher, then in 2021 mortality was higher for women. Excesses in the average Russian mortality from COVID-19 in 2021 were recorded in the Northwestern Federal District, Central Federal District, and UFD.

8. The increase in mortality from COVID-19 in 2021 was noted in all age groups; however, the highest levels were recorded in patients over the age of 85: among men — 2.7 times; among women — 3.8 times.

9. Due to the continuing circulation of a novel coronavirus infections among the Russian population at the same time as other respiratory diseases, it is necessary to develop a program for the prevention of RD.

References

1. Bystritskaya EV, Bilichenko TN. The morbidity, disability and mortality associated with respiratory diseases in the Russian Federation in 2015-2019. *Pul'monology*. 2021;31(5):551–61 (In Russ.). https://journal.pulmonology.ru/pulm/article/view/2875
2. Bilichenko TN. Epidemiology of Coronavirus disease 2019 (COVID-19). *Academy of medicine and sports*. 2020;1(2):14–20 (In Russ.) https://doi.org/10.15829/2712-7567-2020-2-15
3. The incidence of the total population of Russia in 2021 with a diagnosis established for the first time in life: Statistical materials. M.;2022;partI.
4. The incidence of the total population of Russia in 2016, 2017, 2018, 2019: Statistical materials. M.;2017, 018,2019,2020;part II.
5. Total morbidity of the adult population of Russia in 2021: Statistical materials. M.;2022;part IV.
6. Medical and demographic indicators of the Russian Federation. 2021: Statistical materials. M.;2022.
7. Federal State Statistics Service. Demographic yearbook of Russia. 2017; Available at: https://rosstat.gov.ru/storage/mediabank/Dem_ejegod-2017.pdf
8. Federal State Statistics Service. Demographic yearbook of Russia. 2019; Available at: https://rosstat.gov.ru/storage/mediabank/Dem_ejegod-2019.pdf.
9. Federal State Statistics Service. Demographic yearbook of Russia. 2022; Available at: https://rosstat.gov.ru/storage/mediabank/Ejegodnik_2022.pdf
10. Gruzdeva OA, Bilichenko TN, Baryshev MA, Zhukova AV. The impact of vaccination against influenza and pneumococcal infection on the incidence of acute respiratory viral infections and community-acquired pneumonia in the Central Administrative District of Moscow. *Epidemiology and Vaccinal Prevention* 2021; 20(2):28–41. https://doi.org/10.31631/2073-3046-2021-20-2-28-41
11. Williamson EJ, Walker AJ, Bhaskaran K, et al. Open SAFELY: factors associated with COVID-19 death in 17 million patients. *Nature*. 2020;584:430–6. https://doi.org/10.1038/s41586-020-2521-4
12. Molochkov AV, Karateev DE, Ogneva EYu, Zulkarnaev AB, Luchikhina EL, Makarova IV, Semenov DYu. Comorbidities and predicting the outcome of COVID-19: the treatment results of 13,585 patients hospitalized in the Moscow Region. *Almanac of Clinical Medicine.* 2020;48(S1):S1–10 (In Russ.). https://doi.org/10.18786/2072-0505-2020-48-040
13. Selective monitoring of the health status of the population. Accessed July 07, 2022 (In Russ.). https://rosstat.gov.ru/itog_inspect
14. Bilichenko TN, Shutov AA. The achievements of pulmonology and the main directions of further improvement of medical care to the population of the Russian Federation. *Pulmonology*. 2021;31(6):782–91 (In Russ.). https://doi.org/10.18093/0869-0189-2021-31-6-782-791

Authors' contributions. All authors confirm that their authorship meets the ICMJE criteria. The largest contribution is distributed as follows: Tatiana N. Bilichenko — collection, preparation and systematization of materials, analysis and discussion of the results obtained, writing and editing of the article; Elena V. Bystritskaya — analysis of materials and discussion of the results obtained, editing of the article, approval of the final version of the article. Viktor M. Misharin — formulation of the purpose and objectives of the study, analysis of materials and discussion of the results obtained, approval of the final version of the article.

AUTHORS

Tatiana N. Bilichenko, Dr. Sci. (Med.), Professor
https://orcid.org/0000-0003-3138-3625
tbilichenko@yandex.ru

Elena V. Bystritskaya, Cand. Sci. (Med.),
https://orcid.org/0000-0001-8447-5801
bystritskaia@yandex.ru

Viktor M. Misharin, Cand. Sci. (Med.)
secretary@pulmonology-russia.ru

Scientific and practical reviewed journal
of FMBA of Russia
extrememedicine.ru